THE
PHYSICAL REVIEW
A Journal of Experimental and Theoretical Physics
VOL. 49, NO. 2 JANUARY 15, 1936 SECOND SERIES

Fluctuations in Cosmic-Ray Ionization as Given by Several Recording Meters Located at the Same Station

RICHARD L. DOAN, *Ryerson Physical Laboratory, University of Chicago*
(Received November 18, 1935)

A graphical comparison is given of the intensity variations of cosmic rays as registered on several different recording meters located in the same room during a period of ten weeks. As one might expect, the agreement is statistical rather than coincident. The barometer effect as calculated from the data of the individual meters ranges from 1 to 2 percent per cm Hg. A diurnal analysis carried out for a ten-day period during which barometric changes were small indicates a maximum of intensity at about 9:00 A.M. having a magnitude about 0.19 percent greater than the average. A pronounced increase in ionization has been observed during rainfall when the meters were operated with top shield removed. This has been ascribed to γ-radiation from active deposits brought down from the upper atmosphere with the raindrops. The average number of cosmic-ray ionizing particles traversing unit area of the ionization chamber in unit time, as estimated from statistical fluctuation data, is shown to compare favorably with counter observations. As regards ionization bursts: Analysis of distribution-in-time of the bursts shows that they occur in a purely random manner. Size frequency distributions covering a period of several weeks on eight different meters can be represented for the most part by a single exponential function. An analysis of nearly 700 bursts occurring over a 25 mm Hg range of pressure gives no evidence of a barometer effect on burst frequency, although the consistency of the data is not sufficient to rule out the possibility of an effect as large as 8 percent per cm Hg. The frequency is a function of shield thickness, being much greater for a reduced top shield than for the full 12 cm of lead.

PART I—INTENSITY VARIATIONS

THE construction of seven precision cosmic-ray recording meters for permanent installation in various parts of the world[1] provided a unique opportunity for comparing the results obtained from several meters running concurrently at the same location. While it is obviously desirable to make such intercomparisons as an aid in estimating the significance of future differences in data obtained at the various permanent stations, the results are also of general interest because of the information they yield in connection with certain cosmic-ray problems.

The instruments used in these tests have previously been described by Compton, Wollan and Bennett.[2] Briefly, they consist of a spherical ionization chamber of 19.3 liters capacity, filled with 50 atmospheres of highly purified argon and shielded with 2500 lbs. of lead shot equivalent in thickness to 12 cm of solid lead. The ionization is measured by means of a Lindemann electrometer and the optical arrangement is such that the image of the electrometer needle can either be observed visually or recorded on a moving strip of bromide paper. A compensating

[1] This is in accordance with a program for the routine collection of cosmic-ray data originally proposed by A. H. Compton and R. D. Bennett (Bulletin No. 9, Union Géodesique et Géophysique Internationale 1933, p. 311) and sponsored by the Department of Terrestrial Magnetism of the Carnegie Institution of Washington. The permanent stations include the magnetic observatories at Cheltenham, Md., and Huancayo, Peru, as well as locations in Mexico, Greenland, and New Zealand.

[2] A. H. Compton, E. O. Wollan and R. D. Bennett, Rev. Sci. Inst. 5, 415 (1934).

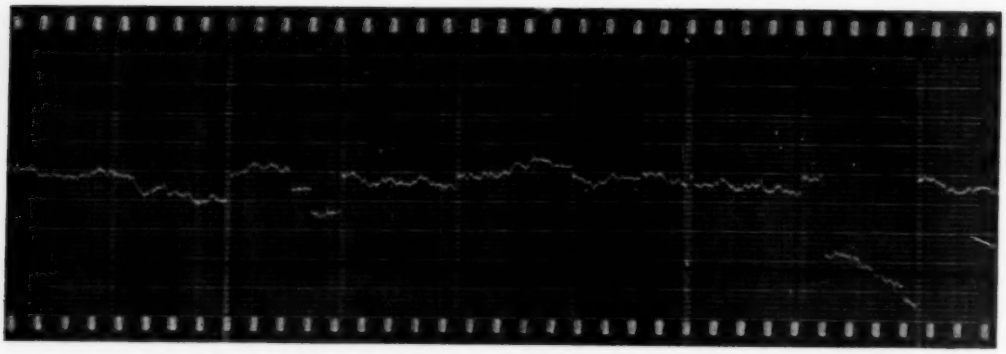

FIG. 1. Portion of record from meter No. 1 for September 21, 1934. Note the bursts in the third and eighth hours. The black line is the barometer trace.

arrangement is employed whereby most of the cosmic-ray ionization is balanced out by the β-ray ionization from a short adjustable uranium rod located in an auxiliary chamber inside the bomb, so that what is actually recorded is the differential between the ionization due to the cosmic rays and that due to the β-ray source. The latter remains constant after it has once been adjusted to the desired intensity and any changes in the intensity of the cosmic rays are indicated on the record. The collecting system is grounded automatically once each hour and the electrometer sensitivity that may be employed is limited only by the necessity of keeping the needle image on the scale during the whole period.

A typical record is shown in Fig. 1. The principal feature to be noted is that the needle drifts from its zero position during the 57.5 minutes that the collecting system is insulated, the amount of the drift being a function of the intensity of the cosmic rays during that period. The total ionization in any period is subject to statistical fluctuations due to the finite number of ionizing particles traversing the chamber, and such fluctuations are evident on the record. An occasional abrupt displacement of the needle image represents a burst of ionization presumably occasioned by the simultaneous passage of a large number of ionizing particles. In the discussion which follows, the bursts are treated separately from the average ionization and so far as possible they have been deducted in making calculations involving variations in ionization.

The hourly scalings of the records from six meters during March and part of April and May are given in Figs. 2 and 3. In each case the top trace indicates the variations in barometric pressure while the lower points show the net unbalance of the electrometer needle in each instrument at the end of the hourly period. The most prominent feature of these plots is the inverse relationship between cosmic-ray intensity and atmospheric pressure. It is also interesting to note that the barometer variations during March were considerably greater than for the later period. For several days around April 19 the total variation in atmospheric pressure was only 2 or 3 mm Hg which is exceptionally small for Chicago. Another point of interest in connection with Fig. 3 is the apparent decrease in cosmic-ray intensity with time which continued throughout the whole period of the test with the possible exception of the last few days (May 20–22) although most of the increase that occurs at this time can probably be attributed to the fall in the barometer.

Statistical fluctuations

Let us now consider the scatter of the points in Figs. 2 and 3 and inquire whether the observed variations in the hourly scalings are such as may reasonably be attributed to statistical fluctuations due to the limited number of ionizing events. The problem of statistical fluctuations of cosmic-ray ionization in a spherical chamber has been worked out by Evans and Neher[3] on the assumption that the ionizing agents are single

[3] R. D. Evans and H. V. Neher, Phys. Rev. **45**, 144 (1934).

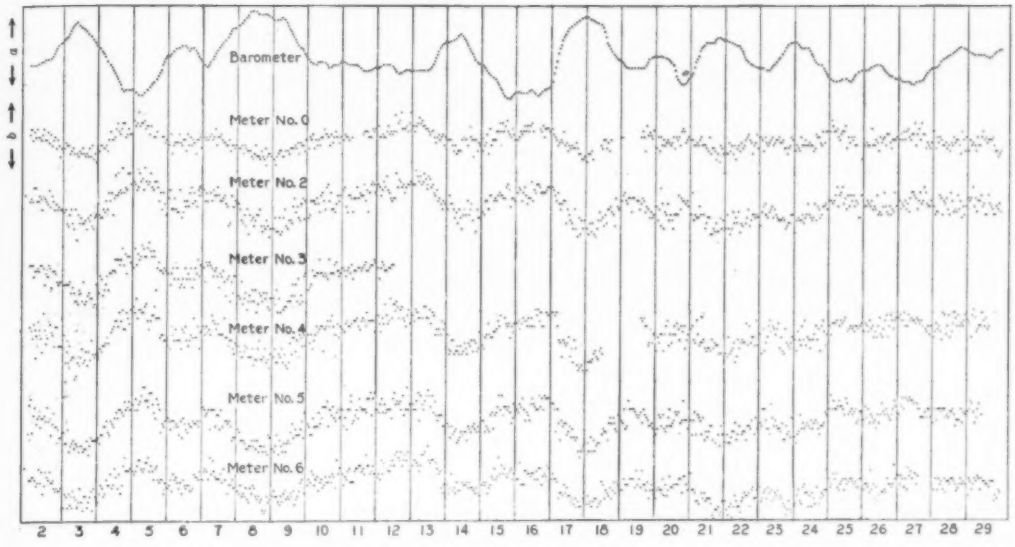

FIG. 2. Variations of cosmic-ray ionization, March 1935 (Chicago). *a*, 20 mm Hg; *b*, 5% I_{750}.

and multiple electron rays which shoot clear through the chamber, the ionization due to a shower of n particles being assumed to be n times that due to a single particle. This leads to the following expression for the total ionization:

$$I = AN\Sigma nr_n/\Sigma r_n, \tag{1}$$

where A is the average ionization produced by a single particle and N the number of ionizing events, an event consisting of the passage of n related particles. The ratio of the frequency of showers to that of single-particle events is designated by r_n.

On the basis of the above picture a series of observations made upon I should show statistical fluctuations around the average value proportional to the inverse square root of N. The relation between N and the standard deviation σ as defined by the root mean square of the deviations from the mean is given by

$$\sigma = FI(N)^{-\frac{1}{2}},$$
$$F^2 = (9/8)[\Sigma r_n \Sigma n^2 r_n/(\Sigma n r_n)^2]. \tag{2}$$

We have thus a means of estimating the rate of passage of ionizing particles through the ionization chamber from measurements of the standard deviation providing we can determine the value of F, which as indicated above, depends upon the distribution of showers and single particles. About the best that we can do here at present is to make an estimate based on the observed distribution of multiples and singles in drop track photographs. If we use the analysis of Anderson,[4] which included about eight hundred events, we get

$$\Sigma r_n = 1.15; \quad \Sigma n r_n = 1.42; \quad \Sigma n^2 r_n = 2.21,$$

from which $F = 1.32$.

This value of F is undoubtedly smaller than that which applies to a spherical ionization chamber completely surrounded by lead, because in the latter case the closer proximity of the shielding material should result in a relatively larger number of showers. It is uncertain as to just what value should be taken but we shall probably not be far off if we use $F = 1.5$, and this is the value adopted in the subsequent calculations.

The standard deviation is obtained from an analysis of the hourly records from the various cosmic-ray meters. If Y_m is the drift of the electrometer needle in scale divisions during the mth hourly period, then σ can be calculated from

$$\sigma^2 = \sum_1^n Y_m^2/n - (\Sigma Y_m/n)^2, \tag{3}$$

where n is the number of hours considered.

[4] C. D. Anderson, Phys. Rev. **44**, 406 (1933).

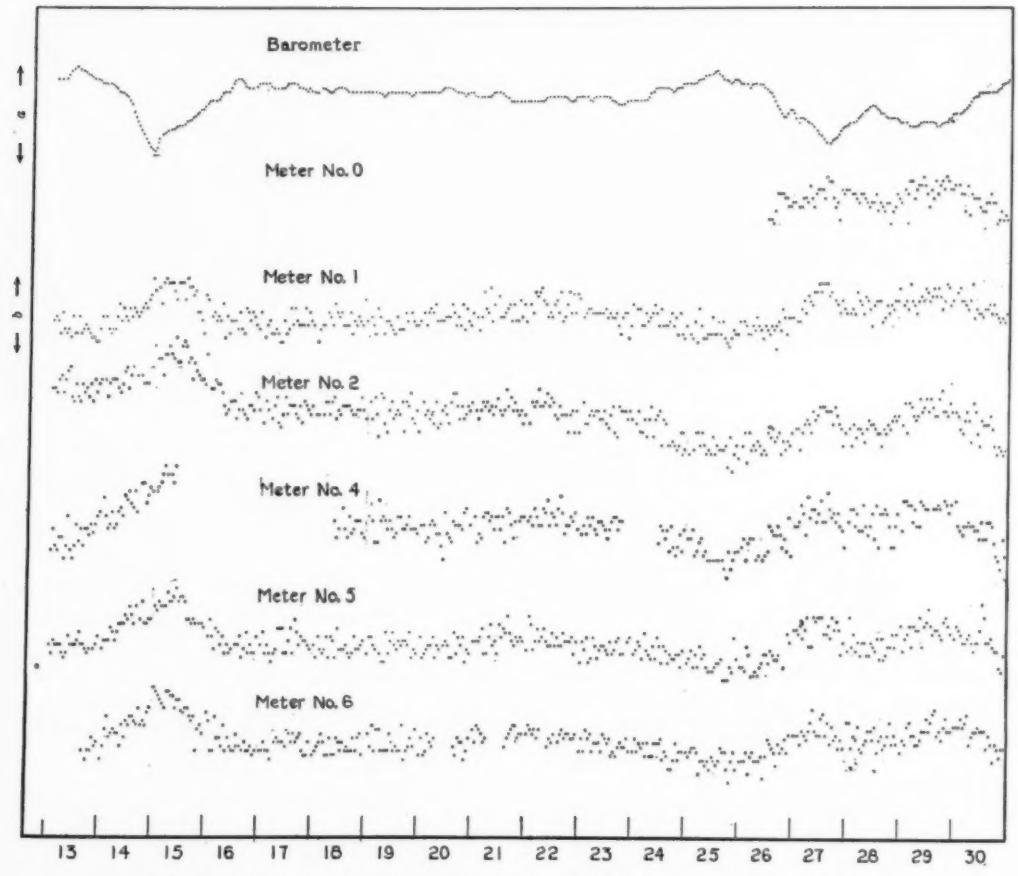

FIG. 3A. Variation of cosmic-ray ionization, April 1935 (Chicago). *a*, 20 mm Hg; *b*, 5% I_{760}.

Since Y varies considerably with the barometer such a calculation can best be made for a period during which the barometer is essentially constant. From Fig. 3 it may be seen that the period April 17–21 was free from barometer changes of any consequence. For this period of approximately 100 hours, the standard deviations as calculated from the records of four meters running simultaneously were as follows:

Meter No.	σ (ions per hour)
1	$33.4(10)^6$
2	34.4
5	35.1
6	30.4

Since the collecting systems were insulated for 57.5 minutes out of each hour the standard deviation for the period of one minute is obtained by dividing the "hourly" deviation by $(57.5)^{\frac{1}{2}}$. Using the average of the above values we obtain

$$\sigma = 4.4(10)^6 \text{ ions per minute.}$$

The mean value of the total ionization as determined by visual observations on the absolute cosmic-ray intensity comes out to be

$$I = 94.8(10)^6 \text{ ions per minute.}$$

Thus, from (2), taking $F = 1.5$ we get

$$N = ((1.5 \times 94.8)/4.4)^2 = 1045 \text{ per min.}$$

The cross-sectional area of the ionization chamber is 995 cm² so that the number of primary ionizing particles per cm² per minute is 1045/995 or 1.05, a value in close enough agree-

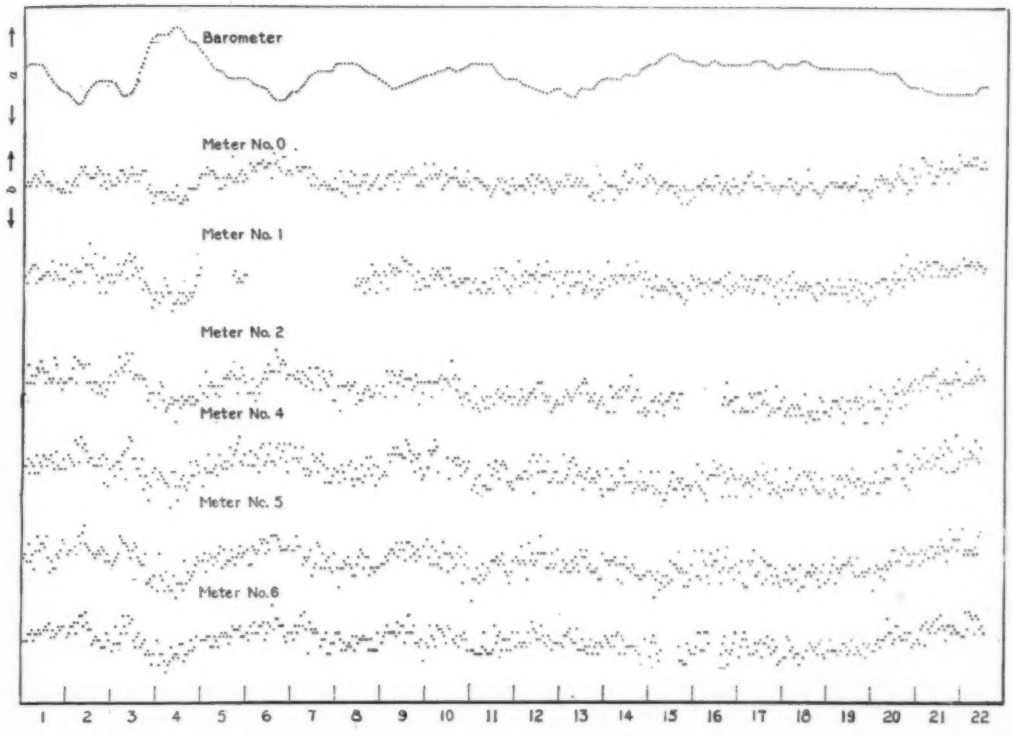

FIG. 3B. Variation of cosmic-ray ionization, May 1935 (Chicago). *a*, 20 mm Hg; *b*, 5% I_{710}.

ment with counter observations[5] to support the conclusion that the observed statistical fluctuation, while too great to be accounted for on the assumption that the ionization is due to randomly distributed single ionizing particles, may reasonably be attributed to a distribution of single and multiple ionizing rays not greatly different from that given by cloud chamber observations. This must mean that the distribution of tertiaries produced by lead secondaries is quite similar to that produced by air secondaries, which is what one might expect if the secondaries in each case are photons but not necessarily so if they are charged particles originating in the nuclei of the respective atoms.

Barometer effect

The variations of cosmic-ray intensity with atmospheric pressure at a given station can be inferred from curves of intensity *vs.* altitude; but for several reasons a straightforward correlation of ionization and barometer differentials does not lead to a constant result when carried out at different times. In the first place the barometer reading gives the weight of air directly above the instrument and therefore gives no accurate measure of the air path of the cosmic rays which come in at appreciable zenith angles. This difficulty is accentuated by the fact that the various high and low pressure areas which pass over the observer do so at different speeds and in different relative positions and have all sorts of pressure distribution. At Chicago during certain times of the year the "highs" and "lows" follow one another in fairly rapid succession as indicated to some extent in Fig. 2. It is not uncommon for the pressure to drop rapidly to a minimum and rise equally fast, and on some of these occasions the cosmic-ray records show that

[5] E.g., The measurements of Street and Woodward gave 0.80 per cm² per min. from unit solid angle at the vertical or 1.48 per cm² per min. from all directions. (Phys. Rev. **46**, 1029 (1934).)

the barometer has passed the low and is rising while the cosmic-ray intensity is continuing the increase which began with the falling barometer. An inspection of Fig. 2 will show that on March 3, 8 and 14 the midpoint of the ionization trough does not coincide with that of the barometer peak but is displaced slightly to the right. This, however, does not appear to be the case for March 17–18.

Another factor which makes the barometer correction difficult if too long a period of time is considered, is an occasional rather large change in cosmic-ray intensity independently of the barometer. Such a change is illustrated in Fig. 3 and has already been mentioned. These so-called "variations of the second kind" have not had a satisfactory explanation.

It is thus well known that the barometer effect as defined by the percentage change in cosmic-ray ionization per cm mercury (or sometimes per meter of water) change in atmospheric pressure may vary widely depending upon the period chosen for analysis. This has led to the practice by European investigators of calculating the barometer effect for short rather than long periods and making the barometer corrections accordingly.

If one plots hourly ionization as ordinates and barometer readings as abscissae a scatter diagram is obtained through which three straight lines may be drawn, two of which represent least-squares adjustment of one variable in terms of the other and *vice versa*, the third being a least-squares adjustment for normal deviations. If we suppose that the barometer readings are relatively exact and that most of the error is in the ionization, then presumably the best line for determining the barometer effect is the one given by averaging all of the ionization values in the various vertical columns of the scatter diagram. The slope of this line which is the so-called regression of y on x, where y represents the ionization and x the barometer, can be calculated from the data obtained from the records. To do this the correlation coefficient r is first calculated making use of the relation

$$n^2\sigma_x\cdot\sigma_y\cdot r=n\Sigma(xy)-\Sigma x\Sigma y, \tag{4}$$

where n is the number of hours considered and the σ's are the respective standard deviations of x and y as defined previously. It should be noted here that the y's and x's are scaled directly from the records and therefore represent departure from an arbitrarily selected base line rather than from the mean.

TABLE I. *Barometer coefficients for March.*

METER No.	r	P_r	a	P_a	$(a/I)\times100$
0	−0.616	±0.016	0.89	±0.003	1.07
2	− .630	.015	1.33	.005	1.60
3	− .845	.012	1.76	.005	2.11
4	− .762	.011	1.43	.004	1.72
5	− .786	.010	1.57	.004	1.89
6	− .572	.017	1.12	.005	1.35

Once the correlation coefficient is obtained, the slope of the regression line is given by

$$a=r(\sigma_y/\sigma_x). \tag{5}$$

The probable error of the correlation coefficient[6] is

$$P_r=0.6745(1-r^2)/n^{\frac{1}{2}} \tag{6}$$

while that of the regression coefficient is

$$P_a=0.6745((1-r^2)/n)^{\frac{1}{2}}\cdot\sigma_y/\sigma_x. \tag{7}$$

In Fig. 4 are plotted the hourly ionization differentials against the barometer readings for meter No. 5 as taken from the March records. The full line drawn through these points is the regression line calculated as described above from the equation

$$y=\bar{y}+r(\sigma_y/\sigma_x)(x-\bar{x}),$$

where $\bar{y}$ and $\bar{x}$ represent mean values. The dashed lines give the probable error of y so calculated and show the limits within which the points fall half of the time. In other words it is equally probable that any given point fall inside or outside the region defined by these lines. Thus the probable error of y

$$P_y=0.6745\sigma_y(1-r^2)^{\frac{1}{2}}$$

is useful in giving some idea of the scatter of the points along the regression line.

The correlation and regression coefficients as given by six different meters for the month of March are grouped in Table I, together with the calculated probable errors. With the exception of Meter No. 3 all of the instruments were

[6] *Handbook of Mathematical Statistics* (Houghton, Mifflin Co.).

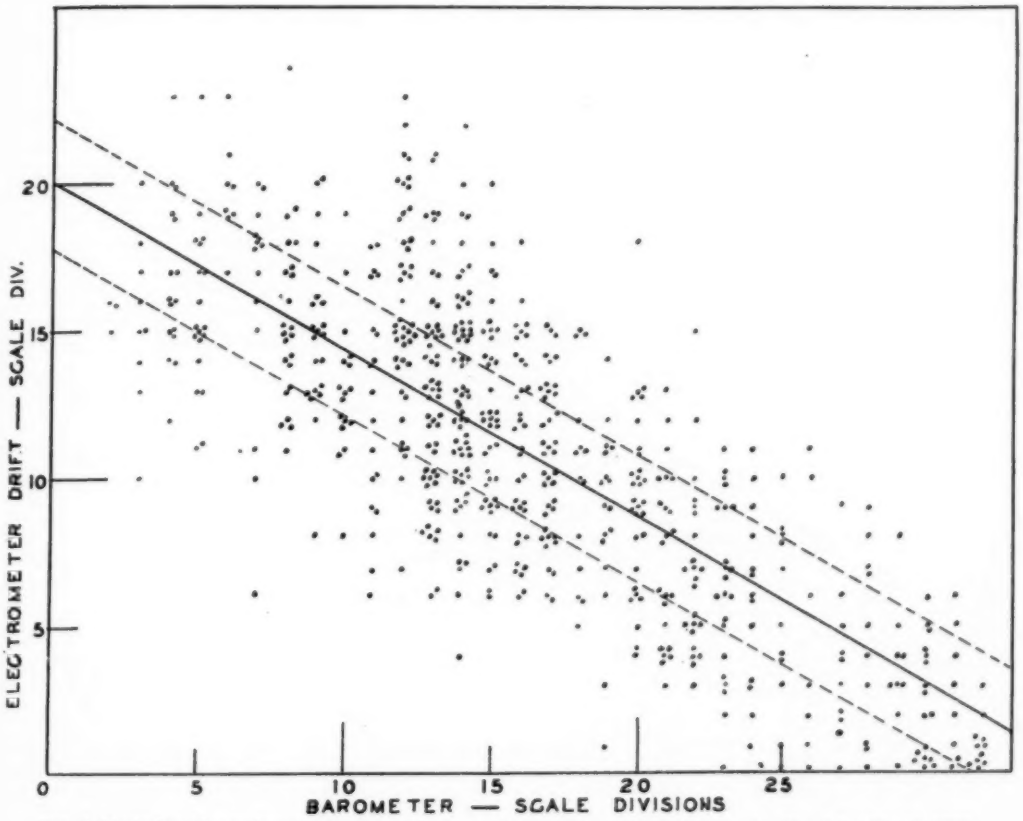

FIG. 4. Variation of cosmic-ray intensity with atmospheric pressure. Data from meter No. 5 for March 1935.

running for the entire month, as may be seen from Fig. 2. The correlation coefficient is given as a negative fraction while the regression coefficient is expressed in terms of ions per cc per sec. per cm Hg and also as percent of the total cosmic-ray ionization per cm Hg.

It will be seen that for the most part the regression coefficients for the various meters differ from one another by more than their probable errors, which is suggestive of the considerable differences noted by other observers when using the same meter at different times. Actually, however, a glance at Fig. 4 will show that the probable error of the calculated ionization is so great that the differences between the various meters indicated in the above table are somewhat exaggerated. A better indication of these differences is obtained by comparing the central regression zones (region between the dashed lines in Fig. 4) of the meters when adjusted to the same mean value. This has been done in Fig. 5 and it will be noted that there is a considerable area common to all zones. Thus in the pressure range 5 to 25 scale divisions (about 20 mm Hg) all of the meters can be said to be giving consistent results about 67 percent of the time within the limits of accuracy of the measurement. If Meter No. 0 be excepted the agreement is much better.

Diurnal variation

The existence of a diurnal variation of cosmic-ray intensity has never been conclusively demonstrated although numerous investigators have reported positive results. Among the best of such studies is that of V. F. Hess and R. Steinmaurer,[13] which covers a period of one year. The situation as of 1933 is summarized very

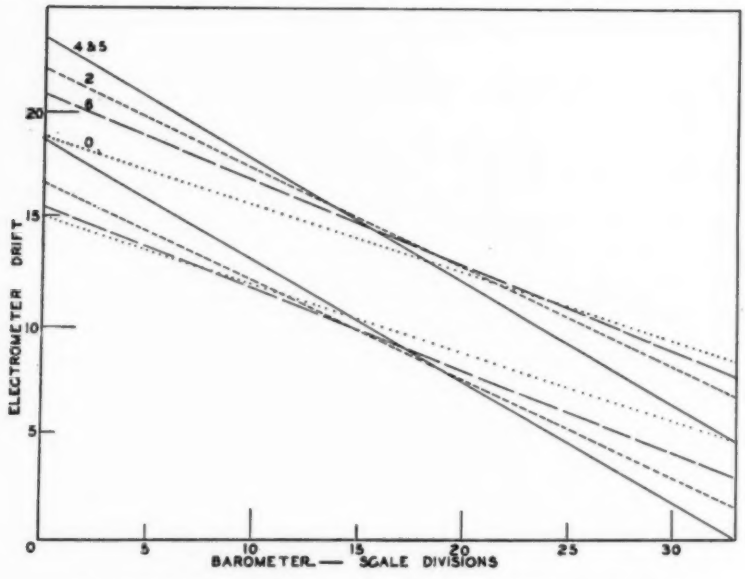

FIG. 5. Barometer variation as given by different cosmic-ray meters.

nicely by Broxon, Meredith and Strait[7] who themselves were unable to detect any significant diurnal variation in a series of experiments carried out on the campus of the University of Colorado only a short distance from the location where Bennett, Stearns and Compton[8] had previously found such a variation with a maximum about noon.

If a solar diurnal variation exists it may mean that a small component of the cosmic rays has its origin either in the sun as suggested by Hess and Pforte[9] or in the general neighborhood of the sun[8] although Gunn[10] has suggested that a diurnal variation might be due to fluctuations in the earth's magnetic field.

Variations according to sidereal time were looked for several years ago, and a sidereal periodicity was reported by Steinke[11] in 1929 as well as by other observers more recently. The search for a sidereal variation has received a new motive in a recent paper by Compton and Getting[12] in which are developed the consequences of the rotation of the galaxy on the intensity of cosmic rays originating in remote space outside the galaxy. A predicted maximum at about 20 hr. 40 min. sidereal time has received a tentative confirmation in some of the results of Hess and Steinmaurer[13] but in general the data needed for a satisfactory test are not yet available.

There are several difficulties in the way of establishing definitely the existence of a diurnal variation. Obviously if the ionization measurements are made during a period when there are any considerable barometric fluctuations, the results must be corrected to a common atmospheric pressure and such a process can easily introduce errors which may mask or distort the relatively small diurnal variation. There is also the possibility that any observed diurnal variation may be largely, if not solely, a temperature effect. Finally, if the measurements cover a long period of time, the situation may be complicated

[7] J. W. Broxon, G. T. Meredith and L. Strait, Phys. Rev. **43**, 687 (1933).
[8] R. D. Bennett, J. C. Stearns and A. H. Compton, Phys. Rev. **41**, 681 (1932).
[9] V. F. Hess and W. S. Pforte, Zeits. f. Physik **71**, 171 (1931).
[10] R. Gunn, Phys. Rev. **41**, 111 (1932).
[11] E. G. Steinke, Physik. Zeits. **30**, 767 (1929).
[12] A. H. Compton and I. A. Getting, Phys. Rev. **47**, 817 (1935).
[13] V. F. Hess and R. Steinmauer, Preuss. Akad. Phys.-Math. Kl. **15** (1933).

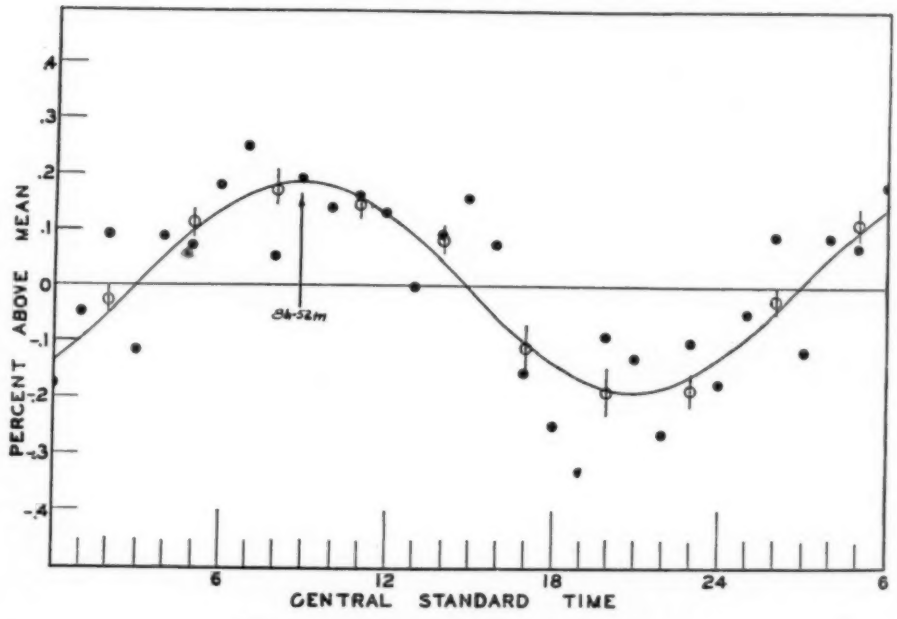

FIG. 6. Diurnal variation of cosmic-ray intensity.

by one or several "variations of the second kind."

In view of the above there should be certain definite advantages in searching for a diurnal effect at a time when the barometer fluctuations are small and in reducing the probable error of the observations by using several instruments rather than by prolonging unduly the period of observation. Ordinarily one cannot choose his experimental conditions so easily; but it just happened that during the intercomparison tests herein described there was a ten-day period, already mentioned, during which the barometer changed very little. Thus it seemed that this period, April 16–26, should be particularly suitable for diurnal analysis.

After making such small barometric corrections as were necessary, the results from all meters were grouped hour by hour on the basis of central standard time and the means calculated. These mean values are plotted as the black dots in Fig. 6. The open circles are the three-hour means, each being the arithmetic average of from 140 to 150 hourly readings on five different meters. The probable errors of the three-hour means as calculated from the relation

$$P = 0.6745\sigma/\sqrt{n}$$

are indicated by vertical lines through the open circles. It will be seen that a definite periodicity is indicated with a maximum at about 9:00 A.M.[14]

The first harmonic of the Fourier analytic curve is shown as the full line, the coefficients having been calculated from the hourly means by least-squares methods. The calculated amplitude and phase together with their probable errors are as follows:

$$\text{Amplitude} = 0.189 \text{ percent } \pm 0.035,$$
$$\text{Phase} \quad = -2 \text{ hr. } 52 \text{ min.} \pm 42 \text{ min.}$$

Thus the amplitude is from five to six times the probable error.

According to these results the maximum intensity occurs in the neighborhood of 9:00 A.M. and cannot therefore be accounted for solely as a solar diurnal variation. It is, however, of

[14] It is not possible to attribute this variation to a temperature effect in the apparatus since careful measurements have shown no detectable temperature coefficient when the temperature of the meter was varied over a range of more than 20°C. Then, too, the diurnal maximum comes several hours earlier than would be expected if it were a temperature effect.

interest to note that 9:00 A.M. Standard Time is about 23 hr. sidereal time on April 21 which is suggestively close to the time 20 hr. 40 min. predicted for the peak on the basis of Compton's theory of the effect due to motion of the galaxy. Perhaps one could consider the observed curve as a sort of combination of the two effects. If solar and sidereal variations are both present then it is to be expected that the diurnal variation will be a maximum about February 16 and a minimum about August 16.

Unshielded chamber; rain effect

Because there is some indication that the softer components of the cosmic rays show more pronounced barometer and diurnal effects than do the more penetrating rays, some European investigators have adopted the practice of operating their recording meters at least a portion of the time with the top shield removed. However, in view of the rather wide variations in γ-ray intensity due to radioactive deposits in the air, it would seem that the results obtained with no top-shielding would be difficult to interpret.

An interesting illustration of the pronounced increase in atmospheric radiation during a rain storm is shown in Fig. 7. The records (tracings) are from three different meters operating side by side, one with no top-shielding, another with 1 cm of lead above the bomb, in the form of a close-fitting hemispherical cap, and the third with several cm of lead shot as top shield. All meters were fully shielded from below.

Weather Bureau records show that during 12 hr. to 14 hr. there was heavy thunder with lightning but no rainfall. The cosmic-ray records show no change during this period. A heavy rainfall started at 16 hr. 28 min. and coincident with this a sharp increase in ionization is noted on the unshielded meter and somewhat later, on the meter shielded with 1 cm of lead. The precipitation was 0.39″ during a period of about 20 minutes, then dropped to 0.03″ and 0.01″ in the ensuing two hours. It may be noted that the ionization excess continued at about the same value for slightly more than two hours after which there was a rapid return to the level existing prior to the storm. No change is evident at any time on the third meter, which was

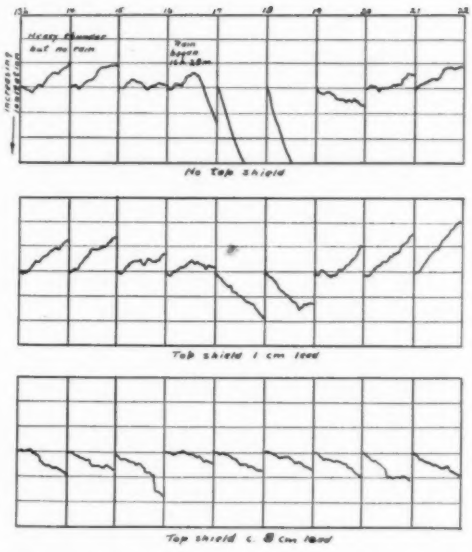

FIG. 7. Tracing of portion of record from three recording meters for August 17, 1935, showing effect of rainfall on ionization.

shielded with lead drop shot to an average thickness of some 6 to 8 cm.

That freshly fallen rain is radioactive was observed several years ago by C. T. R. Wilson[15] who found a half-period of approximately 30 minutes for the active deposit. Since it would be impossible for α- or β-rays to penetrate the half inch of steel comprising the walls of our cosmic-ray ionization chamber, the whole of the observed increase of ionization was presumably due to γ-radiation. Ra B gives off some feeble γ-rays[16] but one would not expect these to be very effective so that the more penetrating rays from Ra C are indicated as the most probable cause of the increase in ionization. Confirming this view is the fact that the observed absorption in 1 cm of lead is just about what we would expect on the basis of the known absorption of γ-rays from radium. If we assume that most of the active deposit came down as Ra B which, being positively charged, would readily form condensation nuclei then the effective period during which γ-rays would be emitted would be about that observed on the records since the half-periods of

[15] C. T. R. Wilson, Proc. Camb. Phil. Soc. **11**, 428 (1902).
[16] Rutherford, *Radioactive Substances and Their Radiations* (1913), p. 488.

Ra B and Ra C are 26.8 and 19.5 min., respectively.

These results emphasize the importance of using heavy shields in making cosmic-ray measurements if such atmospheric effects as the one illustrated here are to be avoided. With the 12 cm shield normally employed on the Compton-Bennett meters, no such effects are detectable.

Part II—Ionization Bursts

A burst of ionization is indicated on the cosmic-ray records by an abrupt displacement of the needle trace by an amount varying from one to twenty or twenty-five scale divisions (see Fig. 1). An event of this kind corresponds to the production of from ten to two hundred million ion pairs presumably by the simultaneous passage of several hundred ionizing particles through the ionization chamber. The actual number of particles involved is somewhat uncertain but can be estimated if we assume that the average rate of occurrence of ionizing events as obtained from statistical fluctuation data is somewhere near correct. This was found to be 1045 per minute for the whole chamber. Since an individual event might consist of the passage of a single particle or of several associated shower particles, the average number of ionizing particles traversing the chamber per minute would be

$$N = 1045 \Sigma n r_n / \Sigma r_n$$
$$= 1045 \times 1.23 = 1285$$

if we use the distribution of multiples and singles given by cloud chamber observations. Since the observed total ionization per minute is, after deducting the zero correction, $94.8(10)^6$ ions the average number of ions produced per particle is $7.36(10)^4$. Thus a burst of magnitude $5(10)^7$ ions corresponds to about 680 ionizing particles. This would be a burst of moderate proportions, a few scale divisions on the record, and many larger ones have been observed.

Table II. *Distribution of bursts according to time of occurrence.*

Hour	No. of Bursts	Hour	No. of Bursts
1	54	13	76
2	80	14	76
3	62	15	65
4	89	16	79
5	73	17	71
6	72	18	68
7	72	19	70
8	66	20	62
9	71	21	66
10	64	22	71
11	78	23	68
12	77	24	80

The data on bursts presented here were obtained by an analysis of the records from (a) three meters located under a slate and steel roof during parts of September, October and November, 1934; (b) six meters stationed under a glass roof in a campus greenhouse during March and parts of April and May, 1935.

In taking out the bursts the smallest one considered was $1.5(10)^7$ ions which according to the analysis of Bennett, Brown and Rahmel[17] is large enough to avoid confusion with the ordinary statistical fluctuations. However, it should be noted that a considerable amount of individual opinion is involved in picking out these smallest bursts, much more so than for the larger ones.

A casual examination of the records from any of the meters will show occasional days when as many as eight or ten bursts are in evidence while at other times not a single burst occurs in a complete day's record. This makes it of interest to examine the time-distribution of the interval between bursts. First in order to see whether the frequency of bursts was greater at certain times of day than at others all of the bursts from a total of 9206 hours of record were arranged according to the hour during which the burst occurred. The results are given in Table II.

Apparently there is no significant variation of burst frequency with the time of day, the results being more suggestive of a random distribution with respect to time. If the distribution is purely random the number of intervals between bursts should vary with the size of the interval in accordance with Poisson's formula

$$n = N(e^{-t_1/T} - e^{-t_2/T}),$$

where n is the expected number of intervals in the group defined by t_1 and t_2, N is the total number of intervals and T the average interval. A comparison of the calculated and observed intervals making use of Pearson's criterion should permit a decision as to whether or not the bursts

[17] R. D. Bennett, G. S. Brown and H. A. Rahmel, Phys. Rev. **47**, 437 (1935).

TABLE III. *Distribution of intervals between bursts.*

LENGTH OF INTERVAL (hr.)	NUMBER OF INTERVALS Obs.	Calc.	Δ	$\Delta^2/N_{calc.}$
0–1	63	56.2	−6.8	0.82
1–2	47	45.1	−1.9	.08
2–3	39	35.7	−3.3	.30
3–4	28	28.1	0.1	.00
4–6	35	40.5	5.5	.75
6–10	32	42.1	10.1	2.42
10–15	25	19.1	−5.9	1.82
15–∞	9	9.1	0.1	00
				$\chi^2=5.89$

occur in a random fashion. The results of such a comparison using the data on bursts obtained from meter No. 0 for the period September 1 to November 17, 1934, are given in Table III.

Reference to a table of chi-square values[18] shows that the probability of departure from the theoretical distribution by an amount equal to or greater than that indicated by $\chi^2=5.89$ is between 0.65 and 0.70 for any random sample. This would indicate strongly that the assumption of random distribution of bursts is correct. A similar analysis carried out for the bursts occurring on five meters during March leads to the same conclusion, which is in agreement with previous results of the Montgomerys.[19]

Burst frequency *vs.* size

The chief importance of a study of burst frequency as a function of magnitude lies in the possibility of learning something about the nature of the burst mechanism. The reality of the burst as a cosmic-ray phenomenon has been questioned by Millikan, Anderson and Neher[20] and defended apparently successfully by Bennett[21] and Hoffman.[22]

If we accept the reality of the phenomenon then we may logically inquire as to its nature. Although several investigators including Hoffman[22] feel certain that a burst is not of the nature of a large "shower," there seem to be enough points of similarity between the two phenomena to justify the opinion that some of the smaller bursts at least must be showers. For example, cloud chamber observations show that the number of particles in a single shower may on occasion be quite large, enough so that the resultant ionization in a high pressure chamber would be comparable with that due to a small burst. Whether all bursts are of this nature is an open question, although it would seem that the frequency with which they occur is much too small to be consistent with observed shower frequencies. However, this objection becomes of less importance as a distinction between showers and bursts in view of the results of Bennett, Brown and Rahmel[17] showing that the relation between burst frequency and magnitude can be expressed as a series of exponentials, because one may reasonably suppose that for the bursts still smaller than those recorded as such the slope of the semi-log curve of frequency *vs.* size would become increasingly steep so that the extrapolation to fewer and fewer ionizing particles would give a more favorable comparison with cloud chamber data. When it is considered that counter-controlled expansion chambers probably give a ratio of multiples to singles which is too high, the picture is still more favorable. However,

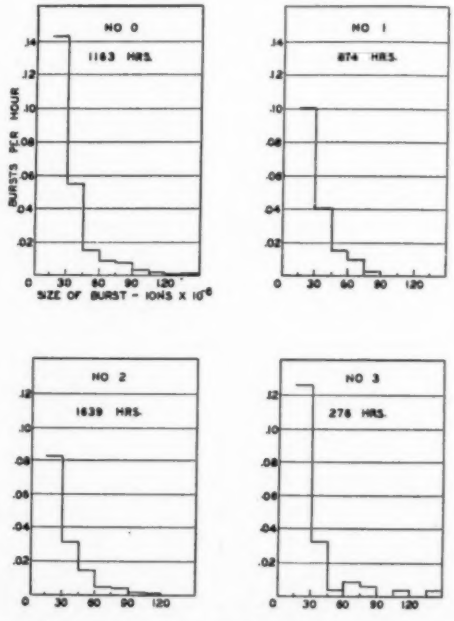

FIG. 8. Burst frequency as a function of magnitude.

[18] T. C. Fry, *Probability and Its Engineering Uses.*
[19] C. G. and D. D. Montgomery, Phys. Rev. **44**, 779 (1933).
[20] R. A. Millikan, C. D. Anderson and H. V. Neher, Phys. Rev. **45**, 141 (1934).
[21] R. D. Bennett, Phys. Rev. **45**, 491 (1934).
[22] G. Hoffman, Int. Conf. on Nuclear Physics (London, 1934), p. 226.

if it should be demonstrated that there is a maximum in the curve of frequency *vs.* size, the extrapolation argument would no longer hold and it would become more evident that the burst is an independent phenomenon. As a matter of fact such a maximum has been reported by Hoffman,[22] at $3.8(10)^6$ ions for lead and $2(10)^6$ ions for aluminum, but the curves of C. G. and D. D. Montgomery[23] covering approximately the same range show no maximum. The reason for the difference in results is not clear.

The number of bursts observed in scaling the records from eight different cosmic-ray meters for a total of about 9000 meter hours during March–July 1935 is given for the separate instruments by the frequency polygons of Figs. 8 and 9. The meters were all located under a glass roof in a campus greenhouse and each was fully shielded with 12 cm of lead.

It will be noted that the bursts occurred considerably more frequently on some instruments than on others. Thus the highest total rate was observed on No. 0 at 0.238 per hour while No. 2 and No. 7 were about equally low at around 0.145 per hour. The total rate for all the other meters did not vary appreciably from 0.190 per hour.

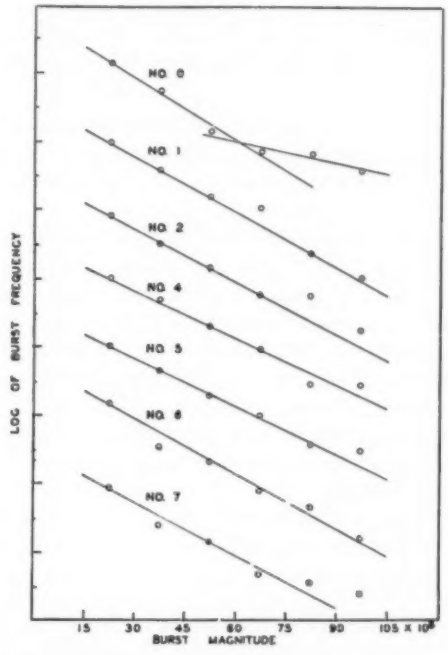

FIG. 10. Exponential relationship between burst frequency and size.

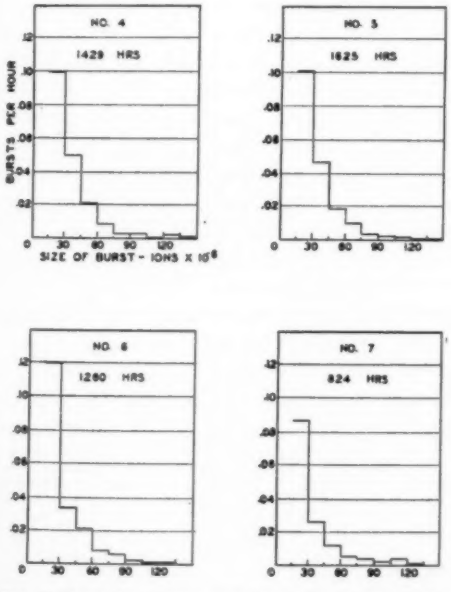

FIG. 9. Burst frequency as a function of magnitude.

[23] C. G. and D. D. Montgomery, Phys. Rev. **47**, 429 (1935).

If one plots the logarithm of frequency against burst magnitude the curves of Fig. 10 are obtained. Here for convenience the burst magnitude has been taken as the midpoint of the various size groups. In order to separate the curves the ordinates for each have been shifted a full unit with respect to the one above and below.

For the most part, the points for each meter fall on or near a single straight line although in the case of No. 0 a better fit is apparently obtained by using two intersecting straight lines. However, the position of the points in the two largest size groups is subject to considerable uncertainty because it is obviously impossible to say very much about the frequency of an event which occurs less than five times in more than 1000 hours unless the observations extend over a much longer period. Taking, then, the single exponential as giving the best representation of the data, the constant F_0 and a in the relation

$$F = F_0 e^{-aS}$$

TABLE IV. *Coefficients relating burst frequency to size.*

Meter No.	0	1	2	4	5	6	7
F_0	0.66	0.44	0.29	0.33	0.33	0.45	0.36
a	.067	.064	.057	.052	.051	.058	.065

are as shown in Table IV. F is the frequency in bursts per hour and S is the midpoint of a size group having a spread of $15(10)^6$ ions. S is expressed in millions of ions

It must be kept in mind that these coefficients are a function of the size group used in the analysis. If we had used a grouping smaller than $15(10)^6$ ions the frequency for each group would have been less. Therefore one cannot obtain the total burst frequency by integrating the exponential expression with respect to the burst magnitude. Neither is it permissible to interpret F_0 as the extrapolated frequency for very small bursts. With the grouping used we can extrapolate only to magnitude $7.5(10)^6$ ions at which point the calculated burst frequency (that is, the frequency of all bursts up to $15(10)^6$ ions) comes out to be 0.40 per hour or about 0.053 percent of the total ionization. Obviously the size group is much too large to attach any particular significance to this value but no smaller grouping was chosen because $15(10)^6$ ions represents one scale division on the record and this is therefore a convenient size of unit. The value 0.053 percent as the total contribution of all bursts up to about two hundred ionizing particles ($7.44(10)^4$ ions per particle) is of course much too small in view of cloud chamber observations on showers; but from the way this value was obtained it is not to be expected that it would have any meaning for very small bursts involving only a few ionizing particles.

The results of two independent investigations on much smaller bursts have been reported recently. C. G. and D. D. Montgomery[23] using a 50-liter ionization chamber filled with 14.5 atmospheres of nitrogen find about the same sort of size-frequency distribution for bursts ranging from $1.5(10)^6$ ions to $7.5(10)^6$ ions as described above for much larger bursts, while Hoffman reporting on some of Messerschmidt's work at the 1934 London International Conference on Physics shows that a maximum frequency is reached at $3.8(10)^6$ ions for lead and that below this size the bursts become decidedly less frequent. The charge sensitivity used was the same in both of these investigations, but no details are given on the ionization chamber used by Messerschmidt, so that it is not possible to state definitely that the range of burst sizes (as regards the number of ionizing particles) was the same in both cases although this seems likely.

If we take the results of the Montgomerys on burst frequency at Swarthmore, an interesting extension of our large burst data to the region below $15(10)^6$ ions is possible. The Dow metal ionization chamber used at Swarthmore had a volume $2\frac{1}{2}$ times as great as ours and was filled with 14.5 atmospheres of nitrogen which, according to Hopfield's curves[24] and some additional data of our own, has an ionization about 1/5 as great as that in 50 atmospheres of pure argon. Thus a burst of a given size in the Dow metal sphere corresponds to one twice as large in the argon-filled chamber, that is, the same number of ionizing particles would be involved in the two cases. At Swarthmore the observed number of bursts having a magnitude greater than $7.5(10)^6$ ions was 0.10 per hour as compared with 0.14–0.24 obtained on our instruments for all bursts larger than $15(10)^6$ ions. If one plots the Montgomery data, log frequency *vs.* magnitude, and extrapolates back to the size group $0-0.5\times10^6$ ions an estimated frequency of 13 per hour is obtained. For our ionization chamber this size group would include all bursts under 10^6 ions; that is, all those involving up to about 14 ionizing particles. Thus it appears that while the frequency of very small bursts is considerably less than the apparent frequency of showers estimated from cloud chamber and counter observations, it is nevertheless sufficiently high to make an appreciable contribution to the shower data and to this extent at least there seems to be little reason for making a distinction between the two.

In the region of larger bursts the situation may be different. During several months of operating from four to eight cosmic-ray meters here in Chicago, a few bursts were observed involving as many as $4(10)^8$ ion pairs, requiring for their production something like 5000 ionizing particles and a total energy of about $1.3(10)^{10}$ electron volts. Still larger bursts were observed by Bennett, Brown and Rahmel on Mt. Evans.

[24] J. J. Hopfield, Phys. Rev. **43**, 675 (1933).

Probably the simplest picture of the mechanism of such a burst is that of an incoming high energy primary transferring its energy in one event into a gigantic photon spray the components of which spend most or all of their energy in the production of positron-negative pairs which are the actual ionizing particles. The occasion for the event is assumed to be an interaction between the cosmic-ray particle and an atomic nucleus in the material surrounding the ionization chamber, and it may be that the nucleus itself makes some contribution to the burst, although it is of course out of the question to suppose that all of the ionizing particles come from the nucleus.

Barometer effect of bursts

It has been found by two different investigators[17, 23] that the frequency of bursts increases with altitude considerably more rapidly than does the total cosmic-ray intensity. Similar conclusions have been reached in regard to showers[25, 26, 27] although Gilbert[28] found the showers and vertical intensity to increase with altitude in about the same proportion. In general, then, one would expect a barometer effect for showers and bursts which would be larger than for the vertical or total intensity. This has been demonstrated experimentally for showers by Stevenson and Johnson[29] who found a barometer effect corresponding to an absorption coefficient of 0.41 per meter of water for out-of-line counter coincidences as compared with 0.28 for in-line coincidences. A less definite barometer effect for small bursts was observed by the Montgomerys[23] amounting to about 0.5 percent per mm of mercury, but an effect ten times this large has been reported by Steinke, Gastell and Nie.[30] No effect at all, however, was found for bursts larger than $7(10)^6$ ions.

An analysis of nearly seven hundred bursts larger than $15(10)^6$ ions during March on five different cosmic-ray meters at Chicago reveals no evidence for a barometer effect, although the consistency of the data is not sufficient to rule out the possibility of a rather large effect. The results are summarized in Table V. A calculation of the correlation coefficient between the two variables leads to a value of 0.056 which is, for practical purposes, zero. The average burst frequency was 0.22 ± 0.0085 per hr. if one assumes zero correlation. However, it is more informative to note that the band within which the frequencies fell half of the time was about 0.045 unit wide or about 20 percent of the average frequency. Since the total range of pressure covered was 25 mm Hg, it may be said that the results are not inconsistent with a barometer effect as large as about 8 percent per cm Hg. It seems certain, however, that the effect can be no larger than this.

TABLE V. *Total burst frequency vs. atmospheric pressure.*

Barometer (mm Hg)	Scale Div.	Total Bursts	Bursts per hr.	Barometer (mm Hg)	Scale Div.	Total Bursts	Bursts per hr.
735	18	14	0.21	749	34	17	0.21
	19	8	.12		35	32	.24
	20	18	.19		36	25	.24
	21	3	.08		37	31	.24
	22	18	.46		38	26	.26
	23	27	.25		39	18	.28
	24	19	.20		40	14	.26
741	25	18	.22		41	10	.29
	26	22	.25		42	11	.22
	27	44	.22		43	9	.18
	28	55	.22		44	9	.21
	29	72	.21		45	16	.19
	30	44	.21		46	15	.25
	31	28	.16	759	47	5	.13
	32	38	.20		48	3	.10
	33	20	.33				

All of the meters were shielded with 12 cm of lead during these tests. In view of the known high absorption coefficient of shower producing radiation and short range of the shower particles it seems likely that most of the bursts registered on this apparatus are due to the higher energy particles and occur within a zone only a few centimeters wide in the immediate neighborhood of the bomb. In the Montgomery apparatus the thickness of lead above the chamber was small enough that one might expect a majority of the bursts to be due to tertiaries produced by air secondaries. They would therefore show a barometer effect in keeping with the known high

[25] T. H. Johnson, Phys. Rev. **45**, 569 (1934); **47**, 318 (1935).
[26] B. Rossi and S. de Benedetti, Ricerca Scient. (5) **1**, 594 (1934).
[27] P. Auger and L. Leprince-Ringuet, Comptes rendus **199**, 785 (1934).
[28] C. W. Gilbert, Proc. Roy. Soc. **A144**, 559 (1934).
[29] E. C. Stevenson and T. H. Johnson, Phys. Rev. **47**, 578 (1935).
[30] E. G. Steinke, H. Gastell and H. Nie, Naturwiss. **51**, 898 (1933).

absorption coefficient of the shower producing radiation. However, for much greater thicknesses of lead it seems necessary to adopt the view that the showers occasioned by the air secondaries do not reach the ionization chamber and that the burst-producing radiation originates in the lead, probably as a result of a close nuclear approach of a high energy primary. On this view any barometer effect would have to be due to the air absorption of the primary particles and should therefore be much smaller than for bursts involving air secondaries.

Burst frequency as a function of shield thickness

The shield of 17 cm of lead shot ordinarily used on the meters described above is apparently thick enough to absorb a considerable portion of the burst-producing radiation and resultant burst particles. Evidence for this is a very considerable, at least twofold, increase in burst frequency which ensues when a few hundred pounds of the shot is drained out.[31] The optimum shield thickness to give maximum burst frequency has not yet been determined but probably lies in the neighborhood of five cm of lead. This corresponds to a similar situation in the case of showers, where the frequency increases with additional top shielding up to about 2 cm of lead and then falls off for greater thicknesses. The size of the bursts seems not to be greatly affected by reducing the shield thickness.

In conclusion the writer wishes to acknowledge his great indebtedness to Professor A. H. Compton for providing the opportunity of making this investigation and also for numerous suggestive discussions during its progress. Thanks are also due to the Carnegie Institution of Washington through whom the necessary funds were provided, and to Dr. J. A. Fleming, Director of the Institution, who emphasized the desirability of such a comparative study. Practically all of the statistical calculations presented here and many more that have not been discussed were carried out by Mrs. Ardis T. Monk with the help of J. O. Pyle, Jr., and James Geary. Needless to say, this assistance has been invaluable from the standpoint of expediting the investigation.

[31] R. L. Doan, Phys. Rev. **48**, 470 (1935).

JANUARY 15, 1936 PHYSICAL REVIEW VOLUME 49

Theory of the Effect of Temperature on the Reflection of X-Rays by Crystals

II. Anisotropic Crystals

CLARENCE ZENER,* *Wayman Crow Hall of Physics, Washington University, St. Louis*

(Received November 29, 1935)

In anisotropic crystals the temperature factor for the reflection of x-rays is a function of the orientation of the reflection plane. The general case of anisotropic metals is here treated by an extension of a simple method recently discussed in this journal. The complete solution is found for metals with hexagonal symmetry. The temperature factor is generally written as e^{-M}. The constant M is explicitly calculated for Zn and Cd (hexagonal symmetry). It is found that for these two metals M is 1.80, 1.73, respectively, as large for the reflection plane normal to the principal axis as for reflection planes parallel to the principal axis.

§1. INTRODUCTION

IN view of the approximations made in the Debye theory of specific heats, its success for isotropic as well as for anisotropic crystals is surprising. An explanation may lie in the relative insensitiveness of the specific heat to the assumptions made about the lattice vibrations. In particular, the specific heat is a scalar quantity, and so does not directly reflect the anisotropic vibrations of the atoms in anisotropic metals. This anisotropy in vibrations may, however, be detected experimentally by a study of the temperature dependence of the atomic

* The author was aided in part by a grant from the Rockefeller Foundation to Washington University for research in science.

structure factor in the reflection of x-rays. Thus the mean square displacement μ of an atom along a definite direction, parallel say to the unit vector $\mathbf{n}$, is related by the formula[1]

$$M = 8\pi^2 \mu \sin^2 \theta / \lambda^2 \tag{1}$$

to the temperature factor e^{-M} for the reflection of x-rays from planes normal to $\mathbf{n}$.

The purpose of this paper is to show how the mean square displacement μ depends upon direction in single crystals of metals not having cubic symmetry.

Assuming only that the amplitudes of vibration are sufficiently small so that the potential energy of the metal may be regarded as a quadratic function of the displacement, one obtains[2]

$$\mu(\mathbf{n}) = \frac{h}{4\pi^2 M} \sum_{j,\,\mathbf{k}} \gamma^2(j, \mathbf{k}) \left\{ \frac{1/\nu}{e^{h\nu/kT} - 1} + \frac{1}{2\nu} \right\}. \tag{2}$$

The vector $\mathbf{k}$ specifies a wave having a direction of propagation along the direction of $\mathbf{k}$, and whose wave-length is $2\pi/k$. The letter j specifies one of the three waves associated with each $\mathbf{k}$, the three waves corresponding to one longitudinal and two transverse waves in isotropic solids. $\nu(j, \mathbf{k})$ is the classical frequency of the wave $(j, \mathbf{k})$. $\gamma^2(j, \mathbf{k})$ is the square of the direction cosine between $\mathbf{n}$ and the direction of vibration of the wave $(j, \mathbf{k})$. M is the mass of the crystal. The summation is over all waves in the crystal.

In isotropic metals μ is the same for all directions $\mathbf{n}$. In anisotropic metals μ is a quadratic function of the components of $\mathbf{n}$, l, m, n. This is readily seen when we expand

$$\gamma_{j,\,\mathbf{k}} = l l_{j\mathbf{k}}' + m m_{j\mathbf{k}}' + n n_{j\mathbf{k}}',$$

where $l_{j\mathbf{k}}'$, $m_{j\mathbf{k}}'$, $n_{j\mathbf{k}}'$ are the direction cosines of the direction of vibration of the wave $(j, \mathbf{k})$. When the coordinate axes are chosen to lie along the principal axes of the crystal, μ will have the form

$$\mu(\mathbf{n}) = \mu_x l^2 + \mu_y m^2 + \mu_z n^2. \tag{3}$$

[1] Waller and James, Proc. Roy. Soc. **A117**, 214 (1927); Zener and Jauncey, Phys. Rev. **49**, 17 (1936) have given a simple and general proof of this formula.

[2] Zener and Jauncey, reference 1. The derivation of this formula given in this reference explicitly assumed the Debye model of a solid. However, one need only assume that the motion of an atom may be represented as the superposition of linearly polarized plane elastic waves.

This equation shows directly that μ has rotational symmetry in metals with a three-, four-, or six-fold axis of symmetry. Further, it shows that $\mu(\mathbf{n})$ is completely determined by its three values for $\mathbf{n}$ pointing along the three principal axes. Hence the mean square displacement μ is completely determined by the experimental determination of the temperature factor for the three (sometimes only two) reflection planes normal to the principal axes.

When evaluating the summation in (2), we shall assume that the velocity of the waves is independent of their wave-length. It is well known that this is incorrect for the shortest wave-lengths. However, it is just these short waves with high frequency which contribute least to the sum (2).

If n is the number of atoms per unit volume, and V is the volume of the solid, the total number of terms included in the summation (2) must be $3nV$. In the customary form of the Debye theory of specific heat this number is obtained, for an analogous summation, by excluding all waves with a frequency greater than a critical frequency ν_m. In this paper the correct number will be obtained by excluding all waves with wave-length shorter than a critical value $\lambda(\boldsymbol{\sigma})$, where $\boldsymbol{\sigma}$ is a unit vector in the direction of propagation, i.e., it is $\mathbf{k}/k$. As indicated, this value will in general be a function of the direction of propagation. Only in this manner can we associate, for short as well as for long waves, three directions of vibration for each $\mathbf{k}$.

The summation over $\mathbf{k}$ in (2) may now be converted into an integral. If $C(j, \boldsymbol{\sigma})$ is the velocity of a "j" wave with the direction of propagation $\boldsymbol{\sigma}$, the number of "j" waves with frequency between ν and $\nu + d\nu$, and having $\boldsymbol{\sigma}$ within the solid angle $d\Omega$, is $VC^{-3}(j, \boldsymbol{\sigma})\nu^2 d\nu d\Omega$.[3] Introducing the notation $\xi = h\nu/kT$, $x(j, \boldsymbol{\sigma}) = h\nu_m(j, \boldsymbol{\sigma})/kT = \Theta(j, \boldsymbol{\sigma})/T$, with $\nu_m(j, \boldsymbol{\sigma}) = C(j, \boldsymbol{\sigma})/\lambda_0(\boldsymbol{\sigma})$, we obtain

$$\mu = \frac{kTV}{4\pi^2 M} \sum_j \int \frac{\gamma^2(j, \boldsymbol{\sigma})}{C^2(j, \boldsymbol{\sigma})\lambda_0(\boldsymbol{\sigma})} \{\Phi(x) + x/4\} d\Omega, \tag{4}$$

where

$$\Phi(x) = \frac{1}{x} \int_0^x \frac{\xi}{e^\xi - 1} d\xi.$$

[3] Jeans, *The Dynamical Theory of Gases* (The University Press, Cambridge, 1925), p. 354.

TABLE I. *Quantization factor.*

x	$\Phi(x)+x/4$	x	$\Phi(x)+x/4$
0.0	1.000	1.2	1.040
0.2	1.001	1.4	1.054
0.4	1.004	1.6	1.069
0.6	1.010	1.8	1.087
0.8	1.018	2.0	1.107
1.0	1.028	2.5	1.164

The factor $\{\Phi(x)+x/4\}$ represents the effect of quantization. From an inspection of Table I, we see that the quantization effect is only of importance when t is considerably less than the maximum $\Theta(j, \sigma)$.

In order that the correct number of waves be included, $\lambda_0(\sigma)$ must satisfy

$$\int\int_{\lambda_0}^{\infty} \lambda^{-4} d\lambda d\Omega = n, \quad \text{i.e.,} \quad \int \lambda_0^{-3}(\sigma) d\Omega = 3n. \tag{5}$$

If the quantization factor differs inappreciably from unity, as in most metals at room temperature, and if $\lambda_0(\sigma)$ is regarded as independent of σ, we obtain

$$\mu(\mathbf{n}) = \frac{3kT}{4\pi^2 m_a} \sum_j \int \frac{\gamma^2(j, \sigma)}{v_0^2(j, \sigma)} \frac{d\Omega}{4\pi}, \tag{6}$$

where $m_a = M/(nV)$, $v_0(j, \sigma) = C(j, \sigma)/\lambda_0$, with $\lambda_0 = (4\pi/3n)^{\frac{1}{3}}$.

In order to evaluate $\mu(\mathbf{n})$, as given in (4), we must know both the velocity and the direction of vibration associated with each "j" wave for all directions of propagation σ. In this paper we first study in detail the waves in a two-dimensional medium (§2). This analysis is given for two reasons. Firstly, the principles involved are identical with the principles for the three-dimensional case, while the analysis is much shorter. Secondly, the problem for crystals with hexagonal symmetry is reducible to the two-dimensional problem. The formal problem of determining the wave velocities and the directions of vibration in a three-dimensional medium[4] is then briefly reviewed (§3) and the solution given for metals with hexagonal symmetry. Finally, the numerical results are given (§4) for all the metals with hexagonal symmetry whose elastic constants have been determined, namely, Zn and Cd.

§2. WAVES IN TWO-DIMENSIONAL MEDIA

Let U, V be the x, y components of the displacement vector of the medium, X_x, Y_y, $Y_x = X_y$ be the stress components, and e_{xx}, e_{yy}, e_{xy} be the strain components. The equations of motion are then[5]

$$\begin{aligned} \delta X_x/\delta x + \delta Y_x/\delta y &= \rho \ddot{U}, \\ \delta Y_x/\delta x + \delta Y_y/\delta y &= \rho \ddot{V}. \end{aligned} \tag{7}$$

The stress components are linear functions of the strain components, i.e.,

$$\begin{aligned} X_x &= c_{11}e_{xx} + c_{12}e_{yy} + c_{13}e_{xy}, \\ Y_y &= c_{12}e_{xx} + c_{22}e_{yy} + c_{23}e_{xy}, \\ Y_x &= c_{13}e_{xx} + c_{23}e_{yy} + c_{33}e_{xy}. \end{aligned} \tag{8}$$

The strain components, in turn, may be expressed in terms of the displacement components by means of the equations

$$e_{xx} = \frac{\delta U}{\delta x}, \quad e_{yy} = \frac{\delta V}{\delta y}, \quad e_{xy} = \frac{\delta U}{\delta y} + \frac{\delta V}{\delta x}. \tag{9}$$

By means of (8) and (9) we may transform (7) into two homogeneous partial differential equations in U and V. If we try as a solution a linearly polarized plane wave, see Fig. 1,

$$(U, V) = (a, b) e^{i\omega(t-(lx+my)/c)}, \quad l^2+m^2 = 1,$$

these two differential equations reduce to

$$\begin{aligned} &\{l^2c_{11} + 2lmc_{12} + m^2c_{33}\}a \\ &\quad + \{lm(c_{12}+c_{33}) + l^2c_{13} + m^2c_{23}\}b = \rho c^2 a, \\ &\{lm(c_{12}+c_{33}) + l^2c_{13} + m^2c_{23}\}a \\ &\quad + \{m^2c_{22} + 2lmc_{23} + l^2c_{33}\}b = \rho c^2 b. \end{aligned} \tag{10}$$

Let c_l and c_t denote the two values of c for which Eqs. (10) have a nontrivial solution, and let c_l be the larger of the two. Further let the corresponding solutions be (a_l, b_l) and (a_t, b_t). The velocities and the corresponding solutions may readily be found in two extreme cases. When the medium is isotropic ($c_{11} = c_{22}$, $c_{12} = c_{33} = 0$, $2c_{33} = c_{11} - c_{12}$), c_l and c_t are independent of

[4] The theory has been presented in an elegant manner by Kelvin, *Baltimore Lectures* (The University Press, Cambridge, 1904), Lecture XI.

[5] Love, *The Mathematical Theory of Elasticity* (The University Press, Cambridge, 1920), p. 83. The notation adopted in this paper is that used by Love.

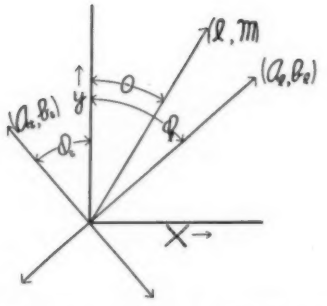

FIG. 1. Vibration directions in anisotropic media. The vector (l, m) is parallel to the direction of propagation. The vectors (a_l, b_l) and (a_t, b_t) are along the directions of vibration.

the direction of propagation, the vector (a_l, b_l) is parallel to the direction of propagation, while the vector (a_t, b_t) is perpendicular to this direction. On the other hand, in the highly anisotropic case $c_{12}=c_{13}=c_{23}=c_{33}=0$, c_l^2 and c_t^2 form the upper and lower branches, respectively, of two intersecting straight lines when plotted as functions of l^2. One of the vectors (a_l, b_l), (a_t, b_t) is parallel to the x axis, one to the y axis. They suddenly interchange directions when $c_l=c_t$, as in Fig. 3. The properties of an actual anisotropic medium will be intermediate between those of these two extreme cases. The interesting case $c_{22}\ll c_{11}$ is illustrated in Fig. 4. c_l^2 and c_t^2 no longer coincide at a critical point, c_l^2 retains a marked variation with l^2, while c_t^2 varies only slightly, being the same for $l=0$ as for $l=1$. The vectors (a_l, b_l), (a_t, b_t) change gradually, as for the case of isotropy, but the component of (a_l, b_l) along the axis of least compressibility, here the x axis, is larger on the average than its component along the axis of greatest compressibility.

This apparent preference of (a_l, b_l) for the direction of least compressibility, so marked in the second limiting case of Fig. 3, may be best understood when Eqs. (10) are put into a variational form. Let us write these equations in the form

$$\lambda_{11}a+\lambda_{12}b=\rho c^2 a, \quad \lambda_{12}a+\lambda_{22}b=\rho c^2 b. \quad (11)$$

Multiplying the first equation by a, the second by b, and adding, we obtain

$$\rho c^2=(\lambda_{11}a^2+2\lambda_{12}ab+\lambda_{22}b^2)/(a^2+b^2). \quad (12)$$

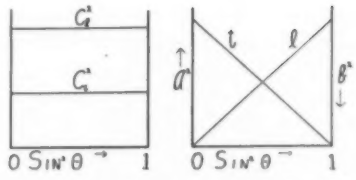

FIG. 2. Isotropic medium. a_l, b_l are the x, y components of the vibration associated with c_l. a_t, b_t are the x, y components of the vibration associated with c_t. c_l is defined as the larger, c_t as the smaller, of the two velocities.

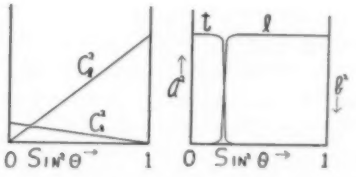

FIG. 3. Highly anisotropic medium. Fig. 2 is reproduced for a medium whose compressibility is much greater along the y axis than along the x axis.

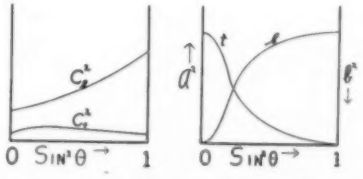

FIG. 4. Moderately anisotropic medium. Fig. 2 is reproduced for a medium which is only slightly anisotropic.

We now regard the left-hand side of this equation as a function of a and b. Eqs. (11) are then equivalent to the statement that c^2, as given by (12), is an extremum. Now the compressional waves have the greatest velocity when the direction of propagation lies along the axis of least compressibility. It is thus evident that when the direction of propagation (l, m) is not along the axis of least compressibility, then c^2, as given by (12), will have its maximum for a direction of (a, b) between (l, m) and this axis.

In the following section we shall need analytic expressions for c_l, c_t and the corresponding solutions of (11). These velocities are given by

$$\rho c_l^2=\frac{\lambda_{11}+\lambda_{22}}{2}+\left\{\left(\frac{\lambda_{11}-\lambda_{22}}{2}\right)^2+\lambda_{12}^2\right\}^{\frac{1}{2}}, \quad (13a)$$

$$\rho c_t^2=\frac{\lambda_{11}+\lambda_{22}}{2}-\left\{\left(\frac{\lambda_{11}-\lambda_{22}}{2}\right)^2+\lambda_{12}^2\right\}^{\frac{1}{2}}. \quad (13b)$$

Since the two solutions (a_l, b_l), (a_t, b_t) are orthogonal, $a_l a_t + b_l b_t = 0$, the normalized solutions may be written in the form

$$(a_l, b_l) = (\cos\varphi, \sin\varphi), \quad (a_t, b_t) = (-\sin\varphi, \cos\varphi).$$

The angle φ, Fig. 1, is given by

$$\varphi = \tfrac{1}{2}\tan^{-1}(2\lambda_{12}/(\lambda_{11}-\lambda_{12})). \tag{14}$$

§3. Waves in Three-Dimensional Media

The method of calculating the velocity and vibration directions of linearly polarized plane waves in a three-dimensional solid is a trivial extension of the method for a two-dimensional solid. This was discussed in the preceding paragraph. We need only give the results for the three-dimensional solid.

Let us consider a plane wave whose direction of propagation has the direction cosines (l, m, n) with respect to the x, y, z axes. The direction cosines α, β, γ of the vibration direction of this wave, as well as the velocity c of this wave, must satisfy the set of equations

$$\begin{aligned} (A_{11}-\rho c^2)\alpha + A_{12}\beta + A_{13}\gamma &= 0, \\ A_{12}\alpha + (A_{22}-\rho c^2)\beta + A_{23}\gamma &= 0, \\ A_{13}\alpha + A_{23}\beta + (A_{33}-\rho c^2)\gamma &= 0. \end{aligned} \tag{15}$$

The coefficients are given in terms of the elastic constants[4] by

$$\begin{aligned} A_{11} &= l^2c_{11} + m^2c_{66} + n^2c_{55} + 2lmc_{16} + 2mnc_{56} + 2nlc_{51}, \\ A_{12} &= l^2c_{16} + m^2c_{26} + n^2c_{45} + lm(c_{12}+c_{66}) \\ &\quad + mn(c_{25}+c_{46}) + nl(c_{14}+c_{56}), \\ A_{13} &= l^2c_{15} + m^2c_{46} + n^2c_{35} + lm(c_{14}+c_{56}) \\ &\quad + mn(c_{36}+c_{45}) + nl(c_{13}+c_{55}), \\ A_{22} &= l^2c_{66} + m^2c_{22} + n^2c_{44} + 2lmc_{26} + 2mnc_{24} + 2nlc_{46}, \\ A_{23} &= l^2c_{56} + m^2c_{24} + n^2c_{34} + lm(c_{25}+c_{46}) \\ &\quad + mn(c_{23}+c_{44}) + nl(c_{36}+c_{45}), \\ A_{33} &= l^2c_{55} + m^2c_{44} + n^2c_{33} + 2lmc_{45} + 2mnc_{34} + 2nlc_{35}. \end{aligned}$$

The exact determination of those values of c^2 for which Eqs. (15) have nontrivial solutions usually involves the solution of a cubic equation, namely, the equation obtained by equating to zero the determinant of the coefficients. There is one case of physical interest, other than the case of isotropy, where an analytical solution may be obtained for the allowed values of c^2 and for the corresponding sets of direction cosines (α, β, γ). This is the case of hexagonal symmetry about a principal axis. Here[6] the elastic constants satisfy the same conditions as in the case of rotational symmetry about a principal axis, namely, the following coefficients must vanish:

$$c_{16},\ c_{26},\ c_{36},\ c_{46},\ c_{56},\ c_{45},\ c_{14},\ c_{24},\ c_{15},\ c_{25},\ c_{34},\ c_{35}$$

and the following relations must hold,

$$c_{11}=c_{22}, \quad c_{13}=c_{23}, \quad c_{44}=c_{55}, \quad c_{66}=(1/2)(c_{11}-c_{12}).$$

An important simplification may now be introduced. Since in this case the elastic constants are invariant with respect to an arbitrary rotation about the principal axis, here the z axis, the x and y axes may be chosen in such a manner as to simplify Eqs. (15). The most apt choice of the x and y axes is to let one, say the x axis, be perpendicular to the direction of propagation, i.e., to set $l=0$. With this choice of axes, and using the simplification imposed by the hexagonal symmetry, we reduce the set of Eqs. (15) to the following:

$$\begin{aligned} \{m^2(c_{11}-c_{12})/2 + n^2c_{44} - \rho c^2\}\alpha &= 0, \\ (m^2c_{11} + n^2c_{44} - \rho c^2)\beta + mn(c_{12}+c_{44})\gamma &= 0, \\ mn(c_{13}+c_{44})\beta + (m^2c_{44} + n^2c_{33} - \rho c^2)\gamma &= 0. \end{aligned} \tag{16}$$

One solution is obvious, namely,

$$(\alpha_1, \beta_1, \gamma_1) = (1, 0, 0), \tag{17}$$

the correct value of c^2, say c_1^2, being given by

$$\rho c_1^2 = m^2(c_{11}-c_{12})/2 + n^2c_{44}. \tag{18}$$

This solution represents a pure transverse wave with its vibration in the plane of symmetry.

Since the second and third solutions must be orthogonal to the first, they are of the form $(0, \beta, \gamma)$. These solutions must thus satisfy the two equations

$$(\lambda_{11}-\rho c^2)\gamma + \lambda_{12}\beta = 0, \quad \lambda_{12}\gamma + (\lambda_{22}-\rho c^2)\beta = 0,$$

[6] Love, reference 5, p. 152.

where

$$\lambda_{11}=m^2c_{44}+n^2c_{33},\quad \lambda_{12}=mn(c_{13}+c_{44}),$$
$$\lambda_{22}=m^2c_{11}+n^2c_{44}. \tag{19}$$

These equations were studied in the preceding section (cf. Eqs. (11)). Let us denote the two values of c^2 for which nontrivial solutions exist by c_2^2 and c_3^2. These are then given by (13a) and (13b), respectively. The corresponding solutions are

$$(\alpha_2, \beta_2, \gamma_2)=(0, \sin\varphi, \cos\varphi),$$
$$(\alpha_3, \beta_3, \gamma_3)=(0, \cos\varphi, -\sin\varphi), \tag{20}$$

where φ is given by (14).

§4. Numerical Results for Zn and Cd

Since $\mu(\mathbf{n})$ has rotational symmetry for metals with hexagonal symmetry, we need explicitly calculate $\mu(\mathbf{n})$ with respect to only two directions for Zn and Cd (see Eq. (3)). This involves merely the evaluation of the integral in (4). Each term with $j=1$, 2, or 3 refers to one type of wave, i.e., to one solution of Eqs. (15). Since the lattice of Zn and Cd is only slightly distorted from an ideal close packed arrangement, λ_0 was taken to be independent of $\mathbf{n}$. Further, the quantization factor $\Phi(x)+x/4$ was found to have a negligible effect at or above room temperatures. Hence the simplified formula (6) was used.

The velocities $c(1, n)$, $c(2, n)$, $c(3, n)$ have been calculated by Grüneisen and Goens[7] by numerical solution of cubic equations. These calculations have been checked by the formulae (18), (13a) and (13b), and found to be correct. The corresponding sets of direction cosines are given by (17) and (20) in terms of an angle φ. This angle was calculated by Eqs. (14), (19) with the elastic constants found by Grüneisen and Goens. It is given in Table II.

Table II.

Θ (in degrees)	10	20	30	40	50	60	70	80	90
φ (in degrees)									
Zn	35.5	45.6	52.0	58.1	64.8	71.0	77.3	83.8	90
Cd	18.4	33.6	45.5	55.4	64.0	70.3	77.0	83.8	90

The integration in (6) was performed numerically. Expressed in terms of M, Eq. (1), the final results are:

$$\text{Zn}: M=1.1\times10^{-3}\{1.80\cos^2\Theta+\sin^2\Theta\}\times T(\sin\theta/\lambda)^2,$$

$$\text{Cd}: M=1.6\times10^{-3}\{1.73\cos^2\Theta+\sin^2\Theta\}\times T(\sin\theta/\lambda)^2,$$

where θ is the angle between $\mathbf{n}$ and the principal axis, and where λ is the wave-length of the incident x-rays expressed in Angstrom units.

[7] Grüneisen and Goens, Zeits. f. Physik **26**, 247 (1924), had occasion to calculate the wave velocities of the hexagonal crystals Zn and Cd. Not observing that Eqs. (15) can be reduced in these special cases, they resorted to a numerical solution, for each direction, of the cubic equation obtained from (15). Their cubic Eq. (4) contains in fact $q-c_{44}'$ (in their notation) as a factor.

X-Ray Studies of Crystals Vibrating Piezoelectrically

CARL V. BERTSCH,* *Physics Department, University of Michigan*

(Received September 5, 1935)

The original investigation has been extended by using both Laue patterns and regular reflection from the crystal surfaces. Much of the previous work was repeated and confirmed. Quartz was found to be more satisfactory for this work than Rochelle salt. A large increase of intensity in the Laue pattern was found for the fundamental of the low frequency mode of vibration with a Y-cut quartz crystal. The large increases found in previous work were due to the high frequency or "thickness" modes of vibration. The modes of vibration determined by the longer dimensions of the crystals gave an intensity increase for the case of regular reflection. It was shown that the negligible increase for the modes of vibration determined by the thickness of the crystals was not caused by an imperfect surface layer. In a complete survey made of a long X-cut crystal, a definite distinction was found between the regions of nodes and antinodes of motion. By direct polishing experiments, it was found that the intensity increases for the cases of regular reflection were due mainly to a reduction of secondary extinction. It is pointed out that in all cases these x-ray methods show a difference in the effect between the X-cut and Y-cut crystals for similar modes of vibration.

INTRODUCTION

IT was first shown by Fox and Carr[1] that a marked increase of the intensity in the Laue pattern of thin quartz crystals occurred when the crystals were vibrating piezoelectrically along the direction of the thickness of the plates. Similar results for thick crystals have been reported by other investigators.[2–6] They observed not only an increase of intensity in the Laue pattern, but also a filling in of the space between the double spots.

Fox and Cork[7] studied this effect further by using the regular x-ray reflection from the major surfaces of thin Y-cut[8] crystals that were vibrating along the direction of their Y axis. They found that this mode of vibration gave no increase of intensity in the reflected line. Colby and Harris[9] in a similar experiment examined the effect upon a line reflected from the middle of a long X-cut quartz bar that was vibrating at the fundamental and second harmonic of its low frequency mode in the direction of its Y axis. They found that the vibration produced a definite increase of intensity for the fundamental but little or no increase for the second harmonic. The middle of their crystal represented a node of motion for the fundamental and an antinode for the second harmonic.

In the case of Laue patterns obtained from quartz crystals, when vibrating at their low frequency modes, several observers[3, 5, 10] have reported little or no intensity increase for the vibration along the Y axis of X-cut crystals. Similar effects have also been reported for the vibration along the Z axis of X-cut crystals.[5]

Some of the work in this investigation has been similar to that of the other observers. The results of these experiments are in agreement with those which have been previously reported. For the vibration determined by the thickness of the crystals, however, more emphasis should be given to the difference in the effect upon the Laue pattern between the thick X-cut and Y-cut crystals. The double spots in the pattern obtained with the thick X-cut crystal were bridged over by the vibration, while this effect was slight for the pattern obtained with the Y-cut crystal. It seems that the vibration made it possible for the interior planes of the X-cut crystal to contribute to the intensity of the spot.

* Now at Western College, Oxford, Ohio.

[1] G. W. Fox and P. H. Carr, Phys. Rev. **37**, 1622 (1931).

[2] S. Nishikawa, Y. Sakisaka and I. Sumoto, Phys. Rev. **38**, 1078 (1931).

[3] C. S. Barrett and C. E. Howe, Phys. Rev. **39**, 889 (1932).

[4] J. M. Cork, Phys. Rev. **42**, 749 (1932).

[5] S. Nishikawa, Y. Sakisaka and I. Sumoto, Sci. Pap. Inst. Phys. and Chem. Res. **25**, 20 (1934); Phys. Rev. **43**, 363 (1933).

[6] G. W. Fox and W. A. Fraser, Phys. Rev. **47**, 899 (1935).

[7] G. W. Fox and J. M. Cork, Phys. Rev. **38**, 1420 (1931).

[8] The terminology used here is in accordance with that suggested by W. G. Cady, Proc. I. R. E. **18**, 2136 (1930). Diagrams of these cuts are also shown in reference 1, in which the X and Y-cuts are referred to as the Curie and 30-degree cuts, respectively.

[9] M. Y. Colby and S. Harris, Phys. Rev. **46**, 445 (1934).

[10] M. Y. Colby and S. Harris, Phys. Rev. **43**, 562 (1933).

On the other hand, the large increase of intensity found for the Y-cut crystal seemed to come from an increased efficiency of the planes which had been reflecting in the nonvibrating case, instead of contributions from additional planes.

The work which is to be reported here represents an extension of this investigation. This intensity effect upon the Laue pattern and a reflected line was studied by using additional modes of vibration. Also, the dependence of the intensity effect upon different parts of the crystals and upon different surface preparations of the crystals was investigated. This additional information gives a better understanding of the relation between this intensity effect and x-ray extinction and the influence upon these effects by certain modes of piezoelectric vibration.

Experimental

Both quartz and Rochelle salt crystals were used in this series of experiments. The quartz crystals were of the conventional X- and Y-cuts and were of various dimensions. Table I will give a brief description of the principal crystals and their fundamental frequencies, which were used in this investigation.

Table I. *Description of crystals.*

Crystal Plate	Cut	x (mm)	y (mm)	z (mm)	Direction of Electric Field	nX (kc)	nY (kc)	nZ† (kc)
A	Y	19.0	6.0	19.7	Y	138.2	371.3	——
B	X	4.2	25.5	27.5	X	638.3	92.3	124.0
C	X	4.0	43.0	16.0	X	——	63.2	——
D*	X	10.0	100.0	20.0	X	——	26.3	——

* This crystal was kindly loaned to the writer by Professor N. H. Williams.

† The terminology suggested by Cady, reference 8, is also used here. The expression nX means, simply, the fundamental frequency of the wave propagated approximately in the direction of the X axis, etc.

The crystals were maintained in vibration at one of their resonance frequencies by an adaptation of the circuit described by Wright and Stuart.[11] The plate voltages were varied from 220 to 500 volts.

The Laue pictures were taken by using the radiation from the tungsten target of a standard 200-kv Coolidge tube, operating at 100 kv and 2 milliamperes. The exposure times were varied from 7 to 15 hours, depending upon the thickness of the crystal. Two cameras were arranged to receive the radiation from the tube, so that it was possible to conduct two experiments simultaneously. One of these cameras has been described elsewhere.[4] The other one was similar, except that it was possible to take the pictures at a crystal-to-plate distance of either 5 cm or 10 cm.

The reflection pictures were taken from an x-ray tube equipped with a tungsten target, with the $L\alpha_1$ and the $L\beta_1$ lines in the first and second orders. The Bragg spectrometer was the same as used by Fox and Cork.[7] Several comparisons between the lines taken with the crystal vibrating and at rest were made on the same plate by moving the plateholder. In order to facilitate the measurement of the intensity change, a line was usually taken at double the exposure time of the comparison lines with the crystal at rest. The exposure times were relatively short, being only 5, 10, and 20 minutes for each line on the plate. These lines were reflected from the planes parallel to the major surfaces of the crystals with but one exception, when the planes parallel to the end of a crystal were used. These planes are the $(2\bar{1}\bar{1}0)$ planes for the X-cut crystals, the $(10\bar{1}0)$ planes for the Y-cut crystals, and also the $(10\bar{1}0)$ planes for the planes parallel to the end of the large X-cut crystal.

Discussion of Results

A study was made to determine the effect upon the Laue pattern obtained from a Y-cut quartz crystal when vibrating at the fundamental of its low frequency mode of vibration along its X axis. This mode of vibration gave an intensity increase comparable to that found for the vibration determined by the thickness of the crystal. This was the only mode of vibration, besides that determined by the crystal thickness, which gave such a pronounced increase of intensity in its Laue pattern. Also, as will be seen later, it is the only case in which a marked effect was found both for the Laue pattern and a reflected line.

The fundamentals of the low frequency modes of vibration gave a marked increase of intensity for the case of regular reflection with all of the crystals used. Two such frequencies were available with the X-cut crystal, B, one of which was presumably determined by its dimension along the Y axis and the other by its dimension along

[11] R. B. Wright and D. M. Stuart, Bur. Standards J. Research **7**, 519 (RP356) (1931).

the Z axis. Typical microphotograms of this effect for the low frequency fundamental determined by the X axis with the Y-cut crystal and the Z axis with the X-cut crystal are shown in Fig. 1 A and B. This definite increase of intensity was unchanged by turning the crystals through 90 degrees for each of the three low frequency fundamentals used with the two crystals. It was also present at various positions on the crystal surfaces. This demonstrated that a "disturbed" area occupied most of the face of the crystal. This observation is in qualitative agreement with the many experiments of Osterberg.[12]

The removal of this intensity effect, due to the piezoelectric vibration, by polishing is illustrated in Fig. 1C. Not only was this effect removed; but it was again made to reappear by appropriately etching the surface. This process of destroying and again creating the intensity effect was done a number of times. It has been well established that polishing removes the extinction effects at the surface of a crystal. Since this polishing experiment was more correctly a fine grinding rather than a high polish, it is evident that the effect found in a reflected line is due to the reduction of the secondary extinction by the vibration. These observations are in accordance with the general agreement that this increase of intensity during vibration is due to a reduction of extinction effects within the crystal. It may be that a reduction of both the primary and secondary extinction occurs in the case of the Laue patterns.

The microphotometer curve in Fig. 1D shows the absence of an intensity effect in the reflected line from the face of the Y-cut crystal while vibrating at its high frequency fundamental in the direction of its thickness. The curve in Fig. 1E shows a small effect for the similar mode of vibration with the X-cut crystal; but it is not comparable to that shown for the low frequency fundamentals, as can be seen by again referring to Fig. 1B.

It has been suggested[3] that the presence of an imperfect surface layer was responsible for the null results of Fox and Cork. This hypothesis has been refuted by this experiment, in which both large and negligible results were obtained from the same crystal by changing the mode of vibration. Both of the crystals, B and C, show a definite effect for the vibrations determined by their longer dimensions, while they show little effect when the motion is determined by the thickness dimension. This is especially convincing, as it was possible to take such a set of

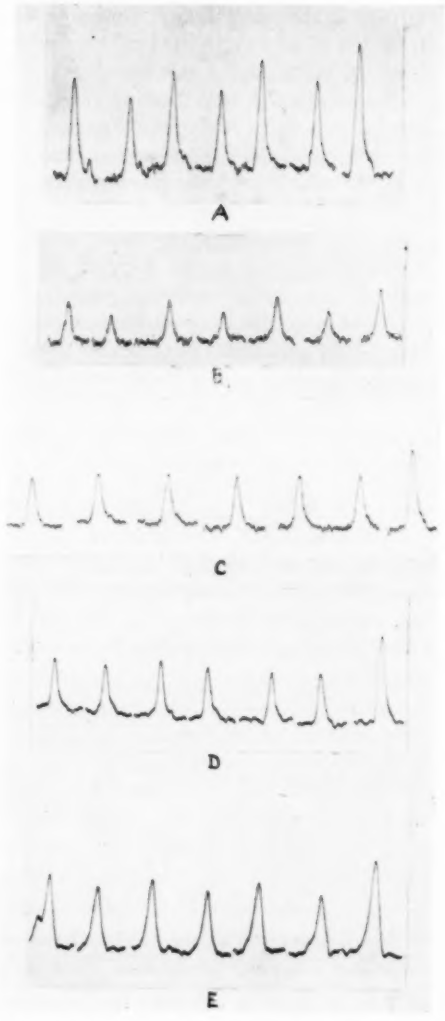

FIG. 1. Typical microphotograms of reflection pictures taken from rectangular quartz plates. Exposures: 10 min., 1st, 3rd, and 5th lines, vibrating; 2nd, 4th, and 6th lines, at rest; 20 min., 7th line, at rest. (A) X vibration of Y-cut crystal. (B) Z vibration of X-cut crystal. (C) Same as (B), except that the crystal surface was polished. (D) Y vibration of Y-cut crystal. (E) X vibration of X-cut crystal.

[12] H. Osterberg, Phys. Rev. **43**, 819 (1933); Rev. Sci. Inst. **5**, 183 (1933).

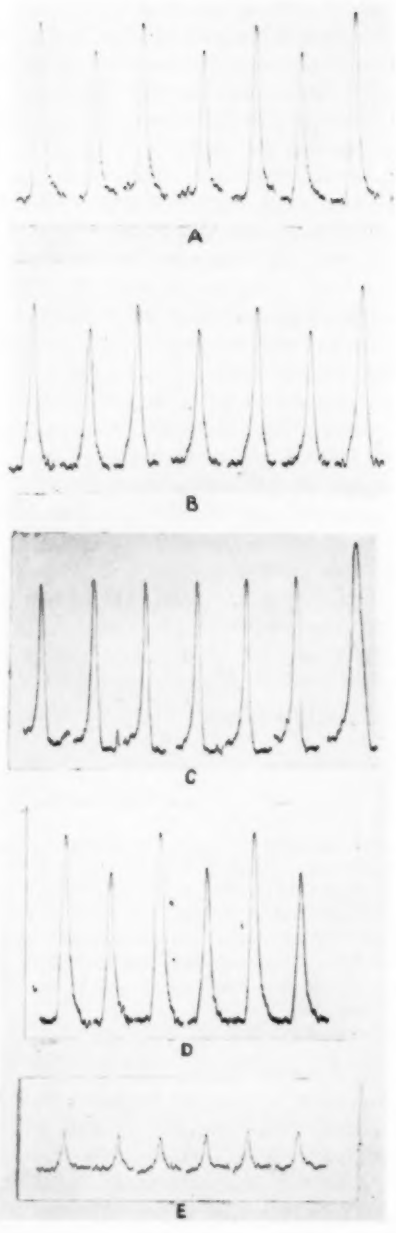

FIG. 2. Typical microphotograms of reflection pictures with the Y vibration of the 10 cm X-cut quartz bar. Exposures: 5 min., 1st, 3rd, and 5th lines, vibrating; 2nd, 4th, and 6th lines, at rest. 10 min., 7th line, at rest. (A) Middle position of bar, plate voltage 320. (B) 3 cm from middle of bar, plate voltage 320. (C) 4.5 cm from middle of bar, plate voltage 320. (D) Same as (B), except plate voltage 500. (E) An end of the bar, plate voltage 500.

pictures by making minor adjustments in the oscillatory circuit, without disturbing the crystal.

The negligible effect for the "thickness" mode of vibration in the reflection pictures is explained by the absence of change in lattice constant at the surface.[7, 9] The motion must also be of such a nature that no breaking up of the "mosaic blocks" occurs in a manner as to produce a change in the secondary extinction. The small effect in the Laue patterns for the low frequency fundamentals of the X-cut crystals may be due to the fact that a similar configuration exists within the region through which the x-ray beam is passing. Thus, there would be no changes in the crystal lattice or "mosaic blocks" which in turn would give a change in the extinction effects.

A complete survey of one face of the quartz bar, D, was made while it was vibrating at the fundamental of its low frequency mode of vibration in the direction of its length. By using a narrow electrode with a slit in its center for maintaining the vibration, nearly the entire face of the crystal was available for reflection. Comparison pictures using the second order $L\beta_1$ line of tungsten were taken at intervals of 5 mm along the Y axis. The entire crystal holder was moved for obtaining the different positions, so that the crystal was not changed relative to its vibrating system.

Assuming that the crystal motion can be represented as a standing wave with a node of motion at the center and antinodes at the ends, the maximum effect would be expected to occur at the node and a zero effect at the antinodes. Although this was found to be true, there was not a sharp nodal point. Instead, there was a nodal region and an antinodal region in which the effect was a maximum and a minimum. The nodal region extended over a space of about 6 cm in which the effect was a maximum. This nodal region was not quite symmetrical with the center of the crystal. There was only a space of about one cm in length at each end in which the effect could be said to be absent. These regions were studied further by using on the crystal a larger electrode which had only three windows, one at the center, two at a distance of 3 cm from the center, and a space at each of the ends. The microphotometer curves in Fig. 2 A, B, C, and D show a repetition of the former results.

A similar series of reflection pictures was taken with the same crystal by using the third harmonic of the same mode of vibration. For the third harmonic there was even less distinction between the expected nodal and antinodal regions than existed for the fundamental. Indeed, a "disturbed" area seemed to occupy the major portion of the reflecting surface of the crystal. On the basis of a large number of pictures, the effect was greater for the nodal than for the antinodal regions.

The microphotogram in Fig. 2E shows that no increase of intensity was present in the reflection pictures taken from the end of this long crystal, while it was vibrating at the fundamental of its low frequency mode of vibration. This result was expected since for this mode of vibration the planes parallel to the end of the crystal are in a configuration similar to that of the planes parallel to the face of the crystal for the mode of vibration determined by the thickness of the crystal.

An extensive study was made of a number of Rochelle salt crystals. The increases of intensity were small and could not be consistently repeated. This may be attributed to the difficulty of maintaining the equivalent of an etched surface for the reflection pictures; and for the Laue pictures, to the fact that most of the modes of vibration used were similar to those of quartz which showed little effect in their Laue pattern. Fox and Fraser[6] report an effect for Rochelle salt, but much smaller than for quartz.

The writer wishes to acknowledge his appreciation to Professor J. M. Cork of this department for suggesting the problem and for aid in interpreting the results. He is especially indebted to Professor N. H. Williams also of this department for the loans of equipment from his laboratory, and for valuable criticism and encouragement during this investigation.

JANUARY 15, 1936 PHYSICAL REVIEW VOLUME 49

Excitation Potential of $K\alpha_{3,4}$ Satellite Lines

LYMAN G. PARRATT,*† *Cornell University*

(Received November 4, 1935)

With a two-crystal vacuum spectrometer the curve of the intensity of $K\alpha$ satellite lines *vs.* voltage of the x-ray tube has been determined for the $K\alpha_{3,4}$ lines of titanium. For voltages greater than 11 kv the satellite intensity (total area of the $K\alpha_{3,4}$ satellite structure) relative to the intensity of the Ti $K\alpha_1$ lines is 2.21 percent; the ratio of peak intensities α_4/α_1 is 0.69 percent. The measured excitation potential of the Ti $K\alpha_{3,4}$ lines is 5450±100 volts, 500 volts in excess of the excitation potential of the $K\alpha_{1,2}$ lines. Assuming 0.85 as the screening constant of a missing K electron on an L electron, one calculates that the voltage required to produce a state of KL_{III} ionization in the titanium atom is 5455 volts. This value is in excellent agreement with the measured excitation potential and the conclusions of the experiments are in support of the Wentzel-Druyvesteyn theory of the origin of the $K\alpha_{3,4}$ satellite lines.

I. INTRODUCTION

THE phenomena associated with nondiagram or satellite lines represent an enigma of many years standing in x-ray spectroscopic theory. For some time we have been able to account satisfactorily for the essential features of the production of diagram lines as either dipole or quadrupole radiations, but, perhaps because of a paucity of accurate, unambiguous experimental information, we are confronted with various contradictory theories which attempt to "explain" satellite lines. The voltage required for the production of satellites is of crucial importance in testing the validity of these various theories and in the present paper we shall be concerned with a determination of this excitation voltage.

---

* National Research Fellow.

† The author is indebted to the American Philosophical Society for a grant-in-aid (made to Professor F. K. Richtmyer) which allowed the completion of this research.

In 1921 Wentzel[1] proposed that satellites originate in multiply-ionized atoms. For example, the $K\alpha_4$ line was supposed to arise from a $KK \rightarrow KL$ transition where KK refers to an atomic state in which two K electrons are missing. The probability of two (or more) electrons being ejected from an atom by successive impacts of the cathode-rays is much too low[2, 3] to account for the observed satellite intensities—the multiple-ionization process would have to take place by a single impact. Then, the x-ray tube voltage necessary to excite the $K\alpha_4$ satellite line in accord with Wentzel's proposal is somewhat more than twice the voltage required to excite the $K\alpha_{1,2}$ lines, for which the initial state of the atom is simply K ionization.

Early qualitative determinations[3–7] of the excitation voltage of satellites gave values considerably less than twice that of the parent diagram lines, although in these experiments the satellite excitation voltage seemed consistently to be the higher. Druyvesteyn[3] accordingly[8] modified Wentzel's scheme by proposing that the initial state of the atom giving rise to satellite lines is one in which the double-ionization never refers to the same electronic shell.[8a] In the Wentzel-Druyvesteyn theory the $K\alpha_4$ line is the radiated result of a $KL \rightarrow LL$ transition, and the excitation potential is approximately equivalent to the total energy required to remove the K electron of atom Z plus the energy required to remove an L electron of atom $Z+1$.

So great were the technical difficulties in experimentally measuring the satellite excitation potentials that the early experiments did not clearly defend the Wentzel-Druyvesteyn theory. Except for the work of Jönsson[6] and that of DuMond and Hoyt,[9] all of these experiments employed the photographic method of measuring the x-ray intensities. The photographic method is especially treacherous in these studies because of the great difference in intensity between the satellites and the parent lines. The parent line[10] is of necessity overexposed in order to bring out the faint satellite lines on the photographic plate. The satellites are found on a rapidly changing background, on the side of the overexposed parent line, and we do not know the form of the photographic density curve of the parent line in the satellite neighborhood. The effective resolving power of the spectrograph is not only low but, in part because of the overexposure, is also unknown so far as concerns a possible correction in the relative intensity measurements. DuMond and Hoyt in attempting to eliminate the uncertainties inherent in the photographic method adapted the two-crystal ionization spectrometer to the determination of the excitation potential of the $K\alpha_{3,4}$ satellite lines of copper. This measurement, with the ionization method, gave a value for the excitation potential which is *less* than that required for KL ionization. This value was based, however, on a questionable extrapolation.

DuMond and Hoyt's measurement was in agreement with another theory of satellite origin which had been proposed by Richtmyer.[11] This theory, the "double-jump" theory, based on semi-Moseley graphs of the wave-length separations of the satellites and the parent lines, ascribes the satellite lines to two simultaneous electron transitions in the atom, one transition being that which alone would give rise to the parent line and the second transition being one between two outer or semi-optical levels. In the case of $K\alpha$ satellites this outer transition involves two M levels. The excitation potential of the $K\alpha$ satellite lines according to Richtmyer's hypothesis

[1] G. Wentzel, Ann. d. Physik **66**, 437 (1921); **73**, 647 (1924); Zeits. f. Physik **31**, 445 (1925).
[2] D. Coster, Phil. Mag. **44**, 546 (1922); S. Rosseland, Phil. Mag. **45**, 65 (1923).
[3] M. J. Druyvesteyn, Zeits. f. Physik **43**, 707 (1927); Dissertation, Groningen, 1928.
[4] E. Bäcklin, Zeits. f. Physik **27**, 30 (1924).
[5] M. Siegbahn and A. Larsson, Arkiv f. Matematik, Astronomy och Fysik **18**, 1 (1924).
[6] Axel Jönsson, Zeits. f. Physik **43**, 845 (1927).
[7] S. W. Barnes, Dissertation, Cornell University, 1930, and S. W. Barnes and F. K. Richtmyer, Phys. Rev. **35**, 661A (1930).
[8] Also important in this modification are considerations of the wave-length separations of the satellites and the associated diagram lines.
[8a] To account for certain satellite lines, for example, the $K\alpha_{3,4}$ lines, an initial state of triple-ionization was proposed in which two of the three missing electrons may be from the same electronic shell.
[9] J. W. M. DuMond and A. Hoyt, Phys. Rev. **36**, 799 (1930).
[10] The term "parent line" refers in the present discussion to the nearest intense diagram line. Evidence has been presented (O. R. Ford, Phys. Rev. **41**, 577 (1932), F. K. Richtmyer, Phil. Mag. **6**, 64 (1928), *et al.*) to show that the true parent line may be more distant in wave-length. For example, the $K\alpha_2$ rather than the $K\alpha_1$ line may be the parent line of the $K\alpha_{3,4}$ satellites.
[11] F. K. Richtmyer, J. Frank. Inst. **208**, 325 (1929); see also F. Bloch, Phys. Rev. **48**, 187 (1935).

is in excess of the ionization energy of the K shell of atom Z by approximately the ionization energy of the M shell of atom Z+1.

Recently Coster and Thijssen[12] reported a determination, using the photographic method, of the excitation potential of the $K\alpha_{3,4}$ satellites of sulphur, obtaining a value in agreement with KL ionization. More recently, Coster, Kuipers and Huizinga[13] have measured photographically the excitation potential of the $L\alpha$ satellites of niobium. This value also agrees with LM ionization (which in the Wentzel-Druyvesteyn theory corresponds to KL ionization with K series satellites), and also gives supporting evidence for the Coster-Kronig theory[14] for the augmented intensities in the range of certain atomic numbers of L and M series satellite lines. (The Coster-Kronig theory, based on radiationless transitions as increasing the probability of an atom finding itself in the initial state for satellite emission, does not apply to K series satellites, although it depends for its meaning upon the Wentzel-Druyvesteyn theory.)

It was felt that the status of the problem as described above demanded a new evaluation of the satellite excitation potential using the ionization method of recording the intensities, which method is free from the objections to the photographic method, and using a two-crystal spectrometer which has a much higher resolving power. The excitation potential of the $K\alpha_{3,4}$ satellite lines of titanium has been determined and the value obtained is in agreement with the energy required to produce KL ionization, in support of the Wentzel-Druyvesteyn theory.

II. Experimental Part

The vacuum spectrometer and accessory equipment used in this work have been described in previous papers.[15] Mounted on the instrument were calcite crystals, etched cleavage-surfaces, crystals A_4B_4 of previous reports.[16, 17] These crystals had been found to be "spectrometrically perfect."[18]

The size of the focal-spot of the target of the x-ray tube was adjusted to be about 2 mm in diameter. This diameter matched the height of each of two slits which limited the maximum vertical divergence of the x-ray beam (with respect to the central ray) to 6×10^{-3} radian. The horizontal divergence of the beam was limited by the collimating action of the first crystal and by the effective size of the focal-spot. As mentioned in another paper,[16] this arrangement causes the x-ray beam to shift along the surfaces of both crystals as the angle of the second crystal is altered. The crystals, however, had been previously tested and found to have uniform reflectivity over their surfaces. The advantages of this aperture-arrangement are (1) in utilizing at all times all the intensity generated in the x-ray tube, (2) in obviating the problems of nonuniform intensity distribution in the focal-spot, and (3) in reducing the number of adjustments in going from one point to another on a curve.

The ionization currents were recorded with the constant deflection method by means of an FP-54 amplifying tube in the DuBridge-Brown circuit.[15, 19] Either of two high resistances, 3.4×10^{11} and 6×10^{9} ohms, could be placed in the circuit by a simple switching device. With the alternate use of these two resistances the assumption of linearity of the amplifying system over the large range of a factor of 1000 was not necessary, although by test, applying known voltages with a potentiometer, the circuit and galvanometer (type HS Leeds and Northrup) were linear over a range of more than 100.

Several important features served to increase the accuracy with which the feeble ionization currents were measured. (1) The Pliotron tube was in a vacuum, inside the massive steel tank. (2) This tank, because of its large heat capacity,

[12] D. Coster and W. J. Thijssen, Zeits. f. Physik **84**, 686 (1933).
[13] D. Coster, H. H. Kuipers and W. J. Huizinga, Physica **2**, 870 (1935).
[14] D. Coster and R. de L. Kronig, Physica **2**, 13 (1935).
[15] L. G. Parratt, Phys. Rev. **41**, 553 (1932); Rev. Sci. Inst. **5**, 395 (1934).
[16] L. G. Parratt, Rev. Sci. Inst. **6**, 387 (1935).
[17] L. G. Parratt and F. Miller, Jr., Phys. Rev. in press (1936).
[18] "Spectrometrically perfect" crystals are defined as "perfect" crystals of "Class I." "Perfect" crystals are defined as crystals whose reflectivities (usually taken as merely the widths of the (1, −1) rocking curves) measured in the parallel positions agree with the theoretical reflectivities. "Class I" crystals are crystals whose (1, +1) curve width of the $K\alpha_1$ line of Mo, Cu or Ti is narrow (a minimum) for the corresponding (1, −1) width. See reference 16.
[19] L. A. DuBridge and H. Brown, Rev. Sci. Inst. **4**, 532 (1933).

served to maintain constant temperature conditions. (3) The ionization chamber, filled with one atmosphere of argon, was small,[20] 2.4 cubic inches, and constructed of steel to reduce[21] the number of extraneously produced ions. (4) The effect of an alpha-particle was a rather violent "kick" and since these kicks were rare, a maximum range alpha-particle (causing a scale deflection of about 12 cm) being observed about one per hour, the x-ray intensity readings could be taken between them or their effects visually discounted. (5) And, finally, the wave-lengths studied are relatively long with correspondingly small disturbances due to the statistical variations in the number of quanta entering the ion chamber to produce a given ionization current.

From the observed variations in the scale position of the light-beam of the galvanometer an ionization current of 10^{-16} ampere could be measured with an estimated accuracy of ± 15 percent. Assuming an energy of 35 electron volts per ion pair,[22] one calculates that a current of 10^{-16} ampere is produced by less than 5 quanta ($\lambda = 2.75$A) completely absorbed per second. The time constant of the measuring system (given by $T = RC$ of the ion chamber-Pliotron circuit rather than by the period of the galvanometer) is approximately 6 seconds. In 6 seconds, then, 30 quanta are absorbed and the standard deviation in measuring 10^{-16} ampere is given by

$$\sqrt{n}/n = \sqrt{30}/30 = 18 \text{ percent.}$$

The ballastic type of recordings, in which the charge is accumulated for several minutes would, statistically, increase the sensitivity without sacrificing accuracy but, when one considers the observer's opportunity with the constant deflection method to discount the alpha-particle kicks and to further smooth out the fluctuations by watching the scale position of the light-beam for a period of time longer than 6 seconds, one is justified in concluding that in measuring the ionization currents produced by x-rays the present techniques have practically reached the theoretical limits. In the actual recordings, except with the tube voltages of 5.75 and 6 kv, the ionization currents observed at the peak of the $K\alpha_4$ line were greater than 10^{-15} ampere: At 20 kv and 20 ma the deflection at the α_4 peak was 100 cm corresponding to an ionization current of 3×10^{-14} ampere.

Many considerations are important in choosing an element for the target of the x-ray tube in this work. (1) The target must be capable of dissipating as much power as possible with constant x-ray emission. (2) The wave-length must not be so long that absorption difficulties become great. (3) The $K\alpha_{3,4}$ satellite intensity relative to that of the parent line should be high. (4) The excitation potential of the parent line should be such (high) that the already small difference between the exciting potential of the parent line and of the satellites be large to allow a relatively more accurate measurement. (5) The satellites should be far removed from the parent line and the width of the parent line should be small so that the uncertainty of the sloping satellite background, actually the side of the α_1 line, may be a minimum. (6) The total internal component structure of the satellites should be narrow to allow the sloping background to be drawn in as accurately as possible. Before the target-element was decided upon, preliminary ionization curves were taken of the satellites from S(16) to Ge(32), and Ti(22) was chosen as being most satisfactory.

A good thermal contact to titanium must be established before it will serve as a satisfactory target. This contact was made with the use of evaporated films.[23] The preparation of the target, discussed elsewhere,[24] was briefly as follows: On a freshly cleaned surface of a Ti disk, about 1/2 inch in diameter and 1/16 inch thick, was condensed in vacuum a layer of chromium and then a layer of copper. The disk was removed from the evaporating jar and more copper electroplated onto the condensed copper until a sufficiently thick deposit allowed the disk to be soldered to the target carriage. This target would

[20] Radiation of 2.75A wave-length is about 95 percent absorbed in a 3 cm path (one atmosphere of argon) in the ionization chamber. With such sudden absorption it is important that there be no "dead pockets" in the electric field in the ion chamber near the entrance window. Accordingly, in the present experiments a cellophane window was used on the inner side of which had been placed a thin but electrically conducting layer of aluminum. The argon path in the chamber was 6 centimeters and in this distance the radiation was completely absorbed.

[21] J. A. Bearden, Rev. Sci. Inst. **4**, 271 (1933).

[22] O. Gaertner, Ann. d. Physik **3**, 325 (1929); **10**, 825 (1931).

[23] The author is indebted to Dr. John E. Ruedy of the Evaporated Films Company for his generous advice and assistance in the preparation of this target.

[24] L. G. Parratt, Rev. Sci. Inst. **6**, 372 (1935).

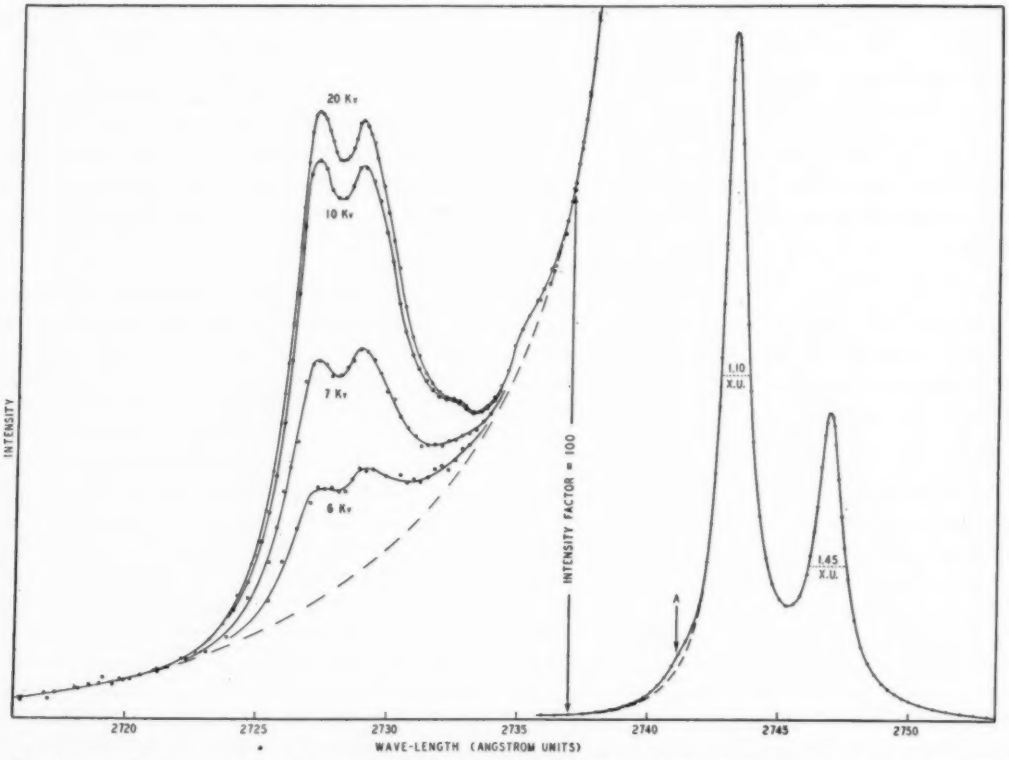

FIG. 1. Ionization curves of the $K\alpha_{3,4}$ region of titanium recorded with various voltages across the x-ray tube. (This particular $\alpha_{1,2}$ curve was recorded at 20 kilovolts.) The four curves are matched for the intensity of the $\alpha_{1,2}$ lines. The satellite lines are plotted to an intensity scale 100 times the scale used in plotting the diagram lines. On the short wave-length side of the $K\alpha_1$ line, at the position of the arrow A, is a new faint component line. See text.

dissipate about 750 watts with a focal-spot about 2 mm in diameter.

Needless to say a good vacuum must be maintained in the x-ray tube to eliminate the intolerable tungsten deposit (from the filament) which would otherwise accumulate on the target surface and on the window of the tube. Because of the x-ray absorption in tungsten a good vacuum becomes rapidly more important as the wave-length is increased. When the vacuum was maintained, and the tube voltage (the primary voltage of the high-tension transformer was supplied by a motor-generator) was held constant by manually adjusting the filament current, the emitted intensity was constant within 2 percent over a period of several hours.

The voltage across the x-ray tube was measured with an accurate milliammeter in series with a three megohm wire-wound resistance. The calibration of this voltmeter was checked by a measurement of the known excitation potential of the Ti $K\alpha_{1,2}$ lines. The ripple in the high voltage was smoothed out by a filter circuit: At 6 kv and 80 ma the ripple was 48 volts as measured with an oscillograph,[25] and about the same as calculated from the constants of the filter circuit.

III. Discussion of Results

In Fig. 1 are plotted several ionization curves of the Ti $K\alpha_{3,4}$ region as recorded with various voltages across the x-ray tube. The particular curve of $\alpha_{1,2}$ shown in the figure was recorded at 20 kilovolts. The observed points on these curves

[25] The author is indebted to Mr. T. T. Goldsmith of this laboratory for assisting in this measurement.

illustrate the accuracy with which the intensity measurements were made.

With the tube operating at 30 kv and 9.7 ma the total background radiation, due to the continuous spectrum and to scattering of the x-rays, was less than 1/10 of the peak of the α_4 line or less than 1/1100 of the peak of the α_1 line. This fractional background was less at lower voltages.

Shown in the curves are at least two satellite components, α' and α_3'' (a new component), in addition to the $\alpha_{3,4}$ lines. The α_3' line, which has been observed by Bäcklin and by Ford on photographic plates with elements Si(14) to Cl(17), appears to be changing its wave-length position relative to the $\alpha_{3,4}$ lines, moving from the long wave-length side of α_4 at S(16) to the short wave-length side as the atomic number is increased. In the case of Ti(22) α_3' is about coincident in wave-length with α_4. With this element, Ti, the intensity of the α_3' line is roughly 29 percent of that of α_4. A subsequent paper is being prepared in which is discussed the structure and intensities of the satellites in the $K\alpha_{1,2,3,4}$ region with elements S(16) to Ge(32), and our interest in the present paper will be confined to the satellite intensity as a function of the x-ray tube voltage and current. The above brief mention of the α_3' line is pertinent in the present discussion in view of the possibility that the origin of this satellite is not the same as the origin of the other satellites in the $\alpha_{3,4}$ group. If the origins are different one might expect a different intensity-voltage function for the two types of satellites. Experimentally no change in the Ti $K\alpha_{3,4}$ satellite structure was observed as the tube voltage was varied; but this check was not sufficiently sensitive below 7 or 8 kv to have much significance and it is probably in the low voltage range that the check is most important.

On the short wave-length side of the $K\alpha_1$ line, at the position of the arrow designated by "A" in Fig. 1, there appears a little "bump," evidence of another component satellite line.[25a] This line has been observed in the present work with elements V, Ti, Sc, Ca, K, Cl and S (elements of lower atomic number than that of S(16) have not yet been studied) and will be discussed in more detail in a subsequent paper. The area under this line has not been considered as part of the intensity of the $K\alpha_{3,4}$ satellite group. Rather, it seems possible that this new line is another group of satellites for which the initial atomic state is one of KM ionization.

The definition of the relative intensities of two x-ray lines refers to the ratio of the areas contained under the lines when the spectral analysis is complete, that is, when the lines are observed with an instrument of infinite resolving power. If the instrument used in the analysis is of low resolving power a more fitting definition of relative intensities is simply the ratio of the observed maximum ordinates of the two lines, although (except with extremely low resolving power) unless the x-ray lines in question have identical "true" widths and "true" shapes, the ratio of maximum ordinates does not give the relative intensities.

It is well known that the resolving power of the two-crystal spectrometer is considerably greater[16, 26] than that of the single-crystal instrument, especially when, as is usually the case, the latter is operated with the confining slits so arranged that they, rather than the diffraction pattern of the crystal, are effective in limiting the resolving power. Even with the two-crystal instrument with "spectrometrically perfect" calcite crystals the $d\lambda$ interval due to the finite resolving power of the crystals is about 1/4 of the true width of the Ti $K\alpha_1$ line.[16] As seen from Fig. 1 the observed width at half-maximum intensity of the Ti $K\alpha_{3,4}$ satellite region is much greater than, a factor of about 4.3, the observed width of the sharp $K\alpha_1$ line. The effect of the instrument is (1) to depress the peak of the $K\alpha_1$ line a greater fraction than the depression of the satellite peaks, and (2) to increase the area of the $K\alpha_1$ line a greater fraction than the increase in the satellite area.

An x-ray line having a true shape $L(\theta)$ is transformed, in two successive acts, by the two single-crystal diffraction patterns $F_A(\theta)$ and $F_B(\theta)$ into the line shape $L_B(\theta)$ which is observed after reflection from crystal B. These functions are related[27] by

[25a] This "bump" appears to be the same as the "emission band" reported by Dolejsek, Comptes rendus **174**, 441 (1922), on the short wave-length side of the $K\alpha_1$ line of Sc, Ca, K and Cl.

[26] S. K. Allison, Phys. Rev. **38**, 203 (1931).

[27] For a more accurate discussion of these functions see Compton and Allison, *X-Rays in Theory and Experiment* (D. Van Nostrand Co., 1935), pp. 709–750. See also L. P. Smith, Phys. Rev. **46**, 343 (1934).

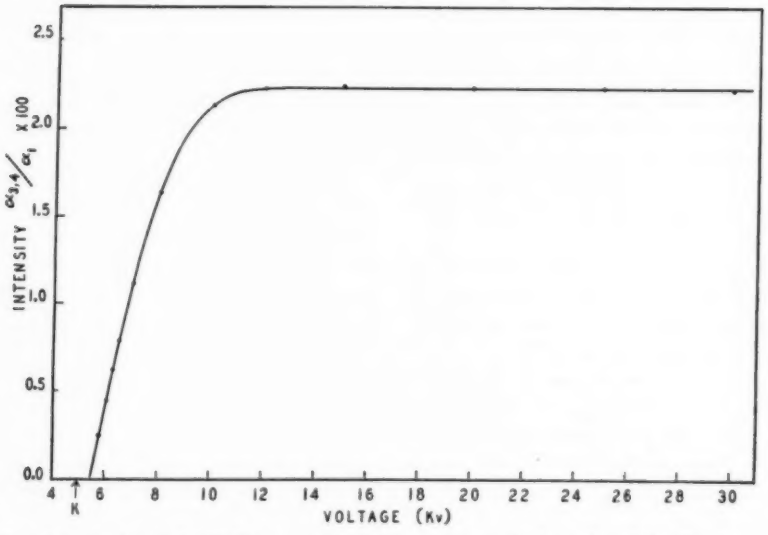

FIG. 2. Intensity of the Ti $K\alpha_{3,4}$ satellite lines relative to the intensity of the $K\alpha_1$ line as a function of tube voltage. The abscissae value at which the intensity ratio $\alpha_{3,4}/\alpha_1$ falls to zero is the excitation potential of the satellite lines. The voltage indicated by K is the excitation potential of the $K\alpha_{1,2}$ diagram lines.

$$L_A(\theta)=\int_{-\infty}^{+\infty} L(\theta-\beta_A)F_A(\beta_A)d\beta_A$$

and

$$L_B(\theta)=\int_{-\infty}^{+\infty} L_A(\theta-\beta_B)F_B(\beta_B)d\beta_B,$$

in which $L_B(\theta)$ is the only shape that is experimentally known. The order of magnitude of the width at half-maximum of the crystal functions F_A and F_B can be inferred from the width of the observed $(1, -1)$ curve. The shape of the theoretical diffraction pattern $F(\theta)$ is not symmetrical. We know also that the width of $L_B(\theta)$ at half-maximum intensity is about 25 percent greater than the width of $L(\theta)$. From this incomplete information we are interested in obtaining $L(\theta)$.

For the present purposes we will be content with an approximate solution, one which gives the maximum ordinate and the area of $L(\theta)$ within about ± 3 percent. A graphical solution has been discussed by Spencer[28] in which each of several types of $F(\theta)$ are considered. None of Spencer's $F(\theta)$ types is applicable. If the full width of $F(\theta)$ be taken arbitrarily as the $(1, -1)$ width (0.22 X. U. in the present case) divided by $\sqrt{2}$, the $F(\theta)$ contour may be adjusted by trial and error to give, following Spencer's double inverse graphical method, an $L(\theta)$ whose width agrees with the true width as previously ascertained.[16] In this manner approximate correction factors were evaluated for the Ti $K\alpha$ lines of Fig. 1: The ratio of the observed peak intensities $\alpha_{3,4}/\alpha_1$ are to be multiplied by 0.93 and the ratio of observed areas $\alpha_{3,4}/\alpha_1$ by the factor 1.05. The corrections are of no importance in the value of the excitation potential but they are greater than the estimated maximum error in the relative intensity measurements.

Measurements of the relative intensities of the satellite lines to the α_1 line as recorded at various tube voltages are listed in Table I and given graphically in Fig. 2. These values, the averages of many trials, have an estimated maximum observational error of ± 4 percent, except with the voltages of 5.75, 6.0 and 6.25 kv where the error may be as large as ± 15 percent. No satisfactory analytical method of drawing in the satellite background, the side of the asymmetrical α_1 line, has been developed and the uncertainty of the arbitrary way in which this background was determined (drawn in free-hand) introduces the greatest error in the relative intensity measurements. The area under the α_1 line was taken as 2/3 the area under the $(\alpha_1+\alpha_2)$ contour.

[28] R. C. Spencer, Phys. Rev. **38**, 618 (1931).

TABLE I. *Intensity of the Ti $K\alpha_{3,4}$ x-ray satellite lines, relative to the intensity of the Ti $K\alpha_1$ diagram line, with various x-ray tube voltages.* (Area of satellites, designated $\alpha_{3,4}$, refers to the area of the total satellite structure which may include component satellite lines in addition to the α_3 and α_4 lines.)

Corrections:
(1) The subtraction of the intensity of the overlapping α_2 line from the observed intensity at the peak of the α_4 line.
(2) For the finite resolving power of the spectrometer (see text).

Tube Voltage (kv)	Tube Current (ma)	Ratio of Obs. Peaks α_4/α_1 (percent)	Ratio of Peaks α_4/α_1 (percent) Corrected (1) (2)	Ratio of Obs. Areas $\alpha_{3,4}/\alpha_1$ (percent)	Ratio of Areas $\alpha_{3,4}/\alpha_1$ (percent) Corrected (2)
5.75	80.0	0.26	0.079	0.237	0.249
6.00	80.7	0.326	0.140	0.423	0.444
6.25	80.6	0.39	0.200	0.603	0.633
6.50	80.5	0.44	0.247	0.749	0.785
7.00	78.5	0.55	0.345	1.05	1.10
8.00	66.0	0.72	0.505	1.54	1.62
10.00	54.6	0.89	0.664	2.07	2.17
12.00	32.3	0.92	0.690	2.11	2.21
15.00	22.2	0.93	0.700	2.12	2.22
20.00	21.4	0.92	0.690	2.11	2.21
25.00	20.0	0.92	0.690	2.11	2.21
30.00	9.7	0.91	0.690	2.10	2.20

Matching the various satellite curves for the same α_1 peak intensity affords a much more sensitive test than has ever before been made of the shape of the α_1 line with different tube voltages and currents. The side of the α_1 line adjacent to the satellite region in all of the matched curves agrees within the experimental error—the ratio of the intensity at this remote part of the α_1 line to the intensity at the peak of the line does not vary with voltage or current within the experimental error of about five percent of one percent. The voltage range used is admirably suited to this test.

For voltages less than twice the excitation potential the intensity of the $K\alpha_{3,4}$ satellite lines is not the same function of voltage that applies in the case of the diagram lines; for voltages greater than twice the excitation potential the functions are the same. The ratio of satellite intensity to that of the α_1 line was found to be linear with the x-ray tube current over a factor range of 4. Since the intensity of the α_1 line is known to be linear with tube current it follows that the same relation holds for the satellite intensity.[29]

[29] The possibility of the double ionization process being one of successive cathode-ray impacts, tandem style, has been ruled out as being too improbable to account for the observed satellite intensities. The fact that the satellite intensity is linear with tube current rules out on a second score the tandem process which requires the intensity to be proportional to the square of the current.

An extrapolation of the curve of Fig. 2 to zero satellite intensity gives the excitation potential. This potential, 5450 volts, is 500 volts in excess of the ionization energy of the K shell of electrons. Great care was taken in determining the relative intensities at the low voltages and if these experimental values are assumed to be accurate without any observational error the uncertainty in the extrapolation is less than ± 40 volts. This assumption may seem warranted from the internal consistency of the data but it is not justified. The estimated maximum observational error is about 100 volts.

Of course, it is not certain that the extrapolation in Fig. 2 is the correct one: A point of inflection below 5.75 kv would bring the satellite excitation potential more nearly in agreement with that of the parent line. Such an inflection point is, however, unlikely.

IV. Conclusions

The ionization energy[30] of a K electron of atom $Z=22$ (titanium) is 4950 volts. The ionization energy of an L_{III} electron of atom $Z+1=23$ (vanadium) is 514 volts; the L_{III} energy of an hypothetical atom[31] $Z+0.85$ is 505 volts. The sum of the two energies, approximately the energy required to produce a state of KL ionization in the Ti atom, is 5455 volts, taking the screening constant as 0.85 instead of unity. This energy is in excellent agreement with the measured excitation potential of the Ti $K\alpha_{3,4}$ satellites, 5450 ± 100 volts, and the conclusions of the experiments are in support of the Wentzel-Druyvesteyn theory of the origin of the $K\alpha_{3,4}$ satellite lines.

Acknowledgments

The author is pleased to express his indebtedness to Professor F. K. Richtmyer for his interest and generous discussions in the course of this work, and to the University of Chicago for the loan of the double spectrometer with which the data were recorded.

[30] The ionization energies are calculated from the ν/R values given in Siegbahn, *Spectroscopie der Röntgenstrahlen* (Julius Springer, 1931), p. 348.

[31] J. C. Slater, Phys. Rev. **36**, 57 (1930) gives 0.85 as the approximate screening constant of a missing K electron on an L electron.

Collision Induced Emission

WILLIAM M. PRESTON, *Harvard University*

(Received November 15, 1935)

A new continuous spectrum, associated with the weak forbidden mercury line λ2269.80A, has been found in a low pressure mercury discharge with a few centimeters pressure of argon or helium added. The continuum lies on the short wave-length side of the line, rising steeply to maximum intensity at about 2259A, and then falling more slowly to 10 percent near 2237A. It is attributed to radiation from excited mercury atoms in the $^3P_2$ metastable state, perturbed by the close approach of rare gas atoms, at which time the thermal energy may be added to the energy of excitation to give a larger quantum. Since the total intensity of the continuum is many times that of the line, although the time during which an excited atom is appreciably perturbed is much less than the time between collisions, we must assume that during a collision the probability of emission is enormously increased. The j selection rule, which normally inhibits the transition $^1S_0-{}^3P_2$, evidently breaks down in the field of the colliding atom. This is shown to be reasonable on theoretical grounds.

INTRODUCTION

WHEN an excited atom is perturbed by the close approach of a colliding neutral atom or molecule, it might be supposed that, in some cases, its probability of emission would be momentarily increased. This effect may be called "collision induced emission," and distinguished from the case in which a stable molecule, with quantized energy states, is formed. The halogens, for example, show intense band spectra due to transitions between molecular levels derived from atomic states between which transitions cannot take place. The time of interaction or the "duration" of a collision is very short, and we are chiefly interested in comparing the emission probability of the excited atom in the perturbed and unperturbed conditions.

It has, of course, been suggested before that a collision might increase the emission probability of an excited atom, but experimental evidence bearing on the question has never been satisfactory. Hamos,[1] for example, looked for this effect in a study of the intensity of the sodium D lines in fluorescence, with and without the addition of foreign gases. He decided that the changes he observed could be adequately explained by ordinary collision broadening of the absorption line, without the additional hypothesis of induced emission.[2] More recently, a diffuse helium band at 600A was investigated by Nickerson.[3] This seemed to be associated with the forbidden line λ602.418, $1\,^1S_0-2\,^1S_0$, although the connection was not very well established. Nickerson first suggested that the band might be due to induced emission during the close approach of a normal to an excited helium atom, since this would account for its location and comparatively great intensity relative to the line. However, he was forced to decide against this interpretation because the potential curves, which are known for the lower states of the helium molecule with considerable accuracy, indicated that no radiation could be emitted in this transition, of frequency greater than that of the atomic line itself.[4]

In the course of work on diffuse bands of the type, first reported by Oldenberg,[5] and in more detail by Kuhn and Oldenberg,[6] which accompany certain strong metallic lines in a discharge when a considerable pressure of one of the rare gases is added, a short continuum has been observed which is believed to give definite indication of collision induced emission. This continuum occurs on the short wave-length side of the weak forbidden mercury line λ2269.80, and

[1] Hamos, Zeits. f. Physik **74**, 379 (1932).

[2] There was no disproof of this hypothesis. Hamos's results were difficult to interpret, because only the *total* intensity of the fluorescent D lines was directly measured. A collision able to modify substantially the emission probability must also modify the interaction potential curves and hence, ordinarily, the frequency radiated. The total intensity, on the other hand, may remain unchanged.

[3] Nickerson, Phys. Rev. **47**, 707 (1935).

[4] That is, the potential curves for the ground state, $2p\sigma\ ^1\Sigma_g$ and the upper state, $2s\sigma\ ^1\Sigma_u$, are further apart at infinite nuclear separation than at any other time. Nickerson suggested that two somewhat similar diffuse bands, at 647A and 662A, may be due to transitions from the first two *vibration* levels of the $2s\sigma\ ^1\Sigma_u$ state, and the possibility remains that the band at 600A comes similarly from a vibration level of some higher state.

[5] Oldenberg, Zeits. f. Physik **47**, 184 (1927).

[6] Kuhn and Oldenberg, Phys. Rev. **41**, 72 (1932).

has been obtained when a few centimeters of helium or argon were added to a low pressure mercury discharge.

Experimental

The simple Pyrex discharge tube had a capillary 5 mm in diameter and 10 cm long, and was supported within an electric furnace which maintained a temperature just sufficient to give a weak mercury discharge with a 0.5 kw, 15,000-volt transformer. Observations were made with a medium-sized quartz prism Hilger spectrograph.

High purity of conditions in the discharge was essential, because of the comparative weakness of the phenomena to be observed. Clean mercury was distilled into a side arm attached to the discharge tube, which was previously baked out carefully. The argon and helium were purified for several days in a misch metal arc, until a spectrogram of long exposure showed no lines or bands due to impurities.

The addition of a rare gas over a wide range of pressures makes a discharge through mercury vapor of low pressure run smoothly and without much heating. The ionization voltage of mercury is 10.38, while the lowest excited levels of both helium and argon lie higher. For this reason, even with 10 cm of rare gas and only 0.01 mm of mercury vapor, the spectrum obtained is that of the metal alone, neither lines nor continua of the rare gases appearing.

Description of the Continuum

A microphotometer trace of the new continuum is shown in Fig. 1. It extends from the forbidden line to short wave-lengths, reaching a maximum near 2259A, 200 cm^{-1} from the line. From that point it falls uniformly, reaching 10 percent of its maximum intensity at about 2237A. To long wave-lengths, the continuum falls steeply to 10 percent at the line, and fades out near 2272A. No trace of structure can be made out. The ratio of the intensity of the line λ2269.80 to that of the maximum of the continuum is close to 0.50, in the case of 10 cm of added argon. This ratio is arbitrary, of course, since it depends on the width of the slit[7] of the spectrograph. The latter was kept constant throughout the experiment, so that the above ratio will be useful for purposes of comparison. It was estimated that the *total* intensity represented by the continuum was about 100 times that of the line.

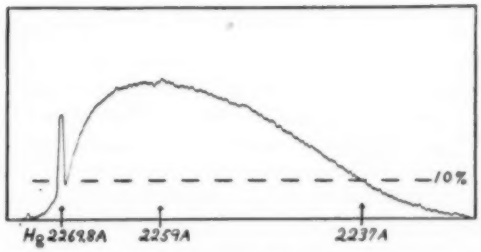

Fig. 1. Densitometer trace of the mercury-argon continuum associated with the forbidden line Hg λ2269.80A. The dotted line indicates the level at which the intensity is 10 percent of that at the maximum. Mercury v.p. 0.02 mm, argon pressure 10 cm, exciting current 1 ma a.c., exp. 24 minutes, medium sized Hilger.

The addition of 10 cm of helium in place of the argon gave rise to a similar continuum with its maximum in the same place, as closely as could be measured. In this case, however, the line was more intense than the maximum, in the ratio 1.4 to 1. When the pressure of helium was reduced to 11 mm, the continuum grew relatively weaker, and the ratio was measured roughly as 28, by comparing the exposure times necessary to give equal densities. For low densities and large intervals, this method is very inaccurate, and the above figure is not to be relied upon. It appears to indicate a variation of intensity with pressure more nearly linear than second power.

Careful measurements were made in an attempt to determine any change in the line-to-maximum ratio with variation of the exciting current. Exposures were made with 1.0, 0.25, and 0.05 amp. primary current, giving currents through the discharge tube of from 11 to less than 1 ma. In all three cases, the ratio remained constant at 0.50.[8]

[7] The intensity of a continuum varies directly as the slit width, while that of a line is independent of slit width if the latter is considerably greater than the spacing of the diffraction pattern of the collimating lens. In this experiment, the slit was kept at 0.05 mm, while the diffraction pattern spacing was less than 0.01 mm. In determining the line-to-maximum ratio, no correction was made for dispersion or plate sensitivity variation, because of the small range involved.

[8] The maximum experimental error in this measurement was probably less than 10 percent. The fact that all three determinations coincided is certainly accidental.

Discussion

It is of primary importance to make certain that the continuum is really due to a mercury-rare gas association, and not to either alone, or to an impurity. As stated above, great care was taken in the preparation of pure gases. Argon and helium have no lines or bands in this region, and in any case were not excited under the experimental conditions. The spectrum of mercury is well known, and although the molecule has a great number of diffuse bands and continua, none have been found in this region. The present structure was found only in the mixture of mercury and a rare gas, and with an intensity roughly proportional to the pressure of the latter. While similar in appearance, it was, for equal pressures of argon and helium, distinctly different in intensity relative to the line.

The further association of the continuum with the particular mercury line λ2269.80 is natural because of its proximity. It has the appearance of an unresolved rotation band coming to a head at the forbidden line. Unlike the case of helium, in which there are several other relatively distant unexplained molecular bands in the neighborhood of the λ600 band discussed by Nickerson,[3] in Hg+A the only diffuse bands which occur are close to atomic lines, namely, the one reported in this paper near λ2269.80, and those found near λ2536.5 by Oldenberg.[5] Even more conclusive is the constancy of the line-to-maximum ratio when the exciting current is varied twenty-fold. The three lowest excited states of mercury are ^3P levels. Of these, the $^3P_2$ (origin of λ2269.80) and the $^3P_0$ are metastable, and the associated lines are weak or missing in the ordinary discharge. Rayleigh[9] mentions that the intensity of both forbidden lines relative to the rest of the spectrum is greatly increased by lowering the exciting current.[10] In

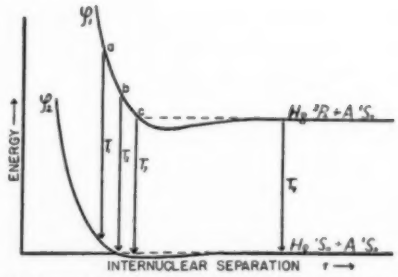

Fig. 2. Hypothetical potential curves, φ_1 for a $^3P_2$ mercury atom colliding with a normal rare gas atom, φ_2 for two normal atoms.

the present case, this effect was very marked. Relative to all surrounding lines, λ2269.80 increased in intensity several times when the current was lowered twenty-fold, so that in Fig. 1, taken with lowest current, only a trace of one other line appears in the 50A covered. Now if the continuum were close to the forbidden line only by chance, the current change would certainly produce a change in the line-to-maximum ratio. The constancy of this ratio allows us to conclude definitely that the two have a common origin, and our ability to establish this relationship gives particular interest to the continuum here reported.

The occurrence of a continuum on the *short* wave-length side of the line may be explained if the interaction potential curves have the qualitative course indicated in Fig. 2. The attractive van der Waals force between two normal atoms will be very small. For Hg $^3P_2$+A $^1S_0$ the attraction will be somewhat greater, but for the present we are not concerned with the resulting minimum in the curve φ_1. At the position of closest approach, which coincides with the maximum of the wave function of nuclear motion, the thermal kinetic energy will be available as potential energy, as represented by some point between *a* and *c* on φ_1. If emission takes place, the corresponding transitions between T_1 and T_2 will give a continuous spectrum of shorter wave-length than the atomic line,[11] provided that the lower potential curve starts to rise at a smaller

[9] Rayleigh, Proc. Roy. Soc. **A114**, 620 (1927).

[10] However, Takamine (Zeits. f. Physik **37**, 72 (1926)) found that the intensity of λ2269.80 relative to surrounding lines was a maximum for a current density of about 0.2 amp./cm², decreasing for higher and lower currents. His more complicated branched arc is perhaps not comparable. It is to be noted that the variable intensity of this line under different conditions of excitation is due to changes in the density of population of the metastable state, rather than to the breakdown of selection rules in high ionic fields, as in the case of many ordinarily forbidden lines involving a change in the electronic angular momentum quantum number *l* other than ±1. High current density would be expected to remove a larger proportion of atoms from the $^3P_2$ metastable state, by secondary excitation and second kind collisions, to states from which transitions can readily occur.

[11] The idea of the addition of thermal to excitation energy at the moment of a collision was used by Oldenberg, reference (5) and Kuhn and Oldenberg, reference (6) to explain the mercury-rare gas bands near the resonance line, λ2536.5, without any suggestion of induced emission probability.

internuclear separation than the upper. This is reasonable, since the outer electron is on a higher orbit in the excited state and there are no strong attractive forces of valence or resonance type.[12]

There are now two reasons why it seems necessary to make the assumption that the probability of emission at close approach must be enormously increased. First, the mean free path of a mercury atom in argon at 10 cm pressure is about 5×10^{-5} cm, while the distance over which repulsive interaction extends is probably about 1×10^{-8} cm. Therefore we should expect that the vast majority of radiation processes would occur uninfluenced by the close approach of a neutral atom.[13] In other words, the intensity of the line proper should be very much greater than that of any accompanying continuous spectrum on the short wave-length side, if the emission probability remained constant. Actually, however, this continuum has a total intensity about 100 times that of the line.

Second, consider the distribution of intensity. The probability P of finding a rare gas atom in a spherical shell of radius r and thickness dr about an excited mercury atom will be proportional simply to the geometrical factor r^2 at large distances, while within the range of interaction there will be an additional factor $e^{-\varphi_1/kT}$, the Maxwell-Boltzmann distribution function. Thus P is a rapidly increasing function of r in the range of repulsion, and the corresponding chance of finding a colliding atom at a point on φ_1 of Fig. 2 decreases rapidly from c to a. As a result, were the probability of emission Q[14] independent of r, we should expect to find on the short wave-length side of the line, a "tail" with uniformly decreasing intensity. Suppose, however, that Q, while constant at large r, increases rapidly at small internuclear distances. Then the product PQ, which will be roughly proportional to the intensity of radiation, may have a maximum. In Fig. 2, the emission probability at a will be large, but few atoms will approach so closely, and transitions T_1 with large wave-length shift will be comparatively few. At c, there will be many more perturbing atoms, but a small emission probability, and transitions T_3 giving radiation only slightly shifted will also be rare. At some intermediate point, say b, the greatest number of transitions will occur, and the continuum will have a separate maximum, as is actually observed.

We may describe two colliding atoms as a molecule, keeping in mind that it is in a continuous positive energy state.[15] If the interaction is weak, as it certainly is in the present case in which the attractive force is of the van der Waals type and the thermal energy is limited to a few hundredths of a volt, the coupling will be of the type of Hund's case C. The number of molecular states is then determined by the possible values of the quantum number Ω, the sum of the projections of the j's of the individual atoms on the internuclear axis. Three molecular states arise from the combination of two unlike atoms in $^3P_2$ and $^1S_0$ levels, namely, 2, 1, and 0^-.[16] Two unlike $^1S_0$ atoms give only a 0^+ state. Since the selection rules are $\Delta\Omega=\pm1$, 0^- does not combine with 0^+, there is one and only one excited molecular state in the present case which can combine with the ground state.

If the unperturbed Hg $^3P_2$ atom had a zero transition probability, we could accordingly predict from molecular theory that it would acquire a chance of radiating during a collision with a neutral atom. The magnitude of this induced transition probability should be proportional to the perturbation, and from a knowledge of the Paschen-Back effect, we can say that it should not approach the transition probability of the $^3P_1$ state until the perturbation is of the order of the multiplet separation. The maximum of the continuum lies about 0.025 volt from the line,

[12] Finkelnburg, Zeits. f. Physik **96**, 699 (1935), discusses this matter from a qualitative theoretical point of view.

[13] All emission is of course *slightly* affected by neighboring atoms. In the different problems of collision broadening and Stark effect broadening, in which nearly all radiation is shifted by a very small amount, it is the combined effect of many distant atoms or ions which is important. Large shifts must arise from the rare close approach of single bodies, and it is only for such comparatively large perturbations that we should expect a considerable change in the emission probability, in the present case.

[14] Q here refers to electronic transitions, and is not to be confused with the transition probability derived from the wave functions of nuclear motion. The latter we ignore, in the absence of any accurate knowledge of the repulsive potential curves, except in so far as we assume that the Franck-Condon rule applies.

[15] This is sometimes called a "quasi molecule": Born and Franck, Zeits. f. Physik **31**, 411 (1925).

[16] Mulliken, Rev. Mod. Phys. **4**, 26 (1932), gives rules for determining the case C states arising from unlike atoms with given l, s, and j.

while the $^3P_2-{}^3P_1$ separation is 0.57 volt. Therefore we should expect that the intensity of the continuum at its maximum should still be far less than that of the line λ2536.5 $^1S_0-{}^3P_1$, and such is the case experimentally.

The free $^3P_2$ mercury atom has actually always a slight chance of radiating, since we observe the sharp atomic line in the discharge, so the most we can say is that it is theoretically reasonable that a collision should *increase* its transition probability, in accordance with our interpretation of the experimental facts. If we consider a Hg $^3P_1$ atom, on the other hand, we should not suppose that a collision would greatly modify its already large transition probability. The rare gas bands found by Oldenberg,[5] on the short wave-length side of λ2536.5, have a total intensity very much less than that of the line proper, and perhaps they must be explained without collision induced emission.

Other forbidden lines ought to be accompanied by continua like that found near Hg λ2269.80, in particular, the corresponding cadmium line, λ3141.01. Investigation showed that unfortunately the neighboring cadmium resonance line has an intense tail, when rare gases are added to the discharge, which covers the region of the forbidden line and makes observation of weak spectra impossible. It is interesting to note that the $^3P_0$ metastable state of cadmium and mercury gives only a 0^- state in combining with a foreign $^1S_0$ atom. Transitions from this to the 0^+ ground state are excluded, and therefore no collision induced emission should be found near these lines, if the theory is correct. Experimentally, they are both obscured by the resonance line tails. In the case of pure mercury, no bands have been found to accompany the line λ2269.80 on the short wave-length side, although a series of what appear to be vibration bands commences at 2345A and gradually merges into a continuous spectrum extending to the long wave-length side of the line.[17] Corresponding vibration bands appear to be lacking in mercury-rare gas mixtures (see below), and we can suppose that the larger binding energy of Hg_2 results in the shift of the repulsive portion of the upper state potential curve to smaller internuclear distances, so that transitions to the ground state liberate *less* energy than the atomic line.

Mention should be made of a paper by Finkelnburg,[18] in which he discusses two diffuse bands at 2285A and 2365A, found by Kessel in a discharge through mercury vapor at 4 mm pressure with 1 mm of argon added.[19] Finkelnburg proposed that these bands came from the lowest vibration levels of states $\Omega=1$ and $\Omega=0$ of stable Hg $^3P_2-\mathrm{A}\ {}^1S_0$ molecules with a considerable binding energy. He further suggested that two bands of some sort should be found on the short wave-length side of the forbidden line λ2269.80, due to collision induced emission at the moment of closest approach. These latter were not found by Kessel.

On some early plates, the author found a faint band at 2365A which was almost certainly that described by Kessel. It has never appeared under conditions of high purity in the discharge. Moreover, one such early plate showed an exposure taken with 2 mm of added argon beside one taken with 90 mm of argon, and in each the 2365A band was of nearly the same intensity. If due to Hg+A molecules, it would surely have been much more intense at the higher pressure. Possibly Kessel's bands were caused by some impurity. Theoretically, as we have said, the $\Omega=0$ excited molecular state cannot combine with the ground state because one is 0^- and the other 0^+. It is also most unlikely that Hg+A should have a larger binding energy than Hg_2, in similar molecular states.[20] Since the author found no trace of spectra on the long wave-length side of λ2269.80 in Hg+A, it is probable that the binding energy of Hg $^3P_2+\mathrm{A}\ {}^1S_0$ is very small. The continuum on the short wave-length side, however, corresponds in principle to Finkelnburg's prediction.

In conclusion, the author wishes to express his deep gratitude to Professor Otto Oldenberg, who directed this work, for his unfailing interest and helpful advice; also to Professor Van Vleck for a discussion of the theoretical aspects of this paper.

[17] Rayleigh, Proc. Roy. Soc. **A116**, 702 (1927); Kuhn, Zeits. f. Physik **76**, 50 (1932).

[18] Finkelnburg, Zeits. f. Physik **81**, 781 (1933).

[19] Kessel, Zeits. f. Physik **70**, 623 (1931).

[20] For mercury, the polarizibility $\alpha=5.2\times10^{-24}$, for argon $\alpha=1.6\times10^{-24}$. In addition, mercury will show resonance attraction. Kuhn calculates a dissociation energy of about 0.1 volt for Hg $^3P_2+$Hg $^1S_0$, while Finkelnburg obtained a dissociation energy of 0.2 volt from Kessel's bands, for Hg $^3P_2+A\ {}^1S_0$.

An Extension of the Thallium II Spectrum

CECIL B. ELLIS AND RALPH A. SAWYER, *University of Michigan*

(Received November 29, 1935)

The spectrum of thallium from the hollow cathode discharge in He has been photographed in the region from 9250A to 600A. The classification of the first spark spectrum has been approximately doubled by the assignment of 160 new lines, which locate 35 new levels. These include members up to $n=11$ and 12 of the s, p, and d series (which establish the ionization potential as 164,765±5 cm^{-1}), the first two members of the g series, and six levels of the $5d^9 6s^2 6p$ configuration. Perturbations are present in many of the series, due to their interaction with the $6p^3$ and $5d^9 6s^2 6p$ configurations. The $6s6g$ term appears to have hyperfine structure larger than its multiplet structure. Practically all of the hollow cathode lines of thallium in the entire spectrum have now been classified.

1. INTRODUCTION

THE classification of the first spark spectrum of thallium has been the subject of papers by Rao, Narayan and Rao,[1] Smith,[2] McLennan, McLay and Crawford,[3] and McLennan and Crawford,[4] using both their own experimental data and the earlier measurements of Lang[5] and Carroll.[6] These investigations established the lowest terms of the various series—with the classification of about 100 lines—but left the upper part of the level diagram, including the interesting $5d^9 6s^2 6p$ configuration, incomplete. The lines which would give the clues to the upper levels should fall in the far ultraviolet below 2000A, in which region thallium has only been studied with the vacuum arc and condensed spark as sources. The most efficient means of producing these lines should be the hollow cathode discharge in He. In this source the Tl atom or ion is excited by collision with a metastable He atom (energy ~160,000 cm^{-1}) or with a He$^+$ ion (energy ~198,000 cm^{-1}).[7] Since these energies are just a little less than that required to ionize doubly the Tl atoms (~213,000 cm^{-1}), very many of the latter will be excited to the upper levels of Tl II. With this in mind we have photographed the hollow cathode spectrum in the entire range from 9250A to 600A with the view of completing the energy level scheme of Tl II.

2. EXPERIMENTAL PROCEDURE

The hollow cathode was filled with He at about one cm pressure which was continuously circulated and purified throughout the exposures. Small pieces of Tl laid inside the cathode immediately melted when the discharge was started. The source of power was a transformer and vacuum tube rectifier set which delivered 1000 volts d.c.—the discharge drawing around 100 ma. For the vacuum lines a normal incidence concave grating vacuum spectrograph[8] was used. The grating (1 m radius, 15,000 lines/in.) gave a dispersion of about 17A/mm. For the regions 2100–2500A the Hilger Quartz E-2, and 2500–4100A the Hilger Quartz E-1 spectrographs were available. The photographs in the visible and infrared were taken with a spectrograph of the same specifications as the Hilger Glass E-1. In the Schumann region lines of He and of the impurities Ne, Hg, C, and O served as internal wave-length standards. Elsewhere comparison spectra were placed upon the plates: 2100–2500 Ag spark; 2500–5800 Fe arc; and 5800–9250 Ne tube. Besides lines from the above-mentioned atomic impurities there appeared some electronic bands due to the molecules H_2, CO^+, OH, and He_2, for which the hollow cathode seems to be a very powerful source.

Of the thallium lines, in accordance with expectation, the lower series members of Tl I and all of Tl II were very strong; while nothing from

[1] Rao, Narayan and Rao, Ind. J. Phys. **2**, 467 (1928).
[2] Smith, Proc. Nat. Acad. Sci. **14**, 951 (1928); Phys. Rev. **34**, 393 (1929); Phys. Rev. **35**, 235 (1930).
[3] McLennan, McLay and Crawford, Proc. Roy. Soc. **A125**, 570 (1929).
[4] McLennan and Crawford, Proc. Roy. Soc. **A132**, 10 (1931).
[5] Lang, Phil. Trans. Roy. Soc. **224**, 371 (1924).
[6] Carroll, Phil. Trans. Roy. Soc. **225**, 357 (1925).
[7] Sawyer, Phys. Rev. **36**, 44 (1930).
[8] Sawyer, J. Opt. Soc. Am. **15**, 305 (1927).

TABLE I. *Energy levels of Tl II.*

LEVEL	TERM VALUE (cm^{-1})	LEVEL	TERM VALUE (cm^{-1})	LEVEL	TERM VALUE (cm^{-1})	LEVEL	TERM VALUE (cm^{-1})	LEVEL	TERM VALUE (cm^{-1})
$6s^2\ ^1S_0$	0	$6s7p\ ^1P_1^0$	122,379	$6s7d\ ^3D_2$	138,053	$6s8d\ ^3D_1$	147,602	$6s10p\ ^3P_2^0$	153,530?*
$6s6p\ ^3P_0^0$	49,451	$6p^2\ ^3P_1$	125,338	$6s7d\ ^3D_3$	138,203	$6s8d\ ^3D_2$	147,652	$6s10p\ ^1P_1^0$	153,633?*
$6s6p\ ^3P_1^0$	52,393	$5d^96s^26p\ 4_2^0$	125,437#	$6s8p\ ^3P_1^0$	139,365*	$6s8d\ ^3D_3$	147,747	$6s11s\ ^3S_1$	155,181*
$6s6p\ ^3P_2^0$	61,725	$5d^96s^26p\ 5_1^0$	126,204#	$6s8p\ ^3P_2^0$	140,304*	$6s9p\ ^3P_1^0$	148,349*	$6s10d\ ^3D_1$	155,963*
$6s6p\ ^1P_1^0$	75,660	$5d^96s^26p\ 6_2^0$	128,663*	$6s8p\ ^1P_1^0$	141,000*	$6s8d\ ^1D_2$	148,465	$6s10d\ ^3D_2$	155,982*
$6s7s\ ^3S_1$	105,225	$6p^2\ ^3P_2$	128,817	$6p^2\ ^1D_2$	141,982	$6s9p\ ^3P_2^0$	148,825*	$6s10d\ ^3D_3$	156,018*
$6s7s\ ^1S_0$	107,996	$5d^96s^26p\ 7_2^0$	129,158*	$5d^96s^26p\ 10_2^0$	142,781#	$6s9p\ ^1P_1^0$	149,063*	$6s10d\ ^1D_2$	156,177*
$5d^96s^26p\ 1_2^0$	110,387*	$6s8s\ ^3S_1$	133,568*	$5d^96s^26p\ 11_1^0$	143,612*	$6s10s\ ^3S_1$	151,568*	$6s11p\ ^1P_1^0$	156,475?*
$6s6d\ ^1D_2$	115,160	$6s8s\ ^1S_0$	134,292*	$5d^96s^26p\ 12_2^0$	145,092*	$6s7f\ ^3F_2^0$	152,104*	$6s12s\ ^3S_1$	157,481*
$6s6d\ ^3D_1$	116,147	$5d^96s^26p\ 8_1^0$	134,362*	$6s9s\ ^3S_1$	145,415	$6s7f\ ^3F_{3,4}^0$	152,110	$6s11d\ ^3D_2$	158,027?*
$6s6d\ ^3D_2$	116,430	$6s5f\ ^3F_2^0$	136,115	$6s9s\ ^1S_0$	145,591	$6s7f\ ^1F_3^0$	152,140*	$6s11d\ ^3D_3$	158,038?*
$6s6d\ ^3D_3$	116,826	$6s5f\ ^3F_3^0$	136,216	$6s6f\ ^3F_4^0$	146,500	$6s6g$	152,470*	$6s11d\ ^1D_2$	158,136?*
$6p^2\ ^3P_0$	117,408	$6s5f\ ^3F_4^0$	136,230	$6s6f\ ^3F_3^0$	146,523	$6s9d\ ^3D_1$	152,819*		
$6s7p\ ^3P_0^0$	119,361	$6s5f\ ^1F_3^0$	136,263	$6s6f\ ^3F_2^0$	146,534	$6s9d\ ^3D_2$	152,847*		
$6s7p\ ^3P_1^0$	119,576	$6s7d\ ^1D_2$	136,891	$6s6f\ ^1F_3^0$	146,543	$6s9d\ ^3D_3$	152,906*		
$6s7p\ ^3P_2^0$	122,029	$6s7d\ ^3D_1$	137,927	$6s5g$	147,065*	$6s9d\ ^1D_2$	153,200*		

* These terms are newly located from this research.
\# The terms here named $5d^96s^26p\ 4_2^0$, 5_1^0, and 10_2^0 were called 3_2^0, 1_1^0, and 2_2^0, respectively, by McLennan and Crawford.
? These high series members are established by only one vacuum line each, and so their term values may be in error by as much as 5 or 6 cm^{-1}. However these approximate positions are justified by the smoothness of the resulting quantum defect curves.

the higher stages of ionization appeared except a few of the most prominent transitions of Tl III and IV, which gave weak lines. Since the record of the 115 previously classified lines is scattered through three papers—those of McLennan, McLay and Crawford,[3] Smith,[9] and McLennan and Crawford[4]—to provide a complete list of Tl II we have included these lines as well as the 160 new ones found by us in Table II. All of the wave-lengths are our own with the exception of those of the three weak lines noted which we did not obtain. Likewise Table I is a complete list of the Tl II energy levels. The discrepancies between the wave numbers of the lines as measured and as computed from these energy levels, given in the $\Delta\nu$ column of Table II, are the best indications of the degree of accuracy of our results—about 6 cm^{-1} in the vacuum region and about 1 cm^{-1} above 2100A.

3. EXTENSION OF THE SERIES

The normal configuration of Tl II is $5d^{10}6s^2$. Excitation of one of the $6s$ electrons gives rise to the usual singlet and triplet series of the $6snl$ configurations. Inspection of the energy levels given in Table I shows that all the far ultraviolet lines ($\nu > 115{,}000$ cm^{-1}) must represent transitions ending on the normal state $6s^2\ ^1S_0$ and all the lines in the range $\nu = 115{,}000$–$50{,}000$ cm^{-1} (except the resonance lines) transitions ending on one of the $6s6p$ levels—otherwise the initial levels would have to be above the ionization potential. With this clue to the identification of the vacuum lines many higher series members were quickly located. We are greatly indebted to Dr. A. B. McLay, of McMasters University, for the information by personal letter that the level at 145,591 cm^{-1} (called $6s8d\ ^1D_2$ by McLennan and Crawford) is really $6s9s\ ^1S_0$ and that the true position of $6s8d\ ^1D_2$ is 148,465 cm^{-1}—with which we concur. A plot of the quantum defects for each of the series showed that the $^3S_1$ and $^3D_{1,2,3}$ series are unperturbed, so these were used to determine the ionization potential, i.e., that value of the latter was found by trial which made the ends of the quantum defect curves most nearly horizontal. The best value is $164{,}765 \pm 5$ cm^{-1}.

4. OTHER CONFIGURATIONS AND PERTURBATIONS

In addition to the regular series there are two other configurations which should give rise to observable lines: $5d^{10}6p^2$ and $5d^96s^26p$. Of the $6p^2$ configuration the three lower levels, $^3P_{0,1,2}$ were already known, and the position of a fourth, $\nu = 141{,}982$ cm^{-1}, was given us by Dr. McLay, who considered it to be the $^1S_0$ level. However there are three pieces of evidence that this is instead $6p^2\ ^1D_2$. The first is the strong transition to $6s6p\ ^3P_2$ (λ1246A) which would be forbidden from a $J = 0$ level. The second is the perturbation of the $6snd\ ^1D_2$ series shown in Fig. 1 (which is so strong as to depress the lower singlet D's beneath their triplets). The curve locates the perturbing

[9] Smith, Phys. Rev. **35**, 235 (1930).

TABLE II. *Classified lines of Tl II.*

INT.	λ(air)	ν(vac)	TRANSITION	Δν
3	9254 Å	10,803* cm⁻¹	$5f\,^1F_3 - 5g$	1
4	9225	10,837*	$5f\,^3F_4 - 5g$	2
2	9216	10,848*	$5f\,^3F_3 - 5g$	2
20	9130	10,950*	$5f\,^3F_3 - 5g$	−1
00	8935	11,189*	$5f\,^3F_3 - 5g$	0
00	8876	11,263*	$7p\,^1P_1 - 8s\,^3S_1$	0
1	8673.8	11,526*	$8p\,^3P_2 - 10s\,^3S_1$	−1
10	8664.1	11,539*	$8s\,^3S_1 - 5d^96s^26p\ 12_2$	2
8	8632.9	11,580*	$7p\,^3P_2 - 8s\,^3S_1$	0
0	8528.7	11,722*	$7s\,^1S_0 - 7p\,^3P_1$	0
8	8445.8	11,837*	$5d^96s^26p\ 5_1 - 7d\,^3D_1$	−1
2	8436.9	11,849*	$6d\,^3D_2 - 5d^96s^26p\ 6_3$	0
4	8389.9	11,916*	$5d^96s^26p\ 5_1 - 7d\,^3D_2$	0
1	8194.0	12,201*	$7p\,^1P_1 - 8s\,^1S_0$	3
0	7934.0	12,601*	$8p\,^1P_1 - 9d\,^1D_2$	1
1	7683.6	13,011*	$8p\,^3P_2 - 9d\,^3D_3$	−1
2	7144.9	13,992*	$6d\,^3D_1 - 5d^96s^26p\ 7_2$	0
00	7110.2	14,059*	$7p\,^3P_1 - 8s\,^3S_1$	0
4	7073.9	14,133	$8s\,^1S_0 - 9p\,^3P_1$	2
2	7070.8	14,139		
00	7035.6	14,209*	$7s\,^3S_1 - 7p\,^3P_0$	
10	6966.5	14,351#	$7p\,^3P_0 - 8s\,^3S_1$	2
4	6950.5	14,384#	$7s\,^3S_1 - 7p\,^3P_1$	0
2	6888.8	14,512#	$7s\,^1S_0 - 7p\,^1P_1$	1
0	6727.2(c)	14,861	$7p\,^1P_1 - 7d\,^1D_2$	0
0	6587.40	15,176*	$7p\,^3P_2 - 7d\,^1D_2$	
1	6555.70	15,250*	$8p\,^1P_1 - 10d\,^1D_2$	−1
2	6552.63	15,257*	$7d\,^1D_2 - 7f\,^1F_3$	1
0	6452.05	15,495*	$8s\,^3S_1 - 9p\,^3P_2$	0
3	6430.45	15,547#	$8s\,^3S_1 - 9p\,^1P_1$	2
10	6378.32	15,674#	$7p\,^1P_1 - 7d\,^3D_1$	−1
2	6289.74	15,895	$7p\,^1P_1 - 7d\,^3D_2$	0
1	6287.55	15,900*		
8d	6239.03	16,024#	$7p\,^3P_2 - 7d\,^3D_1$	
10	6179.98	16,177#	$7p\,^3P_2 - 7d\,^3D_3$	0
1	6170.03	16,203*	$7p\,^3P_2 - 7d\,^3D_2$	
4	6167.38	16,210*	$5f\,^1F_3 - 6g$	
1	6156.17	16,239*		
4	6154.03	16,245*	$5f\,^3F_4 - 6g$	
2	6151.02	16,253*		
1	6149.01	16,258*	$5d^96s^26p\ 7_2 - 9s\,^3S_1$	0
2	6113.87	16,352*	$5f\,^3F_2 - 6g$	−1
4	6111.50	16,358*	$5f\,^3F_3 - 6g$	
25	5949.48	16,804#	$7s\,^3S_1 - 7p\,^3P_2$	0
3	5828.59	17,152#	$7s\,^3S_1 - 7p\,^1P_1$	
2	5826.58	17,158#		
3	5774.00	17,314#	$7p\,^3P_1 - 7d\,^1D_2$	
2	5772.71	17,318		
4d	5643.00	17,716#	$6p^2\,^3P_2 - 6f\,^1F_3$	−1
4d	5640.06	17,725#	$6p^2\,^3P_2 - 6f\,^1F_3$	−1
2	5581.76	17,911*		
4	5490.47	18,208	$7s\,^1S_0 - 5d^96s^26p\ 5_1$	0
4	5448.77	18,347#	$7p\,^3P_1 - 7d\,^3D_1$	
2	5446.85	18,354#		
10	5410.97	18,476#	$7p\,^3P_1 - 7d\,^3D_2$	
7	5409.92	18,479		
15d	5384.85	18,566#	$7p\,^3P_0 - 7d\,^3D_1$	0
1	5206.29	19,202*	$6d\,^1D_2 - 5d^96s^26p\ 8_1$	0
6	5183.10	19,288		
6	5181.95	19,292	$6d\,^3D_3 - 5f\,^3F_3$	
0	5156.40	19,388		
25	5152.14	19,404#	$6d\,^3D_3 - 5f\,^3F_2$	−2
1	5143.81	19,435#	$6d\,^3D_3 - 5f\,^3F_4$	0
1	5099.71	19,604*	$6d\,^3D_3 - 5f\,^1F_3$	−2
25	5078.54	19,685#	$7p\,^1P_1 - 6p^2\,^1D_2$	1
3	5053.14	19,784#	$6d\,^3D_1 - 5f\,^3F_2$	0
3	5052.35	19,787#		
2	5040.55	19,833#	$6d\,^3D_2 - 5f\,^3F_2$	
15	4981.35	20,069#	$6d\,^3D_2 - 5f\,^1F_3$	0
2	4946.63	20,210#	$6d\,^3D_1 - 5f\,^3F_2$	0
1	4945.53	20,215		
0	4938.20	20,245*	$7s\,^3S_1 - 5d^96s^26p\ 4_2$	
4	4770.70	20,955#	$6p^2\,^3P_2 - 9p\,^1P_1$	−1
2	4765.75	20,977	$6d\,^1D_2 - 5f\,^3F_2$	0
1	4764.58	20,982		
0	4748.05	21,055	$7s\,^3S_1 - 5d^96s^26p\ 5_1$	
20	4737.05	21,104#	$6d\,^1D_2 - 5f\,^3F_2$	−1
0	4661.23	21,448	$6d\,^1D_2 - 5f\,^1F_3$	1
0	4660.75	21,450		
3	4500.03	22,216*	$5d^96s^26p\ 5_1 - 8d\,^3D_2$	
8	4490.77	22,262*	$5d^96s^26p\ 4_2 - 8d\,^3D_2$	1
2	4481.46	22,308*	$5d^96s^26p\ 5_1 - 8d\,^1D_2$	1
2	4480.80	22,311*	$5d^96s^26p\ 4_2 - 8d\,^3D_3$	

INT.	λ(air)	ν(vac)	TRANSITION	Δν
0	4462.02	22,404*		
0	4461.23	22,409*	$7p\,^3P_1 - 6p^2\,^1D_2$	
0	4460.70	22,412*		
2	4358.82	22,936*	$5d^96s^26p\ 7_2 - 10s\,^3S_1$	−2
6?	4340.53 H?	23,032	$6d\,^3D_3 - 8p\,^3P_1$	1
3	4339.55	23,037		
1	4313.22	23,178*	$7p\,^1P_1 - 9s\,^3S_1$	
2	4312.37	23,183*		
10	4306.80	23,213#	$5d^96s^26p\ 1_2 - 8s\,^3S_1$	
0	4292.72	23,289	$7p\,^1P_1 - 9s\,^1S_0$	1
1	4291.72	23,294	$6p^2\,^3P_2 - 7f\,^3F_3$	2
4d	4286.51	23,322*	$6p^2\,^3P_2 - 7f\,^3F_{2,4}$	−1
20	4274.98	23,385#	$6p^2\,^3P_2 - 7f\,^1F_3$	−1
3	4274.24	23,389	$7p\,^3P_2 - 9s\,^3S_1$	
2	4258.07	23,478*		
1	4256.82	23,485*	$6d\,^3D_3 - 8p\,^3P_2$	0
1	4256.09	23,489*		
3	4224.31	23,666*	$6p^2\,^3P_1 - 9p\,^3P_2$	
8	4223.05	23,673*		
0	4187.41	23,874*		
3	4177.46	23,931*	$6d\,^3D_3 - 8p\,^3P_2$	0
1	4176.75	23,935*		
0	4069.05	24,569*	$5d^96s^26p\ 7_3 - 7s\,^3S_1$	
3	3955.65	25,273#	$6d\,^3D_2 - 8p\,^1P_1$	
1	3909.5(c)	25,571#	$7p\,^1P_1 - 8d\,^3D_2$	−1
4	3901.53	25,624#	$7p\,^3P_2 - 8d\,^1D_2$	0
10	3887.15	25,718#	$7p\,^3P_2 - 8d\,^3D_3$	
6	3869.15	25,838#	$7p\,^3P_2 - 8d\,^3D_2$	1
			$\{6d\,^1D_2 - 8p\,^1P_1$	0
2	3851.87	25,954#	$\{7p\,^3P_1 - 9s\,^3S_1$	−2
2	3842.93	26,014#	$6d\,^3D_3 - 5d^96s^26p\ 10_3$	0
4	3836.95	26,055#	$7p\,^3P_1 - 9s\,^1S_0$	−1
10	3832.30	26,087*	$7p\,^3P_0 - 9s\,^3S_1$	−1
8	3793.95	26,350	$7p\,^1P_1 - 8d\,^1D_2$	1
2	3791.56	26,367*	$6d\,^3D_2 - 5d^96s^26p\ 10_2$	1
2	3619.49	27,621	$7s\,^1S_0 - 5d^96s^26p\ 8_1$	−1
3	3593.61	27,819*	$6d\,^1D_2 - 5d^96s^26p\ 10_2$	1
5	3567.67	28,022#	$5d^96s^26p\ 1_2 - 7d\,^1D_2$	0
4	3566.84	28,028#		3
9	3560.68	28,077#	$7p\,^3P_1 - 8d\,^3D_1$	
8	3540.08	28,240#	$7p\,^3P_2 - 8d\,^3D_2$	1
2	3536.70	28,267*	$7p\,^3P_2 - 8d\,^3D_1$	−1
1	3513.80	28,451*	$6d\,^3D_3 - 5d^96s^26p\ 12_3$	1
0	3487.81	28,663*	$6d\,^1D_2 - 5d^96s^26p\ 11_1$	−1
6d	3460.48	28,890*	$6d\,^3D_2 - 5d^96s^26p\ 12_2$	1
3	3453.83	28,945*	$7p\,^3P_1 - 8d\,^1D_2$	2
2	3384.47	29,538*	$6d\,^3D_1 - 5d^96s^26p\ 12_2$	0
6	3381.80	29,562#	$7p\,^3P_2 - 10s\,^3S_1$	−1
8	3381.00	29,569#		
15	3369.15	29,673#	$6p\,^1P_1 - 7s\,^3S_1$	
2	3365.48	29,705#	$6d\,^3D_3 - 6f\,^3F_4$	−1
2	3364.05	29,718	$6d\,^3D_3 - 6f\,^3F_3$	−3
4	3339.91	29,932*	$6d\,^3D_3 - 6f\,^1F_3$	1
8	3322.25	30,092#	$6d\,^1D_2 - 5d^96s^26p\ 12_2$	0
12	3321.04	30,102#	$6d\,^3D_2 - 6f\,^3F_3$	−1
12	3319.91	30,113#	$6d\,^3D_2 - 6f\,^3F_2$	−2
15	3291.01	30,377#	$6d\,^3D_2 - 6f\,^1F_3$	0
4	3243.68	30,820*	$6d\,^3D_1 - 6f\,^1F_2$	1
4	3237.96	30,875*	$7p\,^1P_1 - 9d\,^1D_2$	−1
15	3187.74	31,361*	$7p\,^3P_2 - 9d\,^3D_3$	−2
15	3186.56	31,373#	$6d\,^1D_2 - 6f\,^3F_3$	−2
15	3185.51	31,383#	$6d\,^1D_2 - 6f\,^3F_2$	−1
20	3091.56	32,337#	$6d\,^1D_2 - 6f\,^1F_3$	0
5	3029.01	33,004*	$6p\,^1P_1 - 7s\,^1S_0$	1
0	3015.52	33,152*	$7s\,^1S_0 - 8p\,^1P_1$	0
00	3007.05	33,245*	$7p\,^3P_2 - 11s\,^3S_1$	0
3	3004.71	33,271*	$7p\,^3P_1 - 9d\,^3D_1$	2
2	2987.95	33,458*	$7p\,^3P_1 - 9d\,^3D_2$	0
00	2973.30	33,623*	$7p\,^3P_0 - 9d\,^3D_1$	0
0	2957.85	33,799*	$7p\,^3P_1 - 9d\,^1D_2$	−1
4	2948.73	33,903*	$7p\,^1P_0 - 10d\,^1D_2$	1
0	2941.28	33,989*	$6d\,^1D_2 - 9p\,^1P_1$	0
2	2928.21	34,141*	$7p\,^3P_2 - 10d\,^3D_3$	0
0	2854.25	35,025*	$7s\,^3S_1 - 8p\,^3P_1$	1
1	2853.86	35,030*	$5d^96s^26p\ 1_2 - 9s\,^3S_1$	
10	2849.80	35,081*		
2	2833.31	35,284	$7s\,^3S_1 - 8p\,^3P_2$	−2
0	2807.75	35,605*	$6d\,^3D_3 - 7f\,^3F_{3,4}$	0
2	2806.80	35,617*	$7p\,^3P_1 - 11s\,^3S_1$	0
3	2801.81	35,681	$7s\,^1S_0 - 5d^96s^26p\ 11_1$	1
1	2794.59	35,773*	$6d\,^3D_3 - 7f\,^3F_{2,4}$	1
3	2780.25	35,957*	$7s\,^3S_1 - 8p\,^1P_1$	−2
00	2746.01	36,406*	$6d\,^3D_1 - 7f\,^3F_2$	0
			$7p\,^3P_1 - 10d\,^3D_2$	0

* These lines are newly located and classified.
\# Hyperfine structure, here unresolved, has been observed in these lines by previous investigators.
(a) This line coincides with $6p_{\frac{1}{2}} - 13d$ of Tl I.
(b) This line coincides with the third order of λ670.87.
(c) These wave-lengths are taken from previous lists, and included for the sake of completeness, but they were not observed by us.
d An unresolved doublet.
R, *r* Reversed lines.
In the above term designations the "6*s*" has been omitted from the symbols for the 6*snl* configurations.

TABLE II.—*Continued.*

INT.	λ(air)	ν(vac)	TRANSITION	Δν
00	2731.29	36,602*	$7p\ ^3P_2 - 10d\ ^3D_1$	0
3	2705.55(c)	36,950	$6d\ ^1D_2 - 7f\ ^3F_{3,4}$	
2	2703.36	36,980*	$6d\ ^1D_2 - 7f\ ^1F_3$	0
2	2682.61	37,266*	$5d^96s^26p\ 1_2 - 8d\ ^3D_2$	1
4	2676.03	37,358*	$5d^96s^26p\ 1_2 - 8d\ ^3D_3$	
4	2675.76	37,362*		
2	2604.32	38,386*	$7s\ ^3S_1 - 5d^96s^26p\ 11_1$	
1	2604.01	38,391*		
20	2530.86	39,500≠	$6p\ ^1P_1 - 6d\ ^1D_2$	0
4	2507.70	39,865*	$7s\ ^3S_1 - 5d^96s^26p\ 12_2$	
3	2507.39	39,870*		
4?	2477.40(a)	40,353*	$7s\ ^1S_0 - 9p\ ^3P_1$	0
6	2469.03	40,489≠	$6p\ ^1P_1 - 6d\ ^3D_1$	2
8	2451.83	40,773≠	$6p\ ^1P_1 - 6d\ ^3D_2$	3
2	2434.28	41,067*	$7s\ ^1S_0 - 9p\ ^1P_1$	0
2	2403.57	41,592*		
0	2394.71	41,746	$6p\ ^1P_1 - 6p^2\ ^3P_0$	−2
0	2318.20	43,124*	$7s\ ^3S_1 - 9p\ ^3P_1$	0
30	2298.04	43,502≠	$6p\ ^3P_2 - 7s\ ^3S_1$	2
4	2292.97	43,598*	$7s\ ^3S_1 - 9p\ ^3P_2$	−2

INT.	λ(vac)	ν(vac)	TRANSITION	Δν
0	2070.20	48,305*	$7s\ ^3S_1 - 10p\ ^3P_2$	0
5?	2012.57(b)	49,688	$6p\ ^1P_1 - 6p^2\ ^3P_1$	10
25R	1908.64	52,393	$6s^2\ ^1S_0 - 6p\ ^3P_1$	0
8	1892.72	52,834	$6p\ ^3P_1 - 7s\ ^3S_1$	2
3	1881.15	53,159	$6p\ ^1P_1 - 6p^2\ ^3P_2$	2
4	1871.39	53,436	$6p\ ^3P_2 - 6d\ ^1D_2$	1
3	1837.45	54,423	$6p\ ^3P_2 - 6d\ ^3D_1$	1
5	1827.86	54,709	$6p\ ^3P_2 - 6d\ ^3D_2$	4
12R	1814.85	55,101	$6p\ ^3P_2 - 6d\ ^3D_3$	0
4	1798.36	55,606	$6p\ ^3P_1 - 7s\ ^1S_0$	3
10R	1792.76	55,780	$6p\ ^3P_0 - 7s\ ^3S_1$	6
2	1726.92	57,908*	$6p\ ^1P_1 - 8s\ ^3S_1$	1
3	1705.55	58,632*	$6p\ ^1P_1 - 8s\ ^1S_0$	0
4	1633.23	61,228	$6p\ ^1P_1 - 7d\ ^1D_2$	−3
1	1606.21	62,258*	$6p\ ^1P_1 - 7d\ ^3D_1$	−9
1	1602.54	62,401*	$6p\ ^1P_1 - 7d\ ^3D_2$	8
7R	1593.26	62,764	$6p\ ^3P_1 - 6d\ ^1D_2$	−3
4	1572.16	63,607	$6p\ ^3P_2 - 6p^2\ ^3P_1$	−6
10R	1568.57	63,756	$6p\ ^3P_1 - 6d\ ^3D_1$	2
15R	1561.58	64,038	$6p\ ^3P_1 - 6d\ ^3D_2$	1
4	1538.19	65,012	$6p\ ^3P_1 - 6p^2\ ^3P_0$	−3
10R	1507.82	66,321*	$6p\ ^1P_1 - 6p^2\ ^1D_2$	−1
10R	1499.30	66,698	$6p\ ^3P_0 - 6d\ ^3D_1$	2
5r	1490.50	67,092	$6p\ ^3P_2 - 6p^2\ ^3P_2$	0
3	1433.60	69,755°	$6p\ ^1P_1 - 9s\ ^3S_1$	0
2	1430.00 Hg?	69,930*	$6p\ ^1P_1 - 9s\ ^1S_0$	−1
4R	1391.88	71,845*	$6p\ ^3P_2 - 8s\ ^3S_1$	2
1	1390.05	71,940*	$6p\ ^1P_1 - 8d\ ^3D_1$	−2
0	1389.08	71,990*	$6p\ ^1P_1 - 8d\ ^3D_2$	−2
10R	1373.52	72,806*	$6p\ ^1P_1 - 8d\ ^1D_2$	1
3	1370.88	72,946	$6p\ ^3P_0 - 6p^2\ ^3P_1$	1
8R	1330.40	75,165	$6p\ ^3P_2 - 7d\ ^1D_2$	−1
25R	1321.71	75,660	$6s^2\ ^1S_0 - 6p\ ^1P_1$	0
3r	1317.75	75,887	$6p\ ^3P_0 - 6p^2\ ^3P_1$	0

INT.	λ(vac)	ν(vac)	TRANSITION	Δν
2	1312.42	76,195*	$6p\ ^3P_2 - 7d\ ^3D_1$	−7
8R	1310.20	76,324	$6p\ ^3P_2 - 7d\ ^3D_2$	−4
4R	1308.50	76,423	$6p\ ^3P_1 - 6p^2\ ^3P_2$	−1
15R	1307.50	76,482	$6p\ ^3P_2 - 7d\ ^3D_3$	4
4r	1289.58	77,545*	$6p\ ^1P_1 - 9d\ ^1D_2$	5
2	1254.34	79,723*		
5R	1246.00	80,257*	$6p\ ^3P_2 - 6p^2\ ^1D_2$	0
3	1242.00	80,515*	$6p\ ^1P_1 - 10d\ ^1D_2$	−2
8	1231.81	81,181*	$6p\ ^3P_1 - 8s\ ^3S_1$	6
2	1221.02	81,899*	$6p\ ^3P_1 - 8s\ ^1S_0$	0
1	1212.47	82,476*	$6p\ ^1P_1 - 11d\ ^1D_2$	0
12R	1194.84	83,693*	$6p\ ^3P_2 - 9s\ ^3S_1$	3
3r	1188.83	84,116*	$6p\ ^3P_0 - 8s\ ^3S_1$	−1
10R	1183.41	84,501	$6p\ ^3P_1 - 7d\ ^1D_2$	3
5R	1169.17	85,531	$6p\ ^3P_1 - 7d\ ^3D_1$	−3
10R	1167.43	85,658	$6p\ ^3P_1 - 7d\ ^3D_2$	−2
2	1164.50	85,874*	$6p\ ^3P_2 - 8d\ ^3D_1$	−3
4R	1163.80	85,925*	$6p\ ^3P_2 - 8d\ ^3D_2$	−2
15R	1162.55	86,018	$6p\ ^3P_2 - 8d\ ^3D_3$	−4
3	1152.90	86,738*	$6p\ ^3P_2 - 8d\ ^1D_2$	−2
10R	1130.17	88,482*	$6p\ ^3P_0 - 7d\ ^3D_1$	6
4	1113.06	89,850*	$6p\ ^3P_2 - 10s\ ^3S_1$	7
2	1097.43	91,130*	$6p\ ^3P_2 - 9d\ ^3D_2$	8
3r	1096.73	91,188*	$6p\ ^3P_2 - 9d\ ^3D_3$	7
1	1093.25	91,470*	$6p\ ^3P_2 - 9d\ ^1D_2$	−5
5R	1074.97	93,026*	$6p\ ^3P_1 - 9s\ ^3S_1$	4
3	1072.99	93,198*	$6p\ ^3P_1 - 9s\ ^1S_0$	0
2	1070.08	93,451*	$6p\ ^3P_2 - 11s\ ^3S_1$	−5
2	1060.93	94,257*	$6p\ ^3P_2 - 10d\ ^3D_2$	0
3	1060.53	94,292*	$6p\ ^3P_2 - 10d\ ^3D_3$	−1
8R	1050.30	95,211*	$6p\ ^3P_1 - 8d\ ^3D_1$	2
10R	1049.73	95,263*	$6p\ ^3P_1 - 8d\ ^3D_2$	4
2	1044.37	95,752*	$6p\ ^3P_2 - 12s\ ^3S_1$	−4
3r	1042.00	95,969*	$6p\ ^3P_0 - 9s\ ^3S_1$	5
3r	1040.88	96,072*	$6p\ ^3P_1 - 8d\ ^1D_2$	10
2	1038.28	96,313*	$6p\ ^3P_2 - 11d\ ^3D_2$	0
8R	1018.85	98,150	$6p\ ^3P_0 - 8d\ ^3D_1$	−1
3	1008.33	99,174*	$6p\ ^3P_1 - 10s\ ^3S_1$	−1
4r	995.54	100,448*	$6p\ ^3P_1 - 9d\ ^3D_2$	−6
1	991.99	100,808*	$6p\ ^3P_1 - 9d\ ^1D_2$	1
3	979.30	102,114*	$6p\ ^3P_0 - 10s\ ^3S_1$	−3
4	967.42	103,368*	$6p\ ^3P_0 - 9d\ ^3D_1$	0
4	965.41	103,583*	$6p\ ^3P_1 - 10d\ ^3D_2$	−6
1	963.60	103,778*	$6p\ ^3P_1 - 10d\ ^1D_2$	−6
1	951.55	105,092*	$6p\ ^3P_1 - 12s\ ^3S_1$	4
2	946.70	105,630*	$6p\ ^3P_1 - 11d\ ^3D_2$	0
2	945.79	105,732*	$6p\ ^3P_0 - 11s\ ^3S_1$	2
2	938.82	106,517*	$6p\ ^3P_0 - 10d\ ^3D_1$	5
5R	836.34	119,569*	$6s^2\ ^1S_0 - 7p\ ^3P_1$	−7
10R	817.18	122,372	$6s^2\ ^1S_0 - 7p\ ^1P_1$	−7
4r	792.40	126,199	$6s^2\ ^1S_0 - 5d^96s^26p\ 5_1$	−5
4r	744.27	134,360*	$6s^2\ ^1S_0 - 5d^96s^26p\ 8_1$	−2
4	717.55	139,363*	$6s^2\ ^1S_0 - 8p\ ^3P_1$	−2
5R	709.23	140,998*	$6s^2\ ^1S_0 - 8p\ ^1P_1$	−2
15R	696.30	143,616*	$6s^2\ ^1S_0 - 5d^96s^26p\ 11_1$	4
4	674.10	148,346*	$6s^2\ ^1S_0 - 9p\ ^3P_1$	−3
5R	670.87	149,060*	$6s^2\ ^1S_0 - 9p\ ^1P_1$	−3
3	650.90	153,633*	$6s^2\ ^1S_0 - 10p\ ^1P_1$	0
1	639.08	156,475*	$6s^2\ ^1S_0 - 11p\ ^1P_1$	0

term, which can only be $6p^2\ ^1D_2$, in the region of the new level in question. Thirdly, the curve for the $6sns\ ^1S_0$ series (Fig. 2), which can only be perturbed by $6p^2\ ^1S_0$, points to the location of the latter somewhere above $6s9s\ ^1S_0$—probably around 151,000 cm^{-1}. For these reasons we have called the level at 141,982 cm^{-1} $6p^2\ ^1D_2$. (However, since the perturbation is so strong, the "$6s7d\ ^1D_2$" and "$6p^2\ ^1D_2$" levels must each have both *sd* and p^2 properties, so that these two names might very well be interchanged, and have really become meaningless.) The $6p^2\ ^1S_0$ level could not be located.

To the three previously known levels of $5d^96s^26p$ we have added six, leaving from the predicted twelve levels only three missing. As these three, with $J=0$, 3, and 4, should probably give rise each to only one observable line they could not be reliably established. The distribution of the levels found indicates near-*jj* coupling and is very similar to that of the d^9p levels of the Pt I sequence recently studied by Mack and Fromer,[10] and Goble,[11] as shown by the comparison with Au II in Fig. 3. However, differences between these two configurations should arise not only from differences in coupling between Tl II and Au II, but from displacements of some of the thallium levels due to interactions with the odd

[10] Mack and Fromer, Phys. Rev. **48**, 357 (1935).
[11] Goble, Phys. Rev. **48**, 346 (1935).

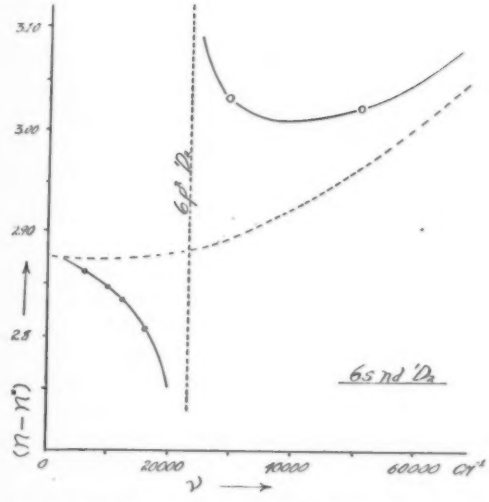

FIG. 1. Perturbation of the singlet D series by $6p^2\,{}^1D_2$.

sp and sf series. The effect of the perturbations upon these series is very marked. Fig. 2 shows the disturbance of the $^1P_1$ series by 8_1, (the reaction upon the latter level being evident in Fig. 3). The $7p\,{}^3P_1$ and the $7p\,{}^3P_0$ are probably displaced downwards slightly by 5_1 and the missing $J=0$ level. The repulsion due to the levels 10_2 and 12_2, lying between $5f$ and $6f$, displaces $5f\,{}^3F_3$ downwards and $6f\,{}^3F_{2,3}$ upwards—leading to the partial inversions apparent in these configurations.

5. Hyperfine Structure

The dispersion of our plates did not permit accurate measurements of the hyperfine structure. However, McLennan and Crawford's[4] h.f.s. term separations were confirmed to the extent that those of our new lines whose structure was large enough to be observed fitted into the system as transitions to just those levels known to have the largest separations. In the case of the $6f$ multiplet the large h.f.s. explains the nearly equal intensities of the lines from $6f\,{}^3F_3$ and $6f\,{}^1F_3$ to $6d\,{}^{3,1}D_2$. These levels, $6d\,{}^{3,1}F_2$, are so near together that their h.f.s. components can interact, since their F values are the same,

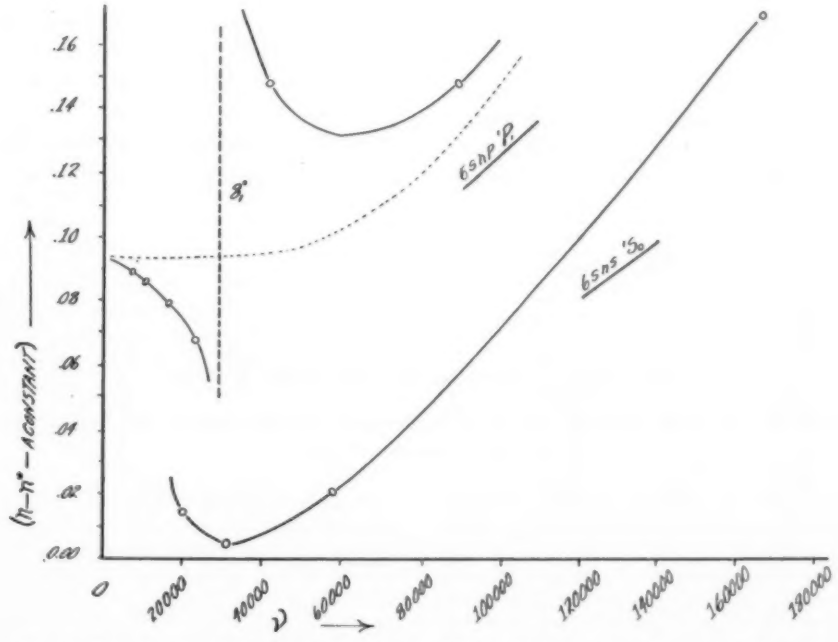

FIG. 2. Perturbation of the singlet P series by $5d^96s^26p8_1$, and of the singlet S series by the unlocated $6p^2\,{}^1S_0$. A constant has been subtracted from the quantum defects (4.20 for the S, and 3.63 for the P series) in order to bring both curves into the same figure.

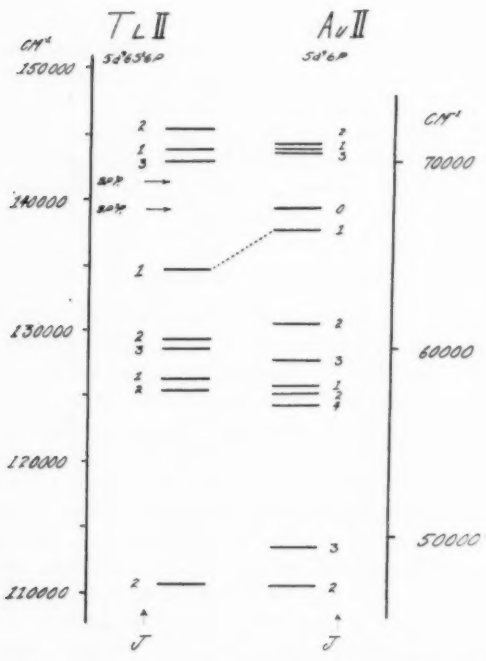

FIG. 3. A comparison of the configurations $5d^9 6s^2 6p$ of Tl II and $5d^9 6p$ of Au II. The arrows show the positions of $6s8p\ ^3,^1P_1$ which probably cause the large shift in the middle $J=1$ level. Three of the Tl levels are still unlocated.

causing the two terms to share their properties—each being partly ^1F and partly ^3F. With the newly found 6*g* configuration the ratio of h.f.s. to multiplet separation is even larger. The 5*f*–6*g* transitions indicate the presence of two 6*g* levels, separated by about 6 cm^{-1}. These are probably the two hyperfine structure components, the multiplet structure being too small to observe. A similar case of h.f.s. larger than multiplet structure has been found in Al II.[12] Structure could not be observed in 5*g* since the transitions fall in a region of low dispersion.

6. Remaining Lines

In the entire spectrum there now remain only five unclassified lines of intensity greater than 1, these being also included in Table II. Besides these five our plates showed one important line (2210.75A; 45,219 cm^{-1}; int. 10) which must belong to the arc spectrum. There seems no possible place for it in the Tl II system; furthermore it has been previously observed as reversed in the arc by Kayser and Runge.[13] An arc line of this frequency, and reversed, can only be a transition ending on the ground state. The initial level is thus established as a new even term in Tl I (with $J=\frac{1}{2}$ or $1\frac{1}{2}$), at an absolute value of 4045 cm^{-1}, and probably belongs to the $6s6p^2$ configuration expected in that region.

We wish to express our appreciation to Dr. S. A. Goudsmit for his interest in the work and to Dr. McLay for the location of the levels previously mentioned.

[12] Paschen, Preuss. Akad. Wiss. Berlin, Ber. **32**, 502 (1932).
[13] Kayser, *Handbuch der Spektroscopie*, Vol. 6, p. 709.

JANUARY 15, 1936 PHYSICAL REVIEW VOLUME 49

Strontium Deuteride and Hydride Spectra

WILLIAM W. WATSON, *Yale University*, AND W. R. FREDRICKSON AND M. E. HOGAN, JR., *Syracuse University*

(Received November 30, 1935)

The analyses of the *B* and *C* band systems of SrD and of a portion of the *D* system of SrH are presented. $B_e^*=1.9427$ for SrD and 3.8788 for SrH for the normal $^2\Sigma$ state. The ratio of these, 0.50635, shows about the expected departure from equality with the ratio $\rho^2=0.50603$ of the reduced masses. The spin doubling of this SrD state is regular, $\gamma_0=+0.0613$ being almost exactly in the ratio ρ^2 with the value for SrH. The spin doubling of the $B\,^2\Sigma$ state of SrD departs markedly from the usual linear variation with $K+\frac{1}{2}$. Multiple perturbations occur in the (0,0) *C* band of SrD, and there is a sharp cut-off of the branches at $K'=29$. For this $C\,^2\Sigma$ state $B_0\leqq 1.95$, but exact analysis is hindered by the lack of any unperturbed lines. Two bands $(v',2)$ and $(v',3)$, with a common upper state, of the $D\,^2\Sigma\rightarrow N\,^2\Sigma$ "many-lined" SrH system have been analyzed. In this *D* state, for which $B_v=1.913$, large irregular perturbations occur. Electronic configurations are discussed.

Introduction

WE have recently described[1] three new band systems of the SrH molecule in the visible and near ultraviolet regions of the spectrum, supplementing the previous analysis[2] of the (0,0) bands of the $B\,^2\Sigma \rightarrow N\,^2\Sigma$ system at 7020A and the $A\,^2\Pi \rightarrow N\,^2\Sigma$ system at 7508A. Of the newly discovered systems we were able to present fairly complete quantum analyses of the abbreviated and strongly perturbed (0,0) and (0,1) $C\,^2\Sigma \rightarrow N\,^2\Sigma$ bands at 3808A and 3984A, respectively, as well as of the (0,0) $E\,^2\Pi \rightarrow N\,^2\Sigma$ band at 5323A. Very probably, however, the upper state of the latter system does not correspond to the upper state of the $E\,^2\Pi \rightarrow N\,^2\Sigma$ bands of CaH at 4900A,[3] and so should be dubbed $F\,^2\Pi$. We give the argument for this change below.

The present report is concerned with the deuteride modification of the B and C systems and with a partial analysis of the complicated "many-lined" D system of SrH. The experimental procedure was similar to that described in the earlier papers. Heavy hydrogen was obtained by vacuum distillation of the vapor of 99 percent heavy water onto metallic calcium. To minimize contamination of the spectrograms with SrH band lines, light from the first few minutes of burning of the arc between a water-cooled copper cathode and an anode of metallic strontium was not used. The gas was then pumped out of the arc chamber, fresh deuterium was admitted to about 7 cm of Hg pressure, and the exposure begun. From time to time during the exposure additional deuterium gas was added because of the consumption of gas in the arc. The few SrH lines occurring on the plates are so faint that they offer no hindrance in the measurement and analysis of the SrD bands. The dispersion for these spectrograms varies from 2.2A per mm for the B bands at 7000A to 2.5A per mm for the C band at 3800A.

The B System of SrD

The analysis of the (0,0) and (1,1) $B\,^2\Sigma \rightarrow N\,^2\Sigma$ bands of SrD has been carried out both to provide lower state combination differences as an aid in analyzing the strongly perturbed (0,0) C band (cf. below) and also for the comparison of constants of the SrH and SrD molecules in connection with isotope effect theory. For this second purpose we have had to provide also the analysis of the (1,1) SrH B band to go with the data for the (0,0) SrH band given in reference 2. In Table I are listed the assignments of frequencies for the (1,1) SrH band, in Table II those for the (0,0) and (1,1) SrD bands. The values of all of the constants of the rotational energy term formula for these states are assembled in Table V. A new calculation of B_0^* for the normal state of SrH yields the value 3.6344, replacing the less accurate value given in reference 2.

In comparing the constants of the two isotopic molecules it should be remembered that all the B's as determined by application of the usual rotational energy formulas are really B^* values,

TABLE I. *Assignment of frequencies in the (1,1) $B\,^2\Sigma \rightarrow N\,^2\Sigma$ band of SrH* (cm^{-1} units).

$J''+\frac{1}{2}$	P_1	R_1	P_2	R_2
1		14377.91		14393.18
2		83.82		403.90
3	14356.63	89.28	14358.61	14.62
4	48.60	96.41	54.80	25.88
5	40.60	403.90	51.28	37.11
6	32.60	11.14	48.05	48.85
7	25.77	18.73	45.29	60.63
8	19.06	26.73	43.00	72.73
9	12.34	35.25	40.60	85.07
10	06.51	43.72	38.60	97.82
11	00.85	52.71	37.21	510.65
12	295.62	62.06	35.99	23.59
13	90.90	71.66	35.13	37.01
14	86.37	81.60	34.20	50.17
15	82.28	91.77	33.80	63.48
16	76.68	502.34	34.20	76.38
17	75.49	13.05	34.20	
18	72.70	24.20	34.00	
19	70.30		35.13	
20	67.92	47.35	35.99	
21	66.08	58.70	37.21	
22	64.65	70.63	38.60	
23	63.56	82.71	40.60	
24	62.89	95.02	42.00	
25	62.33	607.50	43.72	
26	62.33	20.14	45.29	
27	62.89	32.82	47.13	
28	64.65	45.68	49.25	
29	66.08	58.56	51.28	
30	67.92	71.50	53.80	
31	70.30	84.47	57.01	
32	72.50	97.55	60.24	
33	74.89	711.04	63.75	
34	78.03			

[1] W. R. Fredrickson, M. E. Hogan, Jr. and W. W. Watson, Phys. Rev. **48**, 602 (1935).
[2] W. W. Watson and W. R. Fredrickson, Phys. Rev. **39**, 765 (1932).
[3] W. W. Watson and R. L. Weber, Phys. Rev. **48**, 732 (1935).

TABLE II. *Assignment of frequencies in the B $^2\Sigma \rightarrow N\ ^2\Sigma$ system of SrD.*

$J''+\frac{1}{2}$	(0,0) BAND				(1,1) BAND			
	P_1	R_1	P_2	R_2	P_1	R_1	P_2	R_2
1		14346.79						
2		49.51						
3	14335.69	52.77				14368.61		
4	31.43	56.00		14370.59		71.77		
5	27.12	59.36		76.42		75.14		
6	22.97	62.99	14330.16	82.29		78.71		
7	18.81	66.87	28.74			82.29	14345.06	
8	14.96	70.59	27.12	94.34		86.04	43.54	14409.70
9	11.35	74.58	25.72	400.50		89.99	42.12	
10	07.97	78.71	24.43	06.71		93.95	40.85	21.77
11	04.63	83.06	23.34	13.25	14320.83	98.16	39.61	27.89
12	01.52	87.52	22.34	19.94	17.88	402.58	38.68	34.58
13	298.56	92.17	21.47	26.60	14.96	06.90	37.88	
14	95.65	96.94	20.83	33.43	12.19	11.59	37.18	47.79
15	93.03	401.83	20.33	40.34	09.52	16.41	36.67	54.57
16	90.62	06.90	19.98	47.54	07.04	21.32	36.16	61.33
17	88.36	12.08	19.79	54.57	04.63	26.33	35.89	68.32
18	86.21	17.43	19.79	61.77	02.54	31.50	35.69	75.34
19	84.25	22.88	19.79	69.26	00.68	36.83	35.69	82.49
20	82.50	28.52	19.98	76.78	298.67	42.36	35.69	89.67
21	80.87	34.27	20.33	84.42	97.02	47.79	35.89	97.02
22	79.44	40.15	20.83	92.00	95.65	53.53	36.16	504.26
23	78.09	46.14	21.47	99.78	94.22	59.34	36.67	
24	76.95	52.28	22.15	507.58	93.03	65.26	37.18	19.42
25	76.01	58.53	22.97	15.50	92.07	71.31	37.88	26.92
26	75.26	64.87	23.93	23.39	91.19	77.48	38.68	34.28
27	74.64	71.31	24.98	31.45	90.62	83.75	39.61	
28	74.22	77.90	26.19	39.46	89.99	90.09		
29	73.81	84.59	27.43	47.42	89.48	96.56		
30	73.81	91.43	28.74	55.34	89.19	503.10		
31	73.81	98.32	30.16	63.48	89.19	09.77		
32	74.22	505.31	31.43		89.19	16.51		
33	74.64	12.42	33.40		89.48	23.39		
34	75.26	19.57			89.99	30.29		
35	76.01	26.92			90.62	37.03		
36	76.95	34.28			91.19	44.22		
37	77.93	41.66			92.07	51.33		
38	79.03	49.16			93.03	58.56		
39	80.33	56.78			94.22	65.80		
40	81.74	64.38			95.24	73.06		
41	83.25	72.18			96.61	80.45		
42	84.95	79.94			98.00	87.80		
43	86.76	87.80			99.49	95.20		
44	88.68	95.67			301.17	602.71		
45	90.62	603.65			02.83	10.22		

differing from true B_v and B_e values for several reasons. Accurate calculation of the corrections to these B_e^*'s to obtain true B_e values, which should be in the ratio of the reduced masses for the two isotopes, is impossible for these states.[4] Comparison of some of the observed energy constants for the two molecules, however, is of some interest. By using atomic weights 87.63, 1.0081 and 2.0148 for Sr, H and D, respectively, the ratio ρ^2 of the reduced masses of SrH and SrD is 0.50603, $\rho = 0.71136$ and $\rho^3 = 0.35997$. The ratio of the B_e^* values for the $N\ ^2\Sigma$ states of the two molecules is 0.50635, which is larger than ρ^2 by about the expected amount as judged by the results for the hydrogen isotope effect for other molecules. For the B states the B_e^*'s have a ratio 0.50085, the large deviation from ρ^2 in the opposite sense reflecting the large "pure precession" interaction with the neighboring $A\ ^2\Pi$ state. If one corrects these B^*'s by addition of the Λ-doubling constants q_0 of the $^2\Pi$ state[5] ($q_0 = -0.398$ for SrH and -0.102 for SrD), the resulting $B_e = 3.4808$ for SrH and 1.8407 for SrD have the large ratio 0.52882. The excess of this figure over the ρ^2 value would seem to indicate

[4] For a discussion of the relative magnitude of these corrections for some hydride molecules, cf. W. W. Watson, Phys. Rev. **49**, 70 (1936).

[5] For similar calculations for CaH/CaD, cf. W. W. Watson, Phys. Rev. **47**, 27 (1935).

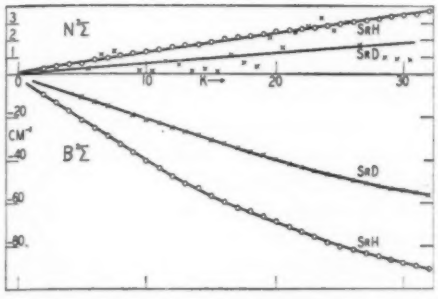

FIG. 1. Comparison of spin doubling in the $N\,^2\Sigma$ and $B\,^2\Sigma$ states for SrH and SrD. The relatively large spread of the values about their mean for the $N\,^2\Sigma$ state of SrD is due to the necessary indirect computation with the aid of the relation $\Delta\nu_{12}(K)=\frac{1}{2}[\Delta_2T_1(K+\frac{1}{2})-\Delta_2T_2(K-\frac{1}{2})](K+\frac{1}{2})$.

strong alteration of the effective potential function for this state because of the perturbing influence of the numerous other near-lying states of the SrH molecule.

The quantity α of the relation $B_v=B_e[1-\alpha(v+\frac{1}{2})]$ should, according to the simple isotope theory, vary as ρ^3. Any change in this variation due to the fact that α is determined from the experimental B^* values should to a first order be negligible. We find that for the $N\,^2\Sigma$ state $\alpha=0.0814$ for SrH. Multiplication by ρ^3 gives 0.0293, as compared to the observed value 0.0292 for SrD. The ratio of the spin doubling constants γ of the relation $\Delta\nu_{12}(K)=\gamma(K+\frac{1}{2})$ for the two molecules should be ρ^2 according to the theory of spin doubling. For the normal state of SrH this linear variation of $\Delta\nu_{12}(K)$ with $K+\frac{1}{2}$ does exist, with $\gamma_0=+0.122$. $\rho^2\times0.122=0.062$, which is almost exactly the observed value $+0.061$ for the $v''=0$ level of SrD. In the $B\,^2\Sigma$ state, however, neither molecule exhibits this ordinary spin doubling. In Fig. 1 the course of the doubling in these states is plotted as a function of K. The slopes of these curves for the B state are large, negative and decrease markedly with increasing molecular rotation. The large, negative γ_0 values reflect the pure precession interaction with the $A\,^2\Pi$ state just below this B state, and the rapid change in slope must be due to the perturbing influence of other close SrH levels. For the B state of SrD $\gamma_0=-2.01$ for $K<10$, while at $K=30$ this slope has dropped to -1.14. This anomalous behavior of the spin doubling for SrD is in contrast with the normal linear variation in the corresponding state of CaD.[5]

THE C SYSTEM OF SrD

As is to be expected from the closer spacing of the rotational levels and the probable near equality of the frequencies of vibration in the two electronic states of each molecule, the (0,0) $C\,^2\Sigma\rightarrow N\,^2\Sigma$ band of SrD has even more perturbations than has the corresponding SrH band[1] and is found at almost exactly the same wave-length. In fact there are no unperturbed lines in this SrD band, which makes the determination of the exact magnitude of the perturbations and the rotational energy constants of the C state rather difficult. We list in Table III the frequencies, intensities and quantum assignments of all the observed lines in this band. Fig. 2 is a comparison of microphotometer traces of these

TABLE III. *Assignment of frequencies in the* $C\,^2\Sigma\rightarrow N\,^2\Sigma$ (0,0) *band of SrD* (cm^{-1} units). Numbers in brackets are estimated intensities.

K''	R	P	K''	R	P
0	26291.02(0)		16	93.83(2)	56.38(7)
1	94.44(1)		17	98.57(4)	54.83(7b)
2	93.69(1)	26280.05(2)	18	406.69(2)	65.74(4b)
				07.85(2)	
3	96.10(3)	76.06(2)			
			19	14.53(1)	63.63(3)
4	300.80(2)	68.07(1)		15.81(1)	
5	05.39(1)	62.66(1)	20	27.01(1)	64.58(1)
	06.18(2)			29.06(1)	65.74(4b)
6	11.69(2)	60.22(3b)	21	36.40(2)	65.74(4b)
				37.05(2)	66.67(2)
7	17.21(2)				
		58.38(12)	22	46.11(2)	71.13(2)
8	22.68(2)	56.38(7)		47.07(2)	73.04(4)
			23	57.10(2)	73.04(4)
9	26.43(1)	54.83(7b)		57.44(2)	74.18(2)
10	44.74(1)	52.87(4)	24	67.36(1)	76.06(2)
				67.97(1)	77.18(2)
11	48.53(2)	49.20(1)			
			25	74.69(1)	80.05(2)
12	54.89(3)	60.22(3b)		76.58(1)	80.55(2)
13	61.92(2)	56.38(7)	26	90.92(2b)	83.61(2)
	62.25(2)			91.78(1)	84.24(2)
14	69.48(2)	56.38(7)	27		84.24(2)
				500.40(2)	86.13(1b)
15	26375.54(2)				
		26256.38(7)	28	16.18(2)	
				16.78(1)	93.69(1)

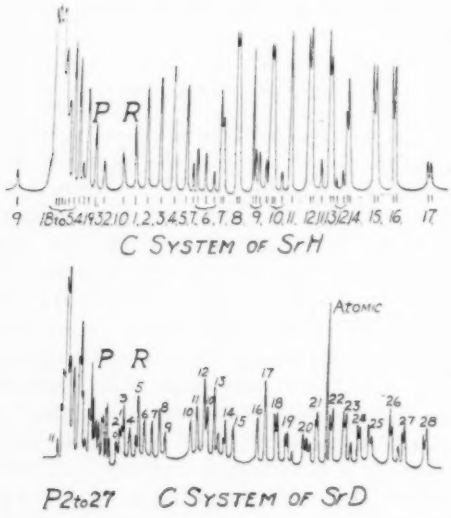

FIG. 2. Microphotometer traces of the $C\,^2\Sigma \rightarrow N\,^2\Sigma$ (0,0) bands of SrH and SrD.

(0,0) C bands of SrH and SrD. The (0,1) SrD band does not occur with appreciable intensity on our spectrograms.

Even though all the lines are perturbed, some violently, producing a confusion of lines in the region of the P branch, assignments of K values may be made with the aid of lower state combination differences known from the analysis of the B bands. As in the SrH band, doubling of some of the lines occurs in an irregular manner. We estimate from the $\Delta_2 T'(K)$ values, none of which are undisturbed by perturbations however, that $B_0^* \leqq 1.95$ for this C state. The sharp cut-off of the branches of the band at $K'=29$ comes at closely the same energy as the corresponding cessation at $K'=19$ in the SrH band. In view of the fact that this breaking-off of the band very probably represents predissociation into the continuum of the less stable $D\,^2\Sigma$ state, the multiplicity of the perturbations is somewhat puzzling. Levels of still another state, such as the $E\,^2\Pi$ or indicated $F\,^2\Pi$ must also be situated so as to perturb these C levels.

THE D SYSTEM OF SrH

The D system of SrH is a complicated, "many-lined" spectrum extending from 5000A to 6700A and containing few regularities. There are no evident series of doublets as in the corresponding CaH D system,[6] probably due both to the larger spin doubling in SrH and to the greater number of perturbations. We have analyzed two bands in this complex, the $(v',2)$ and $(v',3)$ bands, which have a common upper state but with v' unknown.

[6] B. Grundström, Zeits. f. Physik **75**, 302 (1932).

TABLE IV. *Assignment of frequencies in $(v',2)$ and $(v',3)$ $D\,^2\Sigma \rightarrow N\,^2\Sigma$ bands having a common upper state.*

$J''+\frac{1}{2}$	$(v',2)$ BAND				$(v',3)$ BAND			
	P_1	R_1	P_2	R_2	P_1	R_1	P_2	R_2
1				18446.21		17341.39		17342.20
2	18435.31	18446.21	18425.26	43.94	17330.95	42.22	17320.95	40.12
3	25.26	43.94	11.50	37.51	20.95	40.12	08.35	35.09
4	11.50	37.51	395.20	29.63	08.35	35.09	292.71	27.18
5	395.20	29.63	76.02	18.12	292.71	27.18	74.13	16.29
6	76.02	18.12	53.98	03.91	74.13	16.29	52.69	at.
7	53.98	03.71	27.93	386.27	52.69	02.45	28.29	286.59
8	27.93	385.56	299.48	66.10	28.29	285.83	00.93	67.71
9	00.16	65.86	69.03	43.28	00.93	66.51	172.06	46.24
10	268.02	40.84	35.14	17.76	171.14	44.48	39.84	22.49
11	33.69	15.31	198.84	290.33	38.44	19.86	05.17	196.67
12	196.68	286.95	59.62	60.70	03.26	193.46	068.14	69.22
13	57.25	56.81	18.85	30.16	065.58	65.14	29.32	40.63
14	15.31	26.72	076.26	198.84	25.84	37.24	16988.80	11.64
15	071.93	198.84	32.26	63.70	16984.56	11.64	47.21	078.65
16		68.46	17987.88	38.16	43.63	083.60	05.39	56.33
17	17986.71	39.51	41.17	23.44	05.39	58.16	859.24	41.51
18	44.11	17.12	03.06	07.50	864.58	37.37	24.84	29.67
19	03.06	098.72			26.58	22.19	797.73	996.92
20	869.44	60.60			793.02	16984.48	73.32	66.00
21					65.45	61.55	28.24	40.66
22					29.68	37.59	685.39	13.43
23					680.67	12.70	48.52	895.78
24					44.58	883.47		

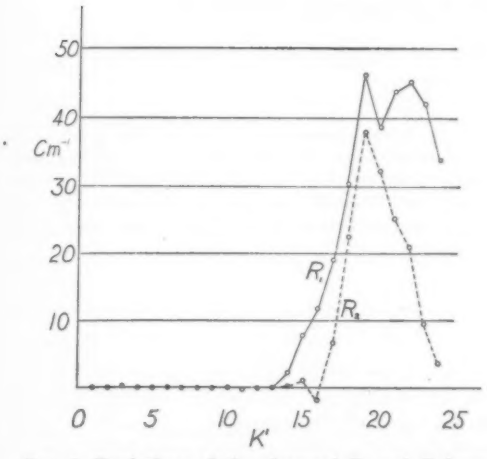

FIG. 3. Deviations of the observed R_1 and R_2-branch lines of the $(v',3)$ SrH D band at $\nu = 17{,}341$ from positions computed with fourth-degree least-squares equations fitting the first 13 lines in each branch. Positive deviation indicates observed frequency to be larger than the calculated frequency.

Table IV contains the assignment of frequencies in these bands. The B'' values as determined from the lower state combination differences agree well with those predicted for $v=2$ and 3 of the $N\,^2\Sigma$ state from the known values of B_0^*, B_1^* and α. Upper state combinations involving unperturbed levels of low K value yield a $B_v^* = 1.913$. This is much lower than the B's for any of the other SrH levels, indicating that this $D\,^2\Sigma$ state has a large equilibrium r value and is less stable.

The peculiar nature of the perturbations in these D levels is illustrated in Figs. 3 and 4. For the first of these diagrams fourth degree equations were developed by the method of least squares to fit the first 13 lines of the R_1 and R_2

TABLE V. *Rotational constants for SrH and SrD.*

	$N\,^2\Sigma$ SrH	$N\,^2\Sigma$ SrD	$B\,^2\Sigma$ SrH	$B\,^2\Sigma$ SrD
B_0^*	3.6344	1.8463	3.8323	1.9252
B_1^*	3.5530	1.8171	3.7393	1.8903
B_2^*	3.471		0.0930	0.0349
B_3^*	3.390		3.8788	1.9427
α	0.0814	0.0292	-1.722×10^{-4}	-4.02×10^{-5}
B_e^*	3.6751	1.8609	-1.732×10^{-4}	-3.81×10^{-5}
D_0	-1.348×10^{-4}	-3.47×10^{-5}	-3.81	-2.008
D_1	-1.293×10^{-4}	-3.64×10^{-5}		
γ_0	$+0.122$	$+0.0613$		

$C\,^2\Sigma$			
B_0^*	3.930		1.95

$D(v)\,^2\Sigma$	
B_v	1.913

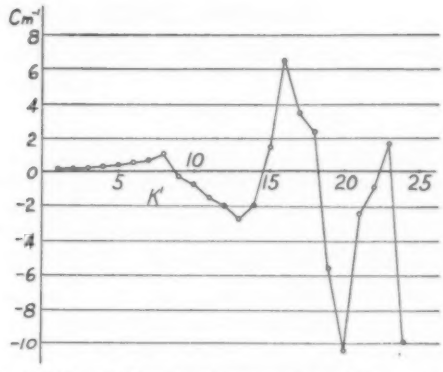

FIG. 4. Spin doubling in the upper state of the $\nu = 17{,}341$ $(v',3)$ SrH D band.

branches of the $(v',3)$ band. The deviations of all the remaining R-branch lines from the frequencies calculated by means of these equations were then plotted. Positive deviations indicate that the observed frequencies are larger than the calculated ones. Fig. 4 gives the course of the spin doubling for this $D\,^2\Sigma$ state as a function of K. Somewhat similar but less marked irregularities exist in the $D\,^2\Sigma$ levels of CaH.[6]

DISSOCIATION PRODUCTS

Because the $^2\Pi \rightarrow {}^2\Sigma$ SrH system at 5323A was thought to correspond with the 4900A E system of CaH, we labeled its upper state $E\,^2\Pi$.[1] Now the only possible electron configurations for these Π states are $\ldots ns\sigma np\sigma np\pi$ or $\ldots ns\sigma^2(n-1)d\pi$, since $\ldots ns\sigma^2np\pi$ is known definitely to give the $A\,^2\Pi$ states. The $E\,^2\Pi$ state of CaH has been shown[3] to have a coupling constant $A=9.3$, fairly close to the value $A=7$ of the $3\,^3D$ level of the Ca atom. We found that for the upper $^2\Pi$ state of the 5323A bands of SrH, however, $A=117$, whereas for Sr $4\,^3D$ A is but 32. Apparently, then, the $E\,^2\Pi$ state of CaH is $\ldots 4s\sigma^23d\pi$, while this $^2\Pi$ state of SrH is $\ldots 5s\sigma5p\sigma5p\pi\,^2\Pi$. We shall therefore refer to this as the $F\,^2\Pi$ state of SrH. Among the large number of lines near 5800A in the SrH spectrum we can trace some of the outline of a $^2\Pi \rightarrow {}^2\Sigma$ band which could not have a very large doubling in its $^2\Pi$ state. This is very possibly the $E\,^2\Pi$ state of SrH. Analysis of this band is unfortunately made very difficult by the considerable overlapping of fine structure from other SrH bands.

Absorption Spectra of Cerium, Neodymium and Samarium

FRED W. PAUL, *George Eastman Laboratory of Physics, Massachusetts Institute of Technology*

(Received November 5, 1935)

A modified King electric furnace, charged with rare earth salts, has been used to observe the absorption spectra of cerium, neodymium and samarium in the region 12,000A to 2500A with a 21-ft. concave grating giving dispersion of 2.5A/mm in the first order. The observations include 600 lines in cerium, 450 in neodymium, and 1500 in samarium. In general the absorption data confirm the line types as given by King's temperature classification in that, of those lines which are absorbed, the class I lines are more strongly absorbed than class II lines, which are in turn stronger than class III lines, and provide additional data in that only those lines of each class which involve the lowest levels appear in absorption.

INTRODUCTION

TEMPERATURE classifications for the spectra of cerium, neodymium and samarium have been published by A. S. King.[1, 2, 3] His emission data do not extend to wave-lengths shorter than 2900A, and absorption data are desirable to supplement these data to aid in the analysis of these spectra. For this reason the absorption spectra of cerium, neodymium and samarium have been photographed with a 21-foot concave grating in the first and second orders at dispersions of 2.5 and 1.25A/mm, over the range 12,000 to 2500A, in extension of the work reported at a meeting of the American Physical Society.[4]

APPARATUS

A vacuum furnace of the type described by King,[5] with modifications introduced by Harrison, has been used to vaporize oxides and oxalates of cerium, neodymium and samarium, to obtain the absorption spectra. The design of the furnace used is shown in Fig. 1. The graphite tube T is held by graphite blocks B which fit into tapered holes in the graphite shields bolted to the water cooling chambers J_1 and J_2. Water and electric current connections are made through the copper tubes $O_{1,2,3,4}$, of which O_1 and O_2 are insulated from the base F at I. The heads carrying the water-cooling chambers J_3 and J_4, the shields D_1 and D_2, and the windows W_1 and W_2 are held to the cover C by air pressure and made vacuum tight with soft vacuum wax. The fitted blocks to hold the tube and the easily removable heads make it possible to recharge the furnace or to replace the tube without removing the cover C.

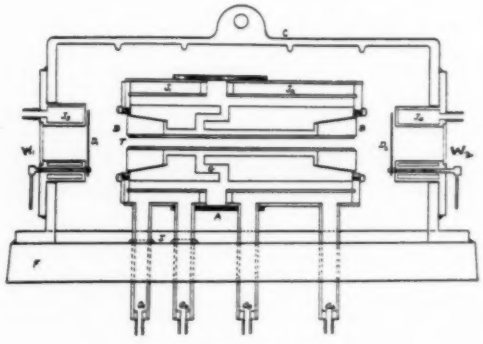

FIG. 1. Vacuum furnace.

The sources of continuous radiation used were: (1) A 500-watt tungsten filament lamp, (2) the positive crater of a carbon arc, and (3) a hydrogen lamp. The first was especially useful in the region 3400 to 8000A. The second, which was arranged in a convenient form with the positive electrode held horizontal, the negative vertical, and the two constantly fed into the arc by clockwork, was used in the short wave-length region from 2900 to 3400A, and was especially valuable from 8000 to 12,000A, because of the high intensity. The third source, a high current, "end-on" hydrogen discharge of conventional type, was operated with a transformer supplying approximately one ampere at 5000 volts, and gave a good continuous background from 2500 to 3500A.

[1] A. S. King, Ap. J. **68**, 194 (1928).
[2] A. S. King, Ap. J. **78**, 9 (1933).
[3] A. S. King, Ap. J. **82**, 140 (1935).
[4] F. W. Paul, Phys. Rev. **47**, 799 (1935).
[5] A. S. King, Trans. A. E. S. **54** (1929).

Experimental Procedure

Since exposure times were rather long in the less easily accessible regions of the spectrum, investigations were carried out to determine in what way the duration of a single charge of salt could most easily be extended. It was found that by concentrating the charge in the central three to five inches of the tube and placing at either end of the packed portion a short half-round graphite plug, a single charge could be made to supply a strongly absorbing column of vapor for an exposure lasting two hours.

A wide range of exposure times was needed to bring out most clearly the different spectral regions. Between 4000 and 6000A, where the grating concentrates a large fraction of the light incident on it, exposure times of the order of one minute gave the best contrast, while between 10,000 and 12,000A exposures of eight hours were necessary to produce a satisfactory blackening of the plates.

Exposures were made at furnace temperatures ranging from 1700° to 2300°C as measured with a Leeds and Northrup optical pyrometer.

The light incident on the slit was observed throughout the exposure by means of a quartz plate which reflected about 8 percent of the light incident upon it, on the slit of a Hilger constant deviation spectrometer. It was necessary to vary this procedure when using the hydrogen lamp as a source because it furnishes no continuous background in the visible region, by replacing the hydrogen lamp by the tungsten filament lamp at regular intervals to observe the absorption lines and make sure there was an absorbing column of vapor.

The use of the type Z plates recently developed by the Eastman Kodak Company permitted photographic investigations between 10,000 and 12,000A.

All the absorption lines were measured against the lines of an international standard iron arc superposed upon part of the absorption picture. For the most part these measurements were used only as a means of identifying the lines, the wave-lengths given in Tables I–III being those obtained in emission by the authors indicated in the references. However, in the short wave-length region (<3000A), many lines are observed which have not been found in emission. The wave-lengths of these lines given in the tables are those determined by the author. Intensity estimates were made on a scale ranging from 1 to 20.

Results

Table I contains approximately 600 lines observed in the absorption spectrum of cerium. Below 3200A the intensity of the absorption lines falls off very rapidly and very few are observed. The wave-lengths with whose emission intensities temperature classifications are given are those recorded by King.[1] The wave-lengths recorded with emission intensities but without temperature classifications to 4670A are those given by King in an unpublished list, and are probably class III lines. Wave-lengths accompanied by emission intensities but without temperature classifications beyond 5500A are those given by Kiess, Hopkins and Kremers.[6] The notations following the emission intensities are those given by these authors. It is seen that the lines listed as possible band structures appear strongly in absorption, and here also they present the appearance of unresolved bands.

Table II contains about 450 lines which were observed in the absorption spectrum of neodymium. This spectrum was somewhat easier to observe between 2600 and 3200A than that of cerium, a more characteristic variation of intensity being apparent. Here again the wave-length recorded with emission intensities and temperature classifications are those given by King.[2] Wave-lengths recorded with emission intensities but without temperature classifications are those given by Kiess.[7]

Table III contains nearly 1500 lines observed in the absorption spectrum of samarium. All wave-lengths with emission intensities are those given by King.[3] This spectrum is remarkable for the number and intensity of the absorption lines. Especially noteworthy are the great number of lines of wave-length shorter than 3000A. The chief absorption lines in the long wave-length region are class I and II lines as one would expect. However, as one goes to shorter wave-

[6] Kiess, Hopkins and Kremers, Bur. Standards Pub. **17**, 318 (1921).
[7] Kiess, Bur. Standards Pub. **18**, 201 (1922).

TABLE I. *Spectra of cerium.*

Wave-length (I.A.)	Intensity Absorption	Intensity Emission
2743.30	1	
2743.47	1	
2757.49	1	
2757.70	1	
2757.82	1	
2758.24	1	
2770.07	1	
2773.57	1	
2811.17	1	
2819.01	1	
2941.85	1	
3001.12	1	
3015.01	1	
3026.27	1	
3030.232	1	6 II
3057.80	1	
3061.236	1	5 II
3082.42	1	
3236.859	1	10 I
3240.393	1	4 II
3240.98	1	
3244.42	1	
3244.69	1	
3247.90	1	
3266.86	1	
3267.18	1	
3272.939	1	8 II
3283.85	1	
3292.35	1	
3294.97	1	
3299.83	1	
3316.539	1	8 II
3325.09	1	
3325.91	1	
3341.292	1	10 I
3355.60	1	
3369.44	1	
3371.20	1	
3371.81	2	
3383.25	1	
3389.636	1	10 I
3408.382	1	6 II
3416.701	1	12 I
3417.11	1	
3420.52	1	
3423.94	1	
3424.36	1	
3435.198	1	20 I
3437.66	1	
3459.01	1	
3461.304	1	8 II
3462.437	1	12 II
3578.831	1—	1
3593.612	1—	1
3606.129	3	12 I
3614.250	3	5 II
3616.469	3	8 I
3625.373	3	10 I
3628.618	1	13 I
3629.807	3	8 I
3637.574	3	12 I
3642.620	8	1
3643.453	8	15 I
3648.530	5	10 II
3654.977	5	8 II
3655.848	5	12 IV
3658.789	5	12 I
3660.640	3	8 IV
3666.023	10	25 I
3667.403	2	2
3671.303	3	6 II
3672.176	5	15 I
3679.075	2	10 IA
3686.050	1	12 I
3687.062	1	2
3688.481	2	2
3689.677	3	15 I
3690.121	5	12 I
3702.636	3	1
3706.932	5	6 II
3723.668	5	15 I
3726.030	3	4 II
3731.192	3	5 II
3732.560	3	10 II
3738.012	1	1
3742.228	8	6 II
3750.067	1—	2
3756.264	8	6 II
3759.757	5	15 I
3763.932	1	1
3766.068	10	15 I
3766.850	1	6 II
3782.524	8	4 IV
3785.016	1	8 II
3789.469	5	10 I
3791.961	3	10 I
3799.098	3	5 I
3884.987	1	3
3885.236	1	8 I
3886.736	3	1
3926.917	3	1
3927.440	1	8 I
3943.906	10	15
3956.768	3	20 I
3957.203	3	15 I
3961.404	10	1—
3967.642	3	5 II
3973.996	3	12 I
3976.256	20	4
3982.164	3	15 I
3986.138	3	5 II
3995.992	1	1
4006.665	20	1
4007.428	3	6
4007.969	12	1—
4011.29	5	6 II
4013.952	2	6 II
4014.847	1	1
4017.791	1	4
4019.195	1	6 II
4044.322	5	1—
4045.976	1	5 I
4051.508	3	1
4055.839	6	20 I
4060.713	3	15 I
4066.576	2	10 I
4068.050	1	8 I
4068.989	2	15 IA
4074.559	1	4
4080.033	1	10 I
4083.159	1	2
4084.785	1	2
4086.373	3	10 I
4088.151	1	1
4093.278	2	15 I
4095.122	4	10 I
4095.449	1	10 II
4096.093	1	8 II
4098.144	1	10 II
4100.901	2	12 I
4103.722	1	2
4105.139	3	3
4107.804	2	3
4112.474	3	2
4114.910	3	15 I
4115.656	3	10 II
4117.573	2	3
4118.319	3	10 II
4122.825	3	3
4126.375	2	10 I
4132.447	3	8 II
4137.956	3	1
4142.113	5	1
4142.719	5	12 I
4144.100	1	1
4150.143	1	10 IA
4151.721	2	8 IA
4156.407	1	1
4157.516	1	4
4162.474	2	5 II
4175.504	1	1
4182.101	1	1
4185.518	2	6 I
4186.821	2	5 I
4188.384	2	10 I
4194.106	3	8 I
4194.854	1	3
4209.366	3	10 I
4211.724	3	7
4217.740	1	2
4221.632	3	10 I
4224.225	2	6 II
4231.606	1	1
4237.153	1	2
4238.071	1	1
4240.053	2	1
4240.594	2	6 II
4241.259	2	6 IIA
4242.280	5	12 II
4247.674	1	5 IIA
4254.371	8	5 II
4254.690	3	15 I
4258.224	2	3
4258.326	2	6 II
4259.034	2	4
4262.810	1	10 II
4266.702	1	8 II
4271.932	1	1
4273.789	2	6 IIA
4279.328	1	12 II
4282.811	3	5 II
4285.783	1	1
4285.847	1	10 IIA
4287.005	2	6 II
4290.289	2	10 II
4293.137	2	15 I
4301.541	2	12 I
4303.63	1	1
4305.425	1	10 I
4324.598	8	25 I
4325.308	2	8 II
4343.567	10	20 I
4351.815	4	15 I
4353.457	2	6 II
4363.51	2	1
4364.502	1	6 II
4368.879	1	8 IIA
4371.694	1	1
4390.382	1	1
4395.052	1	5 II
4396.036	3	20 I
4396.190	3	15 II
4401.523	2	20 I
4403.062	8	15 II
4423.452	10	25 I
4439.515	5	15 I
4447.701	2	15 I
4449.365	1	15 II
4458.601	1	2
4467.319	3	15 I
4475.315	2	4 II
4476.370	1	1
4478.000	1	10 IIA
4479.985	2	15 II
4480.973	2	1
4484.813	1	15 II
4491.539	1	1—
4501.103	2	15 I
4505.121	3	10 I
4506.417	5	25 I
4514.064	2	8 II
4518.023	5	20 I
4521.961	3	10 II
4527.338	5	15 II
4531.308	4	20 I
4532.016	1	8 II
4536.210	1	4 II
4540.632	2	10 I
4541.558	1	2
4545.452	2	8 IIA
4546.064	4	20 I
4548.888	2	20 I
4552.066	2	12 IA
4553.060	3	15 I
4556.351	3	1
4557.973	2	3
4559.607	2	2
4565.242	3	30 I
4570.645	2	10 II
4608.492	2	20 I
4615.195	3	20 I
4624.225	1	10 II
4625.071	3	1
4632.329	3	30 I
4641.071	1	10 II
4643.175	2	6 II
4645.475	5	2
4649.885	1	12 I
4650.514	2	15 I
4661.137	1	1
4670.902	10	8 II
4684.55	1	15 I
4688.90	8	15 I
4696.53	3	15 IIA
4700.62	1	10 IIA
4703.77	1	8 IIA
4705.58	1	15 I
4707.03	1	10 II
4715.07	3	15 I
4719.72	1	8 IIA
4724.30	2	12 I
4724.84	2	20 I
4733.92	3	15 I
4734.67	3	10 I
4743.25	5	15 I
4747.07	5	20 I
4750.23	1	8 I
4750.85	2	10 I
4751.42	1	6 II
4752.59	1	8 II
4758.52	1	5 II
4764.73	20	6 II
4773.84	2	10 II
4775.06	4	25 IA
4776.23	1	8 I
4776.47	1	10 I
4780.73	2	8 II
4781.71	3	8 I
4782.22	3	12 I
4786.53	2	20 I
4803.09	1	5 II
4805.93	3	25 I
4807.66	4	15 I
4820.02	2	15 I
4820.61	2	10 I
4822.53	3	40 I
4836.66	3	25 I
4845.47	2	40 I
4847.72	3	50 I
4852.61	1	6 I
4859.46	1	15 I
4861.72	2	10 I
4863.24	2	12 I
4872.92	10	5 II
4881.52	3	8 IA
4889.57	3	20 I
4892.87	2	10 I
4896.92	3	7 IA
4898.19	1	5 II
4899.91	1	10 II
4901.67	2	12 I
4904.85	8	10 I
4913.40	2	6 IA
4915.30	3	15 I
4919.90	3	10 IA
4924.56	2	8 I
4930.56	3	6 IA
4939.13	2	12 I
4948.67	1	10 I
4958.24	1	4 IIA
4965.25	2	4 II
4970.10	1	5 II
4970.64	1	8 II
4971.66	2	5 II
4974.09	2	6 I
4987.52	1	5 II
4988.68	1	6 I
4990.65	1	6 II
4992.39	1	6 II
4994.61	1	5 II
4995.26	3	4 IIA
4998.12	1	8 I
5009.07	10	15 I
5009.44	1	4 IIA
5016.49	5	10 I
5021.42	2	10 I
5028.31	3	10 I
5036.65	3	8 I
5037.99	1	4 II
5039.74	1	4 II
5040.85	1	12 I
5042.09	1	4 II
5050.98	1	4 II
5053.27	1	5 II
5054.15	3	12 I
5055.77	1	6 II
5063.92	2	6 II
5071.73	1	6 II
5084.81	1	6 IIA
5091.76	3	6 I
5097.29	2	3 II
5099.40	3	5 II
5107.47	1	5 II
5111.59	1	5 II
5115.23	1	6 II
5122.39	2	12 I
5122.68	2	3 II
5125.00	1	6 II
5150.39	2	6 I
5169.74	3	8 IA
5174.58	3	10 II
5177.73	2	4 II
5180.88	5	10 I
5181.91	3	8 I
5183.18	1	5 II
5187.38	2	6 II
5188.64	2	5 II
5191.70	5	5 II
5194.74	3	6 I
5201.39	2	10 I
5211.92	3	12 II
5221.94	1	5 II
5223.48	3	8 II
5229.76	2	12 I
5230.13	1	5 II
5233.79	1	6 IIA
5238.49	2	6 I
5243.06	1	4 II
5244.48	3	10 I
5245.26	3	5 IIA
5245.89	3	10 II
5250.10	2	4 IIA
5261.69	2	6 I
5264.18	1	6 I
5271.87	3	12 I
5276.9	2	4 IIA
5277.49	1	8 IIA
5281.35	1	7 IIA
5290.92	1	8 I
5296.58	3	10 II
5303.31	2	8 I
5335.72	5	10 I
5336.21	5	7 I
5357.21	5	10 IA
5359.91	5	6 IIA
5397.65	5	25 I
5414.15	2	5 II
5418.71	5	10 IA
5426.43	3	10 IIA
5427.29	1	5 II
5433.37	2	4 IIIA
5438.46	2	8 IA
5445.46	3	10 IA
5449.28	1	8 II
5456.40	3	15 IA
5457.22	3	7 IIA
5458.86	5	10 IA
5460.09	5	12 IIA
5465.35	2	20 I
5473.53	3	12 I
5478.61	2	10 I
5498.19	10	10 II
5506.48	1	5 III
5527.15	1	6 III
5527.93	2	6 IIA
5529.48	1	<1
5531.53	1	<1
5535.25	1	20 II
5535.84	1	1
5537.52	1	8 II
5548.81	5	30 I
5551.40	2	12 IIA
5552.30	3	1
5556.26	5	5
5564.26	3	3
5564.99	1	15 I
5567.82	1	3
5582.70	3	4
5590.52	1	4 IIIA
5593.72	1	2
5594.97	1	6 II
5595.89	1	8 II
5597.96	1	8 IIIA
5598.96	2	12 IIA
5601.29	1	25 II
5604.39	1	8 IIA
5606.47	2	12 II
5620.38	1	8 II
5623.76	2	8 IIA
5624.84	1	1
5626.01	1	1
5633.09	1	20 IIA
5634.48	1	6 IIA
5638.18	1	12 I
5646.60	1	4 III
5650.59	1	20 II
5655.17	3	50 I
5662.72	1	1
5664.00	2	7 III
5669.97	5	15 I
5671.92	3	8 I
5675.10	1	10 IA
5676.38	2	1
5677.76	1	12 I
5688.48	1	4 IIIA
5692.98	1	12 I
5695.88	1	20 III
5697.02	2	15 I
5699.24	2	25 I
5702.34	1	8 III
5718.42	2	10 IIA
5719.09	2	20 I
5721.97	4	15 IIA
5725.85	1	10 I
5743.52	2	15 I
5804.42	1	15 I
5810.73	1	5 II
5812.93	1	15 I
5825.22	1	1
5828.00	1	<1
5830.03	1	15 IA
5839.36	1	15 I
5843.73	12	6 II
5863.86	3	1
5871.61	1	15 I
5910.13	1	15 I
5926.28	2	30 I
5927.31	2	1
5940.84	1	25 I
5942.66	1	20 I
5975.25	1	2
6005.85	1	12 I
6139.03	3	3
6162.14	1	25 IA
6269.80	2	20 IIA
6273.71	1	12 IIA
6276.45	1	10 II
6277.10	1	10 II
6295.58	3	50 I
6300.23	1	30 I
6306.63	1	15 IIA
6308.08	1	10 IIA
6310.03	5	30 I
6332.00	3	20 IA
6399.90	3	3 III
6424.47	1	15 IIA
6429.04	1	1
6434.38	5	40 IA
6439.95	2	15 IIA
6441.02	1	8 IIA
6451.38	3	<1
6456.84	2	4 IIA
6458.06	5	60 I
6467.40	1	40 IA
6649.32	10	<1
6679.84	1	8 III
6704.38	1	40 I
6778.23	5	30 IA
6780.15	8	1
6780.72	5	4 III
6785.06	3	<1
6795.46	5	1
6807.83	3	4 III
6818.20	1	20 IA
6850.77	1	1
6857.05	8	1
6867.15	4	<1
6873.86	1	1
6875.43	3	1
6901.50	5	<1
6903.11	6	1
6909.31	2	1
6933.32	1	1
6939.40	5	15 IA
6948.29	4	<1
6956.28	3	1
6957.75	5	1
6959.11	5	1
6960.69	12	2
6963.08	1	1
6981.24	1	1
6985.98	3	15 I
6999.85	3	15 I
7189.40	5	1 n?
7191.70	2	1
7235.70	15	2 n
7241.69	15	2 n
7252.72	5	2
7275.57	10	1 P?
7277.92	10	1 n
7379.64	2	<1
7397.76	3	2
7424.84	8	1 n?
7508.12	2	<1
7509.43	3	1 b
7562.47	4	1
7563.52	2	1
7670.89	5	2
7732.32	1	2
7748.35	1	1
7797.73	2	2
7842.57	5	2
7859.05	10	2
7860.54	8	2
7899.03	6	2 n?
7904.84	6	1 n?
7927.53	10	2 n?
7975.49	8	2 b
8018.94	6	1 b
8109.09	3	1
8114.53	5	1
8120.32	3	2
8171.32	5	1
8220.65	3	1
8223.69	1	2 bd?
8226.94	1	1
8234.12	10	3
8245.10	5	2
8252.52	5	1
8258.35	4	1 b
8261.03	5	2
8310.22	3	2
8352.39	3	2
8363.82	1	2
8368.55	1	1
8371.90	4	2
8503.57	3	1 b
8523.32	2	1
8560.60	3	2
8564.36	3	1
8567.36	3	1
8583.87	7	2 b
8612.62	2	2
8633.25	3	<1
8636.40	2	1
8647.59	3	2
8672.45	1	1
8756.26	1	1
8810.77	3	1
8891.14	1	1
8927.42	3	1

TABLE II. *Spectra of neodymium.*

WAVE-LENGTH (I.A.)	INTENSITY Absorption	INTENSITY Emission	WAVE-LENGTH (I.A.)	INTENSITY Absorption	INTENSITY Emission	WAVE-LENGTH (I.A.)	INTENSITY Absorption	INTENSITY Emission	WAVE-LENGTH (I.A.)	INTENSITY Absorption	INTENSITY Emission	WAVE-LENGTH (I.A.)	INTENSITY Absorption	INTENSITY Emission
2613.35	1		3359.35	1		4343.497	2	20 IA	4778.40	1	15 IA	5213.20	1	8 I	6082.02	1	25 IA
2623.97	1		3359.85	2		4357.789	1	5 IIIA	4779.463	2	40 I	5214.27	1	8 IA	6109.68	1	40 IA
2626.19	1		3360.36	1		4381.878	1	5 IIA	4787.40	1	12 IA	5240.58	0	4 IIIA	6148.60	1	40 IA
2650.73	1		3362.88	1		4393.352	1	6 IIA	4792.62	0	8 IA	5249.30	0	5 IA	6149.28	1	100 IIA
2653.83	1		3363.11	1		4397.320	1	6 IIA	4806.62	1	30 IA	5270.09	1	8 IIIA	6167.40	1	20 IIA
2691.47	1		3363.99	1		4401.063	1	5 IIIA	4833.50	1	8 IIA	5276.27	0	5 IIIA	6174.30	2	50 IA
2712.73	1		3364.46	1		4402.478	1	8 IA	4835.66	1	15 I	5284.11	0	3 IIIA	6223.38	1	40 III
2717.85	1		3373.093	1	8 IIA	4432.220	1	8 IA	4836.62	1	20 I	5298.88	1	6 IA	6225.25	2	30 IA
2733.93	1		3376.83	1		4444.988	2	50 rIA	4845.88	1	8 IIA	5334.33	1	10 IA	6226.50	1	50 IIA
2743.72	1		3379.72	1		4456.132	2	20 rI	4853.33	1	15 IA	5336.84	1	8 IA	6237.34	1	25 IA
2747.72	1		3386.57	1		4469.571	1	8 IIA	4854.22	1	5 IIA	5349.57	1	8 IA	6288.03	4	80 I
2754.20	1		3397.441	1	6 IIA	4477.879	1	50 RI	4855.31	2	15 I	5377.78	1	8 I	6291.48	1	6 IIA
2764.98	3		3410.38	2		4480.972	2	60 RIA	4859.58	2	15 I	5398.11	0	6 IA	6310.48	1	150 I
2765.27	1		3416.18	1		4481.898	2	30 rI	4862.22	0	3 IIIA	5523.88	1	15 IA	6348.78	1	30 IIA
2765.52	1		3416.41	1		4497.379	2	20 rIA	4863.55	0	4 IIIA	5529.07	1	10 I	6360.11	1	30 IA
2765.86	3		3422.02	1		4527.252	1	30 rI	4865.27	1	5 IIIA	5561.16	3	50 I	6372.80	1	5 III
2766.29	1		3431.88	1		4529.944	1	40 rI	4866.74	3	30 I	5576.70	0	4 III	6375.96	1	8 III
2766.78	5		3432.87	1		4542.055	2	30 rI	4869.27	1	6 II	5620.51	3	100 I	6380.40	1	20 IA
2767.28	1		3438.96	2		4548.244	1	20 rI	4875.73	1	8 IIA	5623.70	0	2 IIIA	6385.17	5	300 IA
2768.58	1		3451.84	1		4559.189	1	20 rIA	4879.79	1	10 I	5624.22	0	3 IIIA	6397.84	5	100 IA
2769.40	1		3454.76	3		4559.672	1	40 RI	4881.71	1	5 IA	5651.50	0	4 IIIA	6403.22	1	8 IIIA
2770.04	1		3458.22	1		4560.423	1	20 rI	4883.81	10	60 I	5663.28	2	6 IIA	6408.49	3	25 IA
2771.62	1		3463.60	1		4561.855	1	20 rI	4885.01	1	8 II	5669.77	1	60 IIA	6439.646	0	2 III
2772.29	1		3464.36	5		4562.346	1	8 IA	4887.33	0	4 IIIA	5675.92	3	100 I	6451.21	1	15 IIIA
2780.13	1		3465.43	8		4567.352	1	10 IA	4889.04	0	3 III	5681.16	0	15 IIIA	6455.06	0	10 IIIA
2785.79	1		3466.74	10		4586.617	2	50 RI	4891.07	3	50 I	5686.55	0	5 III	6456.22	5	40 IA
2787.90	2		3467.29	1		4594.676	1	20 rI	4893.23	2	12 I	5693.88	0	5 IIIA	6457.14	1	15 IIA
2792.05	1		3469.93	1		4603.819	1	20 I	4896.93	3	100 I	5702.49	0	3 IIIA	6581.84	1	1
2802.42	1		3474.38	1		4607.378	8	8 IV	4901.53	1	15 I	5704.33	0	3 IIIA	6588.82	0	3 IIIA
2820.41	1		3475.29	2		4607.71	0	4 IVA	4901.84	3	60 I	5710.22	0	3 III	6628.71	2	15 IA
2820.98	1		3529.059	1	4 IIIA	4609.872	2	20 rI	4907.26	1	5 II	5712.94	1	10 IIIA	6630.14	3	60 I
2824.26	1		3585.692	1	6 I	4621.940	1	80 RI	4907.78	1	6 IIA	5727.86	0	30 IIIA	6648.99	2	30 IA
2824.51	3		3593.527	1	3 III	4622.150	1	6 IVA	4910.05	1	30 IA	5729.30	2	60 I	6655.64	1	40 II
2826.75	1		3596.092	1	6 IIIA	4624.210	1	20 rI	4913.41	3	40 I	5734.20	1	20 IIIA	6664.61	3	30 IA
2827.77	1		3610.218	1	3 IIA	4626.034	1	5 IIA	4921.14	0	6 IIA	5749.14	2	40 III	6695.62	1	15 IA
2832.27	2		3658.108	1	10 IIA	4626.498	1	20 rI	4922.45	1	8 IIA	5749.63	2	30 IA	6699.22	1	20 IA
2842.07	1		3701.982	1	6 III	4627.979	1	30 rI	4924.53	8	150 rI	5750.62	0	2 IIIA	6722.72	1	20 IA
2844.82	1		3745.466	1	8 IA	4634.236	5	200 RI	4940.30	1	20 IIIA	5752.36	1	10 IIIA	6753.99	1	15 IA
2923.22	1		3773.338	1	6 I	4636.297	1	12 IIA	4944.83	5	60 I	5772.14	2	20 IA	6770.94	1	12 IIA
2953.32	1		3783.060	1	8 IIIA	4637.198	1	30 rIA	4950.29	0	6 IIIA	5776.10	2	50 I	6784.70	2	20 IA
2968.50	1		3793.64	1	4 I	4639.143	1	40 RIA	4950.67	1	6 IIIA	5784.96	2	25 I	6792.28	1	8 IIA
2968.69	1		3806.540	1	5 IA	4641.103	1	80 RI	4952.46	2	15 IIIA	5788.19	3	30 I	6822.91	2	15 IA
2971.83	1		3807.539	1	4 IA	4646.400	1	50 rI	4954.78	3	40 II	5800.07	0	20 I	6851.79	2	10 IA
3044.44	1		3812.852	1	15 IIA	4649.673	1	60 RI	4963.02	0	4 IIIA	5820.36	2	25 IIA	6904.75	1	8 IA
3061.53	1		3820.866	1	10 IA	4651.020	1	25 rIA	4963.33	0	8 II	5825.11	1	15 IIA	6923.86	5	30 IA
3075.81	1		3830.915	1	10 IA	4651.189	1	12 IA	4969.75	1	8 IIA	5826.75	2	40 IA	6985.26	5	20 I
3082.66	1		3834.404	2	15 IA	4652.390	1	30 rI	4975.50	1	10 II	5829.75	2	15 IIA	6995.27	2	10 IIA
3089.97	2		3840.775	1	5 IA	4654.726	1	50 RI	4982.89	1	8 III	5839.08	2	40 IA	7093.98	3	1
3146.12	1		3842.695	1	4 I	4664.368	1	8 IIA	4988.65	2	8 IIA	5869.57	2	40 IIA	7148.23	1	1
3146.68	1		3887.837	1	6 IIA	4664.613	1	4 IIA	4998.44	1	5 IIIA	5961.86	0	8 IIIA	7183.60	1	1
3203.36	1		3889.214	1	4 IIA	4671.100	1	30 rI	5014.51	1	8 IIA	6463.57	2	20 IIA	7189.42	1	3
3204.82	1		3913.546	1	5 I	4673.971	1	15 IA	5026.42	0	6 IIA	6481.57	3	40 IA	7192.01	1	2
3206.96	1		3935.917	1	4 I	4683.447	3	150 RI	5027.12	1	8 II	6485.69	8	100 I	7198.83	1	2
3215.77	1		3972.753	1	6 IIA	4684.039	1	40 RI	5029.42	2	8 I	6493.54	0	15 IIA	7215.32	0	1
3216.89	2		3981.689	1	4 I	4690.35	2	30 I	5040.17	1	10 II	6500.15	1	15 II	7266.22	1	1
3222.63	1		3982.269	1	4 I	4692.97	0	6 IIA	5045.03	1	5 IIIA	6501.11	1	2 IIIA	7279.36	3	1
3229.73	1		4009.377	1	15 IA	4696.440	3	30 I	5045.52	1	12 IIIA	6516.49	0	4 IIA	7311.91	2	1
3230.43	1		4047.159	1	12 IIIA	4698.30	1	8 II	5051.06	1	8 II	6535.28	1	2 IIIA	7313.70	2	1
3231.84	1		4051.623	1	4 IIA	4706.54	0	4 III	5056.85	3	15 I	5873.33	1	15 IIA	7334.56	5	2
3236.14	1		4053.519	1	4 IA	4706.955	3	40 I	5060.01	1	6 IIIA	5878.88	1	4 IIIA	7378.26	3	2
3259.38	1		4062.897	1	5 IA	4709.53	1	10 IIA	5071.84	1	8 II	5883.66	1	15 IIIA	7401.31	2	3
3279.99	1		4066.860	2	15 IA	4713.05	1	20 IIA	5073.84	0	6 IIIA	5887.89	3	50 IA	7404.78	2	2
3288.50	1		4083.916	1	5 I	4714.233	1	10 IIA	5074.49	1	10 IIA	5896.65	0	3 IIIA	7481.37	1	2
3292.88	1		4100.003	1	4 IIIA	4719.02	2	80 rII	5079.05	0	6 II	5901.59	1	8 IIIA	7547.00	1	3
3293.64	1		4109.162	1	10 IA	4726.550	1	12 I	5081.18	0	8 IIA	5914.91	1	10 IIIA	7555.63	1	1
3313.646	1	5 III	4112.742	1	4 IIIA	4731.770	2	40 I	5089.71	1	4 II	5921.20	1	40 IA	7623.93	2	1
3316.911	1	5 IIId	4122.998	1	10 IA	4734.903	1	10 I	5100.08	0	4 IIIA	5966.01	3	30 IIA	7729.21	1	1
3320.421	1	3 IV	4183.134	1	8 IIA	4749.751	2	30 I	5103.13	2	12 I	5968.30	2	15 IIA	7777.11	2	1
3321.400	2	4 III	4210.988	0	15 IA	4755.847	2	20 I	5105.32	1	10 I	5994.77	2	40 III	7827.90	1	1
3325.732	2	8 II	4256.474	1	30 rIA	4758.49	1	15 IIA	5115.72	0	10 IIIA	6000.09	3	30 IIA	7829.66	4	1
3333.058	2	6 II	4258.106	1	6 IA	4758.89	0	8 IIA	5144.92	0	5 IIIA	6006.44	0	20 IIIA	7842.77	1	1
3346.589	10	4 II	4301.215	1	6 II	4759.34	1	10 IIA	5149.55	2	10 I	6007.67	1	100 II	7858.93	3	4
3353.521	1	5 III	4305.81	1	20 IIA	4760.45	8	10 IA	5178.75	1	8 IIA	6025.54	2	25 IIA	8007.72	2	3
3354.059	1	6 II	4311.254	1	20 IA	4768.96	1	8 IIA	5198.07	1	6 I	6049.92	1	30 IA	8043.33	2	4
3354.534	1	3 IIIA	4329.917	1	5 IIA	4770.20	3	20 I	5199.73	1	6 I	6071.71	1	20 IIA	8082.18	4	1
3358.514	8	8 II	4337.231	1	6 IIA	4772.26	2	10 I	5204.43	2	10 I	6073.96	1	50 I	8164.97	2	3

lengths the class III lines become more and more important in absorption, then the class IV lines appear, and at the shortest wave-lengths many lines appear which are not observed in emission. This is exactly the behavior one would expect if the long wave-length lines correspond to transitions between the ground states and the first excited states, and the shorter wave-lengths to transitions involving progressively higher stages of excitation for the upper state; for then the excitation in ordinary sources would not be sufficient to populate the higher levels enough to

TABLE III. *Spectra of samarium.*

Wave-length (I.A.)	Intensity Absorption	Intensity Emission
2503.89	0	
2518.26	1	
2518.60	1	
2522.55	0	
2522.90	0	
2523.84	1	
2525.99	0	
2528.61	0	
2529.24	0	
2535.77	1	
2536.08	0	
2551.49	0	
2563.84	1	
2566.44	1	
2567.98	2	
2568.47	0	
2568.65	0	
2570.96	0	
2577.06	0	
2577.16	0	
2586.57	0	
2587.88	1	
2588.13	0	
2589.55	0	
2592.75	0	
2598.50	1	
2600.44	0	
2602.46	1	
2603.11	1	
2603.84	1	
2605.60	0	
2609.49	1	
2610.04	1	
2610.43	0	
2610.80	0	
2612.46	0	
2614.95	1	
2615.82	0	
2618.16	1	
2618.99	1	
2619.41	0	
2620.24	0	
2621.17	2	
2621.93	0	
2624.43	2	
2624.92	0	
2625.25	1	
2626.10	0	
2626.44	0	
2627.27	1	
2627.56	0	
2630.18	1	
2630.48	1	
2630.09	1	
2632.05	1	
2632.45	1	
2633.94	1	
2637.15	1	
2637.38	1	
2638.01	1	
2638.57	0	
2638.95	0	
2639.98	1	
2640.87	0	
2641.48	0	
2641.87	1	
2643.10	1	
2643.32	1	
2644.66	1	
2644.89	1	
2645.08	0	
2645.45	1	
2645.70	0	
2647.63	1	
2647.75	0	
2647.89	0	
2649.51	1	
2650.66	1	
2651.96	1	
2652.66	1	
2653.17	2	
2654.40	3	
2654.56	1	
2655.60	1	
2655.87	1	
2656.70	1	
2657.75	1	
2658.46	3	
2658.80	1	
2658.90	1	
2661.05	0	
2662.43	0	
2665.03	1	
2665.98	2	
2666.77	0	
2667.03	1	
2667.42	0	
2668.40	0	
2668.77	3	
2670.74	0	
2671.98	1	
2672.44	0	
2673.03	1	
2673.48	1	
2674.42	2	
2674.79	0	
2676.97	2	
2677.33	0	
2678.08	0	
2679.23	0	
2680.51	0	
2681.13	0	
2681.75	0	
2682.56	1	
2683.28	0	
2684.37	0	
2685.40	2	
2685.59	1	
2685.85	1	
2686.19	1	
2686.37	0	
2687.62	1	
2687.75	1	
2689.01	1	
2691.08	1	
2691.17	0	
2691.55	2	
2691.89	1	
2692.06	0	
2692.34	1	
2693.14	1	
2693.76	1	
2693.89	3	
2694.15	1	
2694.30	1	
2695.78	1	
2695.93	0	
2696.14	1	
2696.36	0	
2696.52	1	
2697.27	1	
2698.85	0	
2699.19	1	
2699.68	1	
2700.67	3	
2700.82	1	
2700.97	1	
2701.23	2	
2703.75	1	
2703.88	1	
2704.06	1	
2704.34	1	
2705.22	1	
2705.51	1	
2705.70	2	
2707.82	3	
2708.01	0	
2708.19	1	
2708.41	1	
2708.63	0	
2708.78	0	
2709.02	2	
2709.60	1	
2709.82	0	
2710.01	1	
2711.24	0	
2711.53	0	
2712.10	4	
2712.33	1	
2713.31	2	
2713.53	1	
2714.21	1	
2714.44	0	
2714.73	1	
2715.07	1	
2716.64	1	
2717.22	2	
2718.38	0	
2718.40	1	
2719.14	2	
2720.09	1	
2720.40	0	
2721.65	2	
2721.94	2	
2722.32	1	
2722.59	1	
2722.83	2	
2723.06	2	
2724.00	2	
2724.09	1	
2724.38	1	
2725.62	1	
2725.94	2	
2727.13	10	
2728.14	0	
2728.36	4	
2728.92	0	
2729.45	1	
2729.69	3	
2730.08	1	
2730.63	0	
2731.26	1	
2731.54	2	
2732.38	3	
2732.54	1	
2732.67	1	
2733.02	0	
2734.10	1	
2734.43	5	
2735.77	3	
2735.95	2	
2736.65	3	
2736.80	1	
2737.36	2	
2737.62	4	
2737.92	1	
2739.35	1	
2739.50	0	
2739.65	0	
2739.79	2	
2740.26	0	
2741.16	3	
2741.35	0	
2742.37	2	
2742.60	0	
2742.98	1	
2743.26	1	
2744.86	5	
2745.27	5	
2745.68	2	
2747.82	2	
2748.50	0	
2749.04	1	
2749.97	1	
2750.41	2	
2750.57	1	
2751.21	2	
2751.88	1	
2752.43	3	
2752.64	1	
2753.15	2	
2753.89	2	
2754.78	1	
2754.81	0	
2755.08	3	
2758.27	1	
2758.95	1	
2759.10	0	
2759.26	0	
2760.64	1	
2761.20	0	
2761.89	2	
2764.37	3	
2766.62	1	
2766.80	0	
2767.60	1	
2768.51	0	
2768.79	0	
2769.47	3	
2770.37	1	
2770.62	0	
2771.14	1	
2771.31	0	
2772.15	1	
2772.41	1	
2773.71	4	
2774.26	1	
2774.79	1	
2775.73	1	
2777.22	3	
2777.94	1	
2778.90	0	
2779.38	1	
2779.67	1	
2780.91	1	
2781.02	0	
2781.14	1	
2782.20	1	
2782.64	1	
2783.17	2	
2784.04	3	
2784.32	1	
2784.77	1	
2785.45	1	
2786.12	3	
2786.58	1	
2787.33	1	
2788.32	1	
2788.45	0	
2788.89	0	
2790.29	0	
2792.80	1	
2793.02	2	
2793.10	2	
2793.98	1	
2796.30	2	
2797.47	0	
2797.68	1	
2798.03	1	
2798.18	1	
2798.50	0	
2799.88	0	
2801.28	1	
2801.87	1	
2803.21	1	
2803.86	0	
2804.09	0	
2805.93	0	
2807.52	1	
2807.87	0	
2808.79	0	
2809.90	1	
2811.07	3	
2811.39	1	
2811.83	0	
2813.13	0	
2814.04	0	
2815.32	2	
2815.65	1	
2816.24	1	
2817.37	1	
2818.77	1	
2819.22	1	
2820.86	1	
2821.88	1	
2822.44	0	
2823.50	0	
2824.49	2	
2827.43	1	
2829.16	2	
2832.68	2	
2833.94	1	
2834.45	1	
2836.46	1	
2839.02	3	
2839.34	1	
2841.64	1	
2841.78	1	
2855.64	1	
2860.20	0	
2860.27	2	
2863.68	1	
2864.22	1	
2864.58	1	
2864.86	1	
2865.56	1	
2866.10	0	
2867.19	1	
2867.46	1	
2868.54	2	
2870.91	1	
2871.04	1	
2874.37	2	
2874.56	1	
2877.00	2	
2878.89	1	
2879.05	0	
2879.41	1	
2879.73	0	
2880.30	5	
2880.60	3	
2881.64	8	
2882.20	0	
2882.26	0	
2884.12	0	
2884.39	0	
2884.86	2	
2885.13	1	
2885.71	3	
2885.96	1	
2886.52	1	
2888.15	1	
2888.54	0	
2889.92	2	
2890.31	4	
2891.60	2	
2892.18	0	
2893.01	2	
2893.72	5	
2894.76	2	
2895.80	1	
2896.47	1	
2896.89	1	
2898.28	1	
2898.56	3	
2898.79	5	
2898.86	5	
2899.81	5	
2899.86	5	
2900.25	0	
2903.25	1	
2905.33	2	
2905.58	2	
2905.83	1	
2905.94	1	
2906.03	1	
2906.77	1	
2906.99	1	
2907.61	2	
2909.80	1	
2911.298	2	1 IV
2911.79	1	
2912.564	4	1 IV
2912.81	2	
2913.28	1	
2914.76	8	
2915.45	1	
2915.70	2	
2916.15	1	
2916.68	3	
2917.386	3	1 IV
2917.97	2	
2919.29	2	
2919.77	2	
2920.828	3	1 IV
2921.07	1	
2921.23	1	
2922.82	3	
2923.54	1	
2924.28	1	
2924.681	1	1 IV
2924.93	2	
2925.45	1	
2926.654	5	2 IV
2927.745	2	1 IV
2928.258	5	1 IV
2929.800	2	1 IV
2929.29	1	
2931.13	0	
2931.49	0	
2931.65	1	
2932.056	2	1 IV
2933.064	1	1 IV
2933.23	1	
2933.40	0	
2933.63	2	
2933.92	1	
2934.19	1	
2934.74	1	
2934.94	0	
2935.413	1	V
2935.90	2	
2936.21	0	
2936.43	1	
2937.48	2	
2937.63	1	
2938.06	1	
2938.94	3	
2939.17	1	
2939.36	1	
2939.52	1	
2939.75	1	
2939.95	3	
2940.46	3	
2941.08	1	
2941.77	8	
2942.11	1	
2943.73	2	
2943.88	1	
2944.31	1	
2944.86	3	
2945.35	2	
2946.23	2	
2946.420	3	1 IV
2947.50	0	
2948.04	1	
2948.80	0	
2950.78	2	
2951.41	0	
2951.96	1	
2952.27	1	
2952.47	4	
2952.91	1	
2954.83	1	
2954.96	0	
2955.31	0	
2955.75	0	
2955.92	1	
2956.22	0	
2956.52	2	
2958.05	1	
2958.34	0	
2959.82	1	
2961.70	1	
2962.032	3	1 IV
2962.65	5	
2963.34	1	
2963.92	4	
2964.40	2	
2964.72	0	
2964.90	1	
2965 13	1	
2965.90	1	
2966.27	2	
2970.483	2	1 IV
2972.65	2	
2972.92	1	
2973.72	3	
2974.60	2	
2975.81	0	
2975.48	1	
2976.92	1	
2977.23	1	
2978.97	3	
2979.59	1	
2979.79	1	
2981.47	2	
2982.894	4	1 IV
2983.42	2	
2986.57	1	
2986.89	3	
2988.14	1	
2988.409	5	1 IV
2989.18	1	
2989.44	3	
2990.62	2	
2992.521	5	2 IV
2992.99	3	
2994.203	3	1 IV
2994.67	0	
2994.75	0	
2995.160	3	1 IV
2995.56	1	
2995.874	1	1 IV
2996.18	1	
2996.32	0	
2996.68	2	
2997.16	1	
2998.263	5	2 IV
2999.54	0	
2999.73	1	
3001.14	1	
3003.66	1	
3004.17	1	
3004.48	0	
3004.914	1	1 IV
3007.85	1	
3009.02	1	
3010.128	1	1 IV

TABLE III.—*Continued.*

Wave-length (I.A.)	Intensity Absorption	Intensity Emission	Wave-length (I.A.)	Intensity Absorption	Intensity Emission	Wave-length (I.A.)	Intensity Absorption	Intensity Emission	Wave-length (I.A.)	Intensity Absorption	Intensity Emission	Wave-length (I.A.)	Intensity Absorption	Intensity Emission	Wave-length (I.A.)	Intensity Absorption	Intensity Emission
3010.327	3	2 IV	3123.029	5	3 IV	3345.763	1	6 IVA	3521.513	2	15 III	3709.023	2	10 III	3972.272	2	8 IIA
3011.862	1	2 IV	3124.307	1	2 IV	3350.664	2	10 III	3522.81	2	6 IIIA	3716.780	3	8 IIIA	3974.865	8	80 RI
3012.183	3	3 IV	3126.002	1	2 IV	3351.689	1	5 IV	3523.416	3	20 III	3719.300	2	6 IIIA	3978.116	2	8 IIA
3012.53	1		3128.864	1	2 IV	3352.727	1	8 IV	3524.108	1	6 IIIA	3719.451	2	6 IIIA	3978.244	2	10 IA
3013.123	1	2 IV	3129.950	4	3 IV	3353.118	0	6 IV	3525.089	1	8 IIIA	3720.345	2	8 III	3990.025	5	50 rI
3013.514	1	3 IV	3132.288	1	1 IV	3356.52	0	4 IVA	3526.779	2	15 III	3721.028	5	50 III	3991.019	3	15 I
3014.52	1		3132.751	4	3 IV	3358.562	0	5 IV	3527.066	2	12 III	3722.026	5	40 III	3998.350	2	15 I
3015.075	3	2 IV	3134.620	8	4 IV	3360.688	1	6 IVA	3530.003	4	10 III	3722.566	0	3 IV	4001.612	1	5 IIA
3015.49	1		3135.985	2	2 IV	3360.938	2	6 IV	3535.143	2	10 IIIA	3728.162	2	20 III	4016.004	2	4 IIA
3016.075	3	2 IV	3142.037	2	3 IV	3363.167	0	3 IVA	3539.88	2	12 IIIA	3730.737	4	25 III	4016.111	2	4 IIA
3016.584	0	1 IV	3142.794	4	4 IV	3366.522	0	4 IVA	3540.525	1	5 III	3737.362	1	4 IIIA	4051.822	1	6 IIA
3017.554	2	2 IV	3144.374	1	2 IV	3376.246	0	2 IVA	3541.390	1	15 III	3737.873	0	3 IIIA	4054.512	3	25 IIA
3019.719	2	2 IV	3147.010	1	2 IVA	3376.817	4	10 III	3545.416	4	10 III	3739.42	1	6 IIIA	4062.320	4	40 IIA
3021.227	2	3 IV	3147.580	3	4 IV	3382.070	1	4 IVA	3546.818	4	8 IIIA	3739.993	3	8 IIIA	4069.751	3	8 IIA
3021.39	1		3148.817	5	5 IV	3384.857	0	3 IV	3550.216	5	40 II	3740.750	3	12 III	4079.834	3	40 IIA
3022.02	1		3149.027	0	2 IVA	3385.017	1	6 IIIA	3552.206	4	10 III	3745.465	10	80 rII	4087.505	2	10 IIA
3023.075	1	1 IV	3150.216	0	1 IV	3385.970	1	12 III	3558.873	2	12 IIA	3747.360	1	15 III	4099.959	1	15 IIA
3025.53	1		3156.784	1	3 IV	3386.609	3	15 III	3562.224	4	15 II	3747.521	1	12 III	4101.317	1	3 III
3026.04	1		3156.977	1	1 IV	3391.024	1	5 III	3563.591	2	6 III	3748.521	10	80 rII	4106.284	1	8 IIA
3026.588	8	3 IV	3157.688	1	1 IV	3394.815	1	6 IV	3564.216	3	8 III	3755.352	1	6 III	4125.233	1	20 IIA
3027.474	3	3 IV	3159.497	1	2 IVA	3395.802	2	8 III	3566.468	2	8 III	3756.411	10	100 RII	4126.117	1	10 IIA
3028.009	1	1 IV	3160.522	0	3 IV	3401.278	0	4 IVA	3569.477	3	6 III	3760.169	2	15 III	4129.994	2	8 IIA
3029.31	0		3165.392	0	3 IV	3406.547	3	8 III	3571.785	5	8 ?III	3760.785	1	6 III	4133.796	1	4 IIA
3029.90	0		3174.507	1	5 IV	3408.049	2	6 III	3573.845	3	8 III	3761.144	1	10 III	4135.505	2	20 IA
3031.06	1		3177.748	1	3 IV	3410.037	1	12 III	3575.451	4	12 III	3763.161	1	6 IIIA	4138.734	1	12 IIA
3031.59	0		3179.507	0	1 IV	3410.286	1	10 III	3586.360	5	40 III	3765.615	0	3 IVA	4142.969	1	4 IIA
3033.393	1	1 IV	3179.725	0	2 IVA	3410.396	2	5 III	3589.301	3	8 ?IIIA	3765.752	0	3 IVA	4145.236	4	30 I
3033.52	1		3181.985	1	4 IV	3412.18	0	4 IVA	3591.679	1	4 IIIA	3766.923	2	20 III	4145.594	1	6 IA
3034.62	1		3182.623	1	3 IV	3412.567	1	8 III	3592.497	1	6 IIIA	3768.311	1	15 III	4146.636	1	4 I
3035.58	0		3182.802	1	2 IVA	3413.609	0	3 IVA	3592.894	2	8 III	3768.807	3	12 IIIA	4147.974	1	6 IA
3035.95	1		3184.192	1	4 IV	3416.198	2	12 III	3594.004	2	12 III	3770.936	1	10 IIIA	4151.135	2	5 IA
3036.60	1		3184.652	1	2 IVA	3416.880	1	6 IVA	3594.508	1	4 IIIA	3772.136	2	15 IIIA	4151.213	2	8 IA
3036.682	2	2 IV	3185.195	1	2 IV	3421.304	1	8 III	3595.929	2	10 IVA	3773.331	8	80 rII	4158.854	1	5 IIA
3038.02	2		3187.566	1	3 IV	3422.067	2	12 III	3596.659	2	8 IIIA	3774.127	1	15 III	4164.709	2	8 IIA
3038.307	1	1 IV	3189.447	1	1 IV	3422.467	0	4 IVA	3597.05	3	15 IIIA	3775.459	2	15 III	4183.333	4	50 rI
3038.52	0		3190.584	2	4 IV	3422.768	2	8 III	3604.714	2	8 IIIA	3775.846	2	12 III	4205.779	3	40 I
3039.705	1	1 IV	3191.031	2	3 IV	3423.499	1	5 III	3606.324	2	8 IIIA	3781.330	1	5 IIIA	4207.250	2	6 IIA
3040.380	5	3 IV	3191.470	1	3 IV	3424.254	3	10 III	3607.644	2	12 III	3782.149	1	10 III	4218.632	4	50 IIA
3041.817	2	2 IV	3196.549	0	3 IV	3427.855	0	6 IVA	3611.055	3	10 IIIA	3782.683	2	20 III	4219.306	4	40 IA
3043.528	3	2 IV	3199.802	1	4 IV	3429.798	1	8 III	3613.910	2	4 IIIA	3783.804	2	20 III	4226.178	4	60 rI
3043.759	1	2 IV	3202.201	2	4 IV	3431.890	3	20 III	3618.531	2	6 III	3787.359	5	30 III	4226.858	3	10 IIA
3046.514	3	3 IV	3209.726	2	5 IV	3434.521	1	8 III	3622.64	1	2 IV	3791.839	2	10 III	4230.727	2	10 IA
3047.254	1	2 IV	3211.227	0	2 IVA	3436.133	1	10 III	3624.414	4	15 IVA	3793.160	1	10 III	4240.450	4	40 IA
3050.20	1		3212.224	0	3 IVA	3438.982	5	10 III	3625.225	1	3 III	3793.334	1	10 IIIA	4244.246	2	12 IA
3051.651	1	2 IV	3213.448	1	3 IV	3441.232	2	6 III	3628.501	1	4 IIIA	3802.416	2	8 III	4248.392	2	4 IIIA
3052.44	0		3214.613	1	4 IVA	3446.58	0	4 IVA	3628.620	1	4 IIIA	3803.942	5	100 RII	4256.309	2	12 IIIA
3053.24	0		3216.234	0	2 IV	3447.790	2	15 III	3628.970	2	6 III	3806.467	1	20 III	4258.168	2	6 IIIA
3053.634	10	5 IV	3216.393	1	3 IV	3448.726	0	4 IVA	3629.120	2	8 III	3809.954	3	30 III	4266.309	5	20 I
3054.313	1	2 IV	3218.260	1	2 IV	3448.868	2	12 III	3629.480	4	40 III	3810.973	3	8 III	4271.862	4	40 I
3054.43	1		3219.041	1	4 IV	3451.533	2	6 III	3636.106	2	8 III	3812.836	3	12 IIIA	4274.011	2	12 IIA
3057.229	2	2 IV	3220.646	3	4 IV	3451.892	1	10 III	3637.563	1	3 IIIA	3813.827	3	30 III	4275.641	1	8 IIIA
3060.054	1	2 IV	3225.622	1	3 IV	3454.784	3	20 III	3641.628	2	10 IIIA	3816.846	2	8 III	4277.404	1	8 IIIA
3060.656	2	2 IV	3231.031	1	6 IV	3457.570	1	8 III	3643.997	3	15 III	3818.363	4	20 III	4282.202	8	100 rI
3060.969	1	1 IV	3232.489	3	6 IV	3458.277	1	6 III	3645.789	3	15 III	3822.972	3	15 ?III	4282.833	8	80 rI
3061.141	3	4 IV	3233.791	1	4 IV	3461.225	0	3 IV	3646.975	2	6 IIIA	3824.811	1	8 III	4283.500	8	80 rI
3063.335	1	2 IV	3234.069	1	2 IV	3463.609	2	10 III	3651.423	5	15 III	3832.808	2	20 III	4283.772	0	8 I
3069.409	5	6 IV	3239.366	2	8 IV	3465.466	3	30 III	3651.516	5	3 III	3834.476	4	80 rII	4290.832	1	8 IIA
3069.78	1		3245.802	2	10 IV	3466.739	5	10 III	3651.825	3	8 IIIA	3834.945	1	8 III	4293.743	1	15 IIA
3070.199	0	2 IV	3247.370	2	6 IV	3466.796	5	20 III	3653.113	1	8 III	3846.277	2	15 II	4296.743	10	300 RI
3070.874	2	3 IV	3249.042	1	4 IV	3469.927	0	8 III	3653.462	3	4 ?III	3846.761	2	15 II	4299.141	4	40 IA
3072.637	2	3 IV	3251.188	0	3 IV	3471.291	1	10 III	3657.312	3	15 III	3853.295	4	50 r?II	4301.275	1	15 IIA
3073.915	5	5 IV	3252.648	2	8 IV	3471.550	1	4 IVA	3661.05	0	4 III	3854.556	4	? II	4305.113	2	10 IIA
3075.309	1	3 IV	3259.418	2	5 III	3472.032	2	12 III	3664.011	1	6 III	3857.339	1	8 II	4312.854	4	30 I
3077.433	1	2 IV	3264.137	2	10 III	3473.05	0	6 IVA	3665.377	2	8 III	3858.517	5	40 ?II	4314.871	4	30 IIA
3084.907	1	1 IV	3265.043	1	3 IV	3473.718	1	8 III	3666.265	1	10 III	3858.737	5	100 r?II	4317.418	1	8 IIIA
3085.017	2	3 IV	3274.430	2	4 IVA	3474.381	2	10 III	3666.972	1	6 IIIA	3860.140	2	30 II	4319.530	10	100 rI
3085.791	1	3 IV	3275.744	1	4 IV	3477.436	3	15 III	3667.932	5	40 III	3873.724	2	15 II	4324.460	5	60 rI
3086.736	1	1 IV	3277.354	2	6 III	3478.445	1	8 III	3668.170	1	4 III	3877.486	2	? II	4325.163	2	30 IIA
3086.867	1	2 IV	3280.218	1	4 IV	3478.955	2	12 III	3668.887	2	10 III	3883.987	1	8 II	4326.145	2	30 IIA
3088.184	3	5 IV	3282.728	0	3 IV	3481.523	1	10 III	3674.345	1	6 III	3886.040	1	8 II	4330.016	10	150 RI
3088.821	5	4 IV	3283.892	3	8 III	3482.828	1	12 III	3675.115	3	8 III	3891.955	1	8 II	4331.447	4	50 I
3089.625	1	3 IV	3287.693	1	3 IV	3483.485	1	12 III	3677.248	5	20 III	3901.046	2	4 II	4336.137	8	125 RI
3090.442	3	8 IV	3291.429	4	10 III	3483.014	1	10 III	3678.081	2	4 III	3904.189	1	3 III	4338.965	5	60 IA
3092.316	1	3 IV	3293.605	1	3 IV	3484.57	1	6 IIIA	3680.983	2	15 III	3908.260	2	8 II	4339.924	2	20 IIA
3094.665	1	4 IV	3294.189	0	4 IV	3484.72	1	8 III	3684.776	1	5 III	3909.946	2	12 I	4344.843	1	8 IIIA
3098.328	1	1 IV	3298.996	4	8 III	3487.3	2	5 III	3687.878	3	20 III	3917.959	1	3 IIIA	4350.815	4	50 IA
3101.927	1	3 IV	3303.606	0	4 IV	3487.612	1	8 III	3688.129	1	10 III	3923.680	1	5 II	4355.835	4	40 IA
3102.867	1	2 IV	3305.434	1	2 IV	3487.049	1	6 III	3689.606	2	12 III	3925.216	5	60 rI	4357.896	2	40 IIA
3103.695	1	1 IV	3307.346	1	3 IVA	3490.705	1	6 III	3690.084	4	50 III	3926.325	2	20 II	4362.912	10	150 RI
3109.964	1	2 IV	3308.546	1	3 IV	3491.040	2	8 III	3690.653	4	15 III	3927.420	1	3 III	4365.954	2	25 IA
3113.407	3	3 IV	3324.022	1	4 IV	3491.905	1	6 III	3694.814	1	10 III	3935.463	1	4 IIIA	4380.423	8	100 rI
3113.496	3	1 IV	3324.615	2	5 IV	3492.898	2	12 III	3695.82	1	6 IIIA	3945.252	2	8 IIA	4381.257	1	8 IIA
3114.629	1	2 IV	3326.984	0	4 IV	3494.826	2	8 III	3699.037	0	2 IV	3949.849	1	10 IA	4388.219	4	60 I
3114.782	5	5 IV	3331.074	2	6 IV	3499.9	0	1 IV	3700.432	3	8 IIIA	3951.887	6	60 rIA	4391.35	0	4 IIIA
3115.542	1	2 IV	3331.935	1	4 IV	3502.818	2	6 IIIA	3701.688	5	20 III	3957.301	1	4 IIIA	4393.170	1	20 IIA
3115.666	2	2 IV	3333.045	1	4 IV	3507.715	2	4 IIIA	3705.995	3	10 IIIA	3960.501	2	8 IIA	4393.354	2	30 IIA
3118.204	1	2 IV	3333.744	0	2 IVA	3508.690	2	12 IIIA	3707.167	4	30 III	3962.136	2	12 I	4397.341	4	60 I
3118.862	2	2 IV	3334.311	1	12 III	3510.15	1	4 IIIA	3707.629	2	12 III	3964.882	2	15 IIA	4401.174	4	60 I?
3120.254	1	2 IV	3338.864	2	8 IV	3511.41	3	8 IIIA	3707.850	4	40 III	3966.144	1	3 IIIA	4403.116	8	150 RI
3121.417	1	1 IV	3341.835	1	10 III	3518.663	1	8 IIIA	3708.77	2	10 III	3968.110	1	4 IIIA	4405.224	1	8 IIIA

TABLE III.—*Continued*

Wave-length (I.A.)	Intensity Absorption	Intensity Emission
4411.585	5	60 rIA
4419.332	8	150 RIA
4423.383	4	20 IA
4429.664	8	80 rI
4433.076	4	30 IA
4433.344	5	50 IIA
4441.812	8	150 RI
4442.276	5	100 rI
4443.270	2	15 IA
4445.153	5	125 rI
4445.881	0	8 IIIA
4452.953	5	50 I
4456.708	5	40 IA
4459.290	4	60 I
4463.897	3	15 IIA
4470.475	4	4 IIA
4470.886	5	100 rI
4471.504	3	8 IIA
4477.505	4	15 IA
4480.316	5	60 IA
4490.019	5	30 IIA
4490.758	1	10 IIA
4499.108	10	150 RI
4503.378	12	125 rI
4504.321	0	6 IIA
4511.327	8	40 I
4522.546	5	30 I
4523.182	4	30 I
4527.418	4	15 IA
4532.444	10	40 IA
4533.799	4	50 II
4534.839	3	20 IA
4536.161	4	20 IA
4537.570	2	10 IA
4539.840	1	5 IIA
4550.032	5	20 IA
4556.628	8	40 IA
4566.767	3	25 IA
4569.579	3	20 IA
4580.188	2	12 IIA
4581.581	5	100 rI
4581.729	5	80 I
4596.743	5	100 rI
4598.285	3	8 IA
4602.024	2	10 IA
4611.248	10	50 IA
4616.615	1	12 IIA
4618.228	2	10 IIA
4629.430	3	20 IA
4632.770	2	8 IA
4640.518	2	8 IA
4643.59	0	1 III
4645.405	8	100 rI
4648.078	3	40 I
4649.491	5	80 rI
4663.556	5	80 rI
4664.509	2	10 IIA
4670.747	6	60 ?I
4670.834	6	80 ?I
4678.114	3	4 I
4681.551	5	40 II
4684.196	2	4 IIA
4688.733	8	100 I
4716.097	5	80 I
4717.071	10	125 I
4718.641	8	30 I
4728.433	10	100 I
4750.725	3	50 II
4760.033	5	60 II
4760.291	8	150 rI
4770.20	4	20 I
4783.125	8	200 I
4785.884	7	125 I
4789.977	5	50 II
4841.701	5	150 I
4848.309	8	100 I
4883.763	10	100 II
4883.971	8	100 II
4904.963	10	80 II
4910.400	10	100 II
4918.994	10	100 I
4924.044	4	30 II
4946.305	10	60 II
4975.949	12	60 I
5010.88	8	10 I A
5044.275	10	40 I
5049.503	10	30 IA
5060.916	8	30 IIA
5071.205	10	60 I
5072.46	1	2 IV
5079.851	2	3 III
5088.347	8	30 I
5091.81	0	2 ?IV?
5100.40	2	2 III
5113.32	0	1 IV
5115.396	1	2 IV
5117.188	12	80 I
5122.159	10	60 I
5132.221	1	1 III
5135.86	1	1 IV
5143.29	2	2 ?III
5145.16	0	1 IV
5145.834	5	12 I
5155.863	3	4 III
5157.260	8	30 I
5172.750	10	40 I
5175.443	10	80 I
5185.550	4	6 IA
5187.131	5	15 I
5194.722	1	4 III
5200.592	12	100 I
5201.454	2	6 III
5209.924	1	4 III
5210.738	4	10 I
5216.44	0	4 IV
5218.388	1	8 III
5221.287	1	6 III
5251.912	10	100 I
5265.646	5	25 I
5269.96	6	10 IA
5271.388	12	125 I
5282.891	8	50 I
5287.66	2	1 IV
5299.21	5	15 IA
5320.572	12	100 I
5341.265	10	50 I
5348.067	5	30 IA
5349.116	5	40 IA
5350.592	4	20 II
5353.701	3	5 IIA
5368.352	8	80 II
5400.85	0	4 III
5402.05	2	20 IIA
5403.70	10	80 I
5405.23	5	125 rII
5411.15	5	40 IIA
5411.39	5	50 II
5415.78	2	4 IIA
5419.47	0	8 III
5421.57	8	30 I
5433.82	5	20 II
5453.00	10	150 rII
5466.72	10	125 rII
5470.29	0	6 III
5485.42	10	100 rII
5493.72	10	200 rII
5498.21	10	150 rII
5500.90	5	25 IIA
5501.78	3	20 IIA
5511.09	10	40 I
5512.10	10	100 I
5516.09	15	300 rII
5517.87	0	4 IIIA
5535.51	5	
5548.95	8	125 I
5550.40	10	200 rII
5561.37	5	20 II
5573.42	8	60 II
5574.89	5	30 II
5575.59	3	20 I
5581.83	3	20 II
5588.20	5	30 II
5591.17	5	40 IA
5591.68	0	6 III
5621.79	10	100 I
5626.01	10	150 rII
5640.25	0	10 III
5641.59	2	10 II
5642.67	3	20 IIA
5644.10	1	20 III
5652.84	5	40 I
5656.34	0	20 III
5659.86	10	200 rII
5678.74	2	15 IIA
5686.98	3	20 I
5693.68	0	10 III
5696.73	1	40 III
5699.61	0	6 III
5706.20	10	100 rII
5706.75	5	80 I
5707.22	3	25 IA
5709.73	0	6 III
5711.45	5	60 II
5720.19	1	60 II
5721.38	0	20 III
5726.06	0	10 IIA
5729.30	0	20 III
5732.95	5	150 II
5741.19	0	4 I
5745.50	2	20 III
5746.50	5	50 IIA
5763.91	0	12 III
5773.77	1	30 III
5778.33	2	50 III
5779.24	5	100 I
5788.38	5	80 I
5790.91	5	50 IA
5800.52	1	50 III
5801.24	0	15 III
5802.84	10	100 I
5814.89	2	60 II
5818.32	0	20 III
5822.61	3	40 IA
5830.51	1	60 III
5860.42	0	30 III
5860.78	1	40 IIA
5866.23	1	20 IIIA
5867.79	3	80 II
5868.61	7	125 I
5871.06	8	125 I
5874.21	8	150 I
5875.92	5	100 IA
5883.68	3	50 IIA
5890.61	1	15 IIIA
5891.41	1	20 III
5895.35	2	20 IA
5898.96	1	30 II
5902.60	2	40 I
5903.50	2	40 III
5906.05	2	40 I
5909.04	2	40 I
5910.83	1	25 III
5912.61	1	30 III
5913.56	0	15 III
5914.91	5	40 IA
5915.36	1	8 III
5916.36	8	150 IA
5921.01	1	12 III
5923.34	0	15 III
5924.23	0	25 III
5924.66	0	25 III
5927.89	5	60 IIA
5936.92	1	8 IIA
5938.86	0	20 III
5946.37	1	30 III
5960.09	1	40 II
5969.49	0	40 III
5979.38	10	200 I
5984.29	1	30 III
5989.68	8	150 IA
5995.09	8	100 I
6001.94	1	40 III
6004.18	15	200 I
6009.89	0	20 III
6016.80	0	15 III
6018.15	2	15 IIA
6027.16	8	150 I
6027.52	8	100 IA
6041.40	1	40 III
6042.84	0	10 III
6045.00	8	150 I
6045.39	0	50 II
6057.69	0	30 III
6059.88	0	20 III
6070.06	10	200 I
6075.72	0	60 III
6084.12	10	250 I
6088.62	0	40 III
6091.40	1	50 III
6096.55	5	80 IA
6099.90	10	200 IA
6103.95	1	15 IIA
6117.79	10	150 IA
6135.85	0	50 II
6159.56	10	200 I
6174.45	8	150 I
6194.39	12	200 I
6196.83	1	25 IIA
6198.37	10	125 IA
6204.72	1	15 IIA
6218.23	10	150 IA
6222.55	5	30 IA
6226.70	1	20 II
6229.07	2	20 IIA
6242.39	12	200 IA
6273.29	10	80 IA
6295.97	8	80 IIA
6345.86	0	30 III
6367.41	12	250 I
6371.01	8	150 I
6373.29	3	60 IIA
6373.50	5	100 IIA
6380.05	0	50 II
6387.79	10	100 IA
6425.90	12	250 I
6428.94	1	80 III
6435.34	1	60 II
6437.62	1	60 II
6471.59	15	60 II
6483.39	0	50 IA
6491.28	8	100 IA
6492.05	1	25 IA
6501.00	5	100 IA
6509.44	15	300 IA
6528.02	12	250 IA
6532.25	15	300 I
6533.96	15	300 I
6536.83	12	150 IA
6544.95	12	150 IA
6551.80	15	300 I
6558.17	3	50 IA
6562.64	5	80 IA
6563.52	10	200 I
6566.36	8	100 I
6580.53	8	200 IA
6588.91	10	300 I
6661.37	0	40 II
6671.51	10	400 I
6678.00	3	60 IIA
6725.88	15	200 I
6775.30	8	150 IA
6779.16	10	200 IA
6790.88	5	60 IA
6802.96	12	150 IA
6827.81	5	150 IA
6853.92	8	150 IIA
6860.93	15	300 I
6864.60	3	15 IIA
6867.11	0	20 III
6880.86	5	200 II
6912.79	3	100 IIA
7002.03	2	60 IA
7026.62	15	200 IA
7051.52	0?	40 II
7056.55	0	40 I
7088.30	15	250 I
7091.16	10	150 I
7095.50	18	200 I
7096.33	18	150 I
7101.46	5	50 I
7104.54	18	200 I
7106.23	18	150 I
7114.50	10	80 I
7115.97	0	30 II
7131.80	15	150 I
7141.13	15	100 I
7172.67	5	30 I
7210.95	0(b)?	100 I
7213.82	18	100 I
7225.62	1(b)?	25 II
7262.69	3	20 IIA
7279.25	15	100 I
7290.23	1	15 II
7332.65	15	100 I
7367.9	1	4 IIA
7378.04	12	60 IA
7403.30	15	60 IA
7446.2	2	5 IIA
7470.72	1	30 II
7479.37	1	15 II
7513.3	2	8 IIA
7554.14	10	60 IA
7580.91	8	60 IA
7590.43	1	25 II
7686.70	4	60 IA
7755.4	4	80 IA
7787.02	2	60 IA
7801.54	1	100 II
7907.48	2	40 IA
7940.31	1	150 I
8027.5	0	15 IIA
8065.16	1	150 I
8203.98	1	150 IA
8267.45	1	100 IA
8301.34	0?	200 IA

produce lines observable in emission, but the lines should appear in absorption, in a manner analogous to the appearance of the higher members of the principal series of sodium in absorption, and their absence in emission. This behavior should be exhibited by cerium and neodymium also, but the data do not indicate it as clearly as those for samarium.

Spectrograms were taken for all three of these elements from 2500 to 10,000A, and for cerium the region was extended to 12,000A; but no absorption lines were observed beyond the extent of the tables.

The author wishes to thank Professor G. R. Harrison for suggesting this problem and for his advice during the course of the work, as well as for the use of the facilities of this laboratory. He is also indebted to Dr. Walter Albertson for his advice and assistance in obtaining and reducing the spectrograms, and to Dr. A. S. King for the use of his unpublished data on cerium.

Diffuse Rings Produced by Electron Scattering

L. H. GERMER, *Bell Telephone Laboratories*
(Received November 25, 1935)

Two diffuse rings produced by electrons scattered from polished metal surfaces have been widely accepted as evidence that such surfaces are amorphous. Similar rings are, however, formed by electrons scattered from vaporized ZnS, and from unpolished surfaces of SiC and Cu_2O, all of which are very probably crystalline. These experiments seem to vitiate the previous interpretation of these rings, although they cannot be construed as definite evidence against an amorphous layer on polished metals.

A NUMBER of experiments have been reported in which electrons incident near grazing have been scattered by highly polished metal targets. The patterns obtained consist of two broad diffuse rings somewhat similar in appearance to rings produced when x-rays are diffracted by a liquid; indeed, the ratio of the radii of the rings (1.8 : 1 approximately) agrees well with prediction based on a simple theory of diffraction by liquids, and with the x-ray patterns of one or two actual liquids.

The obvious inference is that during polishing the material in and near the surface of the target has been rendered amorphous as conceived long ago by Beilby. The surface layer is a supercooled liquid and this is revealed by the pattern of broad rings. This interpretation has been widely accepted, particularly in England, as is evident from the favorable consideration it received at a symposium of the Faraday Society, the papers of which appear in the September number of the Transactions of this society.

In spite of the general acceptance of this interpretation there are certain observations and certain considerations which are not easily reconciled with it, and it is my purpose in this paper to describe still others. Among the difficulties already encountered is the fact that the two diffuse rings are reported to have the same radii for most metals—in the extreme case, for metals for which the cube roots of the atomic densities are in the ratio 1.4 : 1. X-ray diffraction patterns of different liquids do not show such unaccountable similarities.

One of the arguments in favor of the amorphous layer is that if the polished surface were crystalline one would observe the normal Debye-Scherrer pattern of the metal, or possibly the normal pattern as displaced by refraction; since such patterns are not observed the surface cannot be crystalline. The argument is probably not sound, because refraction may easily account for the absence of anything resembling a normal pattern from a crystalline surface from which no points or particles project. This I have attempted to explain in a previous note,[1] and Kirchner also has pointed it out. Kirchner[2] notes that the normal Debye-Scherrer rings should be produced only by projecting roughnesses. If, in reflection experiments, broadening of rings is observed, then any conclusion from this broadening regarding mean size of the crystals must refer only to those portions of the crystal grains which project from the surface, and not to the total sizes of the grains. Kirchner has carried out an instructive experiment upon gold foils in which he shows that the same crystal structure gives, with reflected rays, diffuse rings and with transmitted rays sharp rings. He states finally that "no definite conclusions can be drawn as to the size of crystal grains within the surface layers so far as reflection experiments are used."

DIFFRACTION PATTERNS BY REFLECTION AND BY TRANSMISSION

I have recently repeated Kirchner's experiment using a transparent film of ZnS which had been vaporized in vacuum upon a glass plate. In Fig. 1A is shown the pattern obtained by reflecting electrons from the surface of this film. After this experiment the glass upon which the film had been deposited was broken and, holding the

[1] Germer, Phys. Rev. **43**, 724 (1933).
[2] Kirchner, Nature **129**, 545 (1932); Erg. d. exakt, Naturwiss. **11**, 112 (1932); Trans. Faraday Soc. **31**, 1114 (1935).

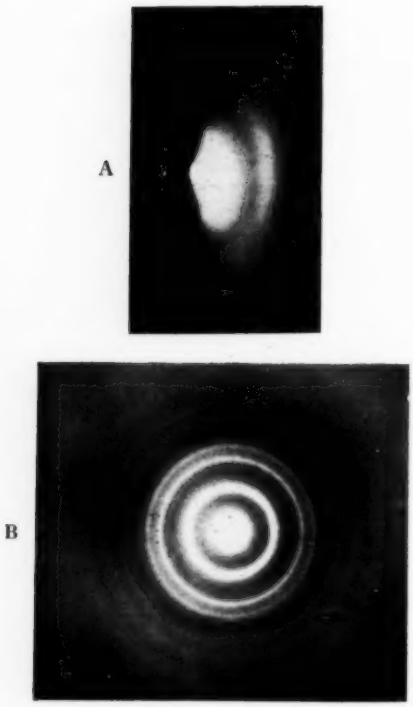

FIG. 1. Diffraction patterns from a ZnS film, deposited by vaporization in vacuum. A, by reflection; B, by transmission.

broken glass under water, portions of the film were chipped off at the edge of the glass. It was easy to capture a minute piece of the film over a 0.1-mm hole in a metal plate. Electrons transmitted through this fragment of film gave the pattern of Fig. 1B.

The ratio of the radii of the rings of Fig. 1A is equal to 1.83. The individual rings correspond, by the Bragg formula, to spacings 2.34A and 1.28A. These values agree well with those of the rings commonly observed from polished metals. The transmission pattern of Fig. 1B, on the other hand, consists of seven sharp rings which correspond both in radii and intensities with rings calculated from the well-known structure of the cubic modification of ZnS,[3] (B3 structure in *Struckturbericht* by Ewald and Hermann). This experiment upon ZnS is substantially a repetition of Kirchner's experiment upon gold mentioned above. It proves again that the occurrence of diffuse rings by reflection cannot be accepted as evidence that the reflecting material is amorphous.

DIFFUSE RINGS FROM NATURALLY FORMED SURFACES

In the present paper I wish to report other objections to the amorphous layer interpretation of the diffuse diffraction rings. The new difficulties are presented by diffraction by glassy smooth surfaces of carborundum single crystals and by glassy smooth surfaces of polycrystalline cuprous oxide. It is difficult to believe that these naturally smooth surfaces are covered by layers of amorphous carborundum and amorphous cuprous oxide, and yet they produce the same type of pattern as polished metals—two broad diffuse rings.

Carborundum crystals were chosen having natural (0001) faces which appeared very smooth and perfect. These crystals were prepared by washing in Merck's thiophene free benzene, in anesthetic ether and in absolute alcohol. From the alcohol each crystal was dried quickly in a stream of dry nitrogen. After this treatment (as well as before) the (0001) faces had a very high gloss and were exceedingly flat. Electron diffraction patterns from these faces always show two rings which are definitely more diffuse than those of Fig. 1A. In addition to these diffuse rings there are traces of extremely weak sharp rings, and sometimes very weak poorly defined spots lying along the intersection of the plane of incidence with the photographic plate. Sometimes also one can detect patterns characteristic of the carborundum crystal, and in one case the carborundum pattern was strong—almost comparable in intensity with that of Fig. 2B. In this case, as well as the others, the two diffuse rings are clearly shown. Usually they are the predominant feature of the plate. The radii of these rings from different specimens appear to be the same, and

[3] The thickness of the film which produced the pattern of Fig. 1B was about 800A, which is somewhat too great to give the best possible pattern. In printing from the original plate it was necessary to employ translucent shields protecting the outer portion of the plate from the intense light necessary for the very dark region near the primary beam. This may be considered a simplified modification of the sector copying method described by Trendelenburg in Wiss. Veröff. a. d. Siemenskonzern **13**, 48 (1934). The rings do not appear with their correct relative intensities in the reproduction. A similar photographic artifice was used in producing the prints of the other figures. In spite of this the rings of Figs. 1A, 2A and 3A are reproduced badly and are much less definite than on the original plates.

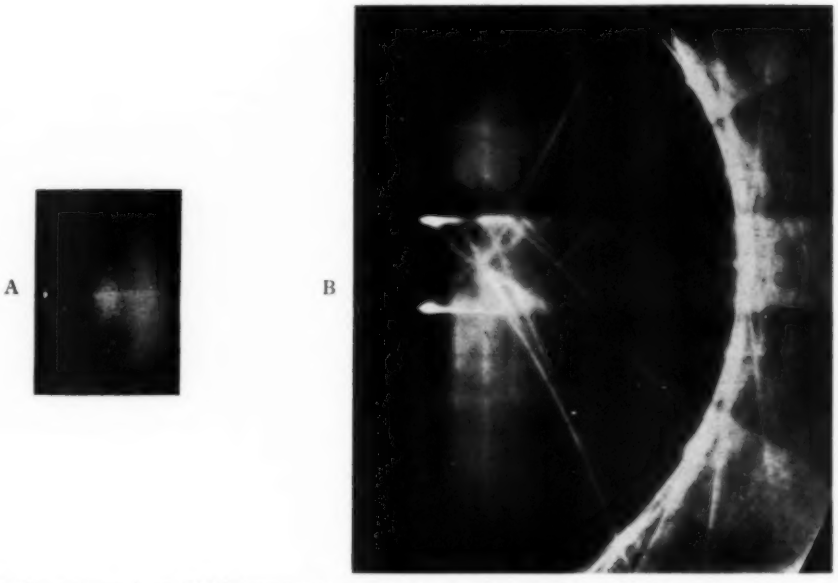

FIG. 2. Reflection patterns from (0001) faces of SiC crystals. A, smooth, unetched surface; B, surface etched in fused KOH.

the mean values of all the measurements correspond, by the Bragg formula, to spacings of 2.26A and 1.23A. These are in good agreement with values obtained from rings produced by polished metals.

The diffuse rings are destroyed by etching in fused KOH. Figs. 2A and 2B show patterns before and after etching. The strongest features of Fig. 2B are readily calculated from the carborundum structure, and it seems highly probable that the entire pattern is due to this structure.[4]

Similar experiments have been carried out upon sheets of red transparent cuprous oxide. This material was formed by oxidizing sheets of copper completely in air. The surfaces of the specimens used had a glassy smoothness, although they were not flat. The individual crystals were very large and the electron beam was probably incident upon only ten or twenty different crystals. The surfaces were prepared by careful washing in benzene, ether and alcohol, and by drying quickly in a stream of nitrogen. The scattering patterns (Fig. 3A) show two diffuse rings, of which the mean values of the measured radii correspond to spacings of 1.7A and 1.1A. These values are distinctly lower than those calculated from the rings from polished metals.

The two diffuse rings cannot be found after the cuprous oxide has been etched. The new pattern which is produced after etching varies greatly with the type of etch. Microscopic examination of some etched surfaces shows minute roughnesses, the various crystals having different appearances. Such a surface gives a diffraction pattern characteristic of some newly formed, and as yet unidentified, surface layer plus what appear to be separate spots falling on the Debye-Scherrer rings of Cu_2O. Under appropriate conditions an etched surface can, however, be produced on which most of the crystals continue to have a rather smooth appearance. The pattern of Fig. 3B came from such a surface. The streaks in this figure, which are approximately parallel to the plane of incidence, appear to be spots on Debye-Scherrer rings which have been displaced and elongated due to refraction and a variable

[4] The crystal which produced the pattern of Fig. 2B was adjusted to make the plane of incidence upon the (0001) face parallel to a [01$\bar{1}$0] direction. It turns out that the strongest features of this pattern are due to the atoms lying along this direction and to planes which pass through this direction as a common zone axis. The spacings and arrangements of these particular atoms and planes happen to be the same for three of the four different crystalline forms of carborundum. Thus one does not readily determine from the pattern of Fig. 2B which of the three structures B5, B6 or even the cubic B3 (Ewald and Hermann *Struckturbericht*) is that of the crystal used. Intensity relations allow one to conclude that the structure is not that described as B7.

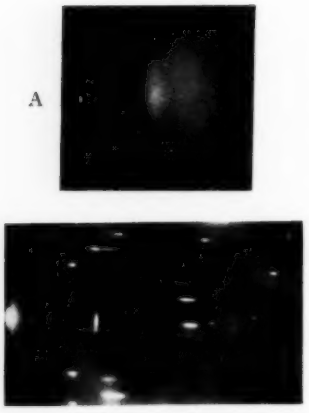

FIG. 3. Reflection patterns from Cu_2O. A, smooth unetched surface; B, etched surface.

glancing angle upon the surface of the individual crystal giving rise to each spot. The elongation seems to be like that observed by French[5] for spots from a silver crystal which had been very lightly polished.

The surfaces which produced the patterns of Figs. 3A and 3B were examined microscopically. Both appeared to be relatively smooth, but they were distinctly different. On the former the crystal boundaries were not marked and the entire surface had a uniform glassy appearance. On the latter the boundaries were well defined and, although most of the crystals still seemed rather smooth, this smoothness had become much less perfect. One cannot, perhaps, be certain that this same difference would still obtain if the observations were concerned with roughnesses sufficiently small to be of importance in the diffraction experiments. There is, however, experimental basis for believing that this would be so; visual examination of roughened metal surfaces is a fairly reliable guide to the suitability of the surfaces for electron diffraction.

It is well known that roughened crystalline surfaces do not show refractive effects. These are appreciable only for surfaces which are so smooth that the *true* glancing angles of incidence or emergence are quite small. From the streaks of Fig. 3B one is able to determine that the surface giving this pattern was sufficiently smooth to cause some refractive displacements of diffraction spots, although less than the displacements which one would expect to observe if the surface had atomic flatness. Judging from the microscopic examinations one must conclude that any diffraction pattern arising from the unetched oxide surface would be displaced by refraction to a still greater extent. Nevertheless the rings of Fig. 3A are similar to those reported from polished metals, and have slightly *larger* radii rather than smaller. The amorphous theory requires that the polished surfaces giving rise to such rings be so rough that refractive effects are nonexistant. The microscopic examinations together with the interpretation of Fig. 3B actually indicate, on the contrary, that the diffuse rings are produced by a surface which is so very smooth that refractive effects must be important —unless, of course, the rings arise from some superficial layer of other material.

No adequate explanation of the diffuse rings from very smooth crystalline surfaces is at hand. The careful washing of these surfaces was expected to remove all grease. Tests have, nevertheless, been made upon thick surface layers of grease. These give interesting patterns which are entirely unlike the diffuse rings. Upon the surfaces of the carborundum crystals there must be some extraneous polycrystalline material to account for the traces of sharp Debye-Scherrer rings which are observed. It appears barely possible that the diffuse rings of Fig. 2A may be made up of a large number of sharp rings very closely packed together. In the case of the ZnS and Cu_2O surfaces, however, there are no traces of the resolution of the diffuse rings into constituent parts.

The present experiments do not offer any definite evidence against the amorphous theory. They simply show that the formation of diffuse rings by electrons scattered from polished metal surfaces cannot, at the present time, be construed as evidence that the surfaces are amorphous.

As a speculation regarding the origin of the diffuse rings it seems worth while to point out that fast electrons have never given rise to diffraction patterns which have been attributed to water or gas molecules adsorbed on a surface. Such adsorbed molecules might be expected to produce appreciable diffraction effects only when lying upon exceedingly smooth surfaces, if at all.

[5] French, Proc. Roy. Soc. **A140**, 637 (1933).

Theory of the Scattering of Slow Electrons by Diatomic Molecules

J. B. Fisk, *Eastman Laboratory, Massachusetts Institute of Technology*

(Received November 29, 1935)

The problem of the Ramsauer effect for diatomic molecules has been treated in a manner analogous to that used by Allis and Morse for atoms. The molecule is represented by a simplified potential field in spheroidal coordinates, and an exact solution is obtained, valid for all velocities of incident electrons. The calculations of "total cross section for elastic scattering" are made in terms of three parameters whose values for a given molecule are definitely determined from data of band spectroscopy and from Slater's rules for atomic shielding constants. Calculations have been carried out in the region of incident electron velocities 0 to 40 volts for N_2, O_2, and H_2, for which molecules excellent agreement is obtained with experiment.

1. Introduction

MEASUREMENTS of the absorption of slow electrons in their passage through a gas have revealed that for molecules, as well as for atoms, the absorption coefficient, α, may change by large amounts for small changes in the velocity of the incident beam, in the range of electron velocities from 0 to 10 or 15 electron volts. The measurements of α, referred to 0°C and 1 mm of mercury pressure, may be correlated with the total cross section for scattering, Q, by the expression $Q=1.02\alpha$ where Q is measured in terms of the square of the first Bohr orbit of hydrogen.

The success of the quantum theory in the hands of Allis and Morse,[1] in resolving this Ramsauer effect for atoms, by assuming a simplified potential, suggested naturally that the molecular problem might be treated in an analogous way. The results of Allis and Morse indicate that the collision cross section is not sensitive to charge distribution provided the potential has the proper characteristics. Their potential was Coulomb-like at small values of r, but went to zero at some distance r_0 from the nucleus. This assumes that the negative charge is distributed over a spherical shell of radius r_0. The effective charge number, and the value of r_0 were calculated from the empirical rules of Slater[2] for the various atoms.

Presumably the molecule may be represented in a similar fashion. Experimental data are available for the internuclear distances, while the other molecular constants, effective charge numbers, and the equivalent of r_0, cannot come far wrong if the atomic analogy be adopted *in toto*.

[1] Allis and Morse, Zeits. f. Physik **70**, 567 (1931).
[2] Slater, Phys. Rev. **36**, 57 (1930).

2. The Molecular Field

Mathematical treatment of the scattering from diatomic molecules requires the wave equation in spheroidal coordinates. Fig. 1 indicates this orthogonal coordinate system where d is the internuclear distance, r_1 and r_2 are the distances from the two nuclei, and

$$\xi=(r_1+r_2)/d\,; \quad \eta=(r_1-r_2)/d.$$

For a symmetrical diatomic molecule the Coulomb potential is given by

$$\Phi_c=2Z\left(\frac{1}{r_1}+\frac{1}{r_2}\right)=\frac{8Z}{d}\cdot\frac{\xi}{\xi^2-\eta^2} \qquad (1)$$

(in atomic units). In order that the potential, Φ, shall represent the field of a molecule it must go to zero on some boundary, such as $\xi=\xi_0$ =constant. But, at the same time, it must leave the Schrödinger equation separable. In other words, Φ must be equal to the Coulomb potential Φ_c multiplied by some function $f(\xi)$, such that

$$\begin{aligned}\Phi &\backsimeq \text{Coulomb} \quad \text{for} \quad \xi \backsimeq 1\\ &=0 \qquad\qquad \text{for} \quad \xi=\xi_0.\end{aligned}$$

The criteria for the function, $f(\xi)$, are

$$\begin{aligned}f(1)&=1, \quad f'(\xi_0)\leqq 0,\\ f(\xi_0)&=0, \quad f'(1)\leqq 0.\end{aligned} \qquad (2)$$

There are numerous forms of $f(\xi)$ which fulfill

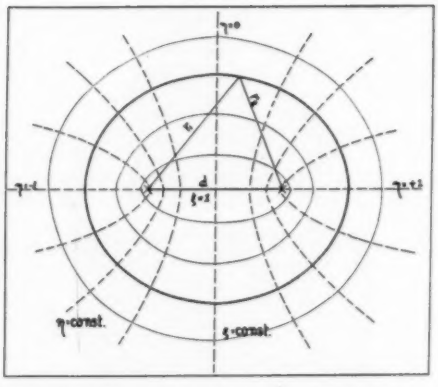

FIG. 1. Spheroidal coordinate system. The heavy line is for $\xi=2$.

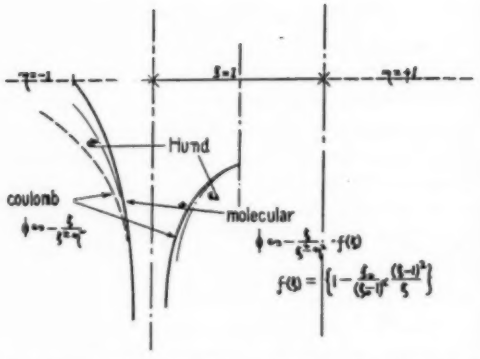

FIG. 2. Potentials plotted along the line of centers of the nuclei.

these conditions. In order to choose among them it is necessary to examine the charge distribution corresponding to each form, and to select that one which best represents the molecule, and which is at the same time simple enough to make the calculations possible.

The following forms of $f(\xi)$ are typical of a number which have been studied:

$$f_A(\xi)=1-[\xi_0/(\xi_0-1)^2][(\xi-1)^2/\xi],$$
$$f_F(\xi)=(\xi_0-\xi)/(\xi_0-1),$$
$$f_S(\xi)=[(\xi_0-\xi)/(\xi_0-1)]^2.$$

These functions, which multiply Φ_C to give Φ, satisfy all the conditions (2). Other f's involving ξ in higher powers may be written down readily. While these latter may possibly represent the charge distribution in a molecule more accurately, it must be kept in mind that the practical problem of solving the wave equation presents itself.

Forms A and F involve ξ, while form S involves ξ^2. Hence, if A or F give reasonable charge distributions they will be preferred. The charge distribution may be readily calculated from Poisson's equation. ρ_A is given by

$$\rho_A=\frac{2\xi_0 Z}{\pi d(\xi_0-1)^2}\cdot\frac{1-\cos^2(\mathbf{r}_1\mathbf{r}_2)}{r_1 r_2}.$$

Φ_A, therefore, represents a distribution of positive charge within the molecule, most of it being concentrated at the two nuclei, none along the line of centers. Or, otherwise, the positive nuclear charge may be considered as being spread out slightly; the negative charge being distributed over the spheroidal surface.

Similarly, ρ_F and ρ_S may be calculated. Φ_F represents both positive and negative charge within the molecule, with a large dipole at each nucleus. Φ_S, which was used by Stier[3] in a calculation for N_2, also has this unsatisfactory dipole at the two centers. The several Φ's do not look appreciably different when plotted together. Φ_A, on a section through the line of centers of the two nuclei, is shown in Fig. 2. The light line is that calculated by Hund using Thomas-Fermi ideas.

Φ_A appears to be best suited to the problem. It avoids the dipoles at the nuclei; it contains ξ in only the second power; and it resembles the Coulomb field as is desired. The additional charge within the molecule may be calculated by integrating over the spheroid, giving for the ρ_A chosen:

$$\int\rho_A d\tau=\frac{2Z}{d}\left[\frac{(\xi_0+1)^2}{2\xi_0}\ln\frac{\xi_0+1}{\xi_0-1}-1\right]=F_0.$$

ξ_0	1.5	2.0	2.5	3.0	4.0
F_0	2.23	1.48	1.07	0.85	0.60

Having chosen a value of ξ_0, F_0 then gives a factor by which the atomic number must be corrected.

It would be desirable, of course, to have a potential which distributed negative charge

[3] Stier, Zeits. f. Physik **76**, 439 (1932).

throughout the molecule to avoid the necessity of having the negative spheroidal surface charge; the positive charge being only at the two nuclei. This appears to be impossible if, at the same time, one demands that the wave equation be solved analytically. The results of Allis and Morse give justification for the use of the molecular potential which has been selected.

3. Calculation of the Total Cross Section for Elastic Scattering

Using the potential field, Φ_S, previously described, Stier[3] has worked through the problem in spheroidal coordinates for N_2, subject to the condition that the energy of the incoming electron be small. Choosing arbitrarily a value of Z, the effective charge, and ξ_0, the shape of the molecule, he has obtained fair agreement with experiment.

The method to be developed presently will be valid for all velocities of incident electrons, and for all symmetrical diatomic molecules. Its chief restriction lies in the potential function, which is subject to the conditions previously enumerated. This difficulty is inherent in all scattering problems.

It is necessary now to obtain two solutions of the wave equation: one outside, and one inside the molecule. One can then determine the amount of "phase" which must be added to the wave outside of the molecule to have it fit onto the inside wave at $\xi=\xi_0=$molecular boundary.

The solution outside the molecule, $(V=0)$, can be given in terms of the spheroidal functions, recently defined by Stratton,[4] to be

$$\Psi_0=\sum_{m,\,l} A_{ml}e^{im\varphi}(1-\eta^2)^{m/2}(\xi^2-1)^{m/2} \times Se^{(1)}_{m,\,l}(c,\eta)\cdot Re^{(1)\text{ or }(2)}_{m,\,l}(c,\xi), \quad (3)$$

where the $Se^{(1)}_{m,\,l}(c,\eta)$ are expressed as an infinite series of Legendre polynomials;

$$Re^{(1)}_{m,\,l}(c,\xi)=\left(\frac{\pi}{2}\right)^{\frac{1}{2}}\frac{(c\xi)^{-m-\frac{1}{2}}}{2^m m!}\sum_k{}'\, i^{m-k}\frac{(2m+k)!}{k!} \times d_k{}^{ml}J_{k+m+\frac{1}{2}}(c,\xi) \quad (4)$$

and $Re^{(2)}_{m,\,l}(c,\xi)$ is a similar expression involving the Neumann function in place of the Bessel function.

The solution inside the molecule,

$$V=(d/2)^2[\xi/\xi^2-\eta^2]f(\xi),$$

differs from (3) only in the ξ part. After separation of variables, the ξ part of the wave equation becomes

$$\left[\frac{\partial}{\partial\xi}(\xi^2-1)\frac{\partial}{\partial\xi}-\frac{m^2}{\xi^2-1}+c^2\xi^2 +2Zd\left\{\xi-(\xi-1)^2\frac{\xi_0}{(\xi_0-1)^2}\right\}-\gamma\right]X=0, \quad (5)$$

the solution of which is

$$X(\xi)=(\xi^2-1)^{m/2}\cdot e^{-\lambda(\xi-1)}\cdot f(\xi-1), \quad (6)$$

where $\lambda^2=\alpha-c^2$; $\alpha=2Zd\xi_0/(\xi_0-1)^2$;

$$c^2=(\pi d/\lambda)^2=((d/2)\cdot k)^2.$$

The equation for $f(\xi-1)$ is solved by an infinite series giving a three-term recursion relationship. This series is absolutely convergent for $\xi<3$.

In terms of these two solutions and their first derivatives one proceeds then to obtain the "phase-defects." Equating the ratio of slope to function at the boundary $\xi=\xi_0$ for the solution inside and the solutions outside the molecule

$$\frac{C_{ml}Re^{(1)'}_{m,\,l}(c,\xi_0)+D_{ml}Re^{(2)'}_{m,\,l}(c,\xi_0)}{C_{ml}Re^{(1)}_{m,\,l}(c,\xi_0)+D_{ml}Re^{(2)}_{m,\,l}(c,\xi_0)}=g_{ml}=\frac{f'(\xi_0)}{f(\xi_0)}-\lambda, \quad (7)$$

one obtains for the tangent of the "phase-defect"

$$\tan\delta_{ml}=(-1)^m\frac{D_{ml}}{C_{ml}}=(-1)^m\left[\frac{Re^{(1)'}_{m,\,l}(c,\xi_0)-g_{ml}\cdot Re^{(1)}_{m,\,l}(c,\xi_0)}{g_{ml}Re^{(2)}_{m,\,l}(c,\xi_0)-Re^{(2)'}_{m,\,l}(c,\xi_0)}\right]. \quad (8)$$

[4] Stratton, Proc. Nat. Acad. Sci. **21**, 51 (1935).

One wishes then to know the total cross section for elastic scattering in terms of the phase defect. If, from the wave function (3), the expression for a plane wave be subtracted, the scattered wave will be obtained, valid in the range of observation. Morse[5] has recently given the expansion of a plane wave in spheroidal coordinates to be

$$e^{ikX}=2\sum_{m,\,l}\cos\left[m(\varphi-\alpha)\right]\frac{c^m i^{m+l}}{N_{ml}}\sin^m\omega\cdot Se^{(1)}_{m,\,l}(c,\cos\omega)(\sinh\mu\sin\vartheta)^m Se^{(1)}_{m,\,l}(c,\cos\vartheta)Re^{(1)}_{m,\,l}(c,\cosh\mu),\quad(9)$$

where N_{ml} is a normalizing factor;

$$\sinh\mu=(\xi^2-1)^{\frac{1}{2}};\quad \sin\vartheta=(1-\eta^2)^{\frac{1}{2}};\quad X=(d/2)[\cos\omega\cos\vartheta\cosh\mu+\sin\omega\sinh\mu\cos(\varphi-\alpha)];$$

and the direction of propagation with respect to the z axis is defined by the angles ω and α.

Subtracting e^{ikX} from Ψ one obtains for the scattered wave $F(\vartheta)\cdot e^{ic\xi}/\xi\cdot d/2$, where

$$F(\vartheta)=2\sum_{m,\,l}\frac{\cos\left[m(\varphi-\alpha)\right]}{k\cdot N_{ml}}\cdot(\sin\vartheta\sin\omega)^m\cdot Se^{(1)}_{m,\,l}(c,\cos\vartheta)Se^{(1)}_{m,\,l}(c,\cos\omega)\sin\delta_{ml}e^{i\delta_{ml}},\quad(10)$$

the A_{ml} of (3) having been so chosen that the solution (10) represents only an outgoing wave.

Averaging $F(\vartheta)$ over all orientations of the molecular axis one obtains the scattered intensity

$$|F(\vartheta)|^2=I(\vartheta)=\frac{4\pi}{k^2}\sum_{m,\,l}\frac{1+\delta_{0m}}{N_{ml}}\sin^{2m}\vartheta\left[Se^{(1)}_{m,\,l}(c,\cos\vartheta)\right]^2\sin^2\delta_{ml},\quad(11)$$

where δ_{0m} is the Kronecker δ-symbol. The total cross section, Q, is obtained immediately from (11) by integrating over ϑ, giving

$$Q=\frac{4\pi}{k^2}\sum_{m,\,l}(2-\delta_{0m})\sin^2\delta_{ml}=4\pi\left(\frac{d}{2}\right)^2\sum_{m,\,l}q_{ml}.\quad(12)$$

The q_{ml} are known as "partial cross sections." The contribution of each to the total cross section, Q, arises from different values of m and l; that is, from different angular momenta of the incoming electrons about the molecule.

Q is calculated in terms of three parameters whose values are fixed for a given molecule by Slater's[5] empirical rules for atomic shielding constants, and by data of band spectroscopy. These parameters are:

$$\beta^2=(Z^*\cdot d\cdot\xi_0)/4;\quad x=\xi_0\cdot c;\quad\text{and}\quad\xi_0.$$

The parameter ξ_0 was chosen to be equal to 2 since this assumes, effectively, that the internuclear distance, d, is twice the "atomic radius," and that the formation of a molecule from two atoms does not push negative charge far beyond the atomic radius on a continuation of the line of centers. The shape of the molecule for $\xi_0=2$ is shown in Fig. 1 by the heavy line. A series of calculations for different values of ξ_0 showed that the cross section was quite insensitive to variations in ξ_0 for ξ_0 between 1.75 and 3.0. This choice of $\xi_0=2$ makes the other parameters

$$\alpha=8\beta^2;\qquad c^2=x^2/4;\quad\text{and}\quad\lambda=(8\beta^2-x^2/4)^{\frac{1}{2}}.$$

A ξ_0 having been chosen, β then determines the molecule uniquely, since Z^* may be calculated. x is the energy of the incident electron in units proportional to (electron volts)$^{\frac{1}{2}}$. β and x have been defined in this manner since they reduce in the limit to the parameters used by Allis and Morse. A series of calculations varying β and x independently should show any periodic phenomena.

The low velocity limit of $Q(x\to0)$ may be obtained by use of Eq. (4). For example: when $m=0$, $l=0$

$$\frac{C}{D}=\tan\underset{\xi\to0}{\delta_{00}}=\frac{g_{00}}{g_{00}+1/\xi_0}\cdot\frac{J_{\frac{1}{2}}(c\xi_0)}{J_{-\frac{1}{2}}(c\xi_0)}\to0,$$

but

$$\underset{x\to0}{q_{00}}=2\cdot\frac{\sin^2\delta_{00}}{c^2}\simeq2\xi_0^2\left[\frac{\xi_0\cdot g_{00}}{\xi_0\cdot g_{00}+1}\right],$$

[5] Morse, Proc. Nat. Acad. Sci. **21**, 56 (1935).

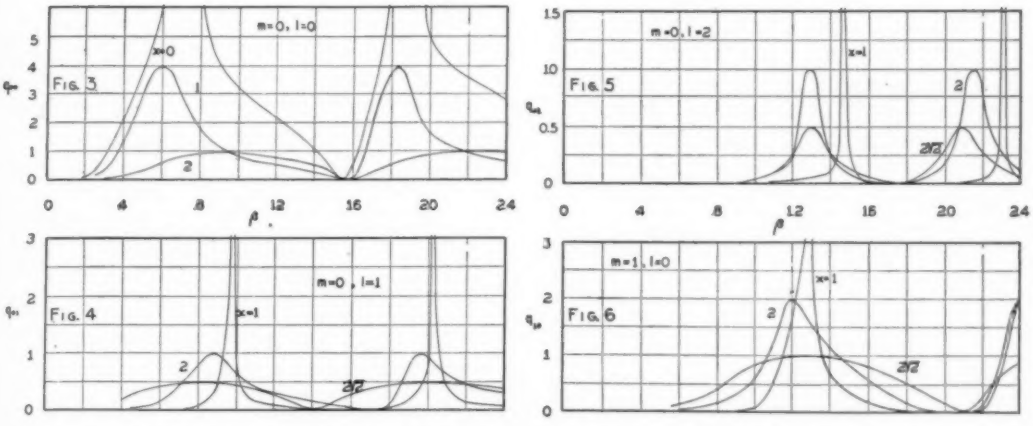

FIGS. 3, 4, 5, 6. Partial cross section as function of the parameter β for different electron velocities, showing occurrence of peaks, and periodicity.

giving a finite value of Q as the energy of the incident electron approaches zero. When $m \neq 0$, $l \neq 0$, the q_{ml} approach zero rapidly as $x \to 0$.

5. Results of Calculations

The total cross section for elastic scattering, Q, has been calculated as a sum of the partial cross sections q_{ml}. The q_{ml} have been calculated as functions of β for a number of values of m and l and for velocities of incident electrons ranging from 0 to 40 volts. It is observed that strong maxima occur in q_{ml} for small values of x as β increases, and that q_{ml} is periodic in β. Figs. 3 through 6 show this behavior for $m=0, 1$; $l=0, 1, 2$ for several values of x. It is observed that as l increases for a given m, the value of β at which a maximum occurs increases. Similarly, for a given l the first peak of q_{ml} for $m>0$ occurs at a considerably larger value of β than for $m=0$. Hence, for small β, the q_{ml} are not affected by neglect of contributions for values of m and l beyond those given.

It is instructive to plot the phase defects, δ_{ml}, for various velocities as functions of β. This has been done for two different m and l combinations in Figs. 7 and 8. The plot brings out the periodicity again indicating the same sort of correlation with the periodic table as was evident in the atomic problem. Here useful information may be obtained concerning the maxima and minima by considering $\sin \delta_{ml}/c$.

Having obtained the q_{ml} as functions of β for various velocities, and for all values of m and l for which there is any appreciable contribution, one can then plot the total cross section Q, as a function of the velocity of incident electrons, for any β. It is to be noted that neglect of partial cross sections beyond q_{00} and q_{01} may lead to serious error. Each q_{ml} becomes most important for some value of β.

It now remains to identify the molecules with values of β in a consistent manner, and to compare the cross sections in theory and experiment.

5. Identification of Symmetrical Diatomic Molecules with the Parameter β

Fig. 9 indicates the method used to determine the effective charge number. The light line is that calculated from the empirical rules of Slater,[3] where the electrons of any shell are considered as forming a uniform charge distribution over a surface whose radius is calculated to give best agreement with spectroscopic properties. The dotted line is that of Allis and Morse[1] where $rV(r)$ has been plotted against r such that the lines enclose equal areas. The curved line has been obtained by plotting

$$[(\xi^2-\eta^2)/\xi]V(\xi, \eta)$$

against ξ for $\xi_0=2$, and adjusting Z such that

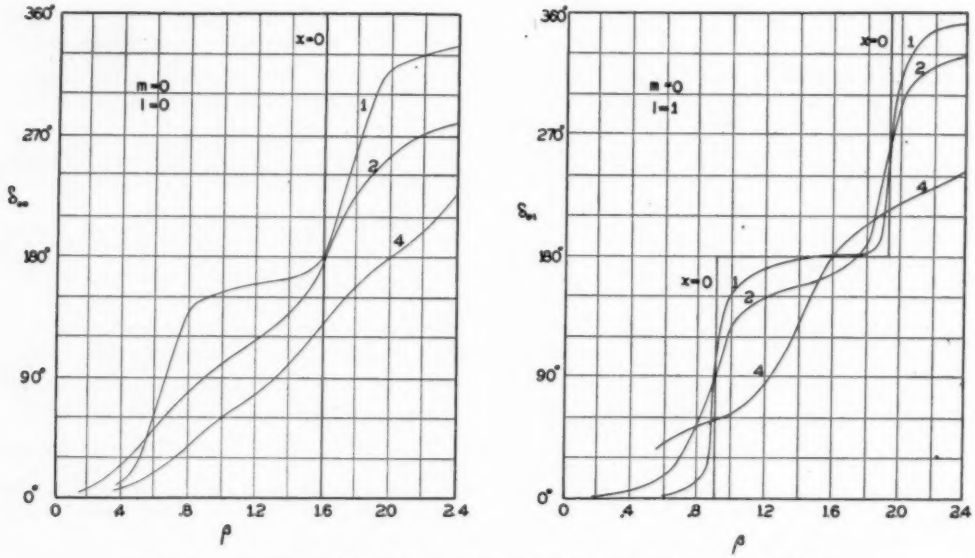

FIGS. 7 AND 8. "Phase defect," δ_{ml}, as function of for different electron velocities.

again the area under this curve equals that under the broken line.

One must correct finally for the additional positive charge introduced by the potential function. From the previous calculations of F one obtains

$$Z^*=Z_0^*/(1+1.48).$$

The internuclear distances are known from band spectra or from crystal structure. One has, therefore, a definite β for each molecule.

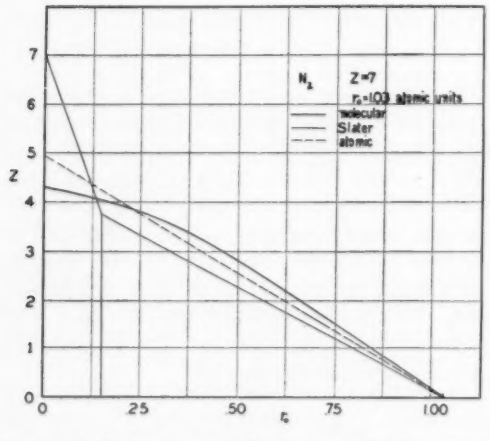

FIG. 9. Method for determination of effective charge number. Plot of V/V (coulomb) as a function of ξ.

6. INTERPRETATION OF EXPERIMENTAL RESULTS

Ramsauer and Kollath,[6] Brüche,[7] Brode,[8] and others, have carried out experiments to obtain the total cross section for elastic scattering in N_2, O_2, and H_2. Fig. 10 shows the structure and final value of Q for N_2, with the experimental results of Brüche for comparison. Apart from the general agreement in shape, position of maxima, and the magnitude of the total cross section as a function of $(\text{volts})^{\frac{1}{2}} \sim x$, it is interesting to note that the theoretical results predict a "fine structure" at about $3.45(V)^{\frac{1}{2}}$. There seems to have been some uncertainty in the experiments regarding this portion of the curve which is generally shown with dotted lines. Of further interest, theory predicts a finite value of Q as $x \to 0$. It also gives the correct magnitude of Q for large values of x. The experimental difficulties in the range 0 to 1 volt are great, hence, the agreement cannot be pushed in this region.

[6] Ramsauer and Kollath, *Handbuch der Physik*, Vol. 22, second edition.

[7] Brüche, Ann. d. Physik **4**, 387 (1930); **83**, 1065 (1927). Also, Ergeb. d. ex. Naturwiss. **8**, 185 (1929).

[8] Brode, Rev. Mod. Phys. **5**, 257 (1933).

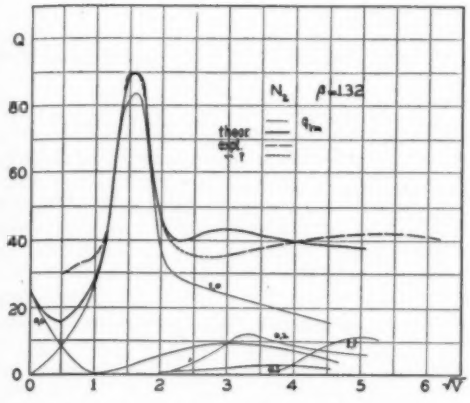

FIG. 10. Total cross section for elastic scattering in N_2 as function of electron velocity in (electron volts)$^{\frac{1}{2}}$. The fine lines are the "partial cross sections."

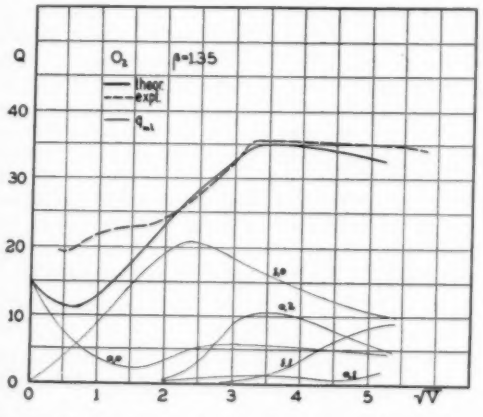

FIG. 11. Total cross section for elastic scattering in O_2.

One might expect to correlate the peak of the cross section curve with the internuclear distance in some manner. No simple correlation has been found for these small velocities. The curve for O_2, Fig. 11, in which there is no sharp peak seems to dismiss the possibility of such a correlation. For low velocities the theory predicts a smaller cross section than that observed. Experimentally, oxygen is a difficult gas with which to work, while low velocity electrons are difficult to obtain. Hence, the agreement may be considered as being good.

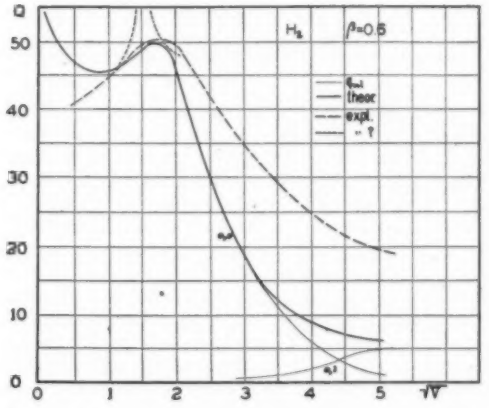

FIG. 12. Total cross section for elastic scattering in H_2.

Fig. 12 compares the results for H_2. The peaks, magnitude, and general shape agree fairly well. As the velocity of the incident electrons increases, the calculated cross section falls below the experimental value. This is, doubtless, due to the fact that the calculations include only elastic collisions, whereas the experiments necessarily include some inelastic scattering and energy going into excitation and rotation. The energy of excitation of H_2 being low renders this explanation plausible.

Calculations for other molecules, Cl_2, etc., can be made quite readily when there is experimental data for comparison.

The fundamental idea and suggestion for this work come from Professor P. M. Morse. It is a pleasure to acknowledge this and the benefit derived from many interesting discussions and helpful suggestions on the subject.

Coulomb Wave Functions in Repulsive Fields

F. L. YOST, JOHN A. WHEELER* AND G. BREIT, *Departments of Physics, University of Wisconsin, University of North Carolina*

(Received December 2, 1935)

Quantitative discussion of nuclear reactions due to bombardment with charged particles requires the knowledge of wave functions in repulsive inverse square fields of force. It is customary to approximate these functions by formulas of the type due to Wentzel, Kramers and Brillouin (referred to as WKB). Errors of unknown amount are frequently introduced by such approximations. Formulas necessary for the *exact* calculation of the needed functions are derived and discussed in the present paper. Results of numerical calculations with estimated total errors are tabulated in a companion article in the *Journal of Terrestrial Magnetism and Atmospheric Electricity*. The proton energy range covered is from 0 to 2 MEV for Li and from 0 to 8 MEV for *C*. For the partial wave with 0 angular momentum the range of radii in proton collisions is covered for Li from 0 to 10^{-12} cm and for *C* from 0 to 0.5×10^{-12} cm. For the partial wave with angular momentum $\hbar$, the range of radii extends to 4×10^{-12} cm in proton collisions with Li and to 2×10^{-12} cm in proton collisions with *C*. The tables are applicable to other reactions as well. Phase shifts necessary for the theory of anomalous nuclear scattering are readily calculated by means of them. The calculation of the regular function and its derivative by means of the tables is easier than that of the irregular solution. The tables are therefore supplemented by graphs in the present paper. By means of these it is possible to calculate the irregular function quickly even though less accurately than by means of the tables. The regular and irregular functions are given, respectively, by $F_L=C_L\rho^{L+1}\Phi_L$, $G_L=D_L\rho^{-L}\Theta_L$. Here the angular momentum of the partial wave is $L\hbar$, C_L and D_L depend only on the energy, ρ is $2\pi r/\lambda$ where r is the radius and λ is the de Broglie wave-length. It is found empirically that for low energies the quantities Φ_L, Θ_L depend only on the radius and not on the energy. This fact is useful in applications and it is explained analytically by means of an apparently new expansion of the confluent hypergeometric function into series of Bessel functions. The successive terms of the series are arranged in ascending powers of the energy and these expansions furnish an independent way of calculating the functions. They are useful for low energies. The exact solutions are compared numerically with the WKB approximations to the functions and to their logarithmic derivatives. The ordinary WKB method is found to give only a crude approximation to the exact solutions in the needed range of energies and radii. The WKB formulas modified by changing $L(L+1)$ into $(L+\frac{1}{2})^2$ are very much better for small energies and small radii but they are not reliable as the region of positive kinetic energies is approached. In some cases the $(L+\frac{1}{2})^2$ method is worse than that using $L(L+1)$. The superiority of the $(L+\frac{1}{2})^2$ method for low energies and constant radii is traced to the fact that in such cases it is identical with the Carlini and Laplace approximations to Bessel functions. From this relationship and graphical comparisons given below errors in the WKB $(L+\frac{1}{2})^2$ approximations can be estimated.

1.

THE radial equation for two particles moving under an inverse square repulsive field of force is:

$$\frac{d^2\bar{F}}{d\rho^2}+\left\{1-\frac{2\eta}{\rho}-\frac{L(L+1)}{\rho^2}\right\}\bar{F}=0, \qquad (1)$$

where

$$\rho=kr;\ k=\mu v/\hbar;\ \eta=(ZZ'/\text{“137”})(c/v)=1/ka$$
$$a=\hbar^2/\mu ZZ'e^2;\quad \text{“137”}=\hbar c/e^2=1/\alpha \qquad (2)$$

and r=distance between particles, v=relative velocity, μ=reduced mass, $L\hbar$=angular momentum of state considered; Ze and $Z'e$ are the charges on the particles; $\bar{F}$ is an arbitrary constant times r times the radial factor of the wave function.

If the inverse square law applies for all r then one needs only the regular solutions $\bar{F}=F$ of the above equation. These are well-known hypergeometric series used by Gordon and Mott[1] in the discussion of Rutherford's formula. These exact forms are convenient for some types of analytical calculation but are cumbersome to use in many problems requiring numerical estimates. In the usual discussion of nuclear collisions one has to suppose that for small values of $r(r<r_0)$ the repulsive inverse square field is changed into another attractive field which represents the "nuclear well." For these smaller values of r the radial function multiplied by r does not satisfy Eq. (1). Instead it satisfies

$$\left[\frac{d^2}{d\rho^2}+1-\frac{2}{\mu v^2}V(r)-\frac{L(L+1)}{\rho^2}\right]\bar{F}=0, \qquad (3)$$

where V is the potential energy at distance r. In

* National Research Fellow.

[1] W. Gordon, Zeits. f. Physik **48**, 180 (1928); N. F. Mott, Proc. Roy. Soc. **A118**, 542 (1928).

applications one needs regular solutions of (3) joined to general solutions of (1) in such a way as to have $\bar{F}$ and its derivative continuous at $r=r_0$. This requires the introduction of solutions for $\bar{F}$ which are linearly independent of F and which are thus irregular solutions of (1) at $\rho=0$. These solutions will be called G. In order to define F and G we have to specify the normalization of the functions and for G we must further define in some way the arbitrary additive constant with which F may enter into G. Now Eq. (1) is a special case of the much studied confluent hypergeometric equation.[2] It is known[1] that the regular solutions of (1) are asymptotic at $\rho=\infty$ to const. $\sin(\rho-L\pi/2-\eta\ln 2\rho+\sigma_L)$ where $\sigma_L=\arg\Gamma(L+1+i\eta)$ and that the irregular solutions are asymptotic at $\rho=\infty$ to forms differing from the above only by the insertion of an arbitrary constant phase into the argument of the sine. It is convenient to standardize both F and G by the requirement that the asymptotic values for large ρ shall be

$$F\sim\sin(\rho-L\pi/2-\eta\ln 2\rho+\sigma_L);\qquad G\sim\cos(\rho-L\pi/2-\eta\ln 2\rho+\sigma_L). \tag{4}$$

Thus F and G are defined by making both have unit amplitude for large ρ and by making the phase of G lead the phase of F by 90°. For the special case of $L=0$ practically explicit forms for G were worked out by Sexl[3] but they are not in a convenient form for calculation on account of the occurrence of imaginaries in real expressions.

The asymptotic forms of the solutions are brought out clearly by using Whittaker's function[2] $W_{\kappa,m}(z)$. Eq. (1) is reduced to the equation of the confluent hypergeometric function by the substitutions

$$z=2i\rho;\quad \kappa=i\eta;\quad m=L+\tfrac{1}{2}. \tag{5}$$

A regular solution of (1) is the function $M_{\kappa,m}(z)$. This may be expressed as a linear combination of $W_{\kappa,m}(z)$ and of $W_{-\kappa,m}(-z)$.

The formula given by Whittaker and Watson at the end of their 16.41 gives an expression for $W_{\kappa,m}(z)$ in terms of $M_{\kappa,m}(z)$ and $M_{\kappa,-m}(z)$ valid for $-\pi/2<\arg z<3\pi/2$; similarly Example 1 immediately following gives $W_{-\kappa,m}(-z)$ in terms of $M_{-\kappa,m}(-z)$, $M_{-\kappa,-m}(-z)$ valid for $-3\pi/2<\arg(-z)<\pi/2$.

We let $\arg z=\pi/2$ and $\arg z=-\pi/2$ so as to correspond to (5) and we have by Kummer's first formula

$$M_{-\kappa,m}(-z)=M_{\kappa,m}(z)\exp\{-(m+\tfrac{1}{2})\pi i\}$$

and

$$M_{-\kappa,-m}(-z)=M_{\kappa,-m}(z)\exp\{(m-\tfrac{1}{2})\pi i\}.$$

We have thus two relations between $W_{\kappa,m}(z)$, $W_{-\kappa,m}(-z)$ and $M_{\kappa,m}(z)$, $M_{\kappa,-m}(z)$.

These can be solved for the latter two quantities and one has

$$M_{\kappa,m}(z)=e^{-\pi i\kappa}\frac{\Gamma(2m+1)}{\Gamma(\frac{1}{2}+m-\kappa)}W_{-\kappa,m}(-z)-e^{\pi i(m-\kappa-\frac{1}{2})}\frac{\Gamma(2m+1)}{\Gamma(\frac{1}{2}+m+\kappa)}W_{\kappa,m}(z).$$

This formula is almost the same as that given in Example 2 of Whittaker and Watson's 16.41, but differs from it by the signs of κ in the exponents. Now $M_{\kappa,m}(z)$ gives a regular solution of (1) if m is real and positive. Similarly $M_{\kappa,-m}(z)$ gives a power series but its first term is $z^{-m+\frac{1}{2}}$. When m is a positive integer $+\frac{1}{2}$ this latter solution is not independent of the first. The asymptotic expansion of $W_{\kappa,m}$ determines the asymptotic form of $M_{\kappa,m}(z)$ and determines the factor by which $M_{\kappa,m}(z)$ should be multiplied to give F as defined by Eq. (4). One thus finds

$$F=\tfrac{1}{2}(Y+Y^*)=\tfrac{1}{2}\left|\frac{e^{\pi i\kappa/2}\Gamma(\frac{1}{2}+m-\kappa)}{\Gamma(2m+1)}\right|e^{-(\pi i/2)(m+\frac{1}{2})}M_{\kappa,m}(z), \tag{6}$$

$$G=\frac{1}{2i}(Y-Y^*)=\tfrac{1}{2}\left|\frac{e^{\pi i\kappa/2}\Gamma(\frac{1}{2}+m-\kappa)}{\Gamma(2m+1)}\right|e^{-(\pi i/2)(m+3/2)}\bar{M}_{\kappa,m}(z),$$

[2] E. T. Whittaker and G. N. Watson, *Modern Analysis*, third edition, Chap. XVI.

[3] Th. Sexl, Zeits. f. Physik **56**, 72 (1929). See especially p. 83. Cf. also Th. Sexl, Zeits. f. Physik **81**, 163 (1933).

where

$$Y=[\Gamma(\tfrac{1}{2}+m-\kappa)/\Gamma(\tfrac{1}{2}+m+\kappa)]^{\frac{1}{2}}\exp\{(\pi i/2)(m+\tfrac{1}{2}-\kappa)\}W_{\kappa,m}(z),$$
$$Y^*=[\Gamma(\tfrac{1}{2}+m+\kappa)/\Gamma(\tfrac{1}{2}+m-\kappa)]^{\frac{1}{2}}\exp\{-(\pi i/2)(m+\tfrac{1}{2}+\kappa)\}W_{-\kappa,m}(-z). \tag{7}$$

The function $\overline{M}_{\kappa,m}$ is defined by Eq. (6) and is analogous to $M_{\kappa,m}$. If m is not a positive half-integer it may be expressed as

$$\overline{M}_{\kappa,m}(z)=\frac{i[\cos 2\pi m+\exp(-2\pi i\kappa)]}{\sin 2\pi m}M_{\kappa,m}(z)-\frac{2i\Gamma(2m+1)\Gamma(2m)}{\Gamma(\tfrac{1}{2}+m+\kappa)\Gamma(\tfrac{1}{2}+m-\kappa)}e^{\pi i(m-\kappa)}M_{\kappa,-m}(z). \tag{8}$$

If m is a positive half-integer the value of $\overline{M}$ can be obtained by passing to the limit in the above Eq. (8).

Substituting into Eq. (6) and expressing the results in terms of ρ, L for integral values of L we have

$$F_L=C_Le^{-i\rho}\rho^{L+1}\left\{1+\frac{L+1-i\eta}{1!(2L+2)}2i\rho+\frac{(L+1-i\eta)(L+2-i\eta)}{(2L+2)(2L+3)}\frac{(2i\rho)^2}{2!}+\cdots\right\}, \tag{8'}$$

where

$$(2L+1)!C_L=2^L[L^2+\eta^2]^{\frac{1}{2}}[(L-1)^2+\eta^2]^{\frac{1}{2}}\cdots[1+\eta^2]^{\frac{1}{2}}(2\pi\eta)^{\frac{1}{2}}(e^{2\pi\eta}-1)^{-\frac{1}{2}}. \tag{9}$$

Similarly one finds from the second Eq. (6)

$$G_L=\text{R.P. }D_Le^{-i\rho}\rho^{-L}\left\{1+\frac{L+i\eta}{2L}\frac{2i\rho}{1!}+\cdots+\frac{(L+i\eta)\cdots(-L+1+i\eta)}{(2L)!}\frac{(2i\rho)^{2L}}{(2L)!}\right\}$$
$$+pD_L\left[\ln 2\rho+2\gamma-\sum_1^{2L+1}s^{-1}+\sum_1^L\frac{s}{s^2+\eta^2}+\text{R.P. }\Gamma'(-i\eta)/\Gamma(-i\eta)\right]F_L/C_L$$
$$-pD_L\text{ R.P. }e^{-i\rho}\rho^{L+1}\sum_{s=1}^{\infty}\frac{(2L+1)!\Gamma(L+1+s-i\eta)(2i\rho)^s}{(2L+1+s)!s!\Gamma(L+1-i\eta)}\sum_{t=1}^{s}\left[\frac{1}{t}+\frac{1}{2L+1+t}-\frac{1}{L+t-i\eta}\right], \tag{10}$$

where

$$(2L+1)D_LC_L=1;$$

$$\gamma=\text{Euler's constant}=0.57721 \tag{11}$$

and

$$p=(2L+1)(e^{2\pi\eta}-1)C_L^2/\pi, \tag{12}$$

while R.P. means real part.

The above formulas could be used for the computation of F_L and G_L but it is inconvenient to do so on account of the occurrence of imaginaries. It is obvious from Eq. (8') that

$$F_L=C_L\rho^{L+1}\Phi_L, \tag{13}$$

where Φ_L is a power series in ρ the first term of which is 1. Substitution of this form into the differential equation satisfied by F_L leads to a recurrence formula between the coefficients of the series and one finds

$$\Phi_L=\sum_{L+1}^{\infty}A_j\rho^{j-L-1};\quad A_{L+1}=1 \tag{14}$$

$$A_j=(2\eta A_{j-1}-A_{j-2})(j+L)^{-1}(j-L-1)^{-1}. \tag{15}$$

For G_L Eq. (10) shows that this function consists of three parts: (a) a power series in ascending powers of ρ, the first term of which is $D_L\rho^{-L}$; (b) $pD_L(F_L/C_L)\ln 2\rho$; (c) an additive term in F_L. The differential equation does not determine G_L from a knowledge of parts (a) and (b) because an arbitrary term in F_L can be added to any solution and thus the power series of part (a) is not uniquely defined. But by requiring that the coefficient of ρ^{L+1} in this power series should vanish it is uniquely determined by substituting it together with $p(F_L/C_L)\ln 2\rho$ into the differential equation. The term in F_L is then also uniquely determined by the coefficient of ρ^{L+1} in Eq. (10). Thus if this coefficient is qD_L/C_L then the term in F_L is $qD_L\rho^{L+1}\Phi_L$. Collecting terms in ρ^{L+1} in Eq. (10) one finds

$$q=p\left[\sum_{1}^{L}\frac{s}{s^2+\eta^2}-\sum_{1}^{2L+}\frac{1}{s}+\text{R.P.}\,\frac{\Gamma'(-i\eta)}{\Gamma(-i\eta)}\right]+(-)^{L+1}\frac{2^L}{(2L)!}\sum_{-L}^{+L}\text{I.P.}\,\frac{2^n(i\eta+n-1)\cdots(i\eta-L)}{(L+n)!(L-n+1)}. \quad (16)$$

We thus have

$$G_L=D_L\rho^{-L}\Theta_L, \quad (17)$$

$$\Theta_L=\Psi_L+\rho^{2L+1}(p\ln 2\rho+q)\Phi_L, \quad (18)$$

where Ψ_L is a power series in ρ beginning with the term 1, having no term in ρ^{2L+1} and having its coefficients determined by the differential equation. It is found that

$$\Psi_L=\sum_{-L}^{\infty}a_j\rho^{j+L}; \quad a_{-L}=1; \quad a_{L+1}=0 \quad (19)$$

$$a_j=[2\eta a_{j-1}-a_{j-2}-p(2j-1)A_j]\times(j+L)^{-1}(j-L-1)^{-1}. \quad (20)$$

The computation of the logarithmic derivative of the gamma-function can be made either by

$$\text{R.P.}[\Gamma'(1+i\eta)/\Gamma(1+i\eta)]=-1/(1+\eta^2)+(1-\gamma)+(S_3-1)\eta^2-(S_5-1)\eta^4+\cdots;$$

$$S_k=\sum_{1}^{\infty}n^{-k} \quad (21)$$

for small η of the order of 1 or less, or else by Stirling's series for $\Gamma'(z)/\Gamma(z)$ as given in Whittaker and Watson's 12.33 for larger η. Differentiating expressions (14), (18) with respect to ρ we also have formulas for the derivatives

$$F_L'=C_L\rho^L\Phi_L^*, \quad G_L'=D_L\rho^{-L-1}\Theta_L^*, \quad (22)$$

$$\Phi_L^*=\sum_{L+1}^{\infty}jA_j\rho^{j-L-1}, \quad (23)$$

$$\Theta_L^*=\Psi_L^*+\rho^{2L+1}(p\ln 2\rho+q)\Phi_L^*+\rho^{2L+1}p\Phi_L, \quad (24)$$

$$\Psi_L^*=\sum_{-L}^{\infty}ja_j\rho^{j+L}. \quad (25)$$

By means of Eqs. (14), (15), (16), (17), (18), (19), (20), (22), (23), (24), (25), the computation of the functions can be carried out by ordinary substitutions.

The functions Φ, Φ^*, Θ, Θ^*, Ψ, Ψ^* vary more slowly than F, G, F', G' both with ρ and with η. It proved practical to calculate Φ, Φ^*, Ψ, Ψ^* at large intervals by means of their power series expansions and to interpolate for the remaining values of ρ, η.

2. Approximations for Small Energies

It was found that the tabulated values of Φ, Φ^*, Ψ, Ψ^* vary slowly in the region of small ρ and $1/\eta$ if the product $\rho\eta=\rho/ka=r/a$ is kept constant. This way of varying ρ, η corresponds to keeping the radius constant and varying the energy. Now it is well known that if the kinetic energy of a particle at ∞ is negligible in comparison with the Coulombian energy one can approximate the wave functions by means of Bessel functions of order $2L+1$ having for argument in our case $i(8\rho\eta)^{\frac{1}{2}}$. It turns out that this approximation is a very good one in a large region, and it proved practical to expand the exact solutions in series of Bessel functions as well as to extend the connection to the irregular function.

The differential Eq. (1) can be transformed by the substitutions

$$F=\zeta f, \quad \zeta=i(8\rho\eta)^{\frac{1}{2}} \quad (26)$$

into

$$\left[\frac{d^2}{d\zeta^2}+\frac{1}{\zeta}\frac{d}{d\zeta}+1-\frac{(2L+1)^2}{\zeta^2}+\frac{\zeta^2}{16\eta^2}\right]f=0. \quad (27)$$

Here the last term may be regarded as small in the region of low energies. If it is neglected one is left with Bessel's equation. The procedure will now be to expand the solution of (27) in a power series in $1/\eta^2$, i.e., in a power of the energy. Thus

$$f=f^{(0)}+(1/16\eta^2)f^{(1)}+(1/16\eta^2)^2f^{(2)}+\cdots \quad (28)$$

and

$$L(f^{(s)})=-\zeta^2f^{(s-1)}, \quad (29)$$

where

$$L=d^2/d\zeta^2+d/\zeta d\zeta+1-\nu^2/\zeta^2, \quad \nu=2L+1. \quad (29')$$

If we set $f^{(0)}=J$, we can obtain a regular solution

of Eq. (1) by solving Eq. (29) always discarding the irregular solutions of these equations. However, it should be remembered that to any $f^{(s)}$ one can add J_ν multiplied by an arbitrary constant involving $1/16\eta^2$ to the 0th and higher powers. Thus an additional restrictive condition must be imposed on each $f^{(s)}$ in order that ζf should differ from F only by a factor independent of ζ and η. This condition is obtained from the exact expression for F given by Eq. (8). We substitute for ρ in terms of ζ and we expand in $1/\eta$. We see then that the lowest power of ζ which occurs with η^{-2p} is $\zeta^{\nu+1+2p}$. Thus each $f^{(s)}$ should be a power series having no terms of order lower than $\zeta^{\nu+s}$. This determines the regular solution uniquely through the successive approximations obtainable from Eq. (29) because the addition of a term in J_ν to any $f^{(s)}$ brings in a term in ζ^ν. The solution of any Eq. (29) can be carried out by using

$$\begin{aligned} L(\zeta^{\mu+1}J_\nu') &= \mu^2\zeta^{\mu-1}J_\nu' + [-2(\mu+1)\zeta^\mu + 2\nu^2\mu\zeta^{\mu-2}]J_\nu, \\ L(\zeta^\mu J_\nu) &= 2\mu\zeta^{\mu-1}J_\nu' + \mu^2\zeta^{\mu-2}J_\nu. \end{aligned} \tag{30}$$

Each approximation is then obtained as a sum of terms of the type $\zeta^\mu J_\nu$, $\zeta^{\mu+1}J_\nu'$. Or else one may use

$$\begin{aligned} L(\zeta^\mu J_\nu) &= (\mu^2+2\mu\nu)\zeta^{\mu-2}J_\nu - 2\mu\zeta^{\mu-1}J_{\nu+1}, \\ L(\zeta^\mu J_{\nu+1}) &= 2\mu\zeta^{\mu-1}J_\nu + (\mu-1)(\mu-2\nu-1)\zeta^{\mu-2}J_{\nu+1} \end{aligned} \tag{30'}$$

and obtain it in terms of $\zeta^\mu J_\nu$, $\zeta^\mu J_{\nu+1}$. On account of the recurrence relation between $J_{\nu+2}$, $J_{\nu+1}$, J_ν one can transform the result into a linear combination of terms in $\zeta^\mu J_{\nu+2}$, $\zeta^\mu J_\nu$. This is convenient for our calculations because $J_{\nu+2}$ is related to Φ_{L+1} in the same way as J_ν is to Φ_L. We thus obtain

$$\begin{aligned} f = J_\nu + \eta^{-2}\Bigg\{\Bigg[-\frac{(\zeta/2)^4}{12(\nu+1)} - \frac{\nu-1}{24}(\zeta/2)^2\Bigg]J_{\nu+2} - \frac{(\zeta/2)^4}{12(\nu+1)}J_\nu\Bigg\} \\ + \frac{1}{24\eta^2}\Bigg\{\Bigg[\frac{(\zeta/2)^6}{5(\nu+1)} + \frac{(\nu+2)(\nu+3)(5\nu-7)}{120(\nu+1)}(\zeta/2)^4 + \frac{(\nu+2)(\nu+3)(5\nu-7)(\nu-1)}{240}(\zeta/2)^2\Bigg]J_{\nu+2} \\ + \Bigg[\frac{7-5\nu}{60(\nu+1)}(\zeta/2)^6 - \frac{(\nu-1)(\nu+3)(5\nu-7)}{240(\nu+1)}(\zeta/2)^4\Bigg]J_\nu\Bigg\} + \cdots. \end{aligned} \tag{31}$$

It is also possible to work out the above expansion directly as an expansion of Eq. (8) and expressing the sth term in terms of $s(s-1)\cdots(s-p+1)$. The series arranges itself then as a sum of terms in powers $\zeta^p J_{\nu+p}$ and then by use of recurrence relations can be brought to the form (31). This calculation is lengthy and need not be mentioned in more detail.

The contour integral for $W_{i\eta,\,m}(2i\rho)$ used as the definition of this function by Whittaker and Watson can be related to the Bessel function contour integral used by them in their 17.2 by observing that

$$(1+i\zeta^2/4\eta\tau)^{i\eta+m-\frac{1}{2}} = e^{-\zeta^2/4\tau}\exp\left\{\frac{1}{\eta}\left[\frac{i}{2}\left(\frac{\zeta^2}{4\tau}\right)^2 + (m-\tfrac{1}{2})\frac{i\zeta^2}{4\tau}\right] + \cdots\right\}.$$

The exponential can be expanded in powers of $1/\eta$ and the result is a sum of powers of ζ and Bessel functions of order higher than ν. However, care must be taken to have the path of integration stay inside the circle of convergence for the power expansion of $\ln(1+i\zeta^2/4\eta\tau)$. This point of view is apparently more troublesome than the use of Eqs. (30) or (30'), but it may have its advantages.

If one omits all but the first term in (31) one obtains an approximation to Φ_L which applies for very large η, i.e., for very small energies. The limiting value of Φ_L for large η and fixed $\rho\eta$ will be written $\mathfrak{F}_L$. We have

$$\mathfrak{F}_L=(2L+1)!(\zeta/2)^{-\nu}J_\nu(\zeta)=(2L+1)!(x/2)^{-\nu}I_\nu(x),\quad x=(8\rho\eta)^{\frac{1}{2}},\tag{32}$$

where I_ν is as defined in Whittaker and Watson's 17.7. Similarly

$$\Phi_L=(2L+1)!(\zeta/2)^{-\nu}f,\tag{32'}$$

where f is the expansion (31); the connection of f and Φ_L is defined uniquely by the coefficients of lowest powers of ρ in both expressions. Expressing all J_ν in terms of the $\mathfrak{F}_L$ in Eq. (31) one obtains an expansion of Φ_L in terms $\mathfrak{F}_L$ and $\mathfrak{F}_{L+1}$. We thus have

$$\Phi_L=\mathfrak{F}_L+\frac{1}{\eta^2}\left\{\left[\frac{(x/2)^6}{12(\nu+1)}-\frac{\nu-1}{24}(x/2)^4\right]\frac{\mathfrak{F}_{L+1}}{(\nu+1)(\nu+2)}-\frac{(x/2)^4}{12(\nu+1)}\mathfrak{F}_L\right\}$$

$$+\frac{1}{24\eta^4}\left\{\left[\frac{(x/2)^8}{5(\nu+1)}+\frac{(\nu+2)(\nu+3)(7-5\nu)}{120(\nu+1)}(x/2)^6-\frac{(\nu+2)(\nu+3)(7-5\nu)(\nu-1)}{240}(x/2)^4\right]\frac{\mathfrak{F}_{L+1}}{(\nu+1)(\nu+2)}\right.$$

$$\left.+\left[-\frac{7-5\nu}{60(\nu+1)}(x/2)^6+\frac{(\nu-1)(\nu+3)(7-5\nu)}{240(\nu+1)}(x/2)^4\right]\mathfrak{F}_L\right\}+\cdots.\tag{33}$$

For $L=0$ the term in η^{-6} to be added in the above expansion is

$$\frac{\rho^2\eta^2}{23{,}040\eta^6}\left\{\left[-\frac{320}{9}\rho^3\eta^3-\frac{640}{7}\rho^2\eta^2-\frac{1280}{21}\rho\eta\right]\mathfrak{F}_0+\left[\frac{320}{27}\rho^4\eta^4+\frac{5056}{63}\rho^3\eta^3+\frac{2560}{21}\rho^2\eta^2+\frac{1280}{21}\rho\eta\right]\mathfrak{F}_1\right\}.\tag{33'}$$

Numerical calculation of successive terms in η^{-2}, η^{-4} shows that the above series converges rapidly even in regions where the power series in ρ requires a large number of terms for its computation. Thus for example for $\rho\eta=0.631$ and $\rho=1.259$ the successive terms of (33) are 1.778, -0.394, $+0.028$ giving $\Phi_0=1.412$ which agrees with $\Phi_0=1.412$ as computed by the power series. By means of Eq. (32) the power series calculations for small ρ were checked satisfactorily.

The recurrence formulae for Bessel functions give the limiting values $\mathfrak{F}_{L+1}$ in terms of $\mathfrak{F}_L$, $\mathfrak{F}_{L-1}$. The relation is

$$\left[1+2\frac{(x/2)^2}{\nu^2-1}\right]\mathfrak{F}_L=\frac{(x/2)^4}{\nu(\nu+1)^2(\nu+2)}\mathfrak{F}_{L+1}+\mathfrak{F}_{L-1}.\tag{34}$$

Similarly recurrence formulae give

$$\mathfrak{F}_L^*=\frac{1}{2}\left[1+\nu+\frac{2(x/2)^2}{\nu+1}\right]\mathfrak{F}_L-\frac{(x/2)^4}{(\nu+1)^2(\nu+2)}\mathfrak{F}_{L+1}=\frac{1}{2}\left[1-\nu+\frac{2(x/2)^2}{1-\nu}\right]\mathfrak{F}_L+\nu\mathfrak{F}_{L-1}.\tag{34'}$$

These relations also determine $\mathfrak{F}_L$, $\mathfrak{F}_{L+1}$ in terms of $\mathfrak{F}_L^*$ and $\mathfrak{F}_{L+1}^*$. The relations

$$\mathfrak{F}_L^*=\frac{1}{2}\left(\nu+1+x\frac{d}{dx}\right)\mathfrak{F}_L,\tag{35}$$

$$\frac{1}{2}\left(\nu+1+x\frac{d}{dx}\right)(x/2)^p\mathfrak{F}_L=\frac{1}{2}\left(\nu+1+p+\frac{(x/2)^2}{\nu+1}\right)(x/2)^p\mathfrak{F}_L-\frac{(x/2)^{4+p}}{(\nu+1)^2(\nu+2)}\mathfrak{F}_{L+1},\tag{35'}$$

$$\frac{1}{2}\left(\nu+1+x\frac{d}{dx}\right)(x/2)^p\mathfrak{F}_{L+1}=(\nu+2)(x/2)^p\mathfrak{F}_L+\left[-\frac{(x/2)^2}{\nu+1}-\frac{\nu+3-p}{2}\right](x/2)^p\mathfrak{F}_{L+1},\tag{35''}$$

determine through (33) the series Φ_L^*. Using the relations (34') one can also express it in terms of $\mathfrak{F}_L^*$, $\mathfrak{F}_{L+1}^*$.

Using Eq. (10) and collecting terms of lowest power in $1/\eta$ we obtain an approximation to

$$\mathfrak{G}_L = -\frac{2}{(2L)!}\left(\frac{x}{2}\right)^{2L+1} K_{2L+1}(x), \tag{36}$$

where K is defined in Whittaker and Watson's 17.71. In our case $K_\nu = (-)^L(\pi/2)H_\nu^{(1)}(\zeta)$. This formula checks satisfactorily the values of $\mathfrak{G}_L$ for small ρ. An expansion of Θ_L similar to (33) is possible but is more complicated. Substitution of K_ν for J_ν in Eq. (31) gives an irregular solution of the differential equation, but we have no proof that this is the irregular solution which is wanted. In special cases numerical trial gave satisfactory results with this expansion.

Both F_L and G_L can be approximated by means of formulae of the type of Wentzel, Kramers and Brillouin (WKB). One can try to use the differential Eq. (1) and to compute the phase integral directly. Such results we will call WKB $L(L+1)$ so as to indicate that the last term is used without any change. In the region of negative kinetic energy the appropriate approximations are

$$F = \tfrac{1}{2}Q^{-\frac{1}{2}} \exp\left\{-\int_\rho^{\rho_0} Q d\rho\right\}; \quad G = Q^{-\frac{1}{2}} \exp\left\{\int_\rho^{\rho_0} Q d\rho\right\}, \tag{37}$$

where $-Q^2$ stands for the coefficient of $\overline{F}$ in Eq. (1) and ρ_0 is the classical turning point, i.e., the positive root of Q^2. Kramers[4] showed that in the case of attractive coulomb fields the correct phase in the region of positive kinetic energies is obtained by using $(L+\frac{1}{2})^2$ instead of $L(L+1)$ in the phase integral. It was subsequently shown by Uhlenbeck and Young[5] that a change from $L(L+1)$ to $(L+\frac{1}{2})^2$ improves the approximation also so far as absolute values of the function are concerned for attractive Coulomb fields. The results of Uhlenbeck and Young are essentially due to a combination of the effect noted by Kramers and of the fact that the $(L+\frac{1}{2})^2$ modification makes the wave function have the correct power dependence on r at small r. *For repulsive fields* the power dependence on r is also given correctly for F by the $(L+\frac{1}{2})^2$ modification but *Kramers' argument about the phase is not applicable* because the regions of positive and negative kinetic energies changed places. We find, *nevertheless*, by trial that *for low energies the* WKB $(L+\frac{1}{2})^2$ *method gives very good results* and on considering the connection with the preceding expansions in Bessel functions a reason for this became apparent.

The values of F_L, G_L obtained by WKB $(L+\frac{1}{2})^2$ are given by

$$F_L = (2\cos u)^{-\frac{1}{2}} \sin^{L+1}\frac{u+u_0}{2} \cos^{-L}\frac{u-u_0}{2} \exp\left\{-\eta\left(\frac{\pi}{2}-u\right)+(L+\tfrac{1}{2})\frac{\cos u}{\cos u_0}\right\}, \quad F_L G_L = 1/2Q \tag{38}$$

where
$$\sin u = (\rho-\eta)[\eta^2+(L+\tfrac{1}{2})^2]^{-\frac{1}{2}}; \quad \sin u_0 = \eta[\eta^2+(L+\tfrac{1}{2})^2]^{-\frac{1}{2}} \tag{38'}$$

and u is supposed to be in the first or fourth quadrant while $0 < u_0 < \pi/2$. This formula is convenient for the computation of F_L. Passing to the limit of small ρ, keeping $\rho\eta$ at a fixed value, one obtains the value of $C_L\mathfrak{F}_L$. Since on the other hand Φ_L is related to J_ν by Eq. (32) this also means that we obtain an approximation for J_ν. We obtain in this way

$$J_\nu(ix) \leqq \frac{(ix)^\nu \exp(\nu^2+x^2)^{\frac{1}{2}}}{(2\pi)^{\frac{1}{2}}(\nu^2+x^2)^{\frac{1}{4}}[\nu+(\nu^2+x^2)^{\frac{1}{2}}]^\nu}, \tag{38''}$$

which will be recognized as Carlini's formula.[6] This is supposed to be valid only for large ν being obtained as a first term of an expansion in descending powers of ν. But even for $\nu=1$ this formula is found, by trial, to be remarkably accurate, deviating from the correct value by not more than 8.5 percent. For $\nu=3$ which corresponds to $L=1$ the agreement is much better, the maximum discrepancy being only 2.8 percent. This agreement applies for all values of x and

[4] H. A. Kramers, Zeits. f. Physik **39**, 828 (1926).

[5] L. A. Young and G. E. Uhlenbeck, Phys. Rev. **36**, 1154 (1930).

[6] G. N. Watson, *Bessel Functions*, pp. 7, 226.

implies a corresponding agreement of the WKB $(L+\frac{1}{2})^2$ method for any radius if the energy is made low enough.

Corresponding to (38″) the approximation to Θ by means of K leads to an approximation for K_ν given by

$$-2(\nu^2+x^2)^{\frac{1}{2}}K_\nu I_\nu = 1, \qquad (38''')$$

where I_ν is as determined by (38″). This approximation is also good. It is apparently a new one mathematically although physical considerations make this approximate connection of K_ν with I_ν very obvious. The exact values of K_ν and I_ν satisfy this formula to within a few percent from $x=0$ to $x=10$.

Keeping η constant and making ρ very small one obtains the region of small radii at constant energy. Here the F_L function can be approximated by $C_L\rho^{L+1}$ and as has been already mentioned the correct power of ρ is obtained by the WKB $(L+\frac{1}{2})^2$ method. We find also that the coefficient of ρ^{L+1} obtained by this approximation agrees well with C_L. Thus for $\eta=1$ this coefficient is 0.120 while $C_L=0.108$; for $\eta=3.162$ the coefficient is 2.35×10^{-4} while the exact value is 2.17×10^{-4}. This agreement causes as well an agreement of G_L with its WKB $(L+\frac{1}{2})^2$ approximation because in this region the approximations satisfy $F_LG_L=\rho/(2L+1)$ and the same formula is obeyed by the exact solutions for small ρ. It is thus seen that both the F and G functions are reproduced quite well by the WKB $(L+\frac{1}{2})^2$ approximation for energies and radii which correspond to the particles being well inside their mutual potential barrier.

It should be remembered, on the other hand, that the $(L+\frac{1}{2})^2$ modification raises the barrier in comparison with its actual value. It is thus not a good approximation in the proximity of the classical turning point, not only because the WKB formulae are always poor close to the turning point but also because the position of the turning point is given incorrectly by the $(L+\frac{1}{2})^2$ modification.

The Carlini formula is obtainable from Meissel's first expansion[6] through the use of Stirling's series and the rapid convergence of this series even for small ν is in part responsible for the practical nature of Carlini's formula for small ν. It is of interest to note that the procedure used in deriving successive terms of Meissel's formula is very closely related to that used in discussing the WKB method. The essential difference lies in the fact that the exponent is expanded in descending powers of ν by Meissel and no such convenient parameter is used in deriving the WKB approximations. The first two terms in the exponent of Meissel's formula given by the first line of V_ν on p. 227 of Watson's Bessel functions give, as is found by trial, a very good approximation which for our purposes is superior to Carlini's. It is not obvious why an expansion in $1/\nu$ should give results so superior to those obtained by treating Eq. (1) by the procedure of WKB.

3. Discussion of Numerical Results[7]

In tables B, C, D, E the coefficients for Φ_L and Ψ_L, are given for $L=0$, 1 and for values of η so chosen that logarithms of η^{-1} extend from $\bar{2}.0$ to 0.5 in steps of 0.1. The values of η^{-1} that were used did not correspond quite exactly to the tabulated values of the logarithms. In some cases it is necessary to know precisely the value of η used in the computation of coefficients and for this reason a separate column giving these values is given in the tables. For a_j, $L=0$, this was not necessary because the same η's were used for them as for A_j, $L=0$. Coefficients for $\Phi_L{}^*$ and $\Psi_L{}^*$, namely jA_j and ja_j can be also obtained from these tables.

Table A gives Φ_L, $\Phi_L{}^*$, Ψ_L, $\Psi_L{}^*$ for $L=0$, 1 obtained using these coefficients. They are calculated for values of ρ chosen in steps of 0.1 on a logarithmic scale to the base 10 from $\ln\rho=\bar{2}.0$ up to $\ln\rho=\bar{1}.9$ and in some cases up to $\ln\rho=0.9$. In this work the values of ρ^n that were used in the computation of the series were each good only to four significant figures.

The probable percentages of error in the values of the series given in Table A are indicated for certain columns of the table as explained in the note at its heading. This was estimated for a large number of them considering: (1) the accu-

[7] The bulk of these tables will be published in the December issue of the Journal of Terrestrial Magnetism and Atmospheric Electricity together with a brief explanation and a collection of formulas. These tables are referred to as A, B, C, D, E, F, G, H, I. In distinction to these the tables of the present paper are numbered: I, II, III, IV, V, VI, VII, VIII.

racy in the coefficients and (2) the slowness of convergence of the series. For Φ and Ψ it was assumed that the first digit discarded in each A_j or a_j was 9. The sum of the squares of the contributions of the errors in individual terms was considered to be the square of the "total error" if the last few terms were small in comparison to previous terms. In case this was not so, additional coefficients were roughly determined to the stage where this condition did exist. The additional contribution of these approximate coefficients was squared and added to the quantity obtained from considering errors in each term. The square root of this sum was used as the "total error." "Total errors" were determined for Φ^* and Ψ^* in the same manner. The error in the powers of ρ was not properly taken into account in these estimates but the fact will probably be of no great importance. The percentages of "total error" increase to the value given for the column at the right more rapidly as the column is approached.

A large number of checks were made on Φ, Φ^*, Ψ, Ψ^* and p_L both for $L=0$ and $L=1$. Use was made of the relation

$$F'G-G'F=1$$

or its equivalent

$$\Phi^*\Theta-\Theta^*\Phi=2L+1.$$

One hundred thirty-five such random checks were made for $L=0$, $\rho\eta\leq 1.259$, $\rho\leq 0.7944$; 145, for $L=1$, $\rho\eta\leq 3.162$, $\rho\leq 1.585$. The majority of these checks were made with values of p_L *slightly* erroneous in a manner to be discussed more fully later. This fact probably does not vitiate the values of $F'G-G'F$ so obtained to any great extent since the checks in Tables VII, VIII (which are a fair sample of those obtained in general) were gotten by using accurate p_L's and do not vary appreciably from original checks with less accurate p_L's. The maximum inaccuracy in $F'G-G'F$ due to this cause was 0.5 percent which was found for $\eta=1$, $L=0$. In other cases the correction due to using quite accurate p_L's had less effect. Thus for $L=0$, $\rho\eta=0.6310$ the effect was less than 0.04 percent and less than 0.3 percent for $L=1$, $\ln\eta^{-1}=0.0$.

The values of $F'G-G'F$ for $L=0$ ranged from 0.9836 to 1.0291. Ninety satisfied the check to 0.1 percent and 135 to 1 percent. The remainder were for $\rho\eta=1.000$ to $\rho\eta=1.259$ where deviations are to be expected. For $L=1$ values lay between 2.82 and 3.24. One hundred eighteen of these satisfied the check to 0.1 percent and 140 to 1 percent. The remainder were for values of $\rho\eta$ from 1.259 to 3.162.

p_L and q_L are given in Table F together with the values of η to which they correspond. The p_0's are accurate as given. The p_1's are accurate to 1 in the last figure. The bothersome part of determining the q_L's is the calculation of R.P. $\Gamma'(1+i\eta)/\Gamma(1+i\eta)$. If one uses the difference equation for the gamma-function this may be written

$$\text{R.P.}\frac{\Gamma'(1+i\eta)}{\Gamma(1+i\eta)}=-\sum_{j=1}^{s-1}\frac{j}{j^2+\eta^2}+\text{R.P.}\frac{\Gamma'(s+i\eta)}{\Gamma(s+i\eta)}.$$

The R.P. $\Gamma'(1+i\eta)/\Gamma(1+i\eta)$ was determined from the above equation by using Stirling's series for $\Gamma'(s+i\eta)/\Gamma(s+i\eta)$ with $s=2$ and $s=6$. This was done for $\eta\geq 1$. Agreement between the two methods was exceedingly good. For $\eta<1$ the calculation was made as above for $S=6$ and this checked satisfactorily with results by Eq. (21). For $\eta\geq 1$ the values for $s=6$ were used inclusive of the first figure in which they disagreed from $s=2$. The difference between $s=2$ and $s=6$ was taken as the probable error. The error due to using a finite number of digits in the other terms in q_L was also taken into account. The square root of the sum of the squares of all these errors was calculated and used as a measure of the error in q. The values of q are so tabulated that the last figure given is not in doubt by more than 5 and generally by less, using the above way of estimating accuracy.

Values of C_L, D_L for $L=0$ and $L=1$ together with the η's to which they correspond are given in Table H.

Tables discussed thus far are auxiliary to the determination of the regular and irregular wave functions, F_L, G_L and their derivatives F_L', G_L'. The latter four quantities are given by Eqs. (13), (17), (18), (22), (24).

Figs. 1, 2 give the values of Θ_0 and Θ_1, respectively. The two families of curves in each graph correspond to constant energies ($\eta=$const.) and constant radii ($\rho\eta=$const.). Some of the

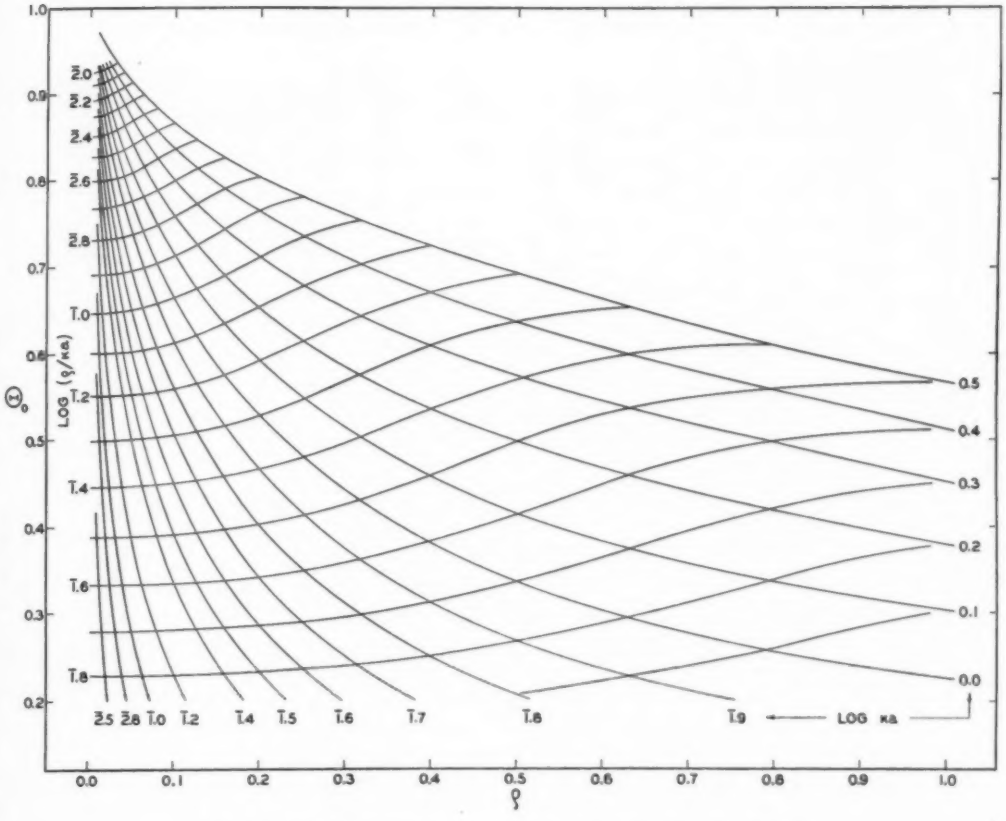

FIG. 1. Graphical representation of Θ_0. Irregular function $G_0 = D_0\Theta_0$.

points of intersection of the two families of curves were obtained by graphical interpolation while other points were obtained by direct calculation.

It is important to note that it is necessary to use accurate values of p, q in order to obtain correct results for Θ because this quantity is often obtained as a difference of two nearly equal numbers. A portion of these values were calculated by using values of p, q, $\ln 2\rho$ which for one reason or another differed slightly from the final accurate values given in the tables.

It is believed that the values of Θ used in plotting the curves of Figs. 1, 2 are good to better than 2.5 percent for $L=0$ and better than 0.5 percent for $L=1$ and in most cases the accuracy is probably higher than just stated. These estimates of accuracy were arrived at by using accurate p's and q's in some representative cases.

Tables I, II of the present paper show the agreement between values of Φ_L for $\rho \to 0$ and $(2L+1)!I_\nu(x)/(x/2)^\nu$. Table III gives the ratios of values of the Carlini formula for certain values

TABLE I. *Values of* $\mathfrak{F}_0/\Phi_0$.

$\rho\eta$	ρ	Φ_0	$\mathfrak{F}_0$	$\mathfrak{F}_0/\Phi_0$
0.01000	0.01000	1.01002	1.01003	1.00001
0.01585	0.01585	1.01589	1.01593	1.00004
0.02512	0.01000	1.02531	1.02532	1.00001
0.03981	0.01585	1.04029	1.04033	1.00004
0.06310	0.01000	1.06442	1.06444	1.00002
0.1000	0.01000	1.1034	1.10339	0.99999
0.1995	0.01000	1.1671	1.16709	0.99999
0.2512	0.01000	1.2730	1.27313	1.00011
0.3981	0.01000	1.4545	1.45458	1.00005
0.6310	0.01000	1.7783	1.77860	1.00017
1.000	0.01000	2.3947	2.3948	1.00004
1.259	0.01259	2.9132	2.91336	1.00006
1.585	0.01585	3.6823	3.68246	1.00004
1.995	0.01995	4.8641	4.86371	0.99992
2.512	0.02512	6.7583	6.75734	0.99986

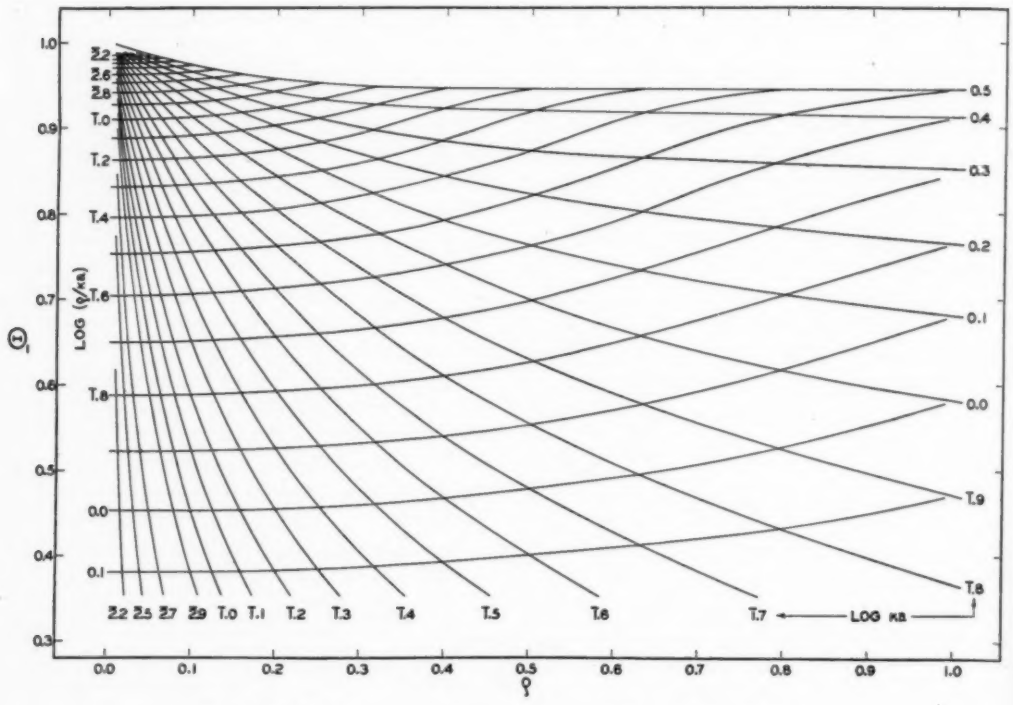

FIG. 2. Graphical representation of Θ_1. Irregular function $G_1 = D_1\Theta_1/\rho$.

of the argument to the actual value of the Bessel function for the same argument. These are for $\nu=1$, $\nu=3$. Table IV gives the ratios of Meissel's first extension of Carlini's formula to the Carlini values and also the ratios of the Meissel form to the actual Bessel functions. The three columns of $\nu=1$, $\nu=3$ give the results of using 1, 2 and 3 terms in Meissel's exponent V.

No tables are given here for the verification of Eqs. (33), (34) and (34′). In testing (33) 51 ratios of $\Phi_0 = f(\mathfrak{J}_0, \mathfrak{F}_1)$ to the actual Φ_0 were taken from $\rho=0.01$ to $\rho=0.6310$, from $\ln\eta^{-1}=\bar{2}.0$ to $\ln\eta^{-1}=0.4$ and uniformly spaced between diagonals $\rho\eta=0.05012$ and $\rho\eta=10$. Bessel function values were used for $\mathfrak{F}_0$ and Φ_1. These ratios were found to lie between 0.9990 and 1.0006. Convergence was such that it was not necessary to consider the term in η^{-6}. The term in η^{-6} was computed for a point beyond the barrier given by $\rho\eta=0.6310$, $\rho=1.259$. The first three terms were 1.778, −0.397, 0.028. The term

TABLE II. *Values of* $\mathfrak{F}_1/\Phi_1$.

$\rho\eta$	ρ	Φ_1	$\mathfrak{F}_1$	$\mathfrak{F}_1/\Phi_1$
0.01000	0.01000	1.00500	1.00515	1.00015
0.01585	0.01259	1.00793	1.00817	1.00024
0.02512	0.01259	1.01261	1.01278	1.00017
0.03981	0.01259	1.02004	1.01983	0.99979
0.06310	0.01259	1.03192	1.03198	1.00006
0.1000	0.01259	1.0509	1.0510	1.00010
0.1995	0.01000	1.1039	1.1038	0.99991
0.2512	0.01259	1.1321	1.1321	1.00000
0.3981	0.01000	1.2155	1.2156	1.00008
0.6310	0.01000	1.3582	1.3582	1.00000
1.000	0.01000	1.6118	1.6120	1.00012
1.259	0.01259	1.8122	1.8123	1.00006
1.585	0.01585	2.0933	2.0934	1.00005
1.995	0.01995	2.4976	2.4976	1.00000
2.512	0.02512	3.0986	3.0991	1.00016

TABLE III. *Values of* $\phi_L/\mathfrak{F}_L$. ϕ_L = *Carlini's approximation to* $\mathfrak{F}_L$.

$x=(8\rho\eta)^{\frac{1}{2}}$	$\mathfrak{F}_0$	ϕ_0	$\phi_0/\mathfrak{F}_0$	$\mathfrak{F}_1$	ϕ_1	$\phi_1/\mathfrak{F}_1$
0.0	1.00000	1.0844	1.0844	1.00000	1.0281	1.0281
0.4				1.01004	1.0373	1.0269
0.8	1.08216	1.1126	1.0281	1.04065	1.0654	1.0238
1.2				1.09331	1.1144	1.0193
1.6	1.35601	1.3348	0.9844	1.17061	1.1871	1.0141
2.0				1.27644	1.2877	1.0088
2.4	1.91510	1.8506	0.9663	1.41621	1.4219	1.0040
3.2	2.95891	2.8610	0.9669	1.82942	1.8230	0.9965
3.6				2.12562	2.1124	0.9938
4.0	4.87973	4.7363	0.9706			
4.4				2.98394	2.9554	0.9904
4.8				3.59824	3.5595	0.9892
5.2				4.38500	4.3347	0.9885
5.6				5.39605	5.3318	0.9881
6.0				6.70012	6.6186	0.9878

TABLE IV. *Ratios of Meissel expansion to Carlini formula.*

$x=(8\rho\eta)^{\frac{1}{2}}$	$\nu=1$	$\nu=1$	$\nu=1$	$\nu=3$	$\nu=3$	$\nu=3$
0.0	0.92214	0.92214	0.92214	0.97271	0.97271	0.97271
0.8	1.00069	0.97039	0.98068	0.97796	0.97642	0.97604
1.6	1.03886	1.03357	1.04465	0.98922	0.98557	0.98560
2.4	1.03925	1.04138	1.04564	0.99957	0.99621	0.99659
3.2	1.03068	1.03358	1.03638	1.00532	1.00300	1.00353
4.0	1.03006	1.03258	1.03483	1.01016	1.00880	1.00941
4.8	1.02634	1.02837	1.03094	1.01205	1.01146	1.01188
Ratios of Meissel expansion to actual Bessel functions for same x and ν						
0.0	0.99997	0.99997	0.99997	1.0000	1.0000	1.0000
0.8	1.0288	0.99766	1.0082	1.0012	0.99966	0.99927
1.6	1.0227	1.0174	1.0284	1.0031	0.99942	0.99944
2.4	1.0042	1.0063	1.0104	1.0036	1.0002	1.0006
3.2	0.9966	0.9994	1.0021	1.0018	0.99946	0.99999
4.0	0.9998	1.0022	1.0044	0.97906	0.97780	0.97833
4.8				1.0012	1.0006	1.00098

due to η^{-6} was 0.003. This indicates that for some values of $\rho\eta$ the first three terms give a good approximation to Φ_0 even beyond the barrier.

In testing (33) for $L=1$ fifty-six values of the ratio of $\Phi_1=f(\mathfrak{F}_1, \mathfrak{F}_2)$ to Φ_1 were taken between $\rho=0.01$ and $\rho=3.981$, $\ln\eta^{-1}=\bar{2}.0$ and $\ln\eta^{-1}=0.4$, evenly spaced between the diagonals $\rho\eta=0.05012$ and $\rho\eta=3.981$. The Bessel function values of $\mathfrak{F}_1$ and $\mathfrak{F}_2$ were used. Out to $\rho=0.7944$ the values of the ratio lay between 0.9993 and 1.0078. This expansion is good within three percent up to $\rho=2.512$, for $\ln\eta^{-1}=0.0$, 0.4 but breaks down for higher ρ. Eqs. (34), (34′) were also verified by numerical trial in a large number of cases. The terms beyond η^{-4} were not considered in these calculations.

The verification of Eq. (36) is shown in Table V. The error in Θ due to the errors in the p's and q's should be small for these values. In fact for $\rho=0.01$ the values for quite accurate p's and q's should not vary from those used by more than 0.17 percent for $L=0$ or by more than 0.24 percent for $L=1$. Similarly the extension of Carlini's result to K_ν given by Eq. (38‴) is verified in Table VI.

A relation giving Θ_0 as a function of $\mathfrak{G}_0$, $\mathfrak{G}_1$ was obtained by analogy with Eq. (33). Thus substituting

$$(x/2)^{-4s}[(\nu+1)\cdots(\nu+2s-1)]^2\nu(\nu+2s)\mathfrak{G}_{L+s}$$

for $\mathfrak{F}_{L+s}$ one obtains an expansion for Θ_L which gives an irregular solution of the differential equation for G. We have no proof that this expansion is equal to Θ because it may differ from it by terms involving the regular solution.

TABLE V. *Values of $\mathfrak{G}_L/\Theta_L$ for $L=0,1$.*

$\ln\eta^{-1}$	ρ	$\mathfrak{G}_0$	Θ_0	$\mathfrak{G}_0/\Theta_0$	$\mathfrak{G}_1$	Θ_1	$\mathfrak{G}_1/\Theta_1$
$\bar{2}.0$	0.01995				0.2386	0.240	0.994
$\bar{2}.0$	0.01000	0.1399	0.136	1.029	0.4496	0.4486	1.0022
$\bar{2}.2$	0.01000	0.2287	0.229	0.9987	0.5866	0.5856	1.0017
$\bar{2}.3$	0.01000				0.6486	0.6479	1.0011
$\bar{2}.4$	0.01000	0.3331	0.333	1.0003			
$\bar{2}.5$	0.01000	0.3880	0.388	1.0000	0.7518	0.7512	1.0008
$\bar{2}.6$	0.01000	0.4438	0.445	0.9973			
$\bar{2}.7$	0.01000	0.5520	0.551	1.0019	0.8333	0.8302	1.0037
$\bar{2}.9$	0.01000				0.8917	0.8870	1.0053
$\bar{1}.0$	0.01000	0.6489	0.6473	1.0025	0.9093	0.9084	1.0010
$\bar{1}.1$	0.01000	0.6917	0.6908	1.0013	0.9266	0.9260	1.0006
$\bar{1}.2$	0.01000	0.7322	0.7305	1.0023			
$\bar{1}.3$	0.01000				0.9592	0.9522	1.0074
$\bar{1}.4$	0.01000	0.8064	0.799	1.0093			
$\bar{1}.5$	0.01000	0.8281	0.8273	1.0010	0.9704	0.9694	1.0010
$\bar{1}.7$	0.01000				0.9809	0.9805	1.0004
$\bar{1}.8$	0.01000	0.9141	0.894	1.0225			
$\bar{1}.9$	0.01000				0.9995	0.9876	1.0120
0.0	0.01000	0.9477	0.9256	1.0239	1.0148	0.9901	1.0249

It is remarkable that this expansion gives good numerical results. Thus for $\rho\eta=0.1000$ the ratio of the values of Θ_0 computed by this expansion to the accurate values increases from 1 to 1.0046 as $\ln(1/\eta)$ varies from $\bar{1}.0$ to 0.0. There is a similar good agreement for $\rho\eta=0.3162$. For $\rho\eta=0.10$ and $\ln(1/\eta)=0.5$ the ratio is 1.3 without using the term in η^{-6} and 2.4 if the term in η^{-6} is used. For such high energies the expansion is not satisfactory but it is apparently safe and accurate in the low energy range.

In applications of the functions one needs the values of F, G as well as the values of the logarithmic derivatives F'/F and G'/G. In view of the fact that the WKB method of approximation is popular and expedient we compare here in some special cases the WKB approximations with the exact values. Figs. 3 and 4 give ratios of approximations to the accurate values of F and G for $L=0$ and for two fixed values of

TABLE VI. *Values of $-2(\nu^2+x^2)^{\frac{1}{4}}I_\nu K_\nu$ for $\nu=1$, $\nu=3$.*

$x=(8\rho\eta)^{\frac{1}{2}}$	$\nu=1$	x	$\nu=3$
0.02	0.99935	0.1	1.00192
0.1	0.99155	0.2	0.99975
0.3	0.97659	0.4	0.99895
0.6	0.95325	0.6	0.99792
0.9	0.95846	0.8	0.99677
1.0	0.96215	1.0	0.99564
2.0	0.99495	1.5	0.99364
3.0	1.00403	2.0	0.99315
4.0	1.00465	2.5	0.99377
5.0	1.00377	3.0	0.99493
6.0	1.00292	3.5	0.99620
7.0	1.00226	4.0	0.99734
8.0	1.00179	4.5	0.99817
9.0	1.00144	5.0	0.99900
10.0	1.00118		
13.0	1.00072		
16.0	1.00048		

the parameter η. It will be noted that the $(L+\frac{1}{2})^2$ modification of the approximation method is in these cases vastly superior to the direct use of $L(L+1)$ in the formulas. The potential barrier in Fig. 3 is at $\rho=2$ and thus corresponds to a point lying $1\frac{1}{2}$ of the marked divisions outside the right end of the figure. For Fig. 4 the potential barrier is reached at log $\rho=\bar{1}.801$. It will be noted that the $(L+\frac{1}{2})^2$ approximation is satisfactory at the barrier and even at values of ρ exceeding 2η. On the other hand the ordinary WKB method breaks down in the well-known manner at the barrier. In Fig. 5 the radius is kept constant and the energy is varied for $\rho\eta=0.631$, $L=0$. It will be noted that here also the $(L+\frac{1}{2})^2$ approximation is superior to that using $L(L+1)$ but at the same time it is clear that even this WKB approximation is consistently incorrect at small energies. This is to be expected from the limiting values obtained by means of the Carlini formula. The barrier is reached in this figure at log $\rho=0.05$. As the barrier is approached there is not much choice between the $(L+\frac{1}{2})^2$ and the $L(L+1)$ approximations for G. In Tables VII and VIII similar comparisons are made for $L=1$. The end column refers to the value of $3(F'G-G'F)$ which corresponds to the values of F', F, G', G used in these calculations. If these values were exact all numbers in the last column would be exactly 3. The amount by which they differ from 3 may be used as a criterion of accuracy. Table VII corresponds to a fixed radius and Table VIII to a fixed energy. The approximations are usually better for $L=1$ than for $L=0$.

Comparison of approximate and exact values for logarithmic derivatives is made graphically in Figs. 6, 7, 8, 9. In these figures the exact values of $\rho F'/F=\Phi^*/\Phi$ and $\rho G'/G=\Theta^*/\Theta$ as well as WKB approximations to these quantities are plotted against ρ. Fig. 6 shows the condition for fixed energy ($\eta=1$) and $L=0$. In the range covered the use of $(L+\frac{1}{2})^2$ is better than that of $L(L+1)$. It will be noted that there is an appreciable region of small ρ where the $L(L+1)$ method gives wrong signs for G'/G. This figure should be compared with Fig. 3 for the direct values of the quantities. In Fig. 7 the radius is kept constant by keeping $\rho\eta=0.631$ for $L=0$. In this case G'/G is approximated somewhat better

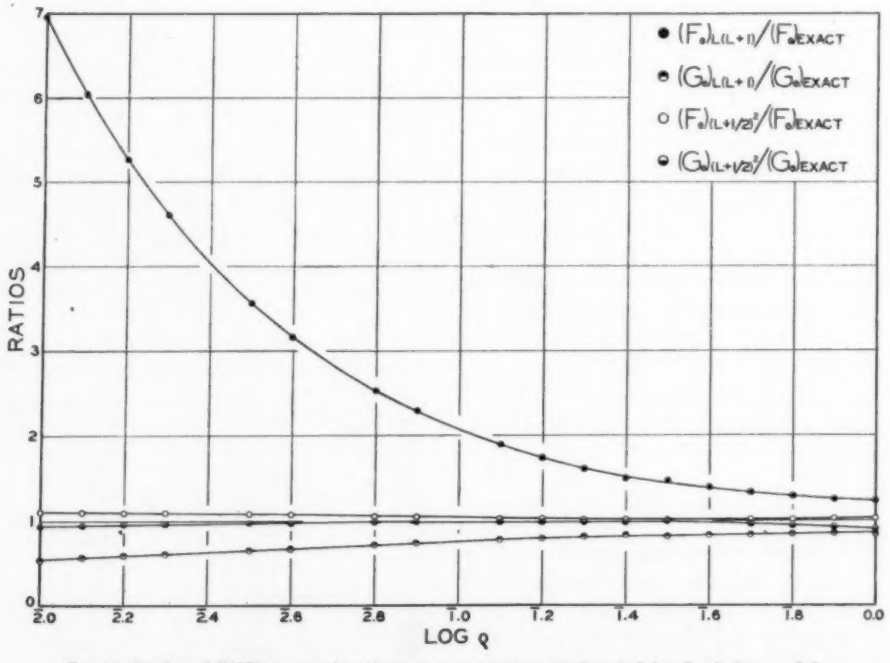

FIG. 3. Ratios of WKB approximations to exact values of F and G for $L=0$, log $\eta=0.0$.

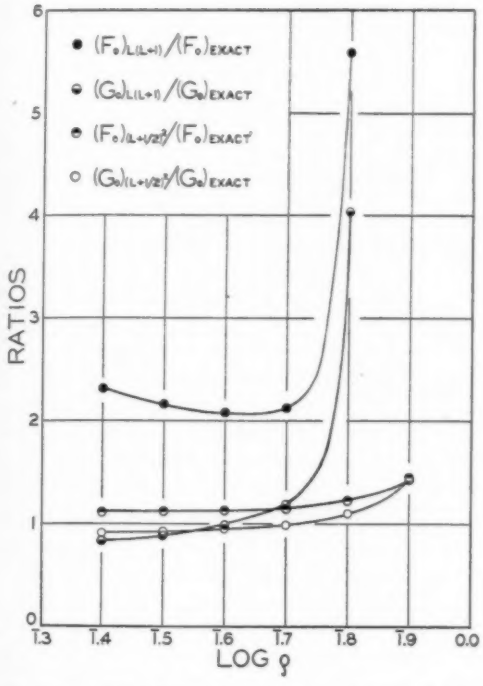

FIG. 4. Ratios of WKB approximations to exact values of F and G for $L=0$, $\log \eta = -1.5$.

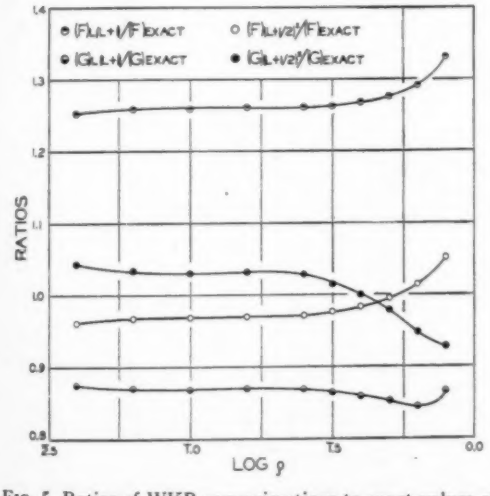

FIG. 5. Ratios of WKB approximations to exact values of F and G for $L=0$, $\rho\eta=0.631$.

by using $L(L+1)$ in the WKB formulas than by using $(L+\frac{1}{2})^2$ at large values of ρ. However, at small values of ρ the $(L+\frac{1}{2})^2$ method is beyond doubt the better. This figure corresponds to Fig. 5 in the values of the parameters used. In Fig. 8 an analogous condition is illustrated for $L=1$, $\rho\eta=1.259$. The values of the parameters used for this figure correspond to Table VII. In Fig. 9 the energy is kept constant for $L=1$, $\eta=1$. Here also the $L(L+1)$ approximation is better than the $(L+\frac{1}{2})^2$ type for G'/G and large ρ. Otherwise the $(L+\frac{1}{2})^2$ method is the better. The analogous comparison of F, G with their approximations was made in Table VIII. It will be noted that the comparisons of approximate and exact values of F and G cannot be used reliably for a discussion of the logarithmic derivatives. Comparisons for many other values of parameters were made in a manner similar to the cases presented here. The same general features are borne out by these calculations. Thus the approximations are usually better for $L=1$ than for $L=0$

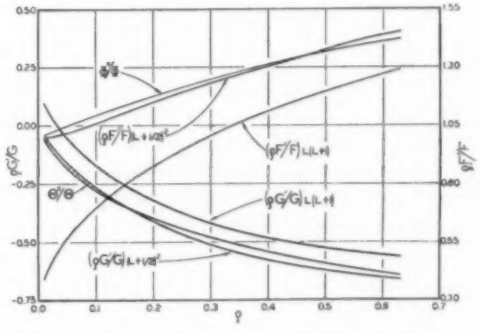

FIG. 6. Comparison of WKB approximations with exact values of F'/F, G'/G for $L=0$, $\log \eta = 0.0$.

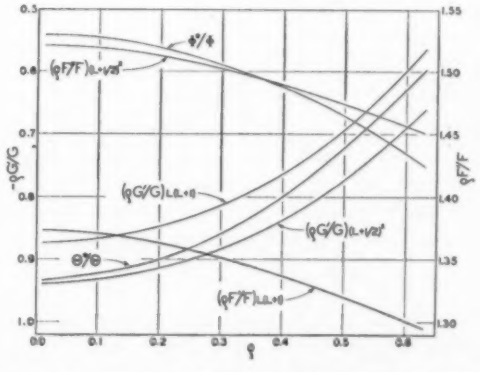

FIG. 7. Comparison of WKB approximations with exact values of F'/F, G'/G for $L=0$, $\rho\eta=0.631$.

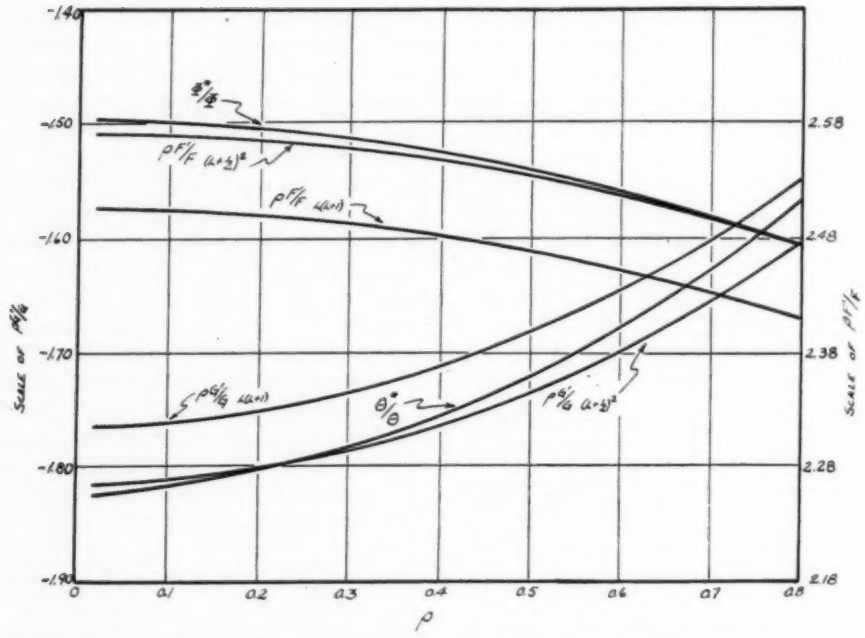

FIG. 8. Comparison of WKB approximations with exact values of F'/F, G'/G for $L=1$, $\rho\eta=1.259$.

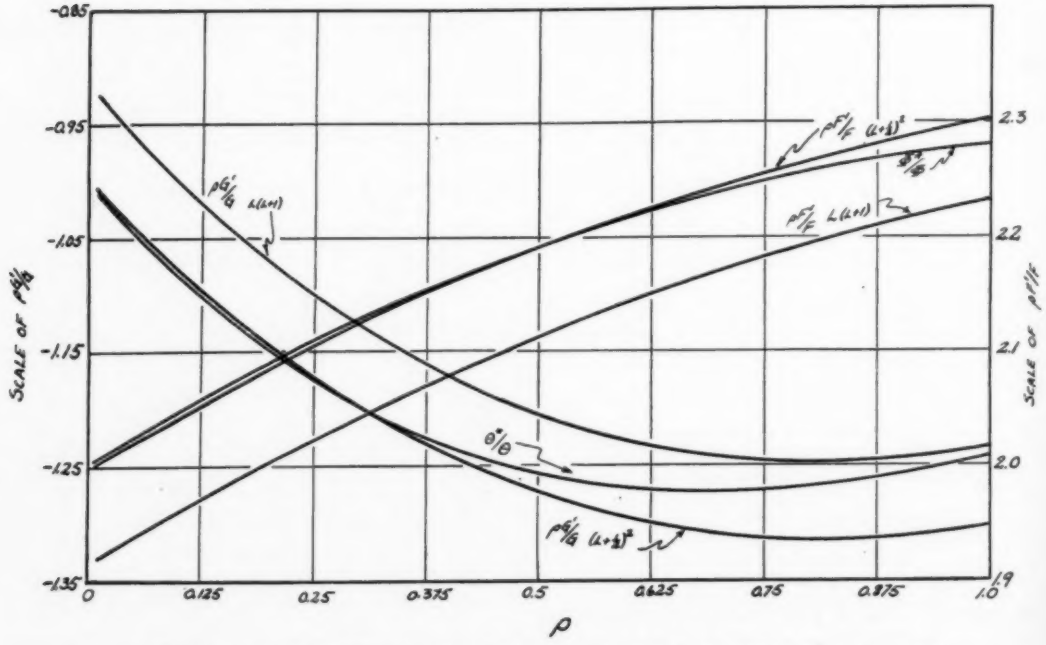

FIG. 9. Comparison of WKB approximations with exact values of F'/F, G'/G for $L=1$, $\log \eta=0.0$.

TABLE VII. *Ratios of WKB approximations to exact values of F, G for $\rho\eta=1.259$, $L=1$.*

ρ	η	$\frac{F_{WKB}}{F_{ex}}$ $L(L+1)$	$\frac{F_{WKB}}{F_{ex}}$ $(L+\frac{1}{2})^2$	$\frac{G_{WKB}}{G_{ex}}$ $L(L+1)$	$\frac{G_{WKB}}{G_{ex}}$ $(L+\frac{1}{2})^2$	Check
0.01585	79.44	1.14	0.96	0.91	1.04	2.9986
0.01995	63.10	1.15	0.96	0.90	1.05	3.0017
0.02512	50.12	1.16	0.99	0.89	1.01	3.0010
0.03162	39.81	1.17	1.00	0.88	1.00	3.0030
0.06310	19.95	1.17	1.01	0.88	1.00	3.0007
0.1000	12.59	1.16	1.00	0.88	1.01	3.0001
0.1259	10.00	1.16	1.00	0.89	1.01	2.9996
0.1995	6.310	1.16	1.00	0.89	1.00	2.9985
0.3162	3.981	1.16	1.00	0.89	1.00	3.0018
0.5012	2.512	1.16	1.01	0.89	0.99	2.9948
0.7944	1.585	1.16	1.02	0.88	0.97	2.9945
1.259	1.000	1.16	1.05	0.86	0.92	3.0019
1.585	0.7943	1.20	1.09	0.90	0.93	3.014

TABLE VIII. *Ratios of WKB approximations to exact values of F, G for $\eta=1$, $L=1$.*

ρ	$\frac{F_{WKB}}{F_{ex}}$ $L(L+1)$	$\frac{F_{WKB}}{F_{ex}}$ $(L+\frac{1}{2})^2$	$\frac{G_{WKB}}{G_{ex}}$ $L(L+1)$	$\frac{G_{WKB}}{G_{ex}}$ $(L+\frac{1}{2})^2$	Check
0.01000	1.72	1.05	0.62	0.96	2.9999
0.01585	1.66	1.05	0.64	0.96	3.0000
0.03162	1.56	1.04	0.68	0.97	3.0000
0.05012	1.50	1.04	0.71	0.96	3.0010
0.06310	1.50	1.04	0.70	0.96	3.0000
0.07944	1.44	1.04	0.74	0.96	2.9998
0.1000	1.41	1.04	0.75	0.96	3.0000
0.1259	1.36	1.04	0.78	0.96	3.0000
0.1995	1.33	1.04	0.79	0.96	3.0000
0.3162	1.28	1.04	0.82	0.97	3.0001
0.5012	1.23	1.04	0.85	0.96	3.0001
0.6310	1.21	1.04	0.86	0.96	2.9991
0.7944	1.19	1.04	0.86	0.95	2.9998
1.000	1.17	1.04	0.87	0.94	3.0063
1.259	1.16	1.05	0.86	0.92	3.0019
1.585	1.17	1.07	0.88	0.93	3.050
1.995	1.19	1.11	0.97	0.99	3.64

for the same ρ, η. Also the $(L+\frac{1}{2})^2$ type of approximation is usually better than the unmodified type of WKB formula. However, there are cases where the opposite is true as has been brought out above. The only absolutely unquestionable region in which the WKB formulas have an easily predictable accuracy is that of small ρ where the $(L+\frac{1}{2})^2$ method holds to within the range of validity of the Carlini formula.

In the calculation of excitation functions of nuclear reactions one is at times concerned only with relative values of F for the same radius and different energies. The above comparison shows that even the $L(L+1)$ method is not bad for such a purpose through considerable ranges of energy. Effects of resonance levels, however, are not represented very well by the approximations because these depend on values of F'/F.

In Table VI we give values of $-2(\nu^2+x^2)^{\frac{1}{2}} \times I_\nu(x)K_\nu(x)$ for $L=0$, 1 which give an idea of the accuracy of the approximate Eq. (38‴). By means of the relation

$$\hat{F}\hat{G}/(\hat{F}\hat{G})_{WKB(L+\frac{1}{2})^2}=-2(\nu^2+x^2)^{\frac{1}{2}}I_\nu K_\nu$$

and this table one obtains the accuracy of the WKB approximation for FG in the limit of small ρ and finite $\rho\eta$. Table III gives directly $(\hat{F})_{WKB(L+\frac{1}{2})^2}/\hat{F}$ and by multiplying corresponding numbers in the two tables one obtains $\hat{G}/(\hat{G})_{WKB(L+\frac{1}{2})^2}$. In this limit the approximation is seen to be good to within a few percent and generally better for $L=1$ than for $L=0$.

JANUARY 15, 1936 PHYSICAL REVIEW VOLUME 49

Probability of Radiative Processes for Very High Energies

L. W. NORDHEIM, *Purdue University*

(Received December 3, 1935)

THE present theory of radiative processes[1] (e.g., radiation of electrons and pair production by photons when passing atomic nuclei), though in quantitative agreement with observations up to several MV, gives far too large effects for higher energies and is therefore not applicable to the discussion of cosmic-ray phenomena. The reasons for this failure can be found in (a) the inapplicability already of classical electrodynamics for too high or too rapidly varying fields; (b) difficulties in the simultaneous application of the principles of quantum mechanics and relativity for field strengths above the critical limit

$$E_c=m^2c^3/e\hbar, \qquad (1)$$

that is a potential difference mc^2/e through a distance $\hbar/mc$; (c) breakdown of the superposition principle in Dirac's hole theory at the same limit.

[1] H. Bethe and W. Heitler, Proc. Roy. Soc. **A146**, 183 (1934).

In the analysis of the radiative processes by the method of v. Weizsäcker[2] and Williams[3] (based on a Fourier decomposition of the nuclear field in a system of reference where the electron is at rest or the photon has the energy mc^2) it was found that actually only Fourier components corresponding to small frequencies ($\sim mc^2/\hbar$) contributed to the total effect. From this it was firstly concluded that no upper limit for the applicability of the formulae would exist. But in this method one has to perform a summation over passages of the electrons at various distances from the nuclei. Part of the processes therefore take place in a region where the field exceeds the critical value (1) which is the case for collision parameters smaller than

$$\rho_c = \Lambda(Z\epsilon/137mc^2)^{\frac{1}{2}}; \quad \Lambda = \hbar/mc \qquad (2)$$

(ϵ = primary energy of electron or photon, Z = atomic number). To estimate the possible influence of a modification of the theory for fields higher than (1) we left out the doubtful regions[4, 5] given by (2), that is we summed only from ρ_c to the atomic radius $\hbar^2/me^2Z^{\frac{1}{3}}$ as outer limit (to include the screening effect of the atomic electrons). In this way the following formulae are obtained:

Cross section for the emission of a quantum in the interval ν to $\nu+d\nu$ by an electron of energy ϵ

$$\phi(\nu)d\nu = \frac{Z^2r_0^2}{137}\cdot\frac{4}{\epsilon^2}\{(4/3)\epsilon(\epsilon-h\nu)+(h\nu)^2\} \times \lg\frac{\Lambda}{\rho}\frac{137}{Z^{\frac{1}{3}}}\frac{d\nu}{\nu}; \quad (r_0=e^2/mc^2); \quad (3)$$

average specific energy loss of electrons due to radiation

$$-\frac{d\epsilon}{dx} = \frac{NZ^2r_0^2}{137}\epsilon\cdot 4\lg\frac{\Lambda}{\rho}\frac{137}{Z^{\frac{1}{3}}} \qquad (4)$$

(N = number of atoms per cm^3); absorption coefficient for photons due to pair production

$$\kappa = \frac{NZ^2r_0^2}{137}\frac{28}{9}\lg\frac{\Lambda}{\rho}\frac{137}{Z^{\frac{1}{3}}}. \qquad (5)$$

For $\rho=\Lambda=\hbar/mc$ (minimum extension of a wave packet for an electron) (3) to (5) go over into the well-known formulae which give far too high cross sections.

But with the value (2) for ρ it seems that quantitative agreement with observation is reached.

(a) The specific energy losses in lead for not too high energy electrons as observed by Neddermeyer and Anderson[6] are compared (see table) with the above formulas[7] (all values in units 1 MV $\cong 2mc^2$) once with $\Lambda/\rho=1$ (old) and the new value (2). The new formula agrees excellently (the experimental values are obtained as an average over largely straggling individual values) whilst the old one gives markedly too high values even for energies as low as 30 MV. At $\sim$300 MV the energy loss in lead according to (4) has its maximum and decreases again for higher ϵ.

Specific energy losses of electrons in lead.

	ϵ	30	70	120	300
$-\frac{d\epsilon}{dx}$	old	88	157	270	570
	new	48	70	87	110
	exp.	51	91	90	

(b) From the latitude effect of showers starting from about 30° downwards Compton[8] has concluded that only electrons with an energy of more than 8000 MV are able to traverse the atmosphere. The range for a reduction of energy from this value to 300 MV leads to 130 cm H_2O according to the old, to 400 cm H_2O for the new

[2] C. F. v. Weizsäcker, Zeits. f. Physik **88**, 612 (1934).
[3] E. J. Williams, Nature **135**, 66 (1935).
[4] Such a procedure has already been proposed by Oppenheimer, reference 5, who suggested different values for ρ. They were (a) the critical field strength "at the border of the electron" m^2c^4/e^3 which means that only the probable limit of classical theory (not the lower one for quantum electrodynamics) is considered. This would leave the cross sections still far too high. (b) Exclusion of all regions where Fourier components of an $h\nu > 137mc^2$ occur. This would practically cut off all radiative effects.
[5] J. R. Oppenheimer, Phys. Rev. **47**, 44 (1935).
[6] S. H. Neddermeyer and C. D. Anderson, Phys. Rev. **48**, 486 (1935).
[7] To the radiative losses (4) the contribution of the ordinary stopping effect ($\sim$17 MV) which according to Oppenheimer, reference 5, is not appreciably affected by the above limit, has been added. Neddermeyer and Anderson, reference 6, have not taken into account this contribution.
[8] A. H. Compton, Proc. Phys. Soc. **47**, 747 (1935).

formula.[9] This seems still to be too small but, according to the discontinuous nature of the radiation losses, rather large individual deviations from the average range will occur. The order of magnitude of this straggling effect can be estimated in the same way as Bethe and Heitler[1] did (the logarithmic term in (3) not varying very much for air or water for energies in the above range) with the result that about 10 percent of the electrons will travel a distance 2.8 times as large as the average range. Therefore just a sensible fraction of 8000 MV electrons will be able to reach the sea level.

(c) If one accepts the natural interpretation of the transition effect for showers[10] as a three-stage process: Primary electrons (I) generate the direct shower-producing photon radiation (S) which then produces pairs which cause the coincidences, the experimental curves lead to the following consequences independent of any further hypothesis.

(1) The coefficient of absorption of S is much higher than the one for I (factor ~ 30).
(2) The equilibrium intensity of S for given I (determined by the ratio of production to dissipation) is higher in air than in lead (this gives just the maximum).

The old formulae are in contradiction to both effects. There the average energy of the photons S should be of the same order ($\sim\frac{1}{2}$) as the average energy of the electrons I, and electrons and photons of similar energy have practically the same coefficient of absorption. Further in the ratio of production to dissipation the nuclear charge Z of the traversed matter drops out. According to the new formulation the situation is quite different. If the ρ from (2) approaches the radius of the atoms the radiative effects will decrease rapidly. This is the case, when the expression under the logarithm in (3) to (5) becomes 1, that is for a critical primary energy

$$\epsilon_c = 137^2 mc^2/Z^{5/3}. \tag{6}$$

This is for lead ~ 1000 MV, for air $\sim 20{,}000$ MV. So all cosmic-ray electrons will radiate strongly in air, but in lead only those below 1000 MV; (as the nuclear field is only gradually screened off by the outer electrons the more energetic electrons will still have a small chance to radiate in Pb). The same considerations apply to photons. The equilibrium intensity in air will therefore be higher than in lead, as more electrons will contribute. As furthermore only the corresponding not too energetic photons should produce the bulk of the pairs responsible for the triple coincidences, their absorption coefficient will be much greater than the one for the primary electrons as the greater part of the latter will practically not radiate in lead.[11]

The coefficient of absorption for S in lead would be, according to the old formula, 1.68 cm^{-1} which certainly is too large. In the new theory it depends on the energy being for 300 MV (which is the most effective part of S) about 0.54 cm^{-1} in comparison to the rough figure of 0.6 cm^{-1} usually given.

The author hopes to give a more complete treatment of the straggling of electron ranges and the energy distribution of the secondary photon radiation (which also should account for finer features of the transition effect as the change of shape of the transition curve with altitude and dependence on the material of the screen) together with a more detailed representation of the subject in the near future.

[9] The range R between ϵ_0 and a final energy ϵ for a specific energy loss

$$-d\epsilon/dx = A \lg B/\epsilon$$

being

$$R = (1/A) \lg [\lg (B/\epsilon)/\lg (B/\epsilon_0)].$$

[10] Number of triple coincidences below a target of lead showing a sharp maximum for about 2 cm Pb, then a rapid decrease with an extinction coefficient of about 0.6 cm^{-1} until a nearly stationary value is reached.

[11] The absorption of the primary electrons and the production of new S in lead has to be interpreted in the following way. Already a broad distribution of energetic electrons will enter the lead and as soon as the ordinary stopping brings down the energy of one electron to about 1000 MV, it will start to radiate and then be soon absorbed. Showers of higher energy as occasionally observed, could still be explained as produced by a number of photons of smaller energy generated already in air by one single primary electron or by one of the rarer processes, where an electron of higher energy than 1000 MV radiates in Pb.

LETTERS TO THE EDITOR

Prompt publication of brief reports of important discoveries in physics may be secured by addressing them to this department. Closing dates for this department are, for the first issue of the month, the twentieth of the preceding month; for the second issue, the fifth of the month. The Board of Editors does not hold itself responsible for the opinions expressed by the correspondents.

Communications should not in general exceed 600 words in length.

The Forces Responsible for Continental Motions and Pacific Type Mountain Building

Geological data indicate that continental motions are characteristic of the earth's surface development but no forces adequate to produce these motions have been known.

Because of the lack of strength of the earth's outer shell below about 1000 km the upper layers are in isostatic equilibrium. The principle of the compensation of continents, as usually stated, suggests simply that the mass per unit area of the surface layers above some reference equipotential surface located at levels of negligible strength, is everywhere constant. This statement is not strictly true because in regions of no strength, motion is determined by *pressure* gradients. Therefore, not the mass per unit area but rather the product of the mass per unit area and mean gravity in the outer layers ($m\,\bar{g}$) must be constant. Average gravity $\bar{g}$ in the outer layers depends on the density of the layers which, to moderate depths at least, is known to be greater under the Pacific than under the continents. The observed distribution of radioactivity suggests that this density difference will persist at considerable depths. Therefore $\bar{g}$ is less and m systematically greater over the Pacific than over the continents. The resulting mass asymmetry gives rise to tangential gravitational forces urging North America, for example, toward the west with a force estimated at 10^{25} dynes.

The ratio of the tangential acceleration (a) to that of gravity (g) is given approximately by

$$\frac{a}{g}=\frac{h^3\rho_1}{2R^2\rho_0^2}\frac{d\rho_1}{d\Delta},$$

where h is the thickness of the earth's outer layer of appreciable strength, ρ_1 its mean density, R the earth's radius, ρ_0 its mean density and Δ the angular coordinate. The average magnitude of this ratio approximates 6×10^{-5}. Therefore the average crushing stress produced at the margin of the Pacific basin approximates 10^8 dynes/cm^2 and may in special surface layers of great strength actually exceed 10^9 dynes/cm^2 which is the crushing strength of basalt. Tangential forces of the calculated magnitude seem adequate to induce continental motions, even against a resisting crust of considerable strength.

The motion of the continent results in a great accumulation of light surface material on its "downstream" face and in considerable overthrusting. These are the principal requirements of physical mountain building (as distinct from mountain building by sedimentation processes with which this investigation is not concerned) and account well for the observed structure and characteristics of Pacific type mountains.

The tangential forces are proportional to the *square* of the *thickness* of the outer layer of appreciable strength and therefore became important only after the earth's cooling and development were well advanced. Thus in accordance with geological observation, the Pacific type mountains and the suspected continental motions were produced at a comparatively late date.

The author's earlier astronomical approach to the problem of the origin of the solar system[1] has been supplemented by a geological investigation. It is shown that the mode of formation of the earth there proposed leads to the production of distinct continental and oceanic hemispheres of the type observed. All other proposed theories lead to a symmetrical earth.

ROSS GUNN

U. S. Naval Research Laboratory,
Washington, D. C.,
December 15, 1935.

[1] R. Gunn, Phys. Rev. **39**, 311 (1932); J. Frank. Inst. **213**, 639 (1932).

On the Slowing Down of Neutrons

"*. . . It is easily shown that an impact of a neutron against a proton reduces, on the average, the neutron energy by a factor 1/e.*"

According to reports from several sides, the above passage in a paper by Professor Fermi[1] is considered somewhat obscure. Since a more detailed explanation might be of interest also to others, it was thought advisable to make it generally known.

The mean energy of a neutron after an impact with a proton at rest is equal to one-half of the initial energy E_0. Therefore, calling E_n the energy after n such impacts, one has:

$$\bar{E}_1=E_0/2, \qquad \bar{E}_n=E_0/2^n.$$

We cannot however apply here Bernoulli's theorem on large numbers and conclude that the mean energy is the most probable, or, indeed, "by far the most probable" value of the energy. Fermi's argument was based on the consideration of the logarithmic decrement of the energy, which, being the sum of the partial decrements due to each collision, is subjected to Bernoulli's theorem.

Put: $\xi=\log(E_0/E_1)$; $x=\log(E_0/E_n)$.

One finds that:

$$\bar{\xi}=1 \qquad \text{and therefore:} \qquad \bar{x}=n.$$

Hence the above statement.

All further possible doubts may perhaps be answered

by giving the entire probability distribution of all values of x. Call $p(x)dx$ the probability that x lies between x and $x+dx$. One finds:

$$p(x) = [x^{n-1}/(n-1)!]e^{-x}.$$

One sees that the bulk of the distribution lies within the region specified by:

$$E_n = E_0 e^{-n \pm \epsilon(n)^{\frac{1}{2}}}; \quad \epsilon \sim 1$$

as one could have told beforehand.

It can be seen, also, that the high value of the mean energy arises from a small percentage of neutrons with a comparatively high energy (around $E_0 e^{-n/2}$).

G. C. WICK

Physical Institute,
Rome, Italy,
December 10, 1935.

[1] Fermi, Proc. Roy. Soc. **A149**, 524 (1935).

Proceedings of the American Physical Society

MINUTES OF THE BALTIMORE MEETING, NOVEMBER 29–30, 1935

THE 201st regular meeting of the American Physical Society was held in Baltimore, Maryland at The Johns Hopkins University in Remsen Hall Friday and Saturday, November 29 and 30, 1935. There were single sessions for the reading of contributed papers both morning and afternoon of each day. The presiding officers were President R. W. Wood, W. E. Forsythe, L. W. McKeehan, and W. L. Severinghaus. The attendance at the meeting was about two hundred.

On Friday after the afternoon session the Society was invited to make a tour of the Physics Laboratories in Rowland Hall. On Friday evening the Society held a dinner at the Baltimore Country Club, with one hundred and twenty-four members and guests present. President Wood presided and called for a few words from each of the following at the speakers' table: President Bowman, J. S. Ames, F. K. Richtmyer, J. B. Whitehead, K. T. Compton, A. H. Compton, and W. F. G. Swann.

Meeting of the Council. At its meeting held on Friday, November 29, 1935 the deaths of five fellows (Carl Barus, D. Roberts Harper, J. C. McLennan, C. E. Mendenhall. and K. K. Smith) and three members (H. Kakeshita, T. Kujirai, and C. W. Robbins) were reported. One candidate was transferred from membership to fellowship. One hundred and eighteen candidates were elected to membership. *Transferred from Membership to Fellowship:* Robert F. Paton. *Elected to Membership:* B. O. Adkerson, Robert L. Anthony, O. W. Baird, George B. Banks, Ernest S. Barr, J. Y. Beach, E. H. Bramhall, R. R. Brattain, Delbert F. Brown, David G. Brubaker, Anna May Callan, Anthony Carnvale, Thomas J. Carroll, Seville Chapman, Harold E. Clearman, Jr., J. J. Coleman, Donald K. Coles, Everett F. Cox, Charles S. Cummings, 2nd, Byron T. Darling, P. I. Dee, Hyman S. Denmark, Howard D. Doolittle, Donald W. Dunipace, Cecil G. Dunn, Olive M. Draper, Milo A. Durand, William C. Elmore, J. B. Fisk, Thomas E. Gilmer, Sister Matthew Marie Grannan, G. K. Green, Nicholas J. Guzik, William W. Hansen, Wilbur Harris, Louis M. Heil, Conyers Herring, John B. Hersey, G. Herzberg, J. A. Hipple, Jr., Frank E. Hoecker, Harold S. Howe, Harold K. Hughes, Gordon F. Hull, Jr., William H. Hulswit, Jr., Robert D. Huntoon, Malcolm C. Hylan, Thomas H. James, George R. Irwin, Yoshinobu Kakiuchi, Clare H. Kean, Donald W. Kerst, Don Kirkham, John D. Kleis, Curtis W. Lampson, Haldon A. Leedy, Hugh L. Logan, Carleton C. Long, Raymond C. Machler, Stephen M. MacNeille, Herbert G. MacPherson, Samuel J. Magarge, Ellis L. Manning, Lauriston C. Marshall, Charles M. Mason, John T. McCarthy, Henry L. McMurry, Russell W. Mebs, R. B. Morrissey, Alvin H. Nielsen, Haskell F. Norman, Charles E. Normand, Howard F. Ott, Charles G. Patten, Fred W. Paul, Hugh C. Paxton, Mahlon F. Peck, Boris Podolsky, Bernard H. Porter, Thomas H. Quigley, William R. Ransome, Rex Rhoten, Richard B. Roberts, Frederick W. Ross, Aydin M. Sayili, Leonard I. Schiff, Earl A. Schuchard, Harvey A. Schultz, Howard L. Schultz, Emilio Segrè, Rubby Sherr, Waldo A. Shipman, I. Żaka Slawsky, L. G. Smith, Newell H. Smith, Roman Smoluchowski, Karl C. Speh, John Sterner, Charles Strachan, Motoyosi Sugita, Melvin C. Terry, F. C. Todd,

Robert E. Tozier, Warren A. Tyrell, Jr., Michael L. Valentino, D. H. van Cittert, James H. Wakelin, Bernard Waldman, Frank C. Walz, Marvin C. Warner, Bernard B. Watson, Clarence E. Weinland, James W. White, David T. Williams, Earl D. Wilson, W. S. Wilson, Robert T. Young, Jr., Paul D. Zottu.

The regular scientific program of the Society consisted of thirty-nine contributed papers of which number one was read by title. The abstracts of the contributed papers are given in the following pages. An *Author Index* will be found at the end.

W. L. SEVERINGHAUS, *Secretary*

ABSTRACTS

1. Gyroscopes and Tops with Bearings.* R. C. COLWELL AND N. I. HALL, *West Virginia University.*—In the usual form of the gyroscopic top, the gyroscope is attached to a rod and is balanced by a weight adjusted along the rod. The support of this rod is rotatable about a horizontal and vertical axis. If the rod is placed in a bearing at the point of support, the gyroscope is given another degree of freedom and some very interesting motions may be produced. A new type of top has been developed consisting of a copper disk two inches in diameter and one inch high. This disk is fixed to a one-foot copper rod by means of a high speed bearing. The top is revolved 35,000 r.p.m. in the rotating field of an Alexanderson alternator. This tall top will stand vertically at first and will finally precess in an almost horizontal position.

* To be read by title.

2. Effect of Deuterium Oxide on Action of Some Enzymes. DAVID I. MACHT, *The Pharmacological Research Laboratory, Hynson, Westcott & Dunning, Inc., Baltimore. (Introduced by A. H. Pfund.)*—Ever since the discovery of heavy water much speculation of very diverse character has been advanced in regard to its possible effects on life. The most extreme views are presented by those who claim, without experimental proof, that deuterium oxide is a most powerful, destructive physiological agent and those who, basing their conclusions on experiments made with deuterium oxide in dilute concentrations, state that its pharmacological effects are of negligible character.[1] The author has recently discovered an interesting and striking contrast in the biophysical and biochemical behavior of H_2O and D_2O, which consists of a difference in velocity of reaction shown by certain animal and vegetable enzymes suspended in them. Studies were made on the behavior of muscle oxydase from the rat and on the reductase of finely ground seeds of Lupinus albus by the Thunberg method of determining the rapidity with which a standard buffered solution of methylene blue is decolorized. A marked difference was found to exist between identical enzymes suspended in H_2O and D_2O, respectively. This difference can be demonstrated not only with concentrations of D_2O, 1 : 100, but also with much *weaker* concentrations. Further studies regarding the activity of another enzyme, catalase, also revealed a difference in the speed of reactions as determined by H_2O and D_2O, respectively.

[1] Cf. Macht and Davis, "Some Pharmacological Experiments with Deuterium," J. Am. Chem. Soc. **56**, 246 (1934).

3. Ratio of Specific Heats of Air, N_2, and CO_2 as a Function of Pressure, by the Ultrasonic Method. J. C. HUBBARD AND A. H. HODGE, *The Johns Hopkins University.*—Measurements have been completed by Hodge of ultrasonic velocities at 27°C at pressures from 1 to 60 atmospheres for CO_2 and to 100 atmos. for air and N_2. The method used[1] permits the use of small scale apparatus and the driving of the source at any desired pressure. The results for CO_2 at a frequency of 88.39 kc, combined with the compressibility data of Amagat, give for γ at 27°C values from 1.304 at 1 atmos. to 3.524 at 60 atmos. The results for air at frequency 286.17 kc and for N_2 at 286.09 kc, combined with the respective compressibility data of Holborn and Otto, give at 27°C for air, values of γ between 1.408 at 1 m Hg and 1.584 at 80 m Hg, and for N_2, 1.402 at 1 m Hg to 1.572 at 80 m Hg. These and the other results between the limits quoted are in excellent general agreement with the few scattered results available for comparison, such results being very meager because of the technical difficulties of methods hitherto used for evaluating C_v or γ under even very moderate pressures.

[1] Hubbard, Phys. Rev. **46**, 525 (1934) *et ante.*

4. Deviations of Ortho- and Parahydrogen from the Laws of Ideal Solutions. F. G. BRICKWEDDE AND R. B. SCOTT, *National Bureau of Standards.*—An explanation of the vapor-pressure differences of *o*- and *p*-H_2 based on energy differences associated with intermolecular forces of orientation in the condensed states is suggested. These forces would be expected to differ for rotating and non-rotating varieties, and hence mixtures of these should show large deviations from ideal solution laws. Subsequent experimental data have confirmed this. Differences in vapor pressures of liquid mixtures containing 0, 19, 38, 57, 66, and 75 percent *o*-H_2 were measured from 14° to 20.4°K, and solid mixtures containing 0, 38, and 75 percent from 10.5° to 14°K; from these data differences in latent and specific heats were calculated. The size of the deviations is indicated by the table for liquid solutions at 20.4°K.

$[o\text{-}H_2]$ CONC. OF $o\text{-}H_2$ IN SOL.	$*\Delta P(p-s)$ AT 20.4°K (mm Hg)	$\frac{\Delta P(p-s)}{[o\text{-}H_2]}$	$\frac{\Delta L(s-p)}{[o\text{-}H_2]}$
0.1889	4.26	22.6	1.97
.3796	10.36	27.3	2.54
.5658	17.86	31.6	3.02
.6573	22.16	33.7	3.27
.7500	26.80	35.7	3.49

* $\Delta P(p-s)$ is the difference between the vapor pressures of *p*-H_2 and the solution.

The nonproportionality of the anomalous specific heat below 10°K of solid solutions[1] of *o*- and *p*-H_2 to the *o*-H_2 concentration is accounted for.

[1] Simon, Mendelssohn and Ruhemann, Naturwiss. **18**, 34 (1930).

5. A Problem in Potential Theory. MORRIS MUSKAT, *Gulf Research & Development Corporation, Pittsburgh, Pa.*—Two methods have been developed for treating a new type of potential problem arising in the study of the encroachment of water into an oil sand. The problem is that of finding the potential distributions in two regions of different "constants" ("conductivities"), separated by a movable surface of unknown shape, its motion and shape to be determined by the conditions that each point of the interface should have a velocity proportional to the vector gradient of the potential at the point, and that the area swept out by it shall assume the "constant" appropriate to that of its encroaching side. The first, a perturbation method, is valid when the difference between the "constants" is small, and reduces the problem of determining the shape and motion of the interface and the potential distributions *simultaneously*, to a series of problems in which potential distributions are to be found on the sides of *known* interfaces, and the motion of the surface is to be found in a *known* (time varying) potential field. This same type of reduction is effected also in the second method, which is one of direct successive approximations, but which may be used for any values of the potential "constants."

6. Residual Moisture in Cellulose Dielectrics. EUGENE W. GREENFIELD, *Anaconda Wire & Cable Co., Hastings-on-Hudson, N. Y.*—This paper discusses in a brief way the chemical and colloidal nature of the structure of cellulose paper as elucidated by the rich background of cellulose research and the more modern physico-chemical studies into the subject. With these theories of structure and our modern ideas of adsorption, the mechanism by which moisture is taken up or eliminated by or from cable paper is discussed. Argument is advanced to demonstrate that practically all of the free water residing in well dried cable paper exists in an adsorbed state upon or between the capillary walls. From a study of the dielectric properties of a sample of cable paper taken over a range of evacuation pressures it was possible to determine the quantity of residual moisture retained by the paper and from this the thickness of the adsorbed moisture films. It is shown that over the drying range studied, the paper exhibits a typical adsorption isotherm the equation of which is derived. Based on the above conclusions, the mechanism of the electrical behavior of adsorbed ion systems is discussed with particular reference to explaining the anomalous behavior of "dry" cable paper.

7. Magnetic Inversion Points by the Diffusion of H_2 Through Nickel and Iron and Through Iron-Nickel and Palladium-Nickel Alloys. W. R. HAM AND J. D. SAUTER, *Pennsylvania State College.*—The diffusion of hydrogen through homogeneous metals follows the formula $R=A[(p_0^y-p_t^y)/X]Te^{-b/T}$, where R=rate of diffusion, A=a constant of the diffusing metal, p_0 and p_t=pressures on ingoing and outgoing sides, y=a variable exponent often nearly 0.5, T=temperature Kelvin, X=thickness of diffusing sheet, b=total work function expressed in equivalent degrees. Over a temperature range between 200° and 800°C the isotherms for the above metals are almost exactly linear between pressures of 74 cm and 1 cm of Hg, but the slopes (y) are not necessarily constant with temperature change, nor are the isobars necessarily linear. Pure nickel shows a discontinuity in diffusion isobars at 360°C which cannot be mistaken, as does also palladium slightly alloyed with nickel. The cooling curves and magnetometer curves for nickel show the magnetic inversion to be very nearly at this same point. In the case of iron alloyed with nickel, the isobars show a sharp change in slope around 600°, whereas pure iron shows a large change in its isobars beginning at 760°C. The energy changes involved in these magnetic transformations are discussed.

8. Recording Field Current Electrons with a Geiger-Müller Counter. R. T. K. MURRAY, *The Johns Hopkins University.*—Preparatory to an attempt to measure directly the temperature dependence of field current emission, single field current electrons have been recorded by means of a Geiger-Müller counter. The cathode consisted of a brass sphere placed in a vacuum over a plane anode containing a small hole covered by a thin aluminum window which looks into a counter. Steady negative potentials between 10 and 20 kv were applied to the sphere. Tests showed that no detectable x-ray quanta were produced and for electrons having energies over 10 kv the window was perfectly transparent within the limits of experimental error. The field at the surface of the sphere necessary to give a threshold defined by an average current of 1 electron per second varied from about 50,000 volts per cm for a polished sphere to 20,000 volts per cm for one artificially roughened with an abrasive. Linear log current against reciprocal field strength relations were obtained over a current range from 1 electron every 10 seconds to 30 electrons per second in accordance with the Fowler-Nordheim relation $i=ae^{-b/F}$. Calculations of the microscopic form factors of the points give values as high as 400 and average emitting areas as low as 10^{-23} cm^2.

9. Photoelectric Work Function of Barium. R. J. CASHMAN AND N. C. JAMISON, *Northwestern University.*—After repeated distillation in high vacuum, barium was deposited on a nearly plane glass surface. The photoelectric work function at room temperature was determined by Fowler's method. In order to obtain accurate values of absorbed energy the reflection coefficient of the surface was measured. It was found to vary from 44.7 to 47.9 percent in the range from 4189 to 5035A, the range used in obtaining Fowler plots. The reflection was measured also at −77°C and as predicted by theory no change from the room temperature value was obtained in the wave-length range investigated. The shift necessary to superimpose the experimental curves upon the theoretical curve due to Fowler could be determined definitely to less than one-tenth of one percent. Measurements made from two hours to three months after laying down different deposits

yielded the value, 2.517 volts, for the work function. The authors do not maintain at present that the work function of pure Ba is 2.517 volts; the data suggest, however, that photoelectric work functions as measured by Fowler's method may be determined more accurately than those reported in the past. Thus far but one sample of barium has been used; work is in progress to obtain even more carefully purified samples of barium.

10. The Filter-Coupled Inductive Glow Discharge Oscillator. WINSTON E. KOCK, *The Institute for Advanced Study.*—The characteristics of an inductive glow discharge oscillator are reported whereby the previous control circuit of inductance and capacity is replaced by a control circuit comprising a multisection filter. The sharper resonance band thus presented effects a greater frequency stability by exerting a more effective control over the oscillations of the glow tube. Various types of filter sections are discussed and comparative curves given.

11. Influence of Physical Development in Region of Solarization.* ANNA JOYCE REARDON, *Saint Louis University.* (*Introduced by F. E. Poindexter.*)—In a previous paper entitled *Solarization at Low Intensity*[1] eight reversals in the region of solarization were established experimentally with chemical development. This same experiment was repeated by using three methods of physical development. The first, physical development before fixation as described by Odell;[2] the second, pre-fixing with acid hypo and then development of latent image in Odell's silver nitrate-amidol developer; and the third, pre-fixing of latent image in 30 percent plain hypo and development in Odell's developer. These three methods of physical development showed no reversal for extra fast, undyed, dry Hammer plates. In each case there was a continuous increase in the density of the latent image. This shows that in the region of solarization there is no decrease in the amount of silver deposited by the light exposure and that the prolonged light action does not decrease the amount of silver which has already been deposited. Therefore when solarization of the latent image occurs it must be due to some other cause. We suggest the possible closing of the fissures in the emulsion as set forth in the crystal cracking hypothesis of the latent image.

* To be read by title.
[1] Reardon, J. O. S. A. **24**, 331 (1935).
[2] Odell, Ind. Eng. Chem. **25**, 877–879 (1933).

12. Spectra of Strontium Deuteride and Hydride. WILLIAM W. WATSON, *Yale University*, W. R. FREDRICKSON AND M. E. HOGAN, JR., *Syracuse University.*—Details of the B and C band systems of SrD and the D system of SrH are presented. For the normal $^2\Sigma$ state $B_v^*=1.9427$ for SrD and 3.8788 for SrH. The ratio of these, 0.50635, shows about the expected departure from equality with the ratio $\rho^2=0.50603$ of the reduced masses. The spin doubling of the normal state of SrD is regular, $\gamma_0=+0.0613$ being almost exactly in the ratio ρ^2 with the value for SrH. In contrast with the corresponding state of CaD, the spin doubling of the $B\,^2\Sigma$ state of SrD departs markedly from the usual linear variation with $K+\frac{1}{2}$. The (0,0) C band of SrD exhibits multiple perturbations and a sharp cut-off of the branches at $K'=29$. For the $C\,^2\Sigma$ state $B_0\leqq 1.95$, but exact analysis of this state is hindered by the lack of any unperturbed lines. Two bands $(v',2)$ and $(v',3)$, with a common upper state, of the $D\,^2\Sigma\rightarrow N\,^2\Sigma$ "many-lined" SrH system having R branch heads at 18,446.21 and 17,341.39, respectively, have been analyzed. In this D state, for which $B_v=1.913$, large irregular perturbations occur. Finally, the nature of and the interactions among the known electronic states of the alkaline earth hydrides are discussed.

13. A Test of the Interval Rule in the $^2D_{3/2}$ State of Bi I. E. U. MINTZ AND L. P. GRANATH, *New York University, University Heights.*—The hyperfine structure of the line $\lambda 4722.5$ $(6p^3\,^2D_{3/2}-6p^27s(1)_{1/2})$ in the arc spectrum of bismuth was investigated using a Fabry-Perot etalon. The intervals between the six hyperfine structure components were measured and corrections were made for their mutual influence. A deviation from the Landé interval rule was found in the $^2D_{3/2}$ state. In the table under (a) and (b) are listed the measured intervals and those calculated from the Landé interval rule using a spin of 9/2 and the total measured separation of the $^2D_{3/2}$ state. The findings here are in accordance with those obtained for lines in europium and lutecium II by Schüler and Schmidt, and can be explained by the addition of a $\cos^2(ij)$ term to the usual cosine law of interaction. Under (c) in the table are the values of the intervals calculated letting $E=E_0+a_1\cos(ij)+a_2\cos^2(ij)$. The constants $a_1(276.7)$ and $a_2(12.9)$ were calculated with the interval $f_{(6-5)}$ (258 $\times 10^{-3}$ cm^{-1}) and the total separation.

Measured and Calculated Intervals (in $\Delta\nu\times 10^{-3}$ cm^{-1}) for $^2D_{3/2}$ State of Bi I.

		(a)	(b)	(c)
Δf	MEASURED	INTERVAL FACTORS	CALCULATED FROM COS LAW	CALCULATED FROM $\cos^2$ LAW
$f_{(6-3)}$	148	37	162	149
$f_{(6-4)}$	200	40	202	199
$f_{(6-5)}$	258	43	243	258

14. The Excitation Function of Lithium Under Proton Bombardment. M. OSTROFSKY, G. BREIT AND D. P. JOHNSON, *Institute for Advanced Study, Princeton, New Jersey.*—It is found that agreement with experiment for 8 cm alpha-particles can be obtained either by using the part of the incident wave having an angular momentum $L=0$ or the part having $L=1$. For the first condition with a radius of 0.35×10^{-12} cm one needs a "well" about 35 MEV deep. For $L=1$ and the same radius a "well" about 21.5 MEV is needed. The saturation of the yield with voltage is not a good measure of the height of the barrier and of the nuclear radius. The position of stationary and resonance levels is important for the shape of the excitation curve. The effect of the decay of the incident wave inside the nucleus is estimated and is found to be small in the present case. The "well" necessary for the representation of the alpha-particle reaction is compared with the mass of Be^8. It is found possible to fit this by attributing the alpha-particle reaction to $L=0$ and the formation of Be^8 from Li^7 to the addition of a proton into a p level.

15. Quantum-Mechanical Calculation of Energy of H_3 and H_3^+. J. HIRSCHFELDER, H. EYRING AND N. ROSEN, *Princeton University.*—The potential energy for all linear symmetrical nuclear configurations of the triatomic hydrogen molecule and ion has been calculated by the variational method with hydrogen-like $1s$ atomic orbitals by varying the screening constant and the amount of all polar and homopolar states in the eigenfunction. The lowest energies (in kcal./mole = 1/23.06 ev) and separations between neighboring atoms (in Bohr radii) are given in the table. The activation energy of the reaction

	E_{H_3} $-3E_H$	$(r_0)_{H_3}$	$E_{H_3^+}$ $-2E_H-E_{H^+}$	$(r_0)_{H_3^+}$	E_{H_2} $-2E_H$	$(r_0)_{H_2}$
Heitler-London approx.	−53.11	2.00	−91.92	2.00	−72.18	1.65
H. L. plus ionic approx.	−60.39	2.00	−108.64	2.00	−74.02	1.70
Wang approx.	−56.16	1.89	−130.89	1.55	−86.94	1.38
Wang plus ionic approx.	−67.09	1.84	−155.35	1.52	−92.24	1.40
Experimental	−101				−108.6	1.40

$H+H_2 \rightarrow H_2+H$ is calculated to be 25.15 kcal., i.e., 18 kcal. greater than the experimental value. The reaction $H_3^+ + H_2 \rightarrow H_2^+ + H$ will take place with at most a small amount of kinetic energy. The difficult three center integrals for the repulsions between pairs of electrons were calculated explicitly in ellipsoidal coordinates without the use of infinite series.

16. Cross Section for the Production of Triples. JOHN A. WHEELER, *University of North Carolina.*—Besides producing pairs in the neighborhood of atomic nuclei, energetic quanta should create positrons and electrons in the fields of the outer electrons. As pointed out by Perrin[1] who originally suggested the possibility of this effect, the low energy limit is not $2mc^2$, as in ordinary pair production, but at $4mc^2$ (2.04 MEV), because of the energy imparted to the electron in whose neighborhood the pair is produced. Indeed, the relations for the final momenta and energies are symmetric in the original electron and the two new ones, and determine a lower bound for the energy of any one of the three. The cross section for the process is calculated by taking account of the symmetry between the original electron and the newly created one. Because of the relativistic velocities, Møller's retarded interaction is used. Detailed probability studies on the effect in a cloud chamber should give a new test of the relativistic interaction between two electrons at high energies. The production of triples may be expected to be of considerable importance in the absorption of high energy quanta in substances of such low atomic number as water and air.

[1] Perrin, Comptes rendus 197, 1100 (1933).

17. The Infrared Absorption of Mixtures of Water and Acetone. E. K. PLYLER AND DUDLEY WILLIAMS, *University of North Carolina.*—A study of the infrared absorption spectra of absolute acetone and acetone containing water showed bands of solvation in the regions of 1.6μ and 2.7μ. The band at 2.7μ was studied for concentrations of water in the acetone of 0.5 percent to 70 percent. The intensity of the solvation band increased with the water content. When the water content was large, the 3μ water band overlapped the solvation band. Absorption spectra were obtained for ten mixtures. It was found that water with concentrations as low as 0.1 percent in the acetone could be detected by the presence of this band.

18. Infrared Absorption of Cyanides, Thiocyanates, and Their Isomers. DUDLEY WILLIAMS, *University of North Carolina.*—Aqueous solutions of inorganic cyanides have been studied in the region from 1.2μ to 7.5μ. In all the materials a characteristic absorption band was observed in the region from 4.38μ to 4.90μ. The exact position of the band was found to be different for the various substances. Bands in this same region were observed for several organic cyanides. This characteristic absorption was attributed to changes in the vibrational energy of the bound CN group. The organic cyanides and thiocyanates furnish an opportunity for a study of the effects of isomerism on infrared absorption. Six organic liquids and their isomers were studied. The bands characteristic of the NC group are of much greater intensity and appear at slightly longer wave-lengths than the corresponding CN bands.

19. Columnar Ionization. W. R. KANNE, *Johns Hopkins University.*—A study has been made of the ionization current produced by alpha-particles as a function of the angle between the path of the particles and the electric field. A polonium source was mounted above a parallel plate ionization chamber so that it could be rotated about an axis lying in the lower surface of the upper plate and passing through the fine hole in this plate which admitted the particles to the chamber. The lower plate, which served as the collecting electrode, was surrounded by a large guard ring and connected to the grid of an FP-54 vacuum tube. It has been found that the increase in ionization current is linear with respect to the angle between the path of the particle and the field. No deviation from linearity occurs as the path and the direction of the field become parallel. The columnar effect becomes slightly less as the field strength is increased. The effect is correspondingly larger for the curves run at two atmospheres than for those run at one atmosphere. For a field of 100 volts per cm and one atmosphere pressure, the number of ions collected changes about 3 percent as the angle changes from 0° to 10°.

20. Theoretical Considerations Concerning Passage of Electrons Through Magnetized Iron. W. F. G. SWANN, *Bartol Research Foundation of the Franklin Institute.*—On the Lorentzian theory the magnetic induction, B, is the average value of the true magnetic field H, averaged throughout the magnetic material. In this average, regions inside the magnetic entities responsible for the polarization make contributions which determine the whole difference between B and the ordinary macroscopically defined field, h, equal to $B-4\pi I$. A study is made of the special case where the entities are rotating electrical spheres. If the entities are very small in volume the chance of an electron missing all of them in its passage through a reasonably

small length of the magnetized material is considerable. For such electrons as miss the entities the effective deflecting force is determined on the average by $h+2\pi I$. The true average for all electrons passing through the material is determined by $B=h+4\pi I$; but, that average is contributed to in appreciable amount by very few electrons which experience deflections much in excess of those determined by B. These considerations have important consequences in relation to the interpretation of experimental results.

21. Deflection of Cosmic-Ray Secondaries by Magnetized Iron. W. E. DANFORTH AND W. F. G. SWANN, *Bartol Research Foundation of the Franklin Institute.*—At a previous meeting we described experiments using Geiger-Müller counters which showed that the cosmic-ray electrons experience a definite deflection when they pass through a magnetized iron core in a direction normal to the magnetization. The more recent appearance of appropriate energy distribution data, as found in a counter controlled Wilson chamber by Anderson and Neddermeyer, enables us to arrive at a more satisfactory interpretation than was possible at that time. We have also been able to set limits to the correction necessitated by the presence of cosmic-ray showers. By taking the various probable errors into account it appears that the experimental results may be accounted for by assigning a value for the effective magnetic vector somewhere between the induction B and $B/3$. The assignment of a value different from B involves no logical difficulties if one allows that the deflections of a number of electrons of the same energy have a statistical distribution. For, although the arithmetic average of the deflections must be determined by B, the effect observed in the counter experiment corresponds to a different sort of average.

22. The Absorption of Cosmic-Ray Electrons at 10,600 Ft. and at Sea Level. R. H. WOODWARD AND J. C. STREET, *Harvard University.*—Counter measurements of the absorption of cosmic-ray electrons have been made at Echo Lake, Colorado, elevation 10,600 ft. Care has been taken to obtain results directly comparable with those previously found at sea level.[1] For this purpose the same counters and geometrical arrangement were used and the efficiencies were measured at each station. The results are sufficiently precise to permit a comparison of the quality and intensity of the radiation at the two elevations. The following abbreviated table illustrates the comparison.

THICKNESS OF LEAD ABSORBER (cm)	COUNTS PER MIN. AT ECHO LAKE (52.5 cm)	COUNTS PER MIN. AT CAMBRIDGE (76 cm)
0	0.540	0.289
15.2	.284	.209
91.5	.132	.107

The atmospheric layer between the two elevations is equivalent to 36.3 cm of lead on the extranuclear electron scale.

[1] Street, Woodward and Stevenson, Phys. 891 (1935).

23. Effect of Rainfall on Ionization Registered by Recording Cosmic Meter with Top Shield Removed. RICHARD L. DOAN, *University of Chicago.*—Several recording cosmic-ray meters operated with bottom shielding only have shown pronounced increases of ionization during thunderstorm periods. Investigation has shown these increases to be associated with rainfall and not with atmospheric electrical discharges. The excess ionization starts at the beginning of the rain and continues for an hour or more after the precipitation has stopped, thus indicating an appreciable life for the responsible ionizing agent. Simultaneous tests with two meters, one with no top shield and the other shielded from above with 1 cm of lead, indicate an absorption coefficient for the radiation about equal to that of gamma-rays, from which it is concluded that the effect is largely due to Ra B and Ra C brought down with the raindrops from the upper atmosphere. The radioactivity of freshly fallen rain was first observed by C. T. R. Wilson in 1902 and the effect reported here is doubtless of a similar nature. Such rapid changes in atmospheric radiation emphasize the importance of using heavy shields in making cosmic-ray observations.

24. Magnetic Spectrum of Positrons Generated in Lead by Th C'' Gamma-Rays. G. L. LOCHER AND C. L. HAINES, *Bartol Research Foundation of the Franklin Institute.*—A special beta-ray spectrograph has been constructed for simultaneous analysis of the energies of positrons and electrons generated in a centrally located metal foil. A collimated beam of γ-rays from 1.7 mg (Ra γ-ray equivalent) of $MsTh_1$, filtered through 1 cm of lead, was used for generating positron-electron pairs in a lead foil 0.02 cm thick (0.227 g/cm^2). The magnetic field, as measured with a Cotton balance, is 503.0 ± 2.0 gauss. Two exposures: 39 days, with a wide source, and 47 days, with a narrower source, respectively, made with the lead generator, gave nearly identical results. The positrons showed a sharp cut-off at $(1.10\pm0.01)\times10^6$ ev ($H\rho=5098$); below this energy, the blackening was continuous. The cut-off is, thus, approximately 500,000 volts lower than the predicted maximum energy for positrons generated in this way. The blackening of the films by negative electrons was continuous up to the energy-limit of the spectrograph. Double emulsion film (Eastman x-ray film) was used; the blackening of each emulsion by positrons and the γ-rays emitted by their annihilation was measured with a microdensitometer. The upper emulsions showed distributions of blackening, on the positron side, similar to those of the lower emulsions, but of lower density. A similar spectrogram, with silver as the generating element, is now being made; the results of this exposure will be available for the meeting.

25. Experiments on Slow Neutrons with Velocity Selector. J. R. DUNNING, G. A. FINK, G. B. PEGRAM AND E. SEGRÈ, *Columbia University.*—Further experiments with the mechanical velocity selector for slow neutrons at room temperature are in agreement with previous results.[1] Considerations of the form of the experimental curve to be expected if the neutrons were in thermal equilibrium within the paraffin with a Maxwellian distribution of velocities, show that within the limits of precision, the experimental results follow this curve. The resolution and precision at present are not sufficient to detect small departures from a

Maxwellian curve. Attempts to measure differences in the absorption of Cd with neutrons selected from the upper and lower parts of the distribution curve have not shown any departures beyond experimental error. The velocity distribution of "cold" neutrons at about 95°K was studied by cooling with liquid air 2000 cc of paraffin contained in a soft glass Dewar, the source being at the center of the paraffin. The number of very slow neutrons is increased, and the maximum of the distribution curve shifted toward lower velocities, as is to be expected.

[1] Phys. Rev. **48**, 704 (1935).

26. Absorption of Neutrons with Lithium and Boron as Detectors. D. P. MITCHELL, J. R. DUNNING AND G. B. PEGRAM, *Columbia University.*—A comparison of Li- and B-lined ionization chambers used as detectors in measuring the transmission of slow neutrons through various substances has been made and absorption (capture plus scattering) with varying thickness has been measured. The cross section of B, Li and Cd measured with similarly constructed Li chambers differed a little more than the statistical error. Measurements with a boron chamber agreed with those from one of the lithium chambers within the statistical error. To test the effect of thickness and surface condition of the Li, chambers having different fronts were compared by measuring the absorption of cadmium. Variations with thickness are insignificant, but the ratio of fast to slow neutrons detected increases when the Li is permitted to oxidize and absorb water vapor. This may be due to the projection of H nuclei and the absorption of the disintegration particles from within the Li by the oxide on its surface.

27. Production and Absorption of Slow Neutrons in Hydrogenic Materials. G. A. FINK, J. R. DUNNING, G. B. PEGRAM AND E. SEGRÈ, *Columbia University.*—A Rn-Be neutron source was placed at the center of several sizes of cylinders containing water and the number of neutrons emerging per minute determined by the use of an 8-cm diameter Li-lined chamber and an amplifier-recorder system. The relation between the number of slow neutrons counted and the thickness of the water layer outside of a Cd shell placed in the water shows rates of production and absorption as in our previous measurements on paraffin spheres of diameters from 4 to 45 cm. From the rate of absorption and the known M.F.P. in paraffin the mean life time of a neutron in paraffin is computed to be of the order of 10^{-4} sec. The number of slow neutrons coming from various zones of the end of a paraffin cylinder 16.6 cm diameter and 22 cm long was counted and the relative number/cm²/min. found to decrease from 1 in central (5.1 cm diam.) to 0.7 for the intermediate (5.1–10.6) and 0.25 for the outside (10.6–16.6) zone, with an average of 0.45 for the whole end surface. The number of fast neutrons not absorbed by Cd is, on the same basis, 0.06.

28. Excitation Potential of $K\alpha_{3,4}$ X-Ray Satellite Lines. LYMAN G. PARRATT, *National Research Fellow, Cornell University.*—With a two-crystal vacuum spectrometer the curve of the intensity of $K\alpha$ satellite lines *vs.* voltage of the x-ray tube has been determined for the $K\alpha_{3,4}$ lines of titanium. For voltages greater than 11 kv the satellite intensity (total area of the $K\alpha_{3,4}$ satellite structure) relative to the intensity of the $K\alpha_1$ line is 2.21 percent; the ratio of peak intensities α_4/α_1 is 0.69 percent. The measured excitation potential of the Ti $K\alpha_{3,4}$ lines is 5450 ± 100 volts, 500 volts in excess of the excitation potential of the $K\alpha_{1,2}$ lines. Assuming 0.85 as the screening constant of a missing K electron on an L electron, one calculates that the voltage required to produce a state of KL ionization in the titanium atom is 5455 volts. This value is in excellent agreement with the measured excitation potential and the conclusions of the experiments are in support of the Wentzel-Druyvesteyn theory of the origin of the $K\alpha_{3,4}$ satellite lines.

29. Practical Analysis by Use of X-Ray Diffraction. J. D. HANAWALT AND H. W. RINN, *The Dow Chemical Company, Midland, Michigan.*—The x-ray diffraction of a crystalline substance provides a practical method of chemical analysis because the diffraction pattern can be used empirically as a unique identification of a substance without any necessity of a theoretical interpretation of the pattern. In the course of a few years of use of x-ray diffraction as a supplement to chemical analysis, the patterns of about one thousand substances have been accumulated. A suitable system of classification of these films makes it possible to use them for crystalline substances in an analogous way to that in which finger prints are used to identify persons. The system of classification which has been adopted allows a pattern to be identified in less than a minute if it is contained in the portfolio of standard patterns. Some improvements in the technique of obtaining good patterns will also be described.

30. The Structure of Ice II. RONALD L. MCFARLAN, *Harvard University.*—The stability of the high pressure ice forms discovered by Tammann and Bridgman at very low temperatures and atmospheric pressure has made it possible to obtain x-ray powder diffraction photographs of these forms. The experimental procedure is very briefly discussed. An analysis of the ice II diffraction patterns leads to a side-centered orthorhombic cell with $a=7.80$A, $b=4.50$A, and $c=5.56$A. This cell contains eight molecules, has the symmetry of space group V^8-C222_1, and gives a value for the density of 1.21. The proposed arrangement of the hydrogen atoms indicates that the transition from ice I to ice II breaks up the water molecule, and that ice II is an ionic crystal. According to the model described the effect of a pressure of 2100 atmospheres in forming ice II is (1) to decrease the packing volume of the oxygen ion approximately three percent; (2) to break down the open ice I structure by a slipping of the oxygen ion layers relative to each other; (3) to give a four-coordinated structure where each oxygen is surrounded by a badly distorted tetrahedron of oxygen ions.

31. The Structure of the Sulphur Molecule by Electron Diffraction. LOUIS R. MAXWELL, S. B. HENDRICKS AND V. M. MOSLEY, *Bureau of Chemistry and Soils, Washington, D. C.*—Considerable uncertainty exists as to the structure

of the S_2 molecule, band spectra values obtained by different authors for the nuclear separation in the normal state ranging from 1.60 to 1.84A. Independent determinations of this distance can be made by means of electron diffraction. A gas boiler containing iron pyrite heated to about 850°C provided a source of hot sulphur vapor calculated to give a very predominant concentration of S_2 molecules. The electron diffraction pattern obtained from this gas showed two outer rings classified as the third and fourth maxima located at $(1/\lambda)\sin\frac{1}{2}\theta=0.827\pm0.008$ and 1.09 ± 0.02, respectively; the inner rings appeared only as halos. Assuming a diatomic structure the two outer rings give a S−S distance of 1.94 ± 0.03A, a distance definitely greater than any of the band spectra values. When the temperature of the boiler is lowered the interference pattern is changed. A prominent second ring comes at $(1/\lambda)\sin\frac{1}{2}\theta=0.516\pm0.005$ while the third maximum has a diameter of 0.790 ± 0.008. This pattern can be satisfactorily explained by the formation in the vapor of S_3 or S_{2+n} molecules where $n=1, 2, \cdots$, with the S−S−S valence angle approximately 100° and the S−S distance between neighboring molecules as 2.10A, entirely consistent with similar constants found from crystal structure data.

32. The Electron Distribution in $(NH_4)_2C_2O_4\cdot H_2O$ and the Structure of the Oxalate Group. S. B. HENDRICKS AND M. E. JEFFERSON, *Bureau of Chemistry and Soils, Washington, D. C.*—The electron distribution of the orthorhombic crystal $(NH_4)_2C_2O_4\cdot H_2O$ projected on (001) was obtained by a Fourier analysis making use of quantitative intensity measurements for (*hko*). This analysis combined with a determination of the atomic parameters perpendicular to (001) gave the complete structure. Separations of covalently linked atoms in the $C_2O_4^{--}$ group are C−C, 1.581 ± 0.01A, C−O, 1.25 ± 0.02A, and C−O, 1.23 ± 0.02A with the angle $O-C-O=129°\pm2°$. In this compound the O−C−O parts of an oxalate group are in planes at an angle of 28° while in $H_2C_2O_4\cdot 2H_2O$, α and β $H_2C_2O_4$ the parts are coplanar.

33. The Anisotropic Growth of Silver Crystals by Condensation from Vapor. JOSEPH H. HOWEY,* *Yale University.*—It has been found that silver vapor condensing in a vacuum on suitable nuclei of solid silver maintained at a temperature just below the melting point forms single crystal needles under certain conditions. The observed habit of growth is probably dependent upon the presence of certain impurities but it is noteworthy that a metal having face-centered cubical symmetry in the solid state should ever condense in the form of needles. The longest needles grown have been about three millimeters long and several tenths of a millimeter in diameter. At least five percent of the needles have abrupt changes in direction, the appearance of which indicates that the boundary between the two linear portions coincides closely with a single crystallographic plane extending across the entire cross section. Abrupt changes in direction both less and greater than 90° have been observed but no branching has been found. One tentative explanation of the growth of these needles is to consider their occurrence as experimental evidence for the idea that the forces between metal atoms in a crystal may be greater in one direction than in others which are crystallographically identical and that the direction of this anisotropy may be constant throughout a domain of considerable size. The existence of such anisotropy would serve to explain the growth of the needles regardless of whether the growth is conditioned by the presence of impurities or not.

* Now at Georgia School of Technology.

34. The Production of Large Single Crystals of Lithium Fluoride. DONALD C. STOCKBARGER, *Massachusetts Institute of Technology.*—Preliminary experiments performed to determine the conditions under which lithium fluoride could be crystallized continuously from the melt indicated that high purity of the salt and steep temperature gradient normal to the freezing layer were important. Accordingly an improved method of synthesizing salt, and a special double furnace, in which the required gradient can be maintained without overheating the melt or chilling the crystal, have been developed. With the aid of these improvements lithium fluoride crystals of excellent optical quality up to three inches in diameter are now being grown regularly. These possess such stability that they can ordinarily be sawed and ground to any desired shape.

35. A Laboratory Induction Pump for Mercury. E. S. GILFILLAN, JR., *National Research Fellow,* AND S. M. MACNEILLE, *Massachusetts Institute of Technology.* (*Introduced by J. C. Boyce.*)—Difficulties were encountered with reciprocating pumps for the continuous circulation of mercury. An all-metal pump, without moving parts, operating on the principle of a polyphase induction motor was developed. The mercury flows in the annular region between two concentric tubes. Surrounding the tubes are coils connected to a polyphase supply. The result is a series of magnetic ripples traveling along the axis of the tubes which drag the mercury along by virtue of the currents induced in it. Lifts in excess of a meter and capacities in excess of 50 cc per second have been obtained. Comparison will be made with the designs of previous investigators.

36. Deflection and Focusing of a Beam of Hydrogen Atoms. I. I. RABI, J. R. ZACHARIAS AND J. M. B. KELLOGG. *Columbia University.*—A beam of hydrogen atoms in the normal $^2S_{\frac{1}{2}}$ state was deflected in a weak inhomogeneous magnetic field. It was then passed through a strong field arranged to produce deflections opposite in direction to those of the weak field. With nuclear spin I, the intensity measured at the undeflected position of the beam should show $2I+1$ peaks when plotted as a function of the first deflecting field. These peaks correspond to focusing by the strong field of the $2I+1$ magnetic states of the atoms in the weak field. From the values of H at these peaks it is possible to calculate the hfs separation for the state irrespective of the velocity distribution of the atoms in the beam. The hydrogen atoms were produced in a Wood discharge tube designed to yield a high ratio of atoms to molecules in the beam. The deflecting fields are of the type previously described. Detection was effected by means of a Pirani gauge. The intensity curve shows two well-defined

peaks which gives a value of the spin of the proton of ½, corroborating the result obtained by alternating intensities in band spectra. Further experiments to determine accurately the hfs separation are in progress.

(To be called for after Paper No. 18.)

37. The Photoelectric Work Function of Ca and Photo-Emission from Nonhomogeneous Surfaces. N. C. JAMISON AND R. J. CASHMAN, *Northwestern University.*—Using Fowler's method, the photoelectric work function of Ca was determined for layers produced by single distillations, using a multiple reflection cell adapted to the study of the variation of work function with temperature. Data in good agreement with Fowler's theory were obtained. The room temperature work function by Fowler's method was 2.704 volts; the greatest variation from the mean of seven determinations was 0.004 volt. After repeatedly heating the surface to approximately 100°C the data did not agree with Fowler's theoretical curve. The departures from the theoretical curve were consistent with the assumption that, after heating, the surface was not homogeneous. Analysis of the data gave evidence of two emitting surfaces, one assumed to be Ca having a work function of 2.704 volts and the other having a work function some 0.2 volt lower. It is concluded that a single distillation cell is not suited to the accurate determination of the temperature coefficient of the work function; also a multiple reflection cell is not desirable. When working with composite surfaces having emitting areas of nearly the same work function, the data will not fit Fowler's theoretical curve.

(To be called for after Paper No. 10.)

38. Proton-Proton Forces in Anomalous Scattering and in Nuclear Binding. R. D. PRESENT, *Purdue University.* (*Introduced by K. Lark-Horovitz.*)—Recent experiments by White on the anomalous scattering of 600–750 kv protons in hydrogen indicate a departure from the Coulomb law at 5×10^{-13} cm. Using the Feenberg-Knipp nuclear model we have calculated the cross section for scattering at 45° and obtained good agreement with experiment. This work quantitatively confirms the use of a spin dependent potential for neutron-proton interaction. For other angles, however, there occur serious difficulties. Perfectly general considerations, which depend only on the asymptotic form of the wave function and are *entirely independent* of the nuclear model, show that it is impossible to explain the angular dependence of the experimental cross section by any form of s and p scattering, while higher orders of scattering are negligible.

39. Further Investigations of the Atmospheric Ionization Associated with Rainfall. G. R. WAIT AND A. G. MCNISH, *Department of Terrestrial Magnetism, Carnegie Institution of Washington.*—Investigations conducted during the past summer on the ionization produced in the atmosphere by rainfall confirm the findings previously reported by the authors[1] that the increased ionization is caused by radioactive matter, principally Ra B and Ra C, brought down to the Earth by the rain. Coating the thin-walled ionization-chamber used in the earlier investigations with paraffin sufficiently thick to stop alpha-particles caused the effect during thunderstorms to be diminished. The diminution was from 40 to 8 ion-pairs per cc per second in the chamber per inch of rain, values referring to accumulated rates. The first number is due to the combined effects of alpha, beta, and gamma-radiation while the second is due to beta and gamma-radiation alone. Considering a uniform distribution of Ra B and Ra C in the free atmosphere the ratio of the ionization due to alpha, beta, and gamma-radiation to that due to beta and gamma-radiation alone should be 6 to 1. Evidence is presented to show that the radioactive substances brought down by the thunderstorm rain are not caught by the drops while falling, as hypothesized by C. T. R. Wilson, but are accumulated in the thunder-cloud into which they are carried from the Earth by ascending air-currents associated with the formation of thunderstorms.

[1] Mon. Weath. Rev. **62**, 1–4 (January, 1934) and Phys. Rev. **45**, 750 (1934).

AUTHOR INDEX TO ABSTRACTS OF BALTIMORE MEETING

Breit, G.—see Ostrofsky
Brickwedde, F. G. and R. B. Scott—No. 4
Cashman, R. J.—see Jamison
—— **and N. C. Jamison**—No. 9
Colwell, R. C. and N. I. Hall—No. 1
Danforth, W. E. and W. F. G. Swann—No. 21
Doan, Richard L.—No. 23
Dunning, J. R.—see Fink
—— see Mitchell
—— **G. A. Fink, G. B. Pegram and E. Segrè**—No. 25
Eyring, H.—see Hirschfelder
Fink, G. A.—see Dunning
—— **J. R. Dunning, G. B. Pegram and E. Segrè**—No. 27
Fredrickson, W. R.—see Watson
Gilfillan, E. S., Jr. and S. M. MacNeille—No. 35
Granath, L. P.—see Mintz
Greenfield, Eugene W.—No. 6
Haines, C. L.—see Locher
Hall, N. I.—see Colwell
Ham, W. R. and J. D. Sauter—No. 7
Hanawalt, J. D. and H. W. Rinn—No. 29
Hendricks, S. B.—see Maxwell
—— **and M. E. Jefferson**—No. 32
Hirschfelder, J., H. Eyring and N. Rosen—No. 15
Hodge, A. H.—see Hubbard
Hogan, M. E., Jr.—see Watson
Howey, Joseph H.—No. 33
Hubbard, J. C. and A. H. Hodge—No. 3
Jamison, N. C.—see Cashman
—— **and R. J. Cashman**—No. 37
Jefferson, M. E.—see Hendricks
Johnson, D. P.—see Ostrofsky
Kanne, W. R.—No. 19
Kellogg, J. M. B.—see Rabi

Kock, Winston E.—No. 10
Locher, G. L. and C. L. Haines—No. 24
Macht, David I.—No. 2
MacNeille, S. M.—see Gilfillan
Maxwell, Louis R., S. B. Hendricks and V. M. Mosley—No. 31
McFarlan, Ronald L.—No. 30
McNish, A. G.—see Wait
Mintz, E. U. and L. P. Granath—No. 13
Mitchell, D. P., J. R. Dunning and G. B. Pegram—No. 26
Mosley, V. M.—see Maxwell
Murray, R. T. K.—No. 8
Muskat, Morris—No. 5
Ostrofsky, M., G. Breit and D. P. Johnson—No. 14
Parratt, Lyman G.—No. 28
Pegram, G. B.—see Dunning
—— see Fink
—— see Mitchell
Plyler, E. K. and Dudley Williams—No. 17
Present, R. D.—No. 38
Rabi, I. I., J. R. Zacharias and J. M. B. Kellogg—No. 36
Reardon, Anna Joyce—No. 11
Rinn, H. W.—see Hanawalt
Rosen, N.—see Hirschfelder
Sauter, J. D.—see Ham
Scott, R. B.—see Brickwedde
Segrè, E.—see Dunning
—— see Fink
Stockbarger, Donald C.—No. 34
Street, J. C.—see Woodward
Swann, W. F. G.—No. 20
—— see Danforth
Wait, G. R. and A. G. McNish—No. 39
Watson, William W., W. R. Fredrickson and M. E. Hogan, Jr.—No. 12
Wheeler, John A.—No. 16
Williams, Dudley—No. 18
—— see Plyler
Woodward, R. H. and J. C. Street—No. 22
Zacharias, J. R.—see Rabi

Proceedings of the American Physical Society

Minutes of the Berkeley Meeting, December 20–21, 1935

THE 202nd regular meeting of the American Physical Society was held in 212 Le Conte Hall at the University of California, Berkeley, California, on Friday, December 20 and Saturday, December 21, 1935. The morning sessions ran from 9 to 12 and the afternoon session from 1:30 until 4:30. Twenty-seven papers were presented on the regular program and ten papers were presented on the supplementary program. About 80 members of the society attended the meetings. The Society met at luncheon at the Faculty Club on Friday and Saturday noons. A business meeting was held during the Friday morning session.

The secretary read a letter from the Pacific Division of the American Association for the Advancement of Science stating that a canvass of the affiliated societies of the Pacific Division had indicated definitely that the Pacific Division was opposed to changing the time of the annual Pacific Division meetings now held near the end of June to the month of September and stating their reasons therefor. This decision on the part of the Pacific Division was a revocation of the plan tentatively proposed at the Pullman, Washington meetings in 1932, at which time the Pacific Division had voted to try the plan of changing the time of the annual meetings from June to September. The letter further expressed the wish of the Executive Committee and of the Pacific Division that the Pacific Coast meetings of the American Physical Society continue to be held in affiliation with the Pacific Division of the A. A. A. S. as in the past. It was further stated that the date of the meetings of the Pacific Division in June was set largely for the convenience of the host institution and that therefore the Physical Society would have to conform to the date set if they were to participate in the meetings. The local secretary explained to the members of the Physical Society that in the event of the Pacific Coast members voting to hold the Pacific Coast meetings in June in affiliation with the Pacific Division, the date for the June meetings of the Pacific Division was always agreed upon in ample time so that the secretary of the American Physical Society could be notified of the date of the meetings to the end that the Executive Committee of the American Physical Society in setting the date for the eastern summer meeting of the Physical Society might be able to avoid a conflict in time between the two meetings. It is the earnest desire of the Pacific Coast members of the Society that such conflict be avoided in order that it will be possible for national officers and other interested members of the Physical

Society to attend the summer meetings on the Pacific Coast in years when such summer meetings are held in the large population centers with a considerable attendance of members of the Society.

After due discussion it was moved, seconded and unanimously voted by the members present that the Pacific Coast meeting of the American Physical Society in summer continue to be held in affiliation with the Pacific Division of the A. A. A. S. This action automatically sets the date of the summer meeting of the American Physical Society as the period of Tuesday, June 16 to Saturday, June 20, 1936, at the University of Washington, Seattle, Washington.

The secretary thereupon notified the members of the Physical Society in attendance at the meetings of his resignation as secretary for the Pacific Coast of the American Physical Society to take effect January 1, 1936, and announced the election of Professor Paul Kirkpatrick of Stanford University as the new local secretary for the Pacific Coast of the American Physical Society. On motion from the floor duly seconded, the members of the Society represented at the meeting voted to express to the local secretary their appreciation for his years of faithful and efficient service in the arrangement of the Pacific Coast programs.

LEONARD B. LOEB
Local Secretary for the Pacific Coast

ABSTRACTS

1. Gamma-Rays Emitted by Several Artificially Produced Radioactive Elements. J. R. RICHARDSON, *University of California.*—The energies of the gamma-rays from several artificially produced radioactive elements have been determined by studying the momentum distribution of the recoil electrons produced from a thin lamina of glass or mica placed in a cloud chamber. Only tracks starting in the lamina and projected within 12° of the forward direction were measured. The cloud chamber was filled with hydrogen (which greatly reduces the scattering of the particles) slightly above atmospheric pressure and was situated in a magnetic field of about 500 gauss. When the lamina had a surface density of about 100 mg/cm² the groups of recoil electrons ascribed to single gamma-ray lines of energy 3 MV or less were found to have a width of about 1200 $H\rho$ at half-maximum value. Measurements have been taken on the following radioactive elements produced from their stable isotopes by deuteron bombardment in the magnetic resonance accelerator of Lawrence:

Element	*Energy of gamma-rays in MV*
Na^{24}	1.2, 2.3, 3.4
Cl	2.5 (weak), 2.0 (strong)
A^{41}	1.5

More exact values of the energies and relative intensities will be given at the meeting.

2. Further Data on the Energies of Beta-Rays Emitted from Artificially Produced Radioactive Bodies. F. N. D. KURIE, J. R. RICHARDSON AND H. C. PAXTON, *University of California.*—The upper energy limits of the β-spectra of N^{13}, Na^{24}, Si^{31}, P^{32}, Cl^{38}, K^{42} were reported by the present authors at the Washington meeting, April 1935. We have repeated all these data with the cloud chamber containing hydrogen instead of oxygen in order further to reduce the scattering of the tracks. The following new elements have also been measured: F^{17}, A^{41}. The radio-argon was made by Dr. A. H. Snell. With these new data on eight elements we have examined the agreement between them and the shape of the distribution curves suggested by the Fermi theory and also by the Konopinski-Uhlenbeck variation of the Fermi theory. We find that the Fermi theory does not fit the data at all and that the K–U theory fits very well but leads to a very high upper limit, due to its demanding a high order of contact with the energy axis. The table gives the values of the upper limit as deduced from the data by fitting a K–U curve to them and also that got from simple inspection.

Substance	Upper Limit *Inspection*	*K–U curves*	*Substance*	Upper Limit *Inspection*	*K–U curves*
$N^{13}+$	1.5 MV	1.8	P^{32}	1.3 MV	2.0
$F^{17}+$	2.1	2.4	Cl	4.8	1.5, 6.1
Na^{24}	1.85	2.0	A^{41}	2.7	1.7, 3.4
Si^{31}	1.85	2.0	K^{42}	3.5	1.4, 4.4

The K–U plots suggest that Cl, A and K are each emitting two groups of β-particles. These are apparently not associated with the γ-rays observed in these elements.

3. Mass of the Neutrino from the Disintegrations of Carbon by Deuterons. T. W. BONNER, L. A. DELSASSO, W. A. FOWLER AND C. C. LAURITSEN, *California Institute of Technology.*—The reactions

$$C_6^{12}+H_1^2 \rightarrow C_6^{13}+H_1^1+Q_1$$
$$C_6^{12}+H_1^2 \rightarrow N_7^{13}+n_0^1+Q_2$$
$$N_7^{13} \rightarrow C_6^{13}+e^+ +\mu+Q_3$$

are typical of a class of reactions in which disintegration proceeds along two lines, one leading to a heavy particle and a proton, the other to the same heavy particle and a neutron, a positron, and a neutrino. Assuming no γ-rays to be emitted in either of the carbon disintegrations and assuming the masses of the proton, neutron, and positron to be known we may determine the mass of the neutrino provided the disintegration energies of the above reactions are found. Since the mass of the neutrino is thought to be small, if not zero, it is necessary to determine all of the energies involved rather accurately and we have thought it desirable

to measure them under the same conditions. Our results are:

$Q_1 = 2.65 \pm 0.07$; $Q_2 = -0.37 \pm 0.03$; $Q_3 = 1.45 \pm 0.10$.

By using Feather's mass of the neutron (1.00859 ± 0.00011) the mass of the neutrino is calculated to be on the $0 = 16$ scale: $\mu = 0.00006 \pm 0.00017$.

4. High Altitude Measurements on the Energies of Cosmic-Ray Tracks. CARL D. ANDERSON, R. A. MILLIKAN AND SETH H. NEDDERMEYER, *California Institute of Technology.*—Ten thousand counter-actuated cosmic-ray photographs have been taken on Pike's Peak with the energy measuring apparatus previously used at sea level. The great majority of the tracks are similar in kind to those obtained at sea level. All but about 100 are lightly ionizing tracks such as we have ascribed to positive and negative electrons. Showers are more frequent and on the average larger than those found at sea level. The few heavily ionizing positive tracks are in general interpretable as protons produced by nuclear disintegration. We wish to acknowledge the aid given to these researches by the Carnegie Institution of Washington and the Union Oil Company of California.

5. Design of Six-Million-Volt Magnetic Resonance Accelerator Unit for the Berkeley Magnet. DONALD COOKSEY, F. N. D. KURIE AND ERNEST O. LAWRENCE, *University of California.*—The need in various branches of science for intense neutron sources over long periods of time and for large quantities of radioactive substances has made it desirable to develop the technical aspects of the magnetic resonance accelerator to deliver high intensity deuteron beams under the exacting conditions of continuous operation. With this in mind a new accelerating unit has been designed to produce a deuteron beam of slightly over 6 MV. The gain over the 5.2 MV attained with the accelerator in present use in our laboratory is accomplished by a ten percent increase of the radius of the final circular path available to the ion beam in its interaction with the accelerating field. It is expected that changes in the ion source filament arrangement, better water-cooling of the various parts of the system and an increase in the effective beam area will result in a marked increase in the present deuteron current of 20 microamperes. Several changes in mechanical and electrical design, suggested by the past two years experience with the present apparatus, have been incorporated with the expectation of gaining thoroughly reliable operation. It is hoped to test the performance of this new unit before the meetings. Its various features will be shown by slides and discussed in some detail.

6. Inter-relations of e, h/e and e/m. R. T. BIRGE, *University of California.*—With the now safe assumption that the grating wave-lengths of x-rays are correct, four points on the e_m diagram[1] are shifted to new values of m. With the additional safe assumption that e/m is approximately 1.7575×10^7, two of the four points are again shifted. The final results are—(1) six methods for determining h/e, with all six results consistent ($r_o/r_i = 0.68$) and with a weighted average $(1.37588 \pm 0.00027) \times 10^{-17}$, (2) four methods for e/m, all consistent ($r_o/r_i = 0.44$) with a weighted average $(1.75762 \pm 0.00026) \times 10^7$, (3) two methods for e, of which only one appears really precise (from λ of x-rays) with the result $(4.8029 \pm 0.0005) \times 10^{-10}$. These three observed results are *not* consistent, *if* Bohr's formula for the Rydberg constant is true. Thus each of the three quantities, as calculated from the other two, deviates from the observed result by over ten times the *sum* of the probable errors of the observed and calculated values. One of the three following assumptions seems necessary: (1) The Bohr formula is incorrect, (2) calcite is not a geometrically perfect crystal, (3) the measured e/m is only 136/137 of its true value (Bond and Eddington theory).

[1] Science **79**, 438 (1934).

7. Ionization by Neutral Atom Beams. ROBERT N. VARNEY, *University of California.*—The balanced space charge method, used in previous experiments[1] to study ionization by positive ion impact, was adapted to the study of ionization of a gas by its own neutral atoms. A neutral atom beam was produced by forming a positive gas ion beam and allowing the beam to become neutralized by passing through its own gas. This charge exchange process has been investigated in the past, and is known to be highly efficient. The accelerated neutrals then entered the space-charge cylinder where any ionization they produced in the gas could be observed. The minimum energy at which ionization began was determined by varying the initial energy of the positive ions which made the beam. Ionization was observed to begin at the following energies of neutrals:

Ne in Ne	74 volts	Kr in Kr	40 volts
A in A	48	Xe in Xe	35

No ionization was observed in helium or in nitrogen. These are the lowest energies yet observed for ionization by heavy bodies. At most, only half of this energy is available for ionization because momentum must be conserved. The available energy is thus:

Ne in Ne	37 volts	Kr in Kr	20 volts
A in A	24	Xe in Xe	17.5

These are very near to the true ionization potentials of the gases.

[1] R. N. Varney, Phys. Rev. **47**, 483 (1935).

8. Negative Terms and Broad Lines in the Neutral Calcium Spectrum. H. E. WHITE, *University of California.*—Among the known energy levels of neutral calcium, strontium, and barium there are a relatively small number of known levels which lie above the common series limit of the regular sharp, principal, diffuse, and fundamental series. Some of these *negative terms* combine with lower terms to give sharp spectrum lines, and others combine to give broad nebulous lines. In strontium, for example, the $4d\ 6p$, $^3F^\circ$ term, in a continuum of $5s\ mf$, $^3F^\circ$, is observed to combine with the lower $5s\ 4d$, ^3D to give rise to five nebulous lines. It has already been proposed that the diffuseness of the lines is due to auto-ionization. It is reasonable to suppose that these same transitions should be observed as broad lines in calcium. A careful search for such lines in the exact spectral region where they are predicted has failed to show any trace of them. This is interpreted to mean that

the levels are so broad that they spread out over the $4s\,mf$, $^1F^\circ$ continuum. If an atom is excited toward one of the $3d\,np$, $^1F^\circ$ states, where $n=5, 6, 7, \ldots$, it automatically goes over into the continuum and auto-ionizes. Combination lines for other predicted negative levels besides those identified by Russell have been looked for in calcium, but none have been identified.

9. Transmutation of Platinum by Deuterons: A Resonance Phenomenon. J. M. CORK AND E. O. LAWRENCE, *University of California.*—We have observed that platinum is rendered radioactive by bombardment with deuterons of energies above 3 MV. There are four distinct induced activities having half-lives of 28 min., 49 min., 8.51 hrs. and 14.5 hrs. Wilson cloud chamber observations show that the disintegration electrons are both + and − in sign and chemical tests show that the active substances are noble metals, iradium and platinum. As deuterons of such low energy would not be expected theoretically to react to such an extent with the highly charged platinum nucleus, the transmutation function for the induced radioactivity was determined. A stack of thin (5-mm stopping power) platinum foils was bombarded with several microamperes of 5 MV deuterons for a few hours and the activities induced in the individual foils were compared. These measurements showed that the transmutation function does not rise monotonically with deuteron energy but exhibits sharp maxima and minima characteristic of resonance effects. For the short period activity the maxima occur at 4.0, 4.35 and 4.5 MV while for the long period activity the maxima are at approximately 3.7, 4.3 and 4.5 MV. These observations are interpreted as indicating resonance penetration of the platinum nucleus by deuterons.

10. Absolute Values of the Electron Mobility in Hydrogen. NORRIS E. BRADBURY AND RUSSELL A. NIELSEN, *Stanford University.*—A new method is described for the measurement of electron mobilities in gases. An electrical shutter method is employed in which the shutters take the form of two fine wire grids, alternate wires of which are connected to a high frequency alternating potential. Electrons pass through the grids only when the potential between adjacent grid wires is zero, and only electrons which cross the gas space in one-half cycle are received at the collecting electrode. A sharp maximum is thus observed in the electrometer current when the drift velocity of the electron multiplied by the time of one-half cycle is equal to the distance between the grids. The theoretical shape of the current curve is compared with experiment and good agreement observed. Measurements have been made between X/p of 0.03 and 20, and the values obtained are compared with the Compton mobility equation. The existence of inelastic impacts for electrons of low energy (1–3 volts) seems highly probable.

11. Progress on a Deflection Determination of (e/m). FRANK G. DUNNINGTON,* *California Institute of Technology.*—Work instigated at the University of California[1] and continued in Pasadena has progressed to the point where final observations are being started. Characteristic probably of most experimental investigations when pursued far enough, the initially observed simple phenomenon has been found to be affected by various secondary phenomena. The first phase of the observational work has been concerned with a study of these and the conditions necessary for their elimination. In the second phase the taking of final observations will be made with a series of varying conditions in such a way as to experimentally determine, if possible, the necessary correction to the angular path of the electrons. A more exact mathematical analysis than that presented in the earlier work is also being made but the assumptions necessary to give a solvable problem make an experimental determination desirable.

* Carried out under grant from the American Philosophical Society.
[1] F. G. Dunnington, Phys. Rev. **43**, 404 (1933).

12. Mass-Ratio of the Lithium Isotopes. F. A. JENKINS, *University of California,* AND ANDREW MCKELLAR, *Dominion Astrophysical Observatory.*—Almy and Irwin[1] have determined the mass-ratio given by the isotope effect in the red band system of Li_2. Their conclusions are tested by new measurements of this system on plates taken with the 35-ft., 30,000 line/in.-grating at the Massachusetts Institute of Technology. The bands 5,0 to 0,0 of the $v',0$ progression and 0,0 to 0,4 of the $0,v''$ progression, as well as 1,1, were measured for both the main and isotopic systems. The vibrational and rotational constants were evaluated by methods previously used by one of us for the blue-green system. The most accurate values found for the isotopic mass-coefficient ρ are $\omega_e''^{6}/\omega_e' = 1.04100$ and $\omega_e'^{6}/\omega_e'' = 1.04107$, compared with the values 1.04141 previously obtained from the blue-green system. Almy and Irwin obtained 1.04077, agreeing exactly with the mass-spectrum value. Our new values have a much greater accuracy than those from the blue-green system, because of the higher dispersion and the elimination of blends, which introduced systematic errors in the earlier results. The difference between the new values and those of Almy and Irwin is ascribed to the method of handling the data, our method having the advantage of directness and emphasis on the states of lower vibrational quantum number, where complications are less likely to be important. Full details will be published, probably in the *Publications of the Dominion Astrophysical Observatory.*

[1] Almy and Irwin, Phys. Rev. **48**, 104 (193

13. Neutrons from the Disintegration of Deuterium by Deuterons. W. M. BRUBAKER AND T. W. BONNER,* *California Institute of Technology.*—The excitation functions for the emission of neutrons from the two reactions $_1H^2 + {}_1H^2 \rightarrow {}_2He^3 + {}_0n^1$ and $_4Be^9 + {}_1H^2 \rightarrow {}_5B^{10} + {}_0n^1$ have been investigated in the energy range of from 0.5 to 0.9 MEV. In this interval the yield of neutrons from a $H_3^2PO_4$ target increases linearly with the bombarding energy while the yield from a Be target increases nearly exponentially. At 0.9 MEV three times as many neutrons were observed from the Be target as from the $H_3^2PO_4$ target. At 0.5 MEV only 1/3 as many neutrons came from the Be as from the $H_3^2PO_4$. The neutrons from deuterium were found to be nearly homogeneous in energy with a maximum of 2.55 MEV when they are observed at right angles to the direction of the incident 0.5-MEV deuterons. The energy of the disintegration is 3.21 ± 0.13 MEV.

* National Research Fellow.

14. Passage of X-Rays Through Oscillating Crystals. R. M. LANGER, *California Institute of Technology.*—The distortions suffered by crystals subjected to piezoelectric oscillations not only broaden the band of wave-lengths the crystal can reflect into a particular spot of a Laue pattern but they widen the cone of reflected light as well. This is the now generally accepted explanation of the enhancement of Laue patterns by piezoelectric oscillations first observed by Fox and Carr.[1] To observe the widening of the spots it is necessary to use a well collimated beam of x-rays. An extension of the original theory[2] shows the necessity of taking into account the reflections from the reflected beams back into the initial direction. Because of the inhomogeneous distortions of the piezoelectric crystal the multiply-reflected portion of the beam will be even more widened than the singly reflected portions. This means that the central spot will be enlarged by contributions from all the other spots. These contributions will amount to a very small fraction of the direct beam intensity but since they appear outside the completely fogged normal spot they make it appear appreciably enhanced. This may be the interpretation of the curious observation reported by Fox and Fraser.[3] The results of Jauncey and Deming[4] are not inconsistent with Fox and Fraser's experiments when the present theory is taken into account.

[1] Fox and Carr, Phys. Rev. **37**, 1622 (1931).
[2] R. M. Langer, Phys. Rev. **38**, 573 (1931).
[3] Fox and Fraser, Phys. Rev. **47**, 899 (1935).
[4] Jauncey and Deming, Phys. Rev. **48**, 462 (1935).

15. Positrons from Deuteron Activated Phosphorus. H. G. PAXTON (*Introduced by E. O. Lawrence*), *University of California.*—Phosphorus activated through deuteron bombardment was investigated in a cloud chamber traversed by a magnetic field. Absorbing screens were placed in the chamber in such a fashion that a definite region was primarily available to positrons. Just after the short contamination periods had died out, about one positron was observed for every fifty electrons from P^{32}. The relative numbers of positrons per expansion on series of photographs scattered over more than a week indicate a half-life of 50 ± 10 hours. Consequently these positrons are neither associated with the electron decay of P^{32}, nor do they arise from any known contaminant. The energy distribution appears to have the form of a disintegration spectrum with its upper limit at about 0.9 MV. Chemical tests to identify this positive activity are in progress.

16. The Calculation of Binding Energies in Light Nuclei. WILLIAM V. HOUSTON, *California Institute of Technology.*—If the forces between the nuclear constituents are proportional to the distances between them, the energy levels can be easily calculated by using normal coordinates. If the functions for the ground state in this model are taken as approximate functions with one variable parameter, the energy of the ground state can be computed on the assumption that the force between protons and neutrons is harmonic out to a given distance and then becomes zero. The correction to the function necessary to minimize the energy is relatively small, which lends support to the belief that the approximation functions are rather good. From the masses of H^2, H^3, and He^4 rather narrow limits can be set to the parameters of the force.

17. Radioactivities of Zinc under Deuteron Bombardment. J. J. LIVINGOOD, *University of California.*—When zinc is bombarded with 4-MEV deuterons, a radioactivity is induced exhibiting several periods. The decay curve can be analyzed into components with half-lives of approximately 100 hours, 15 hours and 1 hour, with the possibility of a shorter period of some minutes. Chemical analysis indicates that the active bodies are zinc isotopes, suggesting that the disintegration is of the Oppenheimer-Phillips type, wherein the neutron of the deuteron is captured. The excitation functions rise rapidly after a threshold near 1.5 MEV, and are sufficiently different from that of sodium bombarded by deuterons to assure that the 15-hour activity is not due to sodium contamination.

18. Spray Electrification. SEVILLE CHAPMAN (*Introduced by L. B. Loeb*), *University of California.*—Preliminary to a study of nonaqueous polar liquids, the mobility spectrum of spray electrified salt solutions has been investigated with an Erickson mobility tube under conditions of high resolving power. In general, the curves of electrometer deflection against mobility show no charged carriers with mobility above 1.6 cm/sec. per volt/cm. About this mobility the curve rises sharply to a roughly constant value with a general broad maximum band in the region 0.05 cm/sec. per volt/cm, and then gradually decreases to zero. Superposed on this "background" *striking* peaks were observed. Negative and positive groups for solutions indicated are shown below. The first number represents approximate mobility in cm/sec. per volt/cm. The letter indicates roughly the strength of the peak with respect to the "background." VS, very strong; S, strong; M, medium; W, weak. The next number indicates relative electrometer deflection.

	Negative			Positive		
Solution	*A*	*B*	*C*	*A'*	*B'*	*C'*
4×10^{-2}N KCl	1.2 W 0.6	0.7 M 1.7		1.1 W 0.5	0.6 M 1.9	
4×10^{-3}N KCl	1.2 W 4	0.5 S 8		1.1 W 3	0.4 M 7	
4×10^{-4}N KCl	1.2 M 9	0.4 S 13		1.0 W 8	0.4 VS 15	
4×10^{-5}N KCl	1.2 S 14	0.36 M 15			0.4 VS 18	
4×10^{-6}N LiCl	1.2 S 11	0.4 M 13		1.0 W 7	0.4 VS 17	
4×10^{-6}N NaI	1.2 S 10	0.36 M 14		1.0 M 7	0.4 VS 20	
4×10^{-4}N KCl	1.2 VS 12	0.3 W 8	0.2 W 10		0.4 S 9	0.2 W 9
Distilled Water	1.2 VS 11	0.3 W 6	0.2 M 9		0.5 M 6	0.22 W 7

19. Electric Influence of the Active Region of the Sun. FERNANDO SANFORD, *Stanford University.*—In the August, 1935, number of *Publications of the Astronomical Society of the Pacific* it was shown that there is a local region of high solar activity and a corresponding region of low solar activity on opposite sides of the sun. These regions are shown to have crossed the sun's central meridian at successive intervals of 27.25 days during two periods of 80 solar rotations each, including two periods of maximum sun-spot activity. It is the purpose of this paper to inquire if the electrical influence of solar activity upon the earth varies with the rotation period of the sun. Five different sets of observations of terrestrial electric phenomena have been compared with the variation of solar activity as shown by relative sun-spot numbers. These consist of daily range of variation of earth potential at Palo Alto, daily range of N–S earth-current variation, daily maximum of

N-S earth-currents, character figures of atmospheric potential curves and missing days in earth-current records, all at Ebro Observatory. In all five cases there are indications of a 27.25-day period in phase with the variation of solar activity.

20. Kinematics and World Structure, II. H. P. ROBERTSON, *Princeton University.*—It has been shown previously that any cosmological theory in which the nebulae are considered as particles in homogeneous flow leads automatically to a space-time line-element whose formal properties are identical with those of the metric on which the general relativistic theory is based. This investigation is here continued with an examination of the equations of motion of test particles in such a universe; these are shown to involve a single unknown function, and the problem of their integration is reduced to the solution of a single ordinary differential equation. The acceleration function implied by various gravitational theories is determined, and the properties of the motion discussed.

21. Artificial Radioactivity Induced in Arsenic, Nickel and Cobalt under Deuteron Bombardment. R. L. THORNTON, *University of California.*—*Arsenic.* A layer of arsenic, sublimed on aluminum, was bombarded with 4.3-MEV deuterons. Observations showed the presence of two additional active substances. Of these, the shorter period effect (2.5 hours) can be ascribed to silicon impurity in the aluminum base. The longer period of 27 ± 1 hours has been shown by Fermi and his collaborators to be due to As^{76}. Strong γ-rays accompany this activity. Rough absorption measurements in lead and copper show these to be considerably less energetic than those of radio-sodium. Absorption measurements have been carried out on the disintegration electrons. These indicate a maximum energy of about 1.5 MEV. *Nickel.* A stack of nickel foils 0.001 inch in thickness was bombarded with 5.2-MEV deuterons. Periods of 10 minutes and $3.5+.1$ hours were observed. Plotting the activities against the deuteron range a differential excitation curve was obtained for the longer period. This gives a linear relation between yield and range for deuteron energies greater than 3 MEV. The short period activity observed is probably due to carbon contamination. The chemical tests have not yet been carried out. *Cobalt.* Activities of at least three periods were observed from a cobalt target bombarded with 4.3-MEV deuterons. These were 10 minutes, 3.6 hours and one or more weak activities of period longer than a day. The 10-minute activity can almost certainly be ascribed to carbon contamination. The 3.6-hour effect may be due to the same active isotope as the one of like period observed in nickel. The relative intensities of the effects observed make Ni impurity as a cause improbable.

22. The Transmutation of Argon by Deuterons. ARTHUR H. SNELL, *University of California.*—When bombarded with high speed deuterons, argon gas is found to yield a radioactive product which emits negative electrons, and decays with a period of 10 ± 1 minutes. Chemical tests show that the activity is due to an isotope of argon, and the reaction is probably $A^{40}+H^2=A^{41}+H^1$. Absorption measurements of the β-particles indicate that their maximum energy is about 1.1 MV. This is in satisfactory agreement with the results of a cloud-chamber study of their energy-distribution curve, which shows an upper limit at about 1.8 MV, although there is some indication of a second group of low intensity and higher energy. The radioactivity is accompanied by the emission of a γ-ray, the energy of which is 1.5 MEV, as measured by the energies of its Compton recoils in a cloud chamber. The excitation curve for the radioactivity has also been studied. It favors the Oppenheimer-Phillips theory for this type of reaction, rather than the Gamow theory of the penetration of the potential barrier by a charged particle. Formation of A^{41} starts when the deuteron energy reaches 2 MEV.

23. Optical Changes in Freshly Evaporated Al-Mg Films. HIRAM W. EDWARDS AND ROBERT P. PETERSEN, *University of California at Los Angeles.*—This paper deals with a study of reflection and transmission characteristics of freshly evaporated films of an Al-Mg alloy. Apparatus was arranged inside of an evaporation chamber so measurements could be made during and after deposition of the metallic film. Three types of changes in reflection and transmission coefficients were observed: (1) Occurring at pressures of 10^{-4} mm or less. This consists of a small, rapid decrease in reflectivity and increase in transmissivity. One minute is required for this change. The transmission coefficient alters more rapidly than the reflection coefficient. No further effect takes place in the vacuum. (2) The second type occurs during admission of air or nitrogen into the vacuum chamber. It consists of decrease in reflectivity and increase in transmissivity. The rate of change is definitely dependent upon the rate of increase of pressure in the vacuum chamber. (3) This type takes place very slowly, over a period of several days. The final value of the reflection or transmission coefficient is approached asymptotically. The magnitudes of the three types of changes for a film having an initial reflection coefficient of 58 percent were observed to be 8 percent, 5 percent, and 10 percent, respectively; and for another film having an initial transmission coefficient of 35 percent were 5 percent, 8 percent, and 5 percent.

24. On the Figuring and Correcting of Mirrors by Controlled Deposition of Aluminum. JOHN STRONG AND E. GAVIOLA, *California Institute of Technology.*—By controlled deposition of metals, evaporated in vacuum, it is possible to change the figure of reflecting surfaces quantitatively. The theory for calculating screens and the experimental technique are described. A spherical 12-inch mirror has been repeatedly parabolized, obtaining a surface perfect within 1/20 of a wave-length. A 5½-inch spherical mirror has been parabolized with the optical axis outside of its periphery. A defective parabolic mirror was corrected of turned up and down edges and asymmetric zones. A convex spherical Cassegrain mirror was hyperbolized. The possible applications and the limitations of the method are discussed.

25. Electric Force *versus* Centrifugal Force. CHARLES T. DOZIER, *Redding, California.*—Revolution of a tungar-type vacuum tube about an external axis, with plate-to-

14. Passage of X-Rays Through Oscillating Crystals. R. M. LANGER, *California Institute of Technology.*—The distortions suffered by crystals subjected to piezoelectric oscillations not only broaden the band of wave-lengths the crystal can reflect into a particular spot of a Laue pattern but they widen the cone of reflected light as well. This is the now generally accepted explanation of the enhancement of Laue patterns by piezoelectric oscillations first observed by Fox and Carr.[1] To observe the widening of the spots it is necessary to use a well collimated beam of x-rays. An extension of the original theory[2] shows the necessity of taking into account the reflections from the reflected beams back into the initial direction. Because of the inhomogeneous distortions of the piezoelectric crystal the multiply-reflected portion of the beam will be even more widened than the singly reflected portions. This means that the central spot will be enlarged by contributions from all the other spots. These contributions will amount to a very small fraction of the direct beam intensity but since they appear outside the completely fogged normal spot they make it appear appreciably enhanced. This may be the interpretation of the curious observation reported by Fox and Fraser.[3] The results of Jauncey and Deming[4] are not inconsistent with Fox and Fraser's experiments when the present theory is taken into account.

[1] Fox and Carr, Phys. Rev. **37**, 1622 (1931).
[2] R. M. Langer, Phys. Rev. **38**, 573 (1931).
[3] Fox and Fraser, Phys. Rev. **47**, 899 (1935).
[4] Jauncey and Deming, Phys. Rev. **48**, 462 (1935).

15. Positrons from Deuteron Activated Phosphorus. H. G. PAXTON (*Introduced by E. O. Lawrence*), *University of California.*—Phosphorus activated through deuteron bombardment was investigated in a cloud chamber traversed by a magnetic field. Absorbing screens were placed in the chamber in such a fashion that a definite region was primarily available to positrons. Just after the short contamination periods had died out, about one positron was observed for every fifty electrons from P^{32}. The relative numbers of positrons per expansion on series of photographs scattered over more than a week indicate a half-life of 50 ± 10 hours. Consequently these positrons are neither associated with the electron decay of P^{32}, nor do they arise from any known contaminant. The energy distribution appears to have the form of a disintegration spectrum with its upper limit at about 0.9 MV. Chemical tests to identify this positive activity are in progress.

16. The Calculation of Binding Energies in Light Nuclei. WILLIAM V. HOUSTON, *California Institute of Technology.*—If the forces between the nuclear constituents are proportional to the distances between them, the energy levels can be easily calculated by using normal coordinates. If the functions for the ground state in this model are taken as approximate functions with one variable parameter, the energy of the ground state can be computed on the assumption that the force between protons and neutrons is harmonic out to a given distance and then becomes zero. The correction to the function necessary to minimize the energy is relatively small, which lends support to the belief that the approximation functions are rather good. From the masses of H^2, H^3, and He^4 rather narrow limits can be set to the parameters of the force.

17. Radioactivities of Zinc under Deuteron Bombardment. J. J. LIVINGOOD, *University of California.*—When zinc is bombarded with 4-MEV deuterons, a radioactivity is induced exhibiting several periods. The decay curve can be analyzed into components with half-lives of approximately 100 hours, 15 hours and 1 hour, with the possibility of a shorter period of some minutes. Chemical analysis indicates that the active bodies are zinc isotopes, suggesting that the disintegration is of the Oppenheimer-Phillips type, wherein the neutron of the deuteron is captured. The excitation functions rise rapidly after a threshold near 1.5 MEV, and are sufficiently different from that of sodium bombarded by deuterons to assure that the 15-hour activity is not due to sodium contamination.

18. Spray Electrification. SEVILLE CHAPMAN (*Introduced by L. B. Loeb*), *University of California.*—Preliminary to a study of nonaqueous polar liquids, the mobility spectrum of spray electrified salt solutions has been investigated with an Erickson mobility tube under conditions of high resolving power. In general, the curves of electrometer deflection against mobility show no charged carriers with mobility above 1.6 cm/sec. per volt/cm. About this mobility the curve rises sharply to a roughly constant value with a general broad maximum band in the region 0.05 cm/sec. per volt/cm, and then gradually decreases to zero. Superposed on this "background" *striking* peaks were observed. Negative and positive groups for solutions indicated are shown below. The first number represents approximate mobility in cm/sec. per volt/cm. The letter indicates roughly the strength of the peak with respect to the "background." VS, very strong; S, strong; M, medium; W, weak. The next number indicates relative electrometer deflection.

	Negative			Positive		
Solution	*A*	*B*	*C*	*A'*	*B'*	*C'*
4×10^{-3}N KCl	1.2 W 0.6	0.7 M 1.7		1.1 W 0.5	0.6 M 1.9	
4×10^{-2}N KCl	1.2 W 4	0.5 S 8		1.1 W 3	0.4 M 7	
4×10^{-1}N KCl	1.2 M 9	0.4 S 13		1.0 W 8	0.4 VS 15	
4×10^{0}N KCl	1.2 S 14	0.36 M 15			0.4 VS 18	
4×10^{-1}N LiCl	1.2 S 11	0.4 M 13		1.0 W 7	0.4 VS 17	
4×10^{-1}N NaI	1.2 S 10	0.36 M 14		1.0 M 7	0.4 VS 20	
4×10^{-1}N KCl	1.2 VS 12	0.3 W 8	0.2 W 10		0.4 S 9	0.2 W 9
Distilled Water	1.2 VS 11	0.3 W 6	0.2 M 9		0.5 M 6	0.22 W 7

19. Electric Influence of the Active Region of the Sun. FERNANDO SANFORD, *Stanford University.*—In the August, 1935, number of *Publications of the Astronomical Society of the Pacific* it was shown that there is a local region of high solar activity and a corresponding region of low solar activity on opposite sides of the sun. These regions are shown to have crossed the sun's central meridian at successive intervals of 27.25 days during two periods of 80 solar rotations each, including two periods of maximum sun-spot activity. It is the purpose of this paper to inquire if the electrical influence of solar activity upon the earth varies with the rotation period of the sun. Five different sets of observations of terrestrial electric phenomena have been compared with the variation of solar activity as shown by relative sun-spot numbers. These consist of daily range of variation of earth potential at Palo Alto, daily range of N–S earth-current variation, daily maximum of

N–S earth-currents, character figures of atmospheric potential curves and missing days in earth-current records, all at Ebro Observatory. In all five cases there are indications of a 27.25-day period in phase with the variation of solar activity.

20. Kinematics and World Structure, II. H. P. ROBERTSON, *Princeton University.*—It has been shown previously that any cosmological theory in which the nebulae are considered as particles in homogeneous flow leads automatically to a space-time line-element whose formal properties are identical with those of the metric on which the general relativistic theory is based. This investigation is here continued with an examination of the equations of motion of test particles in such a universe; these are shown to involve a single unknown function, and the problem of their integration is reduced to the solution of a single ordinary differential equation. The acceleration function implied by various gravitational theories is determined, and the properties of the motion discussed.

21. Artificial Radioactivity Induced in Arsenic, Nickel and Cobalt under Deuteron Bombardment. R. L. THORNTON, *University of California.*—*Arsenic.* A layer of arsenic, sublimed on aluminum, was bombarded with 4.3-MEV deuterons. Observations showed the presence of two additional active substances. Of these, the shorter period effect (2.5 hours) can be ascribed to silicon impurity in the aluminum base. The longer period of 27 ± 1 hours has been shown by Fermi and his collaborators to be due to As^{76}. Strong γ-rays accompany this activity. Rough absorption measurements in lead and copper show these to be considerably less energetic than those of radio-sodium. Absorption measurements have been carried out on the disintegration electrons. These indicate a maximum energy of about 1.5 MEV. *Nickel.* A stack of nickel foils 0.001 inch in thickness was bombarded with 5.2-MEV deuterons. Periods of 10 minutes and $3.5+.1$ hours were observed. Plotting the activities against the deuteron range a differential excitation curve was obtained for the longer period. This gives a linear relation between yield and range for deuteron energies greater than 3 MEV. The short period activity observed is probably due to carbon contamination. The chemical tests have not yet been carried out. *Cobalt.* Activities of at least three periods were observed from a cobalt target bombarded with 4.3-MEV deuterons. These were 10 minutes, 3.6 hours and one or more weak activities of period longer than a day. The 10-minute activity can almost certainly be ascribed to carbon contamination. The 3.6-hour effect may be due to the same active isotope as the one of like period observed in nickel. The relative intensities of the effects observed make Ni impurity as a cause improbable.

22. The Transmutation of Argon by Deuterons. ARTHUR H. SNELL, *University of California.*—When bombarded with high speed deuterons, argon gas is found to yield a radioactive product which emits negative electrons, and decays with a period of 10 ± 1 minutes. Chemical tests show that the activity is due to an isotope of argon, and the reaction is probably $A^{40}+H^2=A^{41}+H^1$. Absorption measurements of the β-particles indicate that their maximum energy is about 1.1 MV. This is in satisfactory agreement with the results of a cloud-chamber study of their energy-distribution curve, which shows an upper limit at about 1.8 MV, although there is some indication of a second group of low intensity and higher energy. The radioactivity is accompanied by the emission of a γ-ray, the energy of which is 1.5 MEV, as measured by the energies of its Compton recoils in a cloud chamber. The excitation curve for the radioactivity has also been studied. It favors the Oppenheimer-Phillips theory for this type of reaction, rather than the Gamow theory of the penetration of the potential barrier by a charged particle. Formation of A^{41} starts when the deuteron energy reaches 2 MEV.

23. Optical Changes in Freshly Evaporated Al-Mg Films. HIRAM W. EDWARDS AND ROBERT P. PETERSEN, *University of California at Los Angeles.*—This paper deals with a study of reflection and transmission characteristics of freshly evaporated films of an Al-Mg alloy. Apparatus was arranged inside of an evaporation chamber so measurements could be made during and after deposition of the metallic film. Three types of changes in reflection and transmission coefficients were observed: (1) Occurring at pressures of 10^{-4} mm or less. This consists of a small, rapid decrease in reflectivity and increase in transmissivity. One minute is required for this change. The transmission coefficient alters more rapidly than the reflection coefficient. No further effect takes place in the vacuum. (2) The second type occurs during admission of air or nitrogen into the vacuum chamber. It consists of decrease in reflectivity and increase in transmissivity. The rate of change is definitely dependent upon the rate of increase of pressure in the vacuum chamber. (3) This type takes place very slowly, over a period of several days. The final value of the reflection or transmission coefficient is approached asymptotically. The magnitudes of the three types of changes for a film having an initial reflection coefficient of 58 percent were observed to be 8 percent, 5 percent, and 10 percent, respectively; and for another film having an initial transmission coefficient of 35 percent were 5 percent, 8 percent, and 5 percent.

24. On the Figuring and Correcting of Mirrors by Controlled Deposition of Aluminum. JOHN STRONG AND E. GAVIOLA, *California Institute of Technology.*—By controlled deposition of metals, evaporated in vacuum, it is possible to change the figure of reflecting surfaces quantitatively. The theory for calculating screens and the experimental technique are described. A spherical 12-inch mirror has been repeatedly parabolized, obtaining a surface perfect within 1/20 of a wave-length. A $5\frac{1}{2}$-inch spherical mirror has been parabolized with the optical axis outside of its periphery. A defective parabolic mirror was corrected of turned up and down edges and asymmetric zones. A convex spherical Cassegrain mirror was hyperbolized. The possible applications and the limitations of the method are discussed.

25. Electric Force *versus* Centrifugal Force. CHARLES T. DOZIER, *Redding, California.*—Revolution of a tungar-type vacuum tube about an external axis, with plate-to-

filament gap radial, alters the plate current at constant plate potential and filament temperature in direction opposed to that hitherto expected from the action of centrifugal force on "positive-mass" electrons in the gap. By postulating the electric current in the gap to consist of a one-to-one exchange of electrons and more massive positive particles, the plate current changes agree, in direction, with observation. Quantitatively there is wide variance. With plate radially outward and sufficient excess voltage to maintain constant plate current against the resultant of centrifugal force on electrons and postulated positive particles in the gap, the ratio of these forces in dynes at varying speeds approximates the number 2.2×10^3. The electric force, in dynes, is the larger. It is noticed that the ratio of this number, (2.19×10^3), to the velocity of light is 137 cm/sec., the fine-structure constant of wave mechanics. The dimensions of the fine-structure constant $hc/2\pi e^2$ are those of $1/\kappa$ and $(L^2/T^2)\mu$. These dimensions agree with the above result when both κ and μ have dimensions of the velocity invert T/L. Then, in dimensions, $1/\kappa\mu = L^2/T^2$.

26. The Spectra of Sa II and Gd I. WALTER ALBERTSON, *National Research Fellow, Mount Wilson Observatory.*—With the use of King's data the major portion of the spectrum of Sa II has been classified (1200 lines). The normal state is $4f^6(^7F)\cdot6s\,^8F$, 1500 cm^{-1} above it is found ^6F from the same configuration. The multiplet intervals are almost identical with those of ^7F of Sa I. Approximately 10,000 cm^{-1} above ^8F is the pentad $4f^6(^7F)\cdot5d\,^8HGFDP$, which, except for $^8G_{\frac{1}{2}}$, $^8F_{\frac{1}{2}}$, has been completely found. No violent overlapping or perturbations occur among the multiplets. The triads $4f^6(^7F)\cdot6p\,^8GFD^0$, $^6GFD^0$ have been tentatively picked out. About 200 other middle odd levels are believed to be due to $4f^65d6s$. The transition $6p-6s$, built on parent ^7F, accounts for nearly every intense line from 5000A to 4200A, and $6p-5d$ nearly every line from 9000A to 5500A. The lines from 4200A to 2900A belong mostly to $4f^65d6s-4f^6(^7F)\cdot6s$. The transition $4f^65d6s-4f^6(^7F)\cdot5d$ is represented by only a few lines, all weak. Zeeman effect measurements and additional data for fainter lines are being obtained by King and the writer. The $^7D^0$ multiplet from $4f^7(^8S^0)\cdot5d6s$, of Gd I has been found at about 6000 cm^{-1} above the normal state, $^9D^0$, from the same configuration. Numerous intense combinations in the orange and red have been classified as combinations to the ground levels, the upper levels being tentatively assigned to $4f^7(^8S^0)6s5d6p\,^{11}FDP$.

27. Transmutation Functions at High Bombarding Energies. HENRY W. NEWSON, *University of California.*—The transmutation functions of the reactions:

$$C^{13}+D^2=N^{13}+N^1,\quad N^{14}+D^2=O^{15}+N^1,$$
$$O^{16}+D^2=F^{17}+N^1$$

have been measured for bombarding energies up to 5 MV. The deuteron beam was passed through a stack of 10 platinum foils, spaced about 3 mm apart in an atmosphere of the gas under investigation. The number of recoil atoms deposited was determined by measuring the activities of the foils with an electroscope. By knowing the stopping power of the gas and of the foils the excitation curve may be plotted. The excitation curves of the three elements showed the rapid initial rise which is to be expected, and then became nearly flat. The bombarding energy at the beginning of the flat portion of the curve is presumably the energy corresponding to the top of the potential barrier. The values for the top of the potential barriers so estimated are 3.3, 3.7 and 3.8 MV for carbon, oxygen and nitrogen, respectively. These values are probably high since no correction was made for the variation of the mean forward range of the radioactive recoil atoms with the bombarding energy. Although the form of this correction is not known, its effect will be to cause the excitation curve to flatten at lower energies and to fall off thereafter as the bombarding energy is increased.

28. The Radiations Emitted by Radio-Aluminum. J. M. CORK, J. R. RICHARDSON AND F. N. D. KURIE, *University of California.*—Radio-aluminum (Al^{28}) is formed from ordinary aluminum when the latter is bombarded by high speed deuterons. This substance can be made in several other ways, and is known to emit both β- and γ-rays. The half-life measured by either of these radiations is the same (2.6 min.). The γ-rays have been studied in a Wilson cloud chamber by measuring the curvatures produced by a known magnetic field on the secondary electrons ejected from a thin glass lamina suspended in the chamber. The electrons are distributed over a range of energies corresponding to what would be expected under these conditions for a monochromatic γ-ray. The energy of this γ-ray is 2.3 MV. The β-ray spectrum is a typical continuous distribution. If the data are considered alone an upper limit of 3.3 MV is indicated, but if the data have a Konopinski-Uhlenbeck curve fitted to them an upper limit of 3.7 MV is found.

29. On a Mechanical Method for Computing the Energy Values to be Associated with a Fork in a Cloud Chamber Caused by the Disintegration of a Nucleus by a Neutron. F. N. D. KURIE AND J. J. LIVINGOOD, *University of California.*—The tedium of computing and rechecking the energies associated with the two visible disintegration particles and the neutron, when a reaction of the type $N^{14}+n^1=B^{11}+He^4$ is observed in a cloud chamber, can be greatly relieved by mechanical means. Such a mechanical device has been constructed. It consists of two arms pivoted at one end bearing scales on which both energy and range are marked at distances from the pivot which are proportional to the momentum of the appropriate particle. Sliders on these arms carry a third arm and pointers. The two sliders are set at the observed ranges of the two disintegration particles and the arms swung on their pivots to the angle between the tines of the fork. The energy of the impinging neutron is read on the third arm and that of each of the observed particles on the other arms. Since the angle between the tines of the fork is not measured directly from the cloud chamber photographs it is computed separately on a sphere from the observed altitude and azimuth of each tine. With this device the complete analysis of a disintegration fork is accomplished in about two minutes as against the twenty to thirty required for the longhand computations.

30. The Measurement of Gamma-Ray Energies with a Cloud Chamber. J. R. RICHARDSON AND F. N. D. KURIE, *University of California.*—The only reliable method of measuring γ-ray energies is by the use of a cloud chamber traversed by a magnetic field. The curvature of the tracks of secondary electrons from the radiator is measured. From a frequency distribution of the tracks in radius (strictly in $H\rho$) one estimates the energy of the γ-ray. This work tests the resolution and defines criteria for a homogeneous γ-ray. For radiators composed of light elements, one may neglect photoelectrons and pair production and consider only Compton electrons. The relative numbers of electrons ejected at various angles may be computed from the Klein-Nishina formula. For any given angular range (here taken as within 10°) of the direction of the γ-ray, one may calculate the distribution in energy of the electrons emerging from various depths in the radiator from the known data on the straggling of β-particles. Thus curves can be constructed which show the energy distribution of these secondary electrons for various thicknesses of radiator. One finds from such an analysis that the best conditions are attained by the use of a thin lamina of the order of 100 mg/cm² thick and using only such tracks as emerge within an angle of about 10° with the γ-ray. In this way peaks whose half-width is about 300 kv can be got for each homogeneous γ-ray (provided the energy is of the order of 3 MV).

31. X-Ray Double Spectrometer with Stationary Source and Ion Chamber. PAUL KIRKPATRICK AND P. A. ROSS, *Stanford University.*—The desirable features of a stationary x-ray source and ion chamber are obtained by mounting both crystals on a common base plate which is movable along horizontal ways bisecting perpendicularly the line joining the target (or other x-ray source) and the center of the ion chamber. The crystal tables are coupled together by a steel tape so that they may be rotated simultaneously in opposite directions about the central verticals of their reflecting faces by a precision Nicholas screw. The detecting chamber is mechanically coupled to the base plate of the crystals so that the chamber points toward B crystal at all times. There is no wandering of the reflecting area of the crystals with variation of θ. The precision of the linear motion of the crystals plays no part in the ultimate wave-length precision of the instrument. Kinematic design of crystal holders makes it possible to remove crystals from the instrument and on replacement to repeat previous observations immediately within a fraction of one second in θ. For measuring ion currents the spectrometer is equipped with both an electrometer-tube circuit and a Hoffman electrometer.

32. Zeeman Effects in the Spectrum of Sa II. WALTER ALBERTSON AND A. S. KING, *Mount Wilson Observatory.*—Measurements of the n components of 300 lines of Sa II have been obtained. A field of 31,100 gauss and a dispersion of 1.86A per mm was used. Many of the patterns are completely resolved. The results show that the low levels of Sa II have surprisingly good *LS* coupling, while the high levels must be greatly perturbed.

normal state $4f^6(^7F)\cdot 6s\ ^8F$	$G_{exp.}$	G_{theory}
$^8F_1$	3.92	4.00
3/2	2.00	2.00
5/2	1.72	1.71
7/2	1.62	1.62
9/2	1.58	1.58

33. The Infrared Absorption Spectra of Water and Alcohols in Nonpolar Solvents. E. L. KINSEY AND J. W. ELLIS, *University of California at Los Angeles.*—The infrared absorption of solutions of water and some of the alcohols in carbon disulfide and carbon tetrachloride has been studied in the 1.0–2.5μ region for the purpose of comparing the absorption of these substances in the three states of liquid, solution and vapor. The results show (1) that the bands which are characteristic of the OH group in all cases are vapor-like in solution rather than liquid-like, and (2) that the bands characteristic of the CH linkages in the alcohols show practically no differences in the three states. These facts are regarded as yielding additional evidence that interaction between water or alcohol molecules in the liquid state occurs through the OH groups. Although strong dipole interactions may be the cause of the destruction of quantization which occurs in the liquid state, the vast differences for the three states suggest the operation of a resonance interchange of protons between OH groups of different molecules, in the manner postulated by Bernal and Fowler[1] to account for the mobility of hydrogen ions in acid solutions.

[1] J. D. Bernal and R. H. Fowler, J. Chem. Phys. 1, 515 (1933).

34. On a Method of Decreasing the Reflection from Nonmetallic Substances. JOHN STRONG, *California Institute of Technology.*—It is well known that flint glass frequently tarnishes, resulting in a decrease of reflectivity and a corresponding increase in transmission. H. Dennis Taylor has developed chemical treatments to produce this desired surface condition artificially on glass. The present contribution involves a physical method of effecting the same end. A film of fluorite is deposited on the glass surface by evaporation. For plate glass at normal incidence in one case the reflection was decreased to 80 percent. This has several applications such as the increase in transmission of lenses and prisms; the reduction of halation due to multiple reflections in fast lenses; the elimination of secondary images from the uncoated surfaces of silvered plates; the increase in possible exposure time for Littrow spectrographs. As for the latter, a reduction of 80 percent in reflection, as reported above, would allow a fivefold increase in exposure time.

35. Radio Noises from the Galaxy. R. M. LANGER, *California Institute of Technology.*—The experiments of Jansky show that a rather considerable (10^{-5}) fraction of the radiation from the Milky Way lies in a wave-length range about 16 meters. As Jansky has pointed out it is difficult to explain this component as an emanation from the stars. There is a much more plausible interpretation of the Jansky radiation. Astronomical considerations demonstrate the existence in the galaxy of cold matter much of which occurs in particles about 1μ in size. The diluted stellar radiation in interstellar space ionizes this solid matter until electrons are captured as fast as the

radiation removes them. The ordinary particle has several hundred electrons thus ionized away on the average. The radiation to be expected when an electron recombines with such a particle will contain a component corresponding to energy differences between adjacent quantized states of the electrons. These energy differences depend on the dimensions of the particles. The dimension which is required to give 16 meter waves is just about 1μ. The intensity of the radiation is also not surprising when one considers that the starlight absorbed by the dust has to be reradiated in its own characteristic wave-lengths.

36. The Stability of Emulsions. HANS M. CASSEL, *Pittsburg, California.*—Emulsions are dispersions of small particles of a liquid or gaseous phase in another one. Such systems, because of the interfacial energy usually collapse returning into the initial state, that of two coexisting phases in bulk. It is possible, however, to stabilize emulsions by adding a third component, capable of building a film around the particles which inhibits the exchange of molecules between the adjacent phases. The stability of the emulsion, therefore depends only and entirely on the stability of the emulsifying film. Since the exchange of the emulsifier molecules is not inhibited, the thermodynamic potential of the film substance is the same in the whole system. It is determined by the capillary pressure $2\sigma/r$ exerted upon the internal phase by the interfacial tension:

$$\mu_r = \mu_0 + 2\sigma/r(D_{\text{in}} - D_{\text{ex}})$$

(D_{ex} and D_{in} designating the densities of the emulsifier in the external and in the internal phase, respectively, μ_0 the potential of the emulsifier for the masses in bulk). Hence, as the emulsifier can be stable only, whenever $\mu_0 > \mu_r$, we conclude that in this case D_{ex} has to be larger than D_{in}. This is in agreement with the well established rule of Bancroft, whose derivation, however, has not been available.

37. A Study of Short Time Lags in Sparks as a Function of Overvoltage. R. R. WILSON, *University of California.* (*Introduced by L. B. Loeb.*)—By using an electro-optical shutter the time lag of sparking was measured for static breakdown as a function of overvoltage in air at atmospheric pressure using a sphere gap illuminated with light from a quartz Hg arc. The overvoltage was applied suddenly to a gap already near the sparking voltage. Definite formative lags were observed whose value clustered about a mean time value in a Gaussian distribution curve. Time lags were taken from the peak of this curve and plotted against overvoltage. At 60 percent overvoltage the lag was about 10^{-7} second, it decreased rapidly with overvoltage; near 100 percent overvoltage the time lag observed was 10^{-8} second and it required a large increase in overvoltage to decrease the lag materially below this value. These lags are such that it would be impossible for an electron to cross the gap of about 5 mm in the time given.

AUTHOR INDEX TO ABSTRACTS OF THE BERKELEY MEETING

Albertson, Walter—No.No. 26
——— **and A. S. King**— 32
Anderson, Carl D., R. A. Millikan and Seth H. Neddermeyer—No. 4
Birge, R. T.—No. 6
Bonner, T. W.—see Brubaker
———, **L. A. Delsasso, W. A. Fowler and C. C. Lauritsen**—No. 3
Bradbury, Norris E. and Russell A. Nielsen—No. 10
Brubaker, W. M. and T. W. Bonner—No. 13
Cassel, Hans M.—No. 36
Chapman, Seville—No. 18
Cooksey, Donald, F. N. D. Kurie and Ernest O. Lawrence—No. 5
Cork, J. M. and E. O. Lawrence—No. 9
———, **J. R. Richardson and F. N. D. Kurie**—No. 28
Delsasso, L. A.—see Bonner
Dozier, Charles T.—No. 25
Dunnington, Frank G.—No. 11
Edwards, Hiram W. and Robert P. Petersen—No. 23
Ellis, J. W.—see Kinsey
Fowler, W. A.—see Bonner
Gaviola, E.—see Strong
Houston, William V.—No. 16
Jenkins, F. A. and Andrew McKellar—No. 12
King, A. S.—see Albertson
Kinsey, E. L. and J. W. Ellis—No. 33
Kirkpatrick, Paul and P. A. Ross—No. 31
Kurie, F. N. D.—see Cooksey
———see Cork
———see Richardson
——— **and J. J. Livingood**—No. 29
———, **J. R. Richardson and H. C. Paxton**—No. 2
Langer, R. M.—Nos. 14, 35
Lauritsen, C. C.—see Bonner
Lawrence, Ernest O.—see Cooksey
———see Cork
Livingood, J. J.—No. 17
———see Kurie
McKellar, Andrew—see Jenkins
Millikan, R. A.—see Anderson
Neddermeyer, Seth H.—see Anderson
Newson, Henry W.—No. 27
Nielsen, Russell A.—see Bradbury
Paxton, H. G.—No. 15
———see Kurie
Petersen, Robert P.—see Edwards
Richardson, J. R.—No. 1
———see Cork
———see Kurie
——— **and F. N. D. Kurie**—No. 30
Robertson, H. P.—No. 20
Ross, P. A.—see Kirkpatrick
Sanford, Fernando—No. 19
Snell, Arthur H.—No. 22
Strong, John—No. 34
——— **and E. Gaviola**—No. 24
Thornton, R. L.—No. 21
Varney, Robert N.—No. 7
White, H. E.—No. 8
Wilson, R. R.—No. 37

lsifier
tively,
bulk).
never
larger
lished
been

nction
fornia.
optical
static
tmos-
light
pplied
ltage.
stered
curve.
e and
oltage
with
ne lag
crease
w this
ole for
e time